

Dave Lage Moderno

Shadow Mapping and Ray-Tracing

Tese de Mestrado
Mestrado em Informática

Trabalho efectuado sob a orientação do
Professor Doutor António Ramires Fernandes

É AUTORIZADA A REPRODUÇÃO INTEGRAL DESTA TESE APENAS PARA EFEITOS DE INVESTIGAÇÃO, MEDIANTE DECLARAÇÃO ESCRITA DO INTERESSADO, QUE A TAL SE COMPROMETE.

Universidade do Minho, ___/___/_____

Assinatura: _____

ACKNOWLEDGMENTS

I would like to thank the following people:

- my family, and especially my parents Celeste and Albino for sponsoring this work (and my life in general);
- my friends, too many to be named here, be it those with whom I studied, those with whom I played (and still play) videogames or those with whom I just hang out with;
- my thesis advisor, PhD António Ramires Fernandes, for putting up with all of my questions (many of which weren't very smart);
- my girlfriend, Helena, for supporting me in finishing this work, even considering all the time it took to finish.

SHADOW MAPPING AND RAY-TRACING

ABSTRACT

Shadow mapping has been one of the most used algorithms for real time calculation of shadows, since it is extremely simple and quick in calculating said shadows, but not always presents the best results. On the other hand, ray-tracing presents pixel-perfect shadows, but it is more demanding from a computational point of view.

Shadow mapping has seen many proposals to increase its accuracy, while retaining its high performance nature. Some of the methods proposed, based solely on the standard shadow mapping technique, do improve significantly the standard shadow mapping result at the expense of a minor decrease in performance. Other approaches propose hybrid methods, using shadow mapping as a way of limiting the number of pixels that require ray-tracing. One of such approaches uses texel coherence to reduce the number of pixels that require testing.

These latter approaches establish the theme for this work. The goal is to narrow down as much as possible the amount of pixels that require a ray-tracer to determine its shadow status.

The first step was to identify the location of the errors present in a shadow map. The tests confirmed the intuition that most of these errors should be located in the contours of the shadow areas.

The next step focuses on these contour areas and looks for ways to determine the correctness of a pixel's shadow status. Several methods were proposed to achieve this goal. Some methods were capable of confirming pixels in shadow. Some were capable of correcting pixels in light.

Each method, with the exception of texel coherence, uses a very selective ray-tracer, i.e. only very few triangles are tested for intersection with a single light ray.

Since each method has its strengths and weaknesses an algorithm was proposed, chaining all these methods together. The first step is to determine the set of pixels in the contours of the shadow areas. Then each method is applied in turn, so that only the pixels the remaining unconfirmed/uncorrected pass on to the next stage.

At the end of the algorithm a very large percentage of pixels in shadow were confirmed and a significant number of pixels in light were corrected. The remaining pixels could then be fed to a full ray-tracer. The load of the ray-tracer is severely reduced under this approach making it an affordable solution to obtain pixel perfect shadows in the contours of the shadowed areas.

SHADOW MAPPING E RAY-TRACING

RESUMO

O *shadow mapping* tem sido um dos algoritmos mais utilizados para o cálculo de sombras em tempo real, já que é extremamente simples e rápido em calcular estas sombras, mas nem sempre apresenta os melhores resultados. Por outro lado, *ray-tracing* apresenta sombras perfeitas ao nível do pixel mas é mais exigente de um ponto de vista computacional.

Têm havido muitas propostas para o aumento de qualidade do *shadow mapping* sem afectar o seu desempenho. Alguns dos métodos propostos, baseados somente na técnica de *shadow mapping* padrão, de facto melhoram significativamente o resultado do *shadow mapping* padrão ao custo de uma pequena diminuição no desempenho. Outras abordagens propõem métodos híbridos, usando o *shadow mapping* para limitar o número de pixéis que requerem *ray-tracing*. Uma destas abordagens usa o *texel coherence* para reduzir o número de pixéis que precisam de ser testados.

Estas últimas abordagens estabelecem o tema deste trabalho. O objectivo é limitar o máximo possível a quantidade de pixéis que requerem um *ray-tracer* para determinar o seu sombreamento.

O primeiro passo foi identificar a localização dos erros presentes num *shadow map*. Os testes confirmaram a intuição de que a maior parte destes erros se deveriam encontrar nos contornos das zonas sombreadas.

O próximo passo foca-se nestas áreas de contorno e procura maneiras de determinar se o sombreamento de um pixel está correcto. Vários métodos foram propostos para conseguir este objectivo. Alguns métodos foram capazes de confirmar pixéis em sombra. Alguns foram capazes de corrigir pixéis em luz.

Cada método, com a excepção do *texel coherence*, usa um *ray-tracer* muito selectivo, isto é, apenas uma muito pequena quantidade de triângulos é testada para intersecção com cada raio de luz.

Como cada método tem as suas vantagens e desvantagens um algoritmo que encadeia todos estes métodos foi proposto. O primeiro passo é determinar o conjunto de pixéis nos contornos das áreas sombreadas. Depois cada método é aplicado à vez de modo a que os pixéis que se mantêm por confirmar ou corrigir passem para o próximo passo.

No fim do algoritmo uma grande percentagem de pixéis em sombra foi confirmada e um número significativo de pixéis em luz foi corrigido. O resto dos pixéis poderia então passar por um *ray-tracer* completo. A carga do *ray-tracer* é severamente reduzida sob esta abordagem tornando-o numa solução acessível à obtenção de sombras perfeitas ao nível do pixel nos contornos das áreas sombreadas.

TABLE OF CONTENTS

1. INTRODUCTION	1
1.1. Motivation	2
1.2. Goals.....	2
1.3. Methodology	3
1.4. Thesis Structure.....	4
2. STATE OF THE ART	5
2.1. Shadow Mapping.....	5
2.1.1. Shadow Mapping Basics.....	5
2.1.2. Shadow Mapping Problems	6
2.1.3. Shadow Mapping Approaches	8
2.2. Ray-Tracing.....	13
2.2.1. Ray-Tracing Basics.....	13
2.3. Combining Both	15
2.3.1. Coherence-Based Ray-Tracing	15
2.3.2. Hybrid GPU Rendering Pipeline for Alias-Free Hard Shadows.....	16
2.3.3. Hybrid GPU-CPU Renderer.....	18
2.4. Conclusion.....	19
3. ALGORITHM DESCRIPTION	21
3.1. Shadow Mapping Errors.....	21
3.1.1. Shadow Status and Errors	21
3.1.2. Error Location.....	23
3.2. Using Texel Information	24
3.3. Using the Information of the Neighbouring Texels	28
3.4. Using Texel Coherence	31
3.5. Using Geometric Adjacency Information	34

3.6.	Putting It All Together	37
3.7.	Conclusion.....	41
4.	ALGORITHM TESTING.....	43
4.1.	Test Scenes	44
4.2.	Ray-Tracer.....	46
4.3.	Shadow Mapping Errors.....	52
4.4.	Using Texel Coherence	55
4.5.	Using Texel Information	60
4.6.	Using the Information of the Neighbours of the Texel.....	63
4.7.	Using Geometric Adjacency Information	67
4.8.	Putting It All Together	71
4.9.	Final Observations.....	76
5.	CONCLUSIONS AND FUTURE WORK.....	81
6.	BIBLIOGRAPHY	85
	APPENDIX.....	87

FIGURE INDEX

Figure 1: How a Shadow Map works.	6
Figure 2: The shadow of the tree presents aliasing.....	6
Figure 3: Perspective Shadow Map example.....	8
Figure 4: Light Space Perspective Shadow Map example.....	9
Figure 5: Trapezoidal Shadow Mapping movement flickering.	10
Figure 6: Adaptive Shadow map result compared to a shadow mapping result (2048x2048 shadow map versus an effective 524288x524288 shadow map result).	10
Figure 7: Parallel-Split Shadow Maps example.....	11
Figure 8: Variance Shadow Map light leaking example.....	12
Figure 9: Comparison between Convolved, Variance and Exponential Shadow Maps respectively.	12
Figure 10: Simple example of Ray-Tracing.....	14
Figure 11: Reference image examples for the coherence based ray-tracing.	16
Figure 12: Resizing the triangle by moving its edges.....	17
Figure 13: Example of the uncertain areas when using the Hybrid GPU Rendering Pipeline for Alias-Free Hard Shadows.....	18
Figure 14: Green pixels mark where shadow mapping samples disagree in the Hybrid GPU-CPU Renderer.	19
Figure 15: Correctly (in green) and incorrectly (in blue) shadowed points by shadow mapping.....	22
Figure 16: Correctly (in green) and incorrectly (in blue) lit points by shadow mapping.	23
Figure 17: Marked contours and errors of the scene.....	24
Figure 18: Cases of using texel information.	25
Figure 19: Correcting a point wrongly defined in light with the triangle stored in the projected texel.....	26

Figure 20: Pixel confirmation using texel information.....	27
Figure 21: The two cases of neighbouring texels.	28
Figure 22: Cases using neighbouring texel information with a triangle stored in the centre texel.....	29
Figure 23: Cases using neighbouring texel information without a triangle stored in the centre texel.....	30
Figure 24: Pixel confirmation using neighbouring texel information with 8 neighbours.....	31
Figure 25: Examples of PCF results.	32
Figure 26: Pixel confirmation using PCF with four texels.	33
Figure 27: Using adjacent geometry information for case a).	35
Figure 28: Using adjacent geometry information for case b).	35
Figure 29: Correcting a point wrongly defined in light using triangle adjacency.	36
Figure 30: Pixel confirmation using geometry adjacency information with 2 levels of adjacency.....	37
Figure 31: Average of corrected/confirmed/hinted contour pixels by each method: a) contour pixels; b) shadow map results separated in shadow (black) and light (white); c) errors of the shadow map (gray); d) correct (blue) and incorrect (red) hints using texel coherence; e) confirmed shadow (dark green) and corrected light (light green) pixels by neighbouring texels; f) confirmed shadow pixels (orange) by adjacent geometry.	38
Figure 32: Average of corrected/confirmed/hinted contour pixels by the chaining of methods: a) contour pixels; b) shadow map results separated in shadow (black) and light (white); c) errors of the shadow map (gray); d) correct (blue) and incorrect (red) hints using texel coherence; e) confirmed shadow (dark green) and corrected light (light green) pixels by neighbouring texels; f) confirmed shadow pixels (orange) by adjacent geometry; g) non-hinted/uncorrected/unconfirmed pixels (yellow).	40
Figure 33: The side (left), with (centre) and against (right) viewpoints of the first scene.	44
Figure 34: The side (left), with (centre) and against (right) viewpoints of the second scene..	45

Figure 35: The with (left), side (centre) and against (right) viewpoints of the third scene.	46
Figure 36: The side (left), against (centre) and with (right) viewpoints of the fourth scene. ...	46
Figure 37: Ray-tracer results for the side viewpoint of the primitives scene.	47
Figure 38: Ray-tracer results for the with viewpoint of the primitives scene.	47
Figure 39: Ray-tracer results for the against viewpoint of the primitives scene.	48
Figure 40: Ray-tracer results for the side viewpoint of the bench scene.	48
Figure 41: Ray-tracer results for the with viewpoint of the bench scene.	49
Figure 42: Ray-tracer results for the against viewpoint of the bench scene.	49
Figure 43: Ray-tracer results for the with viewpoint of the trees scene.	50
Figure 44: Ray-tracer results for the side viewpoint of the trees scene.	50
Figure 45: Ray-tracer results for the against viewpoint of the trees scene.	51
Figure 46: Ray-tracer results for the side viewpoint of the flowers scene.	51
Figure 47: Ray-tracer results for the against viewpoint of the flowers scene.	52
Figure 48: Ray-tracer results for the with viewpoint of the flowers scene.	52
Figure 49: Best case of shadow map errors being caught inside contours with a 2048x2048 shadow map.	53
Figure 50: Worst case of shadow map errors being caught inside contours with a 2048x2048 shadow map.	54
Figure 51: Average case of shadow map errors being caught inside contours.	54
Figure 52: Average shadow map results separated by contour thickness with a 1024x1024 shadow map (top) and a 2048x2048 shadow map (bottom).	55
Figure 53: Best case of texel coherence confirmation using four texels and a 2048x2048 shadow map.	56
Figure 54: Worst case of texel coherence confirmation using four texels and a 2048x2048 shadow map.	57

Figure 55: Average case of texel coherence confirmation using four texels.....	58
Figure 56: Best case of texel coherence confirmation using nine texels and a 2048x2048 shadow map.	59
Figure 57: Worst case of texel coherence confirmation using nine texels and a 2048x2048 shadow map.	59
Figure 58: Average case of texel coherence confirmation using nine texels.....	60
Figure 59: Average results of texel coherence with four texels separated by contour thickness with a 1024x1024 shadow map (top) and a 2048x2048 shadow map (bottom).	60
Figure 60: Best case of only using centre texel information with a 2048x2048 shadow map.	61
Figure 61: Worst case of using centre texel information by itself with a 2048x2048 shadow map.....	62
Figure 62: Average case of using centre texel information by itself.	62
Figure 63: Best case of only using information of four neighbouring texels with a 2048x2048 shadow map.	64
Figure 64: Best case of only using information of nine neighbouring texels with a 2048x2048 shadow map.	64
Figure 65: Worst case of only using information of four neighbouring texels with a 2048x2048 shadow map.	65
Figure 66: Worst case of only information of nine neighbouring texels with a 2048x2048 shadow map.	65
Figure 67: Average case of only using information of four neighbouring texels.....	66
Figure 68: Average case of only using information of nine neighbouring texels.....	66
Figure 69: Average results of neighbouring texels with nine texels separated by contour thickness with a 1024x1024 shadow map (top) and a 2048x2048 shadow map (bottom).	67
Figure 70: Best case of only using centre and first level of adjacent geometry information with a 2048x2048 shadow map.....	68

Figure 71: Best case of only using centre and second level of adjacent geometry information with a 2048x2048 shadow map.....	68
Figure 72: Worst case of only using centre and first level of adjacent geometry information with a 2048x2048 shadow map.....	69
Figure 73: Worst case of only using centre and second level of adjacent geometry information with a 2048x2048 shadow map.....	69
Figure 74: Average case of only using centre and first level of adjacent geometry information.....	70
Figure 75: Average case of only using centre and second level of adjacent geometry information.....	70
Figure 76: Average results of adjacent geometry with two levels of adjacency separated by contour thickness with a 1024x1024 shadow map (top) and a 2048x2048 shadow map (bottom).....	71
Figure 77: Best case of algorithm pixel confirmation after using information of the neighbouring texels with a 2048x2048 shadow map.....	72
Figure 78: Worst case of algorithm pixel confirmation after using information of the neighbouring texels with a 2048x2048 shadow map.....	72
Figure 79: Average case of algorithm pixel confirmation after using information of the neighbouring texels.....	73
Figure 80: Average results of the algorithm after the neighbouring texel step separated by contour thickness with a 1024x1024 shadow map (top) and a 2048x2048 shadow map (bottom).....	73
Figure 81: Best case of algorithm pixel confirmation after using information of the adjacent geometry with a 2048x2048 shadow map.	74
Figure 82: Worst case of algorithm pixel confirmation after using information of the adjacent geometry with a 2048x2048 shadow map.	75
Figure 83: Average case of algorithm pixel confirmation after using information of the adjacent geometry.	75

Figure 84: Average results of the algorithm after the adjacent geometry step separated by contour thickness with a 1024x1024 shadow map (top) and a 2048x2048 shadow map (bottom).....	76
Figure 85: Average results of the algorithm after the adjacent geometry step with pixels that were not confirmed, corrected or hinted marked, separated by contour thickness with a 1024x1024 shadow map (top) and a 2048x2048 shadow map (bottom).	76
Figure 86: Marked errors of the best case when using a 2048x2048 shadow map.	78
Figure 87: Marked errors of the worst case when using a 2048x2048 shadow map.	78
Figure 88: Marked errors of the average case.....	79
Figure 89: Result of the ray-tracing approach for the side viewpoint of the primitives scene.	87
Figure 90: Result of the shadow mapping approach for the side viewpoint of the primitives scene.....	87
Figure 91: Result of texel coherence with four texels for the side viewpoint of the primitives scene.....	88
Figure 92: Result of texel coherence with nine texels for the side viewpoint of the primitives scene.....	88
Figure 93: Result of the single texel approach on the side viewpoint of the primitives scene.	89
Figure 94: Result of the neighbour texels approach using four neighbours for the side viewpoint of the primitives scene.	89
Figure 95: Result of the neighbour texels approach using nine neighbours for the side viewpoint of the primitives scene.	90
Figure 96: Result of the adjacent geometry approach with one level of adjacency for the side viewpoint of the primitives scene.	90
Figure 97: Result of the adjacent geometry approach with two levels of adjacency for the side viewpoint of the primitives scene.	91

Figure 98: Result of the algorithm with a six pixel thick contour and a 2048x2048 resolution shadow map for the side viewpoint of the primitives scene.	91
Figure 99: Corrected/confirmed/hinted contour pixels by each method for the side viewpoint of the primitives scene using a 1024x1024 (top) and a 2048x2048 (bottom) resolution shadow map.....	92
Figure 100: Corrected/confirmed/hinted contour pixels by the chaining of methods for the side viewpoint of the primitives scene using a 1024x1024 (top) and a 2048x2048 (bottom) resolution shadow map.	93
Figure 101: Result of the ray-tracing approach for the with viewpoint of the primitives scene.	104
Figure 102: Result of the shadow mapping approach for the with viewpoint of the primitives scene.....	104
Figure 103: Result of texel coherence with four texels for the with viewpoint of the primitives scene.....	105
Figure 104: Result of texel coherence with nine texels for the with viewpoint of the primitives scene.	105
Figure 105: Result of the single texel approach for the with viewpoint of the primitives scene.	106
Figure 106: Result of the neighbour texels approach using four neighbours for the with viewpoint of the primitives scene.	106
Figure 107: Result of the neighbour texels approach using nine neighbours for the with viewpoint of the primitives scene.	107
Figure 108: Result of the adjacent geometry approach with one level of adjacency for the with viewpoint of the primitives scene.	107
Figure 109: Result of the adjacent geometry approach with two levels of adjacency for the with viewpoint of the primitives scene.	108
Figure 110: Result of the algorithm with a six pixel thick contour and a 2048x2048 resolution shadow map for the with viewpoint of the primitives scene.	108

Figure 111: Corrected/confirmed/hinted contour pixels by each method for the with viewpoint of the primitives scene using a 1024x1024 (top) and a 2048x2048 (bottom) resolution shadow map.	109
Figure 112: Corrected/confirmed/hinted contour pixels by the chaining of methods for the with viewpoint of the primitives scene using a 1024x1024 (top) and a 2048x2048 (bottom) resolution shadow map.	110
Figure 113: Result of the ray-tracing approach for the against viewpoint of the primitives scene.....	120
Figure 114: Result of the shadow mapping approach for the against viewpoint of the primitives scene.	120
Figure 115: Result of texel coherence with four texels for the against viewpoint of the primitives scene.	121
Figure 116: Result of texel coherence with nine texels for the against viewpoint of the primitives scene.	121
Figure 117: Result of the single texel approach for the against viewpoint of the primitives scene.....	122
Figure 118: Result of the neighbour texels approach using three pixels for the against viewpoint of the primitives scene.	122
Figure 119: Result of the neighbour texels approach using eight pixels for the against viewpoint of the primitives scene.	123
Figure 120: Result of the adjacent geometry approach with one level of adjacency for the against viewpoint of the primitives scene.....	123
Figure 121: Result of the adjacent geometry approach with two levels of adjacency for the against viewpoint of the primitives scene.....	124
Figure 122: Result of the algorithm with a six pixel thick contour and a 2048x2048 resolution shadow map for the against viewpoint of the primitives scene.	124

Figure 123: Corrected/confirmed/hinted contour pixels by each method for the against viewpoint of the primitives scene using a 1024x1024 (top) and a 2048x2048 (bottom) resolution shadow map. 125

Figure 124: Corrected/confirmed/hinted contour pixels by the chaining of methods for the against viewpoint of the primitives scene using a 1024x1024 (top) and a 2048x2048 (bottom) resolution shadow map. 126

Figure 125: Result of the ray-tracing approach for the side viewpoint of the bench scene... 136

Figure 126: Result of the shadow mapping approach for the side viewpoint of the bench scene..... 136

Figure 127: Result of texel coherence with four texels for the side viewpoint of the bench scene..... 137

Figure 128: Result of texel coherence with nine texels for the side viewpoint of the bench scene..... 137

Figure 129: Result of the single texel approach for the side viewpoint of the bench scene.. 138

Figure 130: Result of the neighbour texels approach with four neighbours for the side viewpoint of the bench scene..... 138

Figure 131: Result of the neighbour texels approach with nine neighbours for the side viewpoint of the bench scene..... 139

Figure 132: Result of the adjacent geometry approach with one level of adjacency for the side viewpoint of the bench scene..... 139

Figure 133: Result of the adjacent geometry approach with two levels of adjacency for the side viewpoint of the bench scene. 140

Figure 134: Result of the algorithm with a six pixel thick contour and a 2048x2048 resolution shadow map for the side viewpoint of the bench scene..... 140

Figure 135: Corrected/confirmed/hinted contour pixels by each method for the side viewpoint of the bench scene using a 1024x1024 (top) and a 2048x2048 (bottom) resolution shadow map..... 141

Figure 136: Corrected/confirmed/hinted contour pixels by the chaining of methods for the side viewpoint of the bench scene using a 1024x1024 (top) and a 2048x2048 (bottom) resolution shadow map. 142

Figure 137: Result of the ray-tracing approach for the with viewpoint of the bench scene.. 152

Figure 138: Result of the shadow mapping approach for the with viewpoint of the bench scene..... 152

Figure 139: Result of texel coherence with four texels for the with viewpoint of the bench scene..... 153

Figure 140: Result of texel coherence with nine texels for the with viewpoint of the bench scene..... 153

Figure 141: Result of the single texel approach for the with viewpoint of the bench scene. 154

Figure 142: Result of the neighbour texels approach with four neighbours for the with viewpoint of the bench scene. 154

Figure 143: Result of the neighbour texels approach with nine neighbours for the with viewpoint of the bench scene. 155

Figure 144: Result of the adjacent geometry approach with one level of adjacency for the with viewpoint of the bench scene..... 155

Figure 145: Result of the adjacent geometry approach with two levels of adjacency for the with viewpoint of the bench scene..... 156

Figure 146: Result of the algorithm with a six pixel thick contour and a 2048x2048 resolution shadow map for the with viewpoint of the bench scene. 156

Figure 147: Corrected/confirmed/hinted contour pixels by each method for the with viewpoint of the bench scene using a 1024x1024 (top) and a 2048x2048 (bottom) resolution shadow map. 157

Figure 148: Corrected/confirmed/hinted contour pixels by the chaining of methods for the with viewpoint of the bench scene using a 1024x1024 (top) and a 2048x2048 (bottom) resolution shadow map. 158

Figure 149: Result of the ray-tracing approach for the against viewpoint of the bench scene.	168
Figure 150: Result of the shadow mapping approach for the against viewpoint of the bench scene.....	168
Figure 151: Result of texel coherence with four texels for the against viewpoint of the bench scene.....	169
Figure 152: Result of texel coherence with nine texels for the against viewpoint of the bench scene.....	169
Figure 153: Result of the single texel approach for the against viewpoint of the bench scene.	170
Figure 154: Result of the neighbour texels approach using four neighbours for the against viewpoint of the bench scene.	170
Figure 155: Result of the neighbour texels approach using nine neighbours for the against viewpoint of the bench scene.....	171
Figure 156: Result of the adjacent geometry approach with one level of adjacency for the against viewpoint of the bench scene.....	171
Figure 157: Result of the adjacent geometry approach with two levels of adjacency for the against viewpoint of the bench scene.....	172
Figure 158: Result of the algorithm with a six pixel thick contour and a 2048x2048 resolution shadow map for the against viewpoint of the bench scene.....	172
Figure 159: Corrected/confirmed/hinted contour pixels by each method for the against viewpoint of the bench scene using a 1024x1024 (top) and a 2048x2048 (bottom) resolution shadow map.	173
Figure 160: Corrected/confirmed/hinted contour pixels by the chaining of methods for the against viewpoint of the bench scene using a 1024x1024 (left) and a 2048x2048 (bottom) resolution shadow map.	174
Figure 161: Result of the ray-tracing approach for the with viewpoint of the trees scene. ...	186

Figure 162: Result of the shadow mapping approach for the with viewpoint of the trees scene.	186
Figure 163: Result of texel coherence with four texels for the with viewpoint of the trees scene.....	187
Figure 164: Result of texel coherence with nine texels for the with viewpoint of the trees scene.....	187
Figure 165: Result of the single texel approach for the with viewpoint of the trees scene. ..	188
Figure 166: Result of the neighbour texels approach using four neighbours for the with viewpoint of the trees scene.....	188
Figure 167: Result of the neighbour texels approach using nine neighbours for the with viewpoint of the trees scene.....	189
Figure 168: Result of the adjacent geometry approach with one level of adjacency for the with viewpoint of the trees scene.....	189
Figure 169: Result of the adjacent geometry approach with two levels of adjacency for the with viewpoint of the trees scene.....	190
Figure 170: Result of the algorithm with a six pixel thick contour and a 2048x2048 resolution shadow map for the with viewpoint of the trees scene.	190
Figure 171: Corrected/confirmed/hinted contour pixels by each method for the with viewpoint of the trees scene using a 1024x1024 (top) and a 2048x2048 (bottom) resolution shadow map.	191
Figure 172: Corrected/confirmed/hinted contour pixels by the chaining of methods for the with viewpoint of the trees scene using a 1024x1024 (top) and a 2048x2048 (bottom) resolution shadow map.	192
Figure 173: Result of the ray-tracing approach for the side viewpoint of the trees scene.....	203
Figure 174: Result of the shadow mapping approach for the side viewpoint of the trees scene.	203

Figure 175: Result of texel coherence with four texels for the side viewpoint of the trees scene.....	204
Figure 176: Result of texel coherence with nine texels for the side viewpoint of the trees scene.....	204
Figure 177: Result of the single texel approach for the side viewpoint of the trees scene....	205
Figure 178: Result of the neighbour texels approach with four neighbours for the side viewpoint of the trees scene.....	205
Figure 179: Result of the neighbour texels approach with nine neighbours for the side viewpoint of the trees scene.....	206
Figure 180: Result of the adjacent geometry approach with one level of adjacency for the side viewpoint of the trees scene.....	206
Figure 181: Result of the adjacent geometry approach with two levels of adjacency for the side viewpoint of the trees scene.	207
Figure 182: Result of the algorithm with a six pixel thick contour and a 2048x2048 resolution shadow map for the side viewpoint of the trees scene.....	207
Figure 183: Corrected/confirmed/hinted contour pixels by each method for the side viewpoint of the trees scene using a 1024x1024 (top) and a 2048x2048 (bottom) resolution shadow map.....	208
Figure 184: Corrected/confirmed/hinted contour pixels by the chaining of methods for the side viewpoint of the trees scene using a 1024x1024 (top) and a 2048x2048 (bottom) resolution shadow map.	209
Figure 185: Result of the ray-tracing approach for the against viewpoint of the trees scene.	219
Figure 186: Result of the shadow mapping approach for the against viewpoint of the trees scene.....	219
Figure 187: Result of texel coherence with four texels for the against viewpoint of the trees scene.....	220

Figure 188: Result of texel coherence with nine texels for the against viewpoint of the trees scene.....	220
Figure 189: Result of the single texel approach for the against viewpoint of the trees scene.	221
Figure 190: Result of the neighbour texels approach using four neighbours for the against viewpoint of the trees scene.....	221
Figure 191: Result of the neighbour texels approach using nine neighbours for the against viewpoint of the trees scene.....	222
Figure 192: Result of the adjacent geometry approach with one level of adjacency for the against viewpoint of the trees scene.....	222
Figure 193: Result of the adjacent geometry approach with two level of adjacency for the against viewpoint of the trees scene.....	223
Figure 194: Result of the algorithm with a six pixel thick contour and a 2048x2048 resolution shadow map for the against viewpoint of the trees scene.....	223
Figure 195: Corrected/confirmed/hinted contour pixels by each method for the against viewpoint of the trees scene using a 1024x1024 (top) and a 2048x2048 (bottom) resolution shadow map.	224
Figure 196: Corrected/confirmed/hinted contour pixels by the chaining of methods for the against viewpoint of the trees scene using a 1024x1024 (top) and a 2048x2048 (bottom) resolution shadow map.	225
Figure 197: Result of the ray-tracing approach for the side viewpoint of the flowers scene.	235
Figure 198: Result of the shadow mapping approach for the side viewpoint of the flowers scene.....	235
Figure 199: Result of texel coherence with four texels for the side viewpoint of the flowers scene.....	236
Figure 200: Result of texel coherence with nine texels for the side viewpoint of the flowers scene.....	236

Figure 201: Result of the single texel approach for the side viewpoint of the flowers scene.	237
Figure 202: Result of the neighbour texels approach using four neighbours for the side viewpoint of the flowers scene.	237
Figure 203: Result of the neighbour texels approach using nine neighbours for the side viewpoint of the flowers scene.	238
Figure 204: Result of the adjacent geometry approach with one level of adjacency for the side viewpoint of the flowers scene.	238
Figure 205: Result of the adjacent geometry approach with two levels of adjacency for the side viewpoint of the flowers scene.	239
Figure 206: Result of the algorithm with a six pixel thick contour and a 2048x2048 resolution shadow map for the side viewpoint of the flowers scene.	239
Figure 207: Corrected/confirmed/hinted contour pixels by each method for the side viewpoint of the flowers scene using a 1024x1024 (top) and a 2048x2048 (bottom) resolution shadow map.....	240
Figure 208: Corrected/confirmed/hinted contour pixels by the chaining of methods for the side viewpoint of the flowers scene using a 1024x1024 (top) and a 2048x2048 (bottom) resolution shadow map.	241
Figure 209: Result of the ray-tracing approach for the against viewpoint of the flowers scene.	253
Figure 210: Result of the shadow mapping approach for the against viewpoint of the flowers scene.....	253
Figure 211: Result of texel coherence with four texels for the against viewpoint of the flowers scene.....	254
Figure 212: Result of texel coherence with nine texels for the against viewpoint of the flowers scene.....	254
Figure 213: Result of the single texel approach for the against viewpoint of the flowers scene.	255

Figure 214: Result of the neighbour texels approach using four neighbours for the against viewpoint of the flowers scene.	255
Figure 215: Result of the neighbour texels approach using nine neighbours for the against viewpoint of the flowers scene.	256
Figure 216: Result of the adjacent geometry approach with one level of adjacency for the against viewpoint of the flowers scene.	256
Figure 217: Result of the adjacent geometry approach with two levels of adjacency for the against viewpoint of the flowers scene.	257
Figure 218: Result of the algorithm with a six pixel thick contour and a 2048x2048 resolution shadow map for the against viewpoint of the flowers scene.	257
Figure 219: Corrected/confirmed/hinted contour pixels by each method for the against viewpoint of the flowers scene using a 1024x1024 (top) and a 2048x2048 (bottom) resolution shadow map.	258
Figure 220: Corrected/confirmed/hinted contour pixels by the chaining of methods for the against viewpoint of the flowers scene using a 1024x1024 (top) and a 2048x2048 (bottom) resolution shadow map.	259
Figure 221: Result of the ray-tracing approach for the with viewpoint of the flowers scene.	269
Figure 222: Result of the shadow mapping approach for the with viewpoint of the flowers scene.	269
Figure 223: Result of texel coherence with four texels for the with viewpoint of the flowers scene.	270
Figure 224: Result of texel coherence with nine texels for the with viewpoint of the flowers scene.	270
Figure 225: Result of the single texel approach for the with viewpoint of the flowers scene.	271
Figure 226: Result of the neighbour texels approach using four neighbours for the with viewpoint of the flowers scene.	271

Figure 227: Result of the neighbour texels approach using nine neighbours for the with viewpoint of the flowers scene.272

Figure 228: Result of the adjacent geometry approach with one level of adjacency for the with viewpoint of the flowers scene.272

Figure 229: Result of the adjacent geometry approach with two levels of adjacency for the with viewpoint of the flowers scene.273

Figure 230: Result of the algorithm with a six pixel thick contour and a 2048x2048 resolution shadow map for the with viewpoint of the flowers scene.....273

Figure 231: Corrected/confirmed/hinted contour pixels by each method for the with viewpoint of the flowers scene using a 1024x1024 (top) and a 2048x2048 (bottom) resolution shadow map.274

Figure 232: Corrected/confirmed/hinted contour pixels by the chaining of methods for the with viewpoint of the flowers scene using a 1024x1024 (top) and a 2048x2048 (bottom) resolution shadow map.275

TABLE INDEX

Table 1: Information of the first scene.....	44
Table 2: Information of the second scene.	45
Table 3: Information of the third scene.....	45
Table 4: Information of the fourth scene.	46
Table 5: Percentages of errors inside the contours.	53
Table 6: Percentage of contour pixels that are incorrect.....	55
Table 7: Percentage of confirmations by PCF with four texels.	56
Table 8: Percentage of confirmations by PCF with nine texels.....	58
Table 9: Percentage of errors by only using the information of the centre texel.....	61
Table 10: Percentage of errors by only using the information of the centre and neighbouring texels.	63
Table 11: Percentage of errors by only using the information of the centre texel and the adjacent geometry.	67
Table 12: Percentage of confirmations by algorithm after using neighbouring texel information.....	71
Table 13: Percentage of confirmations by algorithm after using adjacent geometry information.....	74
Table 14: Percentage of wrong confirmations after applying the algorithm and ray-tracing uncertain pixels.	77
Table 15: Percentage of wrongly defined pixels if uncertain pixels after algorithm are left in light.	77
Table 16: Difference between the approaches that use ray-tracing and the actual ray-tracer for the side viewpoint of the primitives scene.	94
Table 17: Wrongly defined pixels in the shadow mapping result which are inside the contour in the side viewpoint of the primitives scene.....	94

Table 18: Pixels that the shadow map defines wrongly in the side viewpoint of the primitives scene, separated in pixels defined in light and in shadow, compared to the total amount of pixels lighted in the same way.	95
Table 19: Pixel confirmation when using texel coherence with four texels for the side viewpoint of the primitives scene.	95
Table 20: Pixel shadowing for pixels that don't achieve texel coherence with four texels for the side viewpoint of the primitives scene.	96
Table 21: Pixel confirmation when using texel coherence with nine texels for the side viewpoint of the primitives scene.	96
Table 22: Pixel shadowing for pixels that don't achieve texel coherence with nine texels for the side viewpoint of the primitives scene.	97
Table 23: Pixel correction between the single texel approach and the shadow mapping approach for the side viewpoint of the primitives scene.	98
Table 24: Pixel correction between the neighbour texels approach and the shadow mapping approach for the side viewpoint of the primitives scene.	98
Table 25: Average of triangle intersections when using the neighbour texels approach for the side viewpoint of the primitives scene.	99
Table 26: Pixel correction between the adjacent geometry approach and the shadow mapping approach for the side viewpoint of the primitives scene.	100
Table 27: Average of triangle intersections when using the adjacent geometry approach for the side viewpoint of the primitives scene.	101
Table 28: Pixel correction by the neighbour texels (9 texels) and the adjacent geometry (2 levels) approaches separated by lighting change for the side viewpoint of the primitives scene.	102
Table 29: Algorithm results of the side viewpoint of the primitives scene.	103
Table 30: Difference between the approaches that use ray-tracing and the actual ray-tracer for the with viewpoint of the primitives scene.	111

Table 31: Wrongly defined pixels in the shadow mapping result which are inside the contour in the with viewpoint of the primitives scene.	111
Table 32: Pixels that the shadow map defines wrongly in the with viewpoint of the primitives scene, separated in pixels defined in light and in shadow, compared to the total amount of pixels lighted in the same way.	112
Table 33: Pixel confirmation when using texel coherence with four texels for the with viewpoint of the primitives scene.	112
Table 34: Pixel shadowing for pixels that don't achieve texel coherence with four texels for the with viewpoint of the primitives scene.	113
Table 35: Pixel confirmation when using texel coherence with nine texels for the with viewpoint of the primitives scene.	113
Table 36: Pixel shadowing for pixels that don't achieve texel coherence with nine texels for the with viewpoint of the primitives scene.	114
Table 37: Pixel correction between the single texel approach and the shadow mapping approach for the with viewpoint of the primitives scene.	115
Table 38: Pixel correction between the neighbour texels approach using four neighbours and the shadow mapping approach for the with viewpoint of the primitives scene.	115
Table 39: Pixel correction between the neighbour texels approach using nine neighbours and the shadow mapping approach for the with viewpoint of the primitives scene.	115
Table 40: Average of triangle intersections when using the neighbour texels approach for the with viewpoint of the primitives scene.	116
Table 41: Pixel correction between the adjacent geometry approach with one level of adjacency and the shadow mapping approach for the with viewpoint of the primitives scene.	116
Table 42: Pixel correction between the adjacent geometry approach with two levels of adjacency and the shadow mapping approach for the with viewpoint of the primitives scene.	116

Table 43: Average of triangle intersections when using the adjacent geometry approach for the with viewpoint of the primitives scene.	117
Table 44: Pixel correction by the neighbour texels (9 texels) and the adjacent geometry (2 levels) approaches separated by lighting change for the with viewpoint of the primitives scene.....	118
Table 45: Algorithm results of the with viewpoint of the primitives scene.....	119
Table 46: Difference between the approaches that use ray-tracing and the actual ray-tracer for the against viewpoint of the primitives scene.	127
Table 47: Wrongly defined pixels in the shadow mapping result which are inside the contour in the against viewpoint of the primitives scene.	127
Table 48: Pixels that the shadow map defines wrongly in the against viewpoint of the primitives scene, separated in pixels defined in light and in shadow, compared to the total amount of pixels lighted in the same way.....	128
Table 49: Pixel confirmation when using texel coherence with four texels for the against viewpoint of the primitives scene.	128
Table 50: Pixel shadowing for pixels that don't achieve texel coherence with four texels for the against viewpoint of the primitives scene.	129
Table 51: Pixel confirmation when using texel coherence with nine texels for the against viewpoint of the primitives scene.	129
Table 52: Pixel shadowing for pixels that don't achieve texel coherence with nine texels for the against viewpoint of the primitives scene.	130
Table 53: Pixel correction between the single texel approach and the shadow mapping approach for the against viewpoint of the primitives scene.....	131
Table 54: Pixel correction between the neighbour texels approach using four neighbours and the shadow mapping approach for the against viewpoint of the primitives scene.....	131
Table 55: Pixel correction between the neighbour texels approach using nine neighbours and the shadow mapping approach for the against viewpoint of the primitives scene.....	131

Table 56: Average of triangle intersections when using the neighbour texels approach for the against viewpoint of the primitives scene.....	132
Table 57: Pixel correction between the adjacent geometry approach with one level of adjacency and the shadow mapping approach for the against viewpoint of the primitives scene.....	132
Table 58: Pixel correction between the adjacent geometry approach with two levels of adjacency and the shadow mapping approach for the against viewpoint of the primitives scene.....	132
Table 59: Average of triangle intersections when using the adjacent geometry approach for the against viewpoint of the primitives scene.	133
Table 60: Pixel correction by the neighbour texels (9 texels) and the adjacent geometry (2 levels) approaches separated by lighting change for the against viewpoint of the primitives scene.....	134
Table 61: Algorithm results of the against viewpoint of the primitives scene.	135
Table 62: Difference between the approaches that use ray-tracing and the actual ray-tracer for the side viewpoint of the bench scene.....	143
Table 63: Wrongly defined pixels in the shadow mapping result which are inside the contour in the side viewpoint of the bench scene.	143
Table 64: Pixels that the shadow map defines wrongly in the side viewpoint of the bench scene, separated in pixels defined in light and in shadow, compared to the total amount of pixels lighted in the same way.	144
Table 65: Pixel confirmation when using texel coherence with four texels for the side viewpoint of the bench scene.....	144
Table 66: Pixel shadowing for pixels that don't achieve texel coherence with four texels for the side viewpoint of the bench scene.....	145
Table 67: Pixel confirmation when using texel coherence with nine texels for the side viewpoint of the bench scene.....	145

Table 68: Pixel shadowing for pixels that don't achieve texel coherence with nine texels for the side viewpoint of the bench scene.....	146
Table 69: Pixel correction between the single texel approach and the shadow mapping approach for the side viewpoint of the bench scene.	147
Table 70: Pixel correction between the neighbour texels approach using four neighbours and the shadow mapping approach for the side viewpoint of the bench scene.	147
Table 71: Pixel correction between the neighbour texels approach using nine neighbours and the shadow mapping approach for the side viewpoint of the bench scene.	147
Table 72: Average of triangle intersections when using the neighbour texels approach for the side viewpoint of the bench scene.	148
Table 73: Pixel correction between the adjacent geometry approach with one level of adjacency and the shadow mapping approach for the side viewpoint of the bench scene. ...	148
Table 74: Pixel correction between the adjacent geometry approach with two levels of adjacency and the shadow mapping approach for the side viewpoint of the bench scene. ...	148
Table 75: Average of triangle intersections when using the adjacent geometry approach for the side viewpoint of the bench scene.....	149
Table 76: Pixel correction by the neighbour texels (9 texels) and the adjacent geometry (2 levels) approaches separated by lighting change for the side viewpoint of the bench scene.	150
Table 77: Algorithm results of the side viewpoint of the bench scene.....	151
Table 78: Difference between the approaches that use ray-tracing and the actual ray-tracer for the with viewpoint of the bench scene.	159
Table 79: Wrongly defined pixels in the shadow mapping result which are inside the contour in the with viewpoint of the bench scene.....	159
Table 80: Pixels that the shadow map defines wrongly in the with viewpoint of the bench scene, separated in pixels defined in light and in shadow, compared to the total amount of pixels lighted in the same way.	160

Table 81: Pixel confirmation when using texel coherence with four texels for the with viewpoint of the bench scene.....	160
Table 82: Pixel shadowing for pixels that don't achieve texel coherence with four texels for the with viewpoint of the bench scene.....	161
Table 83: Pixel confirmation when using texel coherence with nine texels for the with viewpoint of the bench scene.....	161
Table 84: Pixel shadowing for pixels that don't achieve texel coherence with nine texels for the with viewpoint of the bench scene.....	162
Table 85: Pixel correction between the single texel approach and the shadow mapping approach for the with viewpoint of the bench scene.....	163
Table 86: Pixel correction between the neighbour texels approach using four neighbours and the shadow mapping approach for the with viewpoint of the bench scene.	163
Table 87: Pixel correction between the neighbour texels approach using nine neighbours and the shadow mapping approach for the with viewpoint of the bench scene.	163
Table 88: Average of triangle intersections when using the neighbour texels approach for the with viewpoint of the bench scene.....	164
Table 89: Pixel correction between the adjacent geometry approach with one level of adjacency and the shadow mapping approach for the with viewpoint of the bench scene....	164
Table 90: Pixel correction between the adjacent geometry approach with two levels of adjacency and the shadow mapping approach for the with viewpoint of the bench scene....	164
Table 91: Average of triangle intersections when using the adjacent geometry approach for the with viewpoint of the bench scene.....	165
Table 92: Pixel correction by the neighbour texels (9 texels) and the adjacent geometry (2 levels) approaches separated by lighting change for the with viewpoint of the bench scene.	166
Table 93: Algorithm results of the with viewpoint of the bench scene.	167

Table 94: Difference between the approaches that use ray-tracing and the actual ray-tracer for the against viewpoint of the bench scene.....	175
Table 95: Wrongly defined pixels in the shadow mapping result which are inside the contour in the against viewpoint of the bench scene.....	175
Table 96: Pixels that the shadow map defines wrongly in the against viewpoint of the bench scene, separated in pixels defined in light and in shadow, compared to the total amount of pixels lighted in the same way.....	176
Table 97: Pixel confirmation when using texel coherence with four texels for the against viewpoint of the bench scene.....	176
Table 98: Pixel shadowing for pixels that don't achieve texel coherence with four texels for the against viewpoint of the bench scene.....	177
Table 99: Pixel confirmation when using texel coherence with nine texels for the against viewpoint of the bench scene.....	177
Table 100: Pixel shadowing for pixels that don't achieve texel coherence with nine texels for the against viewpoint of the bench scene.....	178
Table 101: Pixel correction between the single texel approach and the shadow mapping approach for the against viewpoint of the bench scene.	179
Table 102: Pixel correction between the neighbour texels approach and the shadow mapping approach for the against viewpoint of the bench scene.	180
Table 103: Average of triangle intersections when using the neighbour texels approach for the against viewpoint of the bench scene.....	181
Table 104: Pixel correction between the adjacent geometry approach and the shadow mapping approach for the against viewpoint of the bench scene.	182
Table 105: Average of triangle intersections when using the adjacent geometry approach for the against viewpoint of the bench scene.....	183
Table 106: Pixel correction by the neighbour texels (9 texels) and the adjacent geometry (2 levels) approaches separated by lighting change for the against viewpoint of the bench scene.....	184

Table 107: Algorithm results of the against viewpoint of the bench scene.	185
Table 108: Difference between the approaches that use ray-tracing and the actual ray-tracer for the with viewpoint of the trees scene.	193
Table 109: Wrongly defined pixels in the shadow mapping result which are inside the contour in the with viewpoint of the trees scene.....	193
Table 110: Pixels that the shadow map defines wrongly in the with viewpoint of the trees scene, separated in pixels defined in light and in shadow, compared to the total amount of pixels lighted in the same way.	194
Table 111: Pixel confirmation when using texel coherence with four texels for the with viewpoint of the trees scene.....	194
Table 112: Pixel shadowing for pixels that don't achieve texel coherence with four texels for the with viewpoint of the trees scene.....	195
Table 113: Pixel confirmation when using texel coherence with nine texels for the with viewpoint of the trees scene.....	195
Table 114: Pixel shadowing for pixels that don't achieve texel coherence with nine texels for the with viewpoint of the trees scene.....	196
Table 115: Pixel correction between the single texel approach and the shadow mapping approach for the with viewpoint of the trees scene.....	197
Table 116: Pixel correction between the neighbour texels approach and the shadow mapping approach for the with viewpoint of the trees scene.....	197
Table 117: Average of triangle intersections when using the neighbour texels approach for the with viewpoint of the trees scene.....	198
Table 118: Pixel correction between the adjacent geometry approach and the shadow mapping approach for the with viewpoint of the trees scene.....	199
Table 119: Average of triangle intersections when using the adjacent geometry approach for the with viewpoint of the trees scene.....	200

Table 120: Pixel correction by the neighbour texels (9 texels) and the adjacent geometry (2 levels) approaches separated by lighting change for the with viewpoint of the trees scene..	201
Table 121: Algorithm results of the with viewpoint of the trees scene.	202
Table 122: Difference between the approaches that use ray-tracing and the actual ray-tracer for the side viewpoint of the trees scene.	210
Table 123: Wrongly defined pixels in the shadow mapping result which are inside the contour in the side viewpoint of the trees scene.	210
Table 124: Pixels that the shadow map defines wrongly in the side viewpoint of the trees scene, separated in pixels defined in light and in shadow, compared to the total amount of pixels lighted in the same way.	211
Table 125: Pixel confirmation when using texel coherence with four texels for the side viewpoint of the trees scene.	211
Table 126: Pixel shadowing for pixels that don't achieve texel coherence with four texels for the side viewpoint of the trees scene.....	212
Table 127: Pixel confirmation when using texel coherence with nine texels for the side viewpoint of the trees scene.....	212
Table 128: Pixel shadowing for pixels that don't achieve texel coherence with nine texels for the side viewpoint of the trees scene.....	213
Table 129: Pixel correction between the single texel approach and the shadow mapping approach for the side viewpoint of the trees scene.	214
Table 130: Pixel correction between the neighbour texels approach using four neighbours and the shadow mapping approach for the side viewpoint of the trees scene.	214
Table 131: Pixel correction between the neighbour texels approach using nine neighbours and the shadow mapping approach for the side viewpoint of the trees scene.	214
Table 132: Average of triangle intersections when using the neighbour texels approach for the side viewpoint of the trees scene.....	215

Table 133: Pixel correction between the adjacent geometry approach with one level of adjacency and the shadow mapping approach for the side viewpoint of the trees scene.	215
Table 134: Pixel correction between the adjacent geometry approach with two level of adjacency and the shadow mapping approach for the side viewpoint of the trees scene.	215
Table 135: Average of triangle intersections when using the adjacent geometry approach for the side viewpoint of the trees scene.....	216
Table 136: Pixel correction by the neighbour texels (9 texels) and the adjacent geometry (2 levels) approaches separated by lighting change for the side viewpoint of the trees scene. .	217
Table 137: Algorithm results of the side viewpoint of the trees scene.....	218
Table 138: Difference between the approaches that use ray-tracing and the actual ray-tracer for the against viewpoint of the trees scene.	226
Table 139: Wrongly defined pixels in the shadow mapping result which are inside the contour in the against viewpoint of the trees scene.....	226
Table 140: Pixels that the shadow map defines wrongly in the against viewpoint of the trees scene, separated in pixels defined in light and in shadow, compared to the total amount of pixels lighted in the same way.	227
Table 141: Pixel confirmation when using texel coherence with four texels for the against viewpoint of the trees scene.....	227
Table 142: Pixel shadowing for pixels that don't achieve texel coherence with four texels for the against viewpoint of the trees scene.....	228
Table 143: Pixel confirmation when using texel coherence with nine texels for the against viewpoint of the trees scene.....	228
Table 144: Pixel shadowing for pixels that don't achieve texel coherence with nine texels for the against viewpoint of the trees scene.....	229
Table 145: Pixel correction between the single texel approach and the shadow mapping approach for the against viewpoint of the trees scene.	230

Table 146: Pixel correction between the neighbour texels approach using four neighbours and the shadow mapping approach for the against viewpoint of the trees scene.	230
Table 147: Pixel correction between the neighbour texels approach using nine neighbours and the shadow mapping approach for the against viewpoint of the trees scene.	230
Table 148: Average of triangle intersections when using the neighbour texels approach for the against viewpoint of the trees scene.....	231
Table 149: Pixel correction between the adjacent geometry approach with one level of adjacency and the shadow mapping approach for the against viewpoint of the trees scene.	231
Table 150: Pixel correction between the adjacent geometry approach with two level of adjacency and the shadow mapping approach for the against viewpoint of the trees scene.	231
Table 151: Average of triangle intersections when using the adjacent geometry approach for the against viewpoint of the trees scene.....	232
Table 152: Pixel correction by the neighbour texels (9 texels) and the adjacent geometry (2 levels) approaches separated by lighting change for the against viewpoint of the trees scene.	233
Table 153: Algorithm results of the against viewpoint of the trees scene.	234
Table 154: Difference between the approaches that use ray-tracing and the actual ray-tracer for the side viewpoint of the flowers scene.	242
Table 155: Wrongly defined pixels in the shadow mapping result which are inside the contour in the side viewpoint of the flowers scene.	242
Table 156: Pixels that the shadow map defines wrongly in the side viewpoint of the flowers scene, separated in pixels defined in light and in shadow, compared to the total amount of pixels lighted in the same way.	243
Table 157: Pixel confirmation when using texel coherence with four texels for the side viewpoint of the flowers scene.	243
Table 158: Pixel shadowing for pixels that don't achieve texel coherence with four texels for the side viewpoint of the flowers scene.	244

Table 159: Pixel confirmation when using texel coherence with nine texels for the side viewpoint of the flowers scene.	244
Table 160: Pixel shadowing for pixels that don't achieve texel coherence with nine texels for the side viewpoint of the flowers scene.	245
Table 161: Pixel correction between the single texel approach and the shadow mapping approach for the side viewpoint of the flowers scene.	246
Table 162: Pixel correction between the neighbour texels approach and the shadow mapping approach for the side viewpoint of the flowers scene.	247
Table 163: Average of triangle intersections when using the neighbour texels approach for the side viewpoint of the flowers scene.	248
Table 164: Pixel correction between the adjacent geometry approach and the shadow mapping approach for the side viewpoint of the flowers scene.	249
Table 165: Average of triangle intersections when using the adjacent geometry approach for the side viewpoint of the flowers scene.	250
Table 166: Pixel correction by the neighbour texels (9 texels) and the adjacent geometry (2 levels) approaches separated by lighting change for the side viewpoint of the flowers scene.	251
Table 167: Algorithm results of the side viewpoint of the flowers scene.	252
Table 168: Difference between the approaches that use ray-tracing and the actual ray-tracer for the against viewpoint of the flowers scene.	260
Table 169: Wrongly defined pixels in the shadow mapping result which are inside the contour in the against viewpoint of the flowers scene.	260
Table 170: Pixels that the shadow map defines wrongly in the against viewpoint of the flowers scene, separated in pixels defined in light and in shadow, compared to the total amount of pixels lighted in the same way.	261
Table 171: Pixel confirmation when using texel coherence with four texels for the against viewpoint of the flowers scene.	261

Table 172: Pixel shadowing for pixels that don't achieve texel coherence with four texels for the against viewpoint of the flowers scene.	262
Table 173: Pixel confirmation when using texel coherence with nine texels for the against viewpoint of the flowers scene.	262
Table 174: Pixel shadowing for pixels that don't achieve texel coherence with nine texels for the against viewpoint of the flowers scene.	263
Table 175: Pixel correction between the single texel approach and the shadow mapping approach for the against viewpoint of the flowers scene.	264
Table 176: Pixel correction between the neighbour texels approach using four neighbours and the shadow mapping approach for the against viewpoint of the flowers scene.	264
Table 177: Pixel correction between the neighbour texels approach using nine neighbours and the shadow mapping approach for the against viewpoint of the flowers scene.	264
Table 178: Average of triangle intersections when using the neighbour texels approach for the against viewpoint of the flowers scene.	265
Table 179: Pixel correction between the adjacent geometry approach with one level of adjacency and the shadow mapping approach for the against viewpoint of the flowers scene.	265
Table 180: Pixel correction between the adjacent geometry approach with two level of adjacency and the shadow mapping approach for the against viewpoint of the flowers scene.	265
Table 181: Average of triangle intersections when using the adjacent geometry approach for the against viewpoint of the flowers scene.	266
Table 182: Pixel correction by the neighbour texels (9 texels) and the adjacent geometry (2 levels) approaches separated by lighting change for the against viewpoint of the flowers scene.	267
Table 183: Algorithm results of the against viewpoint of the flowers scene.	268
Table 184: Difference between the approaches that use ray-tracing and the actual ray-tracer for the with viewpoint of the flowers scene.	276

Table 185: Wrongly defined pixels in the shadow mapping result which are inside the contour in the with viewpoint of the flowers scene.	276
Table 186: Pixels that the shadow map defines wrongly in the with viewpoint of the flowers scene, separated in pixels defined in light and in shadow, compared to the total amount of pixels lighted in the same way.	277
Table 187: Pixel confirmation when using texel coherence with four texels for the with viewpoint of the flowers scene.	277
Table 188: Pixel shadowing for pixels that don't achieve texel coherence with four texels for the with viewpoint of the flowers scene.	278
Table 189: Pixel confirmation when using texel coherence with nine texels for the with viewpoint of the flowers scene.	278
Table 190: Pixel shadowing for pixels that don't achieve texel coherence with nine texels for the with viewpoint of the flowers scene.	279
Table 191: Pixel correction between the single texel approach and the shadow mapping approach for the with viewpoint of the flowers scene.	280
Table 192: Pixel correction between the neighbour texels approach using four neighbours and the shadow mapping approach for the with viewpoint of the flowers scene.	280
Table 193: Pixel correction between the neighbour texels approach using nine neighbours and the shadow mapping approach for the with viewpoint of the flowers scene.	280
Table 194: Average of triangle intersections when using the neighbour texels approach for the with viewpoint of the flowers scene.	281
Table 195: Pixel correction between the adjacent geometry approach with one level of adjacency and the shadow mapping approach for the with viewpoint of the flowers scene.	281
Table 196: Pixel correction between the adjacent geometry approach with two level of adjacency and the shadow mapping approach for the with viewpoint of the flowers scene.	281
Table 197: Average of triangle intersections when using the adjacent geometry approach for the with viewpoint of the flowers scene.	282

Table 198: Pixel correction by the neighbour texels (9 texels) and the adjacent geometry (2 levels) approaches separated by lighting change for the with viewpoint of the flowers scene.
.....283

Table 199: Algorithm results of the with viewpoint of the flowers scene.....284

1. INTRODUCTION

Since the appearance of computer rendered graphics, there have been two main approaches in order to render scenes: the first one is to obtain satisfactory images in a fraction of a second and the other is to obtain the best quality images, with no regard to the time spent in creating them. Both of these approaches have their uses, with the first one being important to real time rendering used in virtual interactive walkthroughs, and the second being used to create photo-realistic scenes, be it for simple images or for use in a frame of an animated movie.

One of the most important things in rendering a scene is lighting and consequently, shadows. While it is possible to render shadowed scenes in real time, there is clearly a loss in quality when comparing to more computationally intensive algorithms. Shadow algorithms are available for hard and soft shadows, where being able to establish the former is required for the latter. Hence hard shadows are a very relevant topic.

Real-time rendering shadow algorithms are dominated by two classes: shadow maps and shadow volumes. Shadow volumes are able to compute pixel perfect shadows yet are harder to implement and can suffer from severe overdraw. Shadow maps, on the other hand, are very simple to implement, and are performance friendly.

Recent research has focused on improving the quality of the shadow map basic algorithm result, for instance combining it with other algorithms. Shadow maps have evolved a lot, fixing and improving the basic algorithm, hence providing better and better results.

Another solution that is now possible in real time (at least for direct hard shadows) is ray-tracing. However shadow mapping is much faster than ray-tracing, and while ray-tracing is now a possibility for real-time rendering, one has to consider that the quality standards have gone sky high and hard shadows are not jaw dropping anymore. Shadows are only one of many effects that are used nowadays to improve render quality hence shadows must be computed as fast as possible.

1.1.MOTIVATION

As mentioned before, ray-tracing and shadow maps are two possibilities for computing hard shadows in real-time. Ray-tracing assures that the result is correct for each pixel, where shadow maps guarantee performance. The ideal would be to have the performance of shadow maps with the quality of ray-tracing, or at least some compromise that would improve quality without totally sacrificing performance.

Research has been conducted to achieve the best of both worlds: great quality images that take a small amount of time to render. However, so far no research has been performed to evaluate how good the information stored in a shadow map really is.

1.2.GOALS

Studying the value of the information stored in a shadow map is the main goal of this work.

For instance, quantifying the location of the errors in a shadow map, or how many texels in a shadow map are actually correct, i.e. report the closest triangle to the light in a given direction. And how far can an algorithm improve the basic shadow map just using the information stored in it? For instance, can the shadow map information be used to perform selective ray-tracing for certain pixels, and if so how many pixels are fixed and how many pixels are broken? Although some algorithms use this information to perform selective ray-tracing the published work only focuses on particular cases.

When using shadow mapping to evaluate the shadow areas of a scene, the most problematic areas are the contour regions where the real shadow occurs due to the lack of precision, and aliasing of the shadow mapping technique. Hence, when studying the quality of a solution based on shadow mapping it makes sense to concentrate efforts in the contours of the shadow map. But how thick must a contour be to contain a significant number of wrong pixels? And for those pixels in the contours which approaches can be used, based only on the shadow map information, to validate or fix their shadow status?

Ray-tracing can be a helpful tool, helping in fixing a number of pixels, but is the shadow map information sufficient so that the number of rays is cut down to a very low number? And can

pixels be fixed with just a very small number of ray-triangle intersections, where the triangles are selected based on the information stored in the shadow map?

By limiting the number of ray-triangle intersections new errors will be introduced. Hence quantifying the ratio of fixed/broken pixels, when performing this second pass, is essential to evaluate each approach or approach combinations.

The goal of this work is to provide an answer to these questions, with a quantitative analysis.

1.3.METHODOLOGY

The Curitiba 3D engine is capable of using shadow maps and provides a lot of debug information. It is an extensible engine and adding the required features to quantify information, and test new algorithms is really easy. However no ray-tracing is available in Curitiba, hence the first step was to implement a very basic ray-tracer. This new implementation will contain the required functionalities to provide the answers required for this work. However no performance issues were taken into account due to the timeframe required for the completion of the work.

Once the implementation was completed focus could be directed on studying the shadow map generation process. This provided some clues to the type of problems one can expect when applying shadow maps. The next step was to determine where the majority of errors were located.

Then a study on the pixel shadow status versus its correctness was conducted and hypotheses on how to fix the pixels shadow status were constructed.

Each hypothesis was tested and its results quantified. This in turn gave rise to new hypothesis and the process was iterated and finally hypotheses were combined to evaluate if better results were obtained. Selective ray-tracing with a very limited number of ray-triangle intersections, where the triangles were selected based on the shadow map information, was used to attempt to fix pixels.

During all this process the ray-tracer for the whole image was used as ground truth, and each hypothesis, or combination, was tested both against the ground truth and the shadow map basic solution.

1.4.THESIS STRUCTURE

In chapter 2 the state of the art for the shadow mapping and ray-tracing algorithms will be shown. In chapter 3 the main research of this work, as described in the motivation and goals section is presented. Chapter 4 will report on the tests made and present the results obtained. Finally, chapter 5 will present the conclusion of this work and point to some possible future work.

2. STATE OF THE ART

This chapter will present the state of the art of the shadow mapping and ray tracing algorithms. To be precise, this chapter will show how each one of these algorithms work, the problems that these algorithms have and various approaches proposed to solve these shortcomings. Finally, some approaches that combine both algorithms will be presented, also summarizing how they work and some of their problems.

2.1.SHADOW MAPPING

2.1.1. Shadow Mapping Basics

Shadow Mapping (Williams, 1978) is an algorithm that defines shadows in the scene by determining which areas are behind the closest objects to the light source. This is done in a two-step approach:

1. First, the algorithm renders the scene from the point of view of the light source, saving the shortest distances between the light source and the scene's triangles in the rendered grid. The information of each grid point will be called a shadow texel and the entire grid of shadow texels will be called the shadow map.
2. After obtaining the shadow map, the scene will be rendered from the point of view of the camera. Each 3D point that the camera sees will be tested, in order to verify if it is in the shadow of the light source. In order to do this, each point will be transformed from the coordinates of the camera view to the coordinates of the view of the light source view. With the new coordinates, the algorithm will be able to check which texel in the shadow map intersects the ray that goes from the source of light to the point that is being tested. Finally, the distance to the light source of the point being tested is compared to the distance stored in the texel of the shadow map. If the distance of the point being tested is greater than the stored distance, then it will be shadowed, otherwise, it will not.

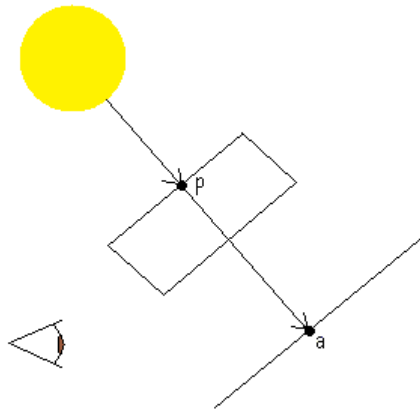


Figure 1: How a Shadow Map works.

In Figure 1, point p is part of the shadow map obtained by the yellow light source, being the nearest surface point to the light source following the shown direction. Following said direction, point a is behind point p of the shadow map, so will be shadowed.

2.1.2. Shadow Mapping Problems

As (Williams, 1978) shows, shadow mapping is a simple, two step way to compute which areas of the scene are shadowed. But it suffers from many problems, many of them related to aliasing. This aliasing is caused by under-sampling, due to insufficient resolution of the shadow map in certain locations. When observing the scenes with aliasing problems, shadows with the wrong contours or highly pixelated can be observed. These problems will be better detailed below.



Figure 2: The shadow of the tree presents aliasing.

Perspective aliasing is a common problem in shadow mapping, since scenes are usually rendered using a perspective view. With a perspective view, objects near the camera are larger than faraway objects. However, unless a headlight is used, the shadow map projection

is not the same as the camera's. This creates a resolution mismatch. The problem appears when there are a lot of points near the camera, but these same points are distant from the light source. Due to the perspective view, a large amount of these points will be behind a single shadow texel, which will provoke aliasing in the shadow. On the other hand, there may be places far away in the camera view where the texel resolution is excessive, resulting in wasted shadow texels. Both these cases are called, respectively, under-sampling and over-sampling.

With a directional light, this mismatch will have its maximum value if the direction of this light is perpendicular to the camera view and will have its minimum value when the light direction is the same as the camera view. For point lights, the mismatch will be greater when the direction of the light and the camera views face each other, a.k.a. the duelling frusta, and minimum when both have the same direction.

Projection aliasing occurs when a surface is parallel (or almost parallel) to the direction of the light. In this case, a single shadow texel will be used to test the occlusion of the light source for a large amount of points, which will cause incorrect shadows. Another problem that comes with projection aliasing is shadow flickering when moving around the scene. This occurs because the perspective aliasing effect is dependent on the position and direction of the camera.

The resolution of the shadow map may also be a problem if it is used for large scenes. The shadow map is usually saved as a texture, but today's hardware limits the size of textures, which limits the size of the shadow map. For example, for a scene with one square kilometre and a perpendicular light direction, a 1024x1024 shadow map has shadow texels that take around one square meter each. While this may give satisfactory results for a bird's eye view over the entire scene, a close-up of this scene will show a large amount of aliasing.

Due to the limited precision of data in computers, calculated distances are in general not exact, but actually an approximation to the real value. Furthermore, the grid that stores the shadow map and the final viewed image are also discrete. These discrete properties and these approximations may cause distances to be calculated in an erroneous way. In the case where the calculated distance of a point to the light source during the second step of the algorithm

does not match the distance of this same point when saved on the shadow map, but is actually bigger, the self-shadowing phenomenon will occur, in which the point shades itself.

2.1.3. Shadow Mapping Approaches

As detailed in the previous section, there are many problems with shadow mapping, mostly aliasing problems. This section will show some approaches to shadow mapping that try to correct these problems.

Percentage Closer Filtering (Reeves, Salesin, & Cook, 1987) is one of the first approaches used to solve the hard shadow problem. This technique will use a filter process in order to calculate which pixels are near the light area and give a percentage to this proximity. This way, a shadow pixel near the light area will have a penumbra colour, instead of having the shadow colour.

Perspective Shadow Maps (Stamminger & Drettakis, 2002) try to correct aliasing by giving more resolution to objects nearby the camera and less resolution to far away objects. This is done by applying a perspective before generating the shadow map. With this perspective, objects near the camera are enlarged and far away objects are shrunk, resulting, respectively, in better and worse shadow map resolutions for near and far objects.

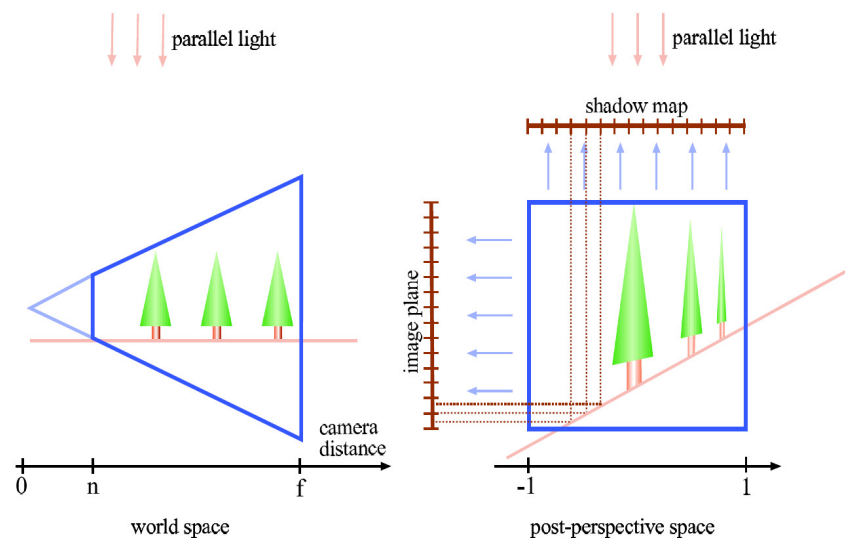


Figure 3: Perspective Shadow Map example.

A Light Space Perspective Shadow Map (Wimmer, Scherzer, & Purgathofer, 2004) uses a perspective transform in light space that does not change the directions of the light sources

and allows treating all lights as directional lights. This allows perspective shadow mapping problems, like missed shadow casters and singularities in post-perspective space, to be avoided.

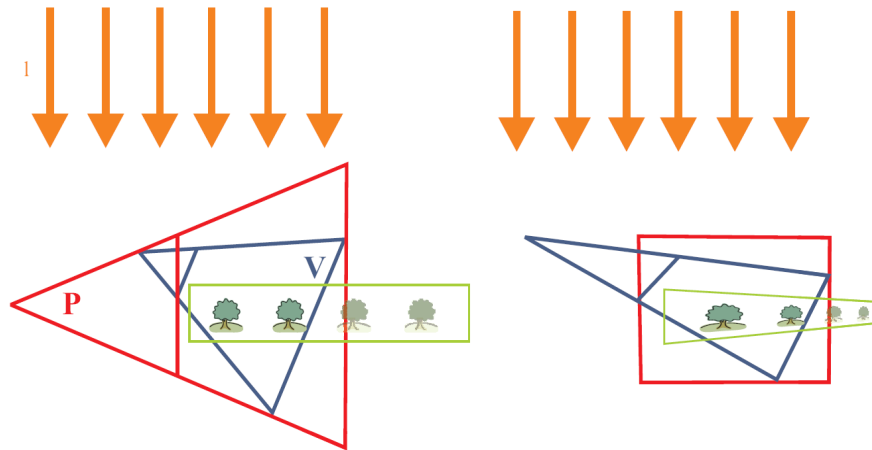


Figure 4: Light Space Perspective Shadow Map example.

Practical Shadow Mapping (Barbec, Annen, & Seidel, 2002) adjusts the view frustum of the light with the visualised objects in mind. Since the view frustum is smaller, the same shadow map resolution can be used for a smaller area, diminishing aliasing. In this case the depth values are distributed uniformly since, as opposed to the camera, objects near the light source might have the same or more importance than those near it, or all important objects could be far from the light source.

The Adaptive Light Frustum technique adapts the view frustum of the light source so that it only includes the objects that are visible from the camera view, allowing for better shadow map resolutions, or more precisely, allows the use of a bigger number of the shadow map's texels for the visible objects. A problem arises from this technique when the camera is moved around. If another object enters or leaves the camera view, the frustum will be readjusted to include the new object, changing the number of texels for the first object and consequently changing the resolution of the shadow of the first object. With camera motion the shadows will flicker.

Trapezoidal Shadow Mapping (Martin & Tanin, 2004) increases the resolution of shadow maps by using trapezoidal approximating to the eye's frusta, as seen from the light source, instead of using the bounding box used in Practical Shadow Mapping. Consecutive

approximations generated by camera moving are treated with smooth changes to the size and shape of the trapezoid, so that shadow flickering is avoided.

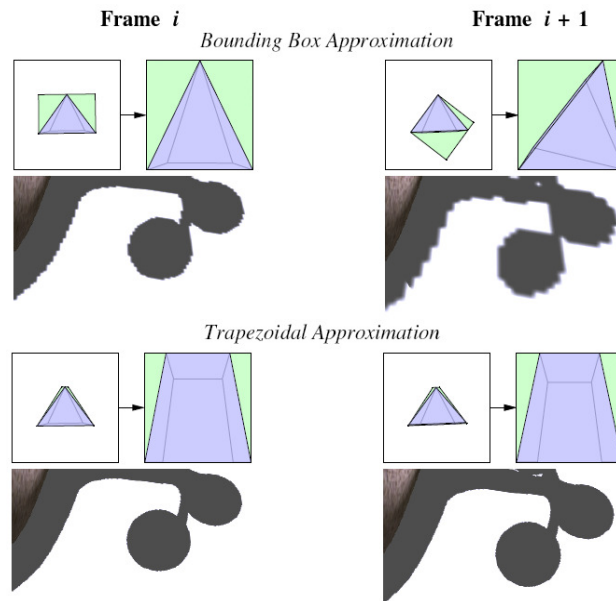


Figure 5: Trapezoidal Shadow Mapping movement flickering.

Adaptive Shadow Mapping (Fernando, Fernandez, Bala, & Greenberg, 2001) is an approach that uses a hierarchical grid structure. With this structure, areas that need a better resolution will have a new child node created, which will increase the resolution of that area. This greatly reduces aliasing artefacts, but the refinement operations require many rendering passes, making this approach not suitable for real time rendering.

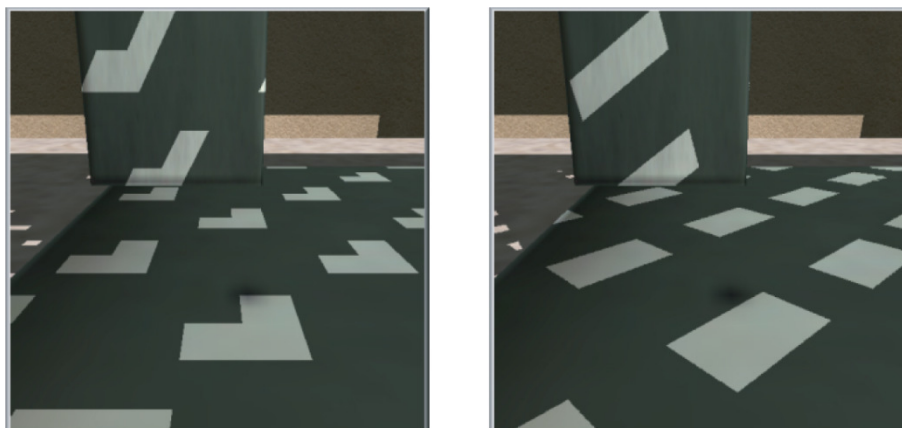


Figure 6: Adaptive Shadow map result compared to a shadow mapping result (2048x2048 shadow map versus an effective 524288x524288 shadow map result).

The Plural Sunlight Depth Buffers Shadow Mapping (Tadamura, Qin, Jiao, & Nakamae, 2001) approach, the shadow map is split in various shadow maps with multiple resolutions. This way places that need better resolutions will be covered by a shadow map with better resolution.

Parallel-Split Shadow Mapping (Zhang, Sun, Xu, & Lun, 2006) splits the view frustum and then creates a shadow map for each one of these splits. The difference between this one and Plural Sunlight Depth Buffers Shadow Mapping is the pre-determined rules for splitting and a uniform resolution distribution, which avoid the need for optimisation computations.

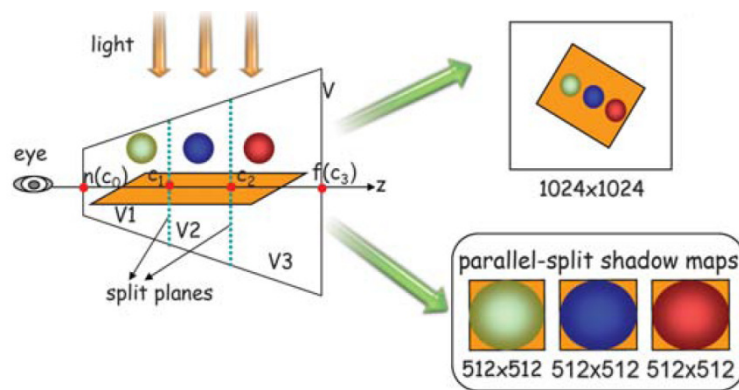


Figure 7: Parallel-Split Shadow Maps example.

Variance Shadow Mapping (Donnelly & Lauritzen, 2006) is a technique that calculates, besides the usual depth value, the depth-squared values. These values will then be used to calculate the probability of each point being lit or not. But due to the fact that the lower bound of brightness is an approximate value derived from using only one single occluder, if a scene has a high depth complexity, there might be light leaking artefacts (areas appearing lit instead of shadowed).



Figure 8: Variance Shadow Map light leaking example.

Convolution Shadow Mapping (Annen, Mertens, Bekaert, Seidel, & Kautz, 2007) avoids aliasing by filtering the shadow map with arbitrary convolution filters. Blurring can be applied afterwards in order to soften the shadow borders, allowing elimination of discretization artefacts and penumbra simulation. Of course, inclusion of many filters can slow down shadow computation, turning this approach into a less desirable one when doing real time rendering.

Exponential Shadow Mapping (Annen, Mertens, Seidel, Flerackers, & Kautz, 2008) is an algorithm inspired on convolution shadow maps, but uses a single term approximation, while convolution shadow maps usually uses sixteen terms. This makes exponential shadow mapping a much faster algorithm, while still avoiding light leaking as seen in variance shadow maps.

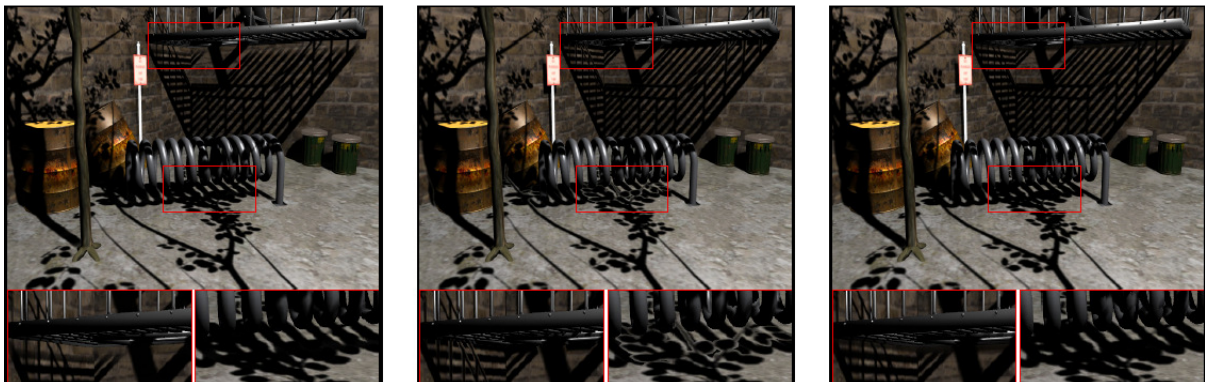


Figure 9: Comparison between Convolution, Variance and Exponential Shadow Maps respectively.

2.2.RAY-TRACING

2.2.1. Ray-Tracing Basics

Ray-tracing (Whitted, 1980) is an algorithm based on the physical properties of light. In the real world, a source of light emanates light rays in many directions. These rays then hit surrounding objects, possibly many times, until they reach the eye of the observer. The surrounding objects may also have different properties, which affect the direction light rays take after hitting these surfaces. For example, they may have a reflective surface, or be translucent, on which a light would bounce off or go through, respectively.

Ray-tracing tries to emulate these physical properties of light on a virtual world. The camera in the scene represents the eye of the viewer. In the real world, there are many light rays that do not reach the eye of the viewer. Obviously, trying to simulate all these rays in a computer would take an enormous amount of time, which would be a waste, since the rays that don't hit the camera don't contribute to what is being seen at the moment. To avoid this, things will be done in reverse order of what actually happens in the real world, that is, rays will be shot from the camera's position into the scene.

The basic ray-tracer works in the following manner:

1. The final view of the camera is basically an image, which corresponds to what the camera is seeing in the actual position and direction. An image is composed of various pixels, which will be used to define the rays that will be shot.
2. For each pixel, a ray will be traced, starting at the camera position and going through the pixel into the scene. These rays are called primary rays.
3. Then for each of these primary rays, a test will be made in order to check if it hits an object in the scene. If it doesn't, the pixel that originated the ray will have the background's colour. If it does, it will declare the place where it hit as the intersection point and the following step will ensue.
4. First, a ray must be traced from the intersection point into each light source in existence in the scene. This way, the contribution of each light source to the intersection point's colour will be known. After this, extra rays will be shot if the object has reflective or refractive surfaces. In these cases, the contribution from the reflection or refraction direction on the intersection

point must be calculated, by respectively tracing a reflective ray or a refractive ray in the direction of reflection or refraction of the ray that originated this calculation. Then for this ray, the process described for the primary rays will be repeated.

5. After calculating all the contributions listed above, the colour of each pixel can finally be calculated.

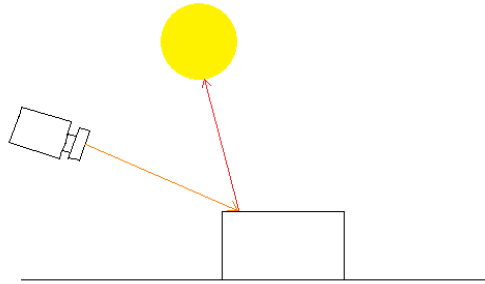


Figure 10: Simple example of Ray-Tracing.

After tracing primary rays, if an object is hit, a ray will be traced from the intersection point into the direction of the light source (see Figure 10), or in the case of various light sources, rays will be traced in the direction of each one of them. If a ray intersects any opaque geometry between the object and the light source then the object is in shadow, otherwise it is lit.

As shown in the algorithm above, ray-tracing can also deal with indirect lighting and transparent surfaces, however in this work only direct lighting and hard shadows will be dealt with.

For this purpose, the initial step of the ray-tracing algorithm, tracing primary rays from the camera into the scene, can be replaced with rasterization. Hence the first step can be performed using standard graphics APIs such as OpenGL. The results obtained using rasterization and ray-tracing for the primary rays are identical. The only requirement is that the coordinates of the 3D point in the scene must be available so that light rays can be cast from these points in the direction of the light source. Casting light rays for each scene point will allow the determination of the shadow status of each pixel.

To improve the performance of the ray-tracer it is fundamental to limit the number of intersection tests performed. Obviously, testing intersection of a ray with every object is an

enormous waste of time, because most objects would probably not be intersected, hence being redundant to the final result. One way to achieve a more rational selection of geometry to intersect is to use hierarchic bounding volumes or spatial partitioning. Under these approaches, various objects will be grouped together in a bounding volume. Checking for intersections is done first with the bounding volume itself, and only if an intersection with the volume exists will the geometry inside be tested. If the ray doesn't intersect the bounding volume, it obviously won't intersect any of the objects within it. A hierarchy of bounding volumes will potentially accelerate the process even further. The most common bounding volumes are the bounding spheres and bounding boxes, which are simple polygons and allow for quick intersection tests. Examples of spatial subdivision include octrees, binary space partitioning (BSP), kD-trees and grids.

2.3.COMBINING BOTH

As seen before shadow mapping is a very efficient algorithm performance wise, yet it is prone to all sorts of aliasing errors, producing shadows containing a large number of artefacts. On the other hand ray-tracing is capable of producing pixel perfect shadows at the expense of a more computational expensive algorithm.

Some researchers have attempted to combine both the performance of the shadow mapping algorithm and the accuracy of the ray-tracer solution.

The common approach behind these methods starts by first computing a shadow map. Ray-tracing is then used selectively for particular pixels that are classified as having an unreliable shadow status.

This greatly reduces the number of rays, and as a consequence the number of intersections to be performed. The results clearly show great improvements when comparing to the shadow map initial result, while still being far lighter than an exclusive ray-tracing solution.

2.3.1. Coherence-Based Ray-Tracing

The Coherence-Based Ray-Tracing (Agrawala, Ramamoorthi, Heirich, & Moll, 2000) algorithm combines a hierarchical ray-tracing technique and a coherence-based sampling technique in order to create soft shadows from area light sources. It starts by creating various reference images from various locations in the scene and saves object depths the same way

shadow maps do. The reference views for these reference images are usually the exterior vertices of the light areas, although no restriction is placed by the algorithm. To shade each point, a shadow ray is traced through each shadow map, until an intersection is met or until the ray passes all shadow maps. To test intersection of this shadow ray with a given reference shadow map the ray will be projected onto the image plane of the shadow map and the resulting epipolar ray will then be followed, from texel to texel, checking for intersections with the geometry of the scene. This intersection will be done in two steps. First, the depth at which the epipolar ray enters and exits a texel will be compared against the depth that the geometry in the texel is found. If the depth of the geometry is between the depths of the epipolar ray then the second step will follow, which is to find the exact depth of intersection.

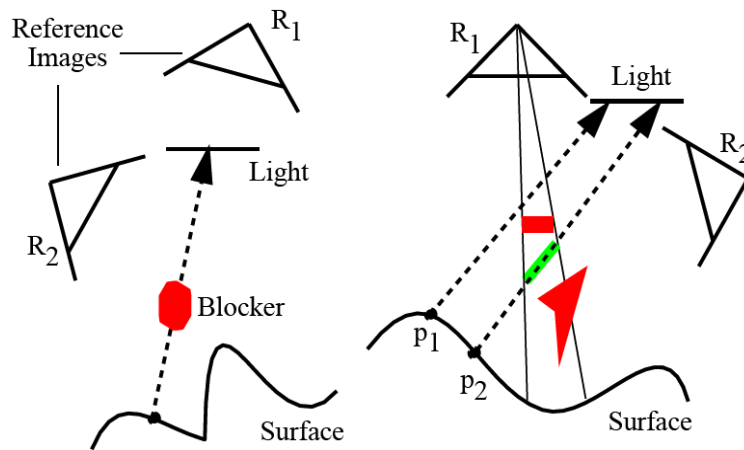


Figure 11: Reference image examples for the coherence based ray-tracing.

The coherence-based sampling algorithm decreases the shadow rays casted by checking where the light source visibility has a higher chance of changing. This may lead to prediction errors where a block or a hole is missed. These may be attenuated by increasing surface sampling density and light sampling respectively,

2.3.2. Hybrid GPU Rendering Pipeline for Alias-Free Hard Shadows

This Hybrid GPU Rendering Pipeline (Hertel, Hormann, & Westermann, 2009) will be used to create alias-free hard shadows. To do this, this algorithm starts by creating a conservative shadow map that works similarly to the usual shadow map, but in this case a triangle will be saved in a pixel if it overlaps said pixel in any place, not only in the centre. This is done by

resizing the edges of the triangles in the direction of the normal of the edge by the length of the diagonal of a texel.

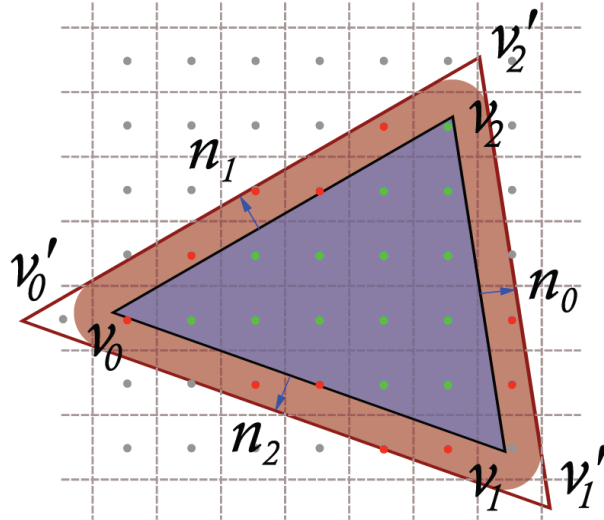


Figure 12: Resizing the triangle by moving its edges.

Normally, if a point is under a pixel, a simple test is made to see if it is lit or shadowed. But in this case, only if a pixel is entirely covered by a triangle will the points that project on it be considered in shadow or in light, depending on the distance of the triangle saved and the points being tested. If a point projects onto one of the pixels that has a triangle that doesn't cover said pixel in its totality, its shadowing will be determined "uncertain". This calculation can be done by testing the distances of the centre of the texel in relation to the triangles edges. To do this, the texel will store the ID of the triangle that covers it. Afterwards, for cases where the shadowing is deemed as uncertain, the GPU will use ray-tracing to verify if the point is actually shadowed or not. This ray-tracer will use the information of the triangle saved by the pixel and a kD-tree in order to speed up intersection tests. The information of the depth at which the triangle is found will allow for the ray-tracer to only start testing for intersections from there, as there should be no other triangle between this point and the light source.

As can be seen in Figure 13, there are many areas classified as uncertain that commonly produce correct results using shadow maps, namely the triangle junctions for triangles in light. The performance of this algorithm is highly dependent on the geometry tessellation hence for highly tessellated models a large number of light rays will be required.

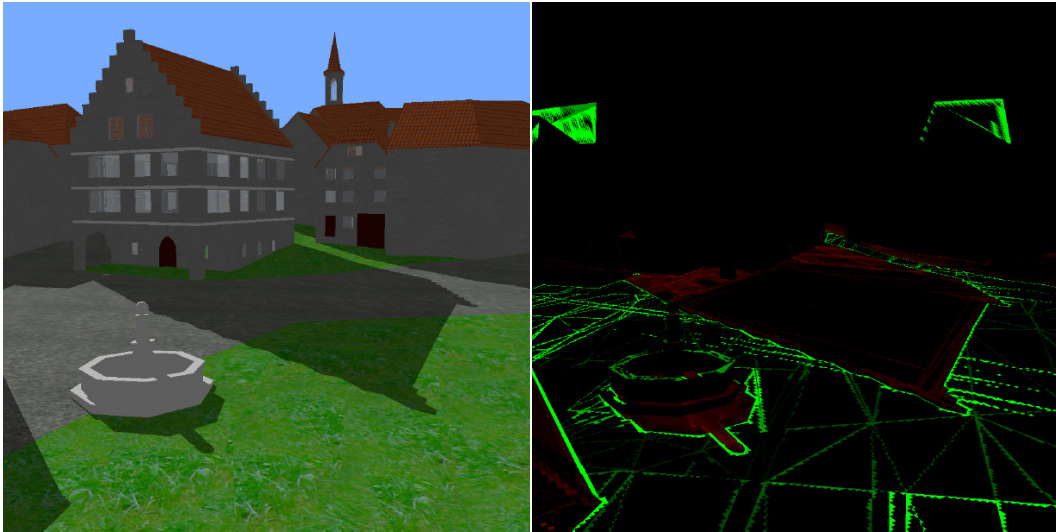


Figure 13: Example of the uncertain areas when using the Hybrid GPU Rendering Pipeline for Alias-Free Hard Shadows.

2.3.3. Hybrid GPU-CPU Renderer

This Hybrid GPU-CPU Renderer (Beister, Ernst, & Stamminger, 2005) also mixes shadow mapping and ray-tracing. This algorithm starts by creating a shadow map with bilinear percentage closest filtering. Then for each pixel the interpolated result is verified and if the result is 0 or 1 then the four surrounding shadow map pixels will agree and the pixel is considered in light or in shadow. If the four surrounding pixels don't agree and the interpolated result is between 0 and 1, then the pixel will be marked and ray-tracing will be used to calculate the shadowing of the point that the pixel observes.

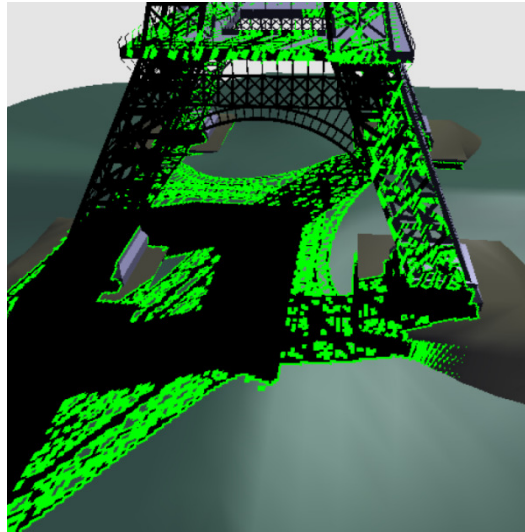


Figure 14: Green pixels mark where shadow mapping samples disagree in the Hybrid GPU-CPU Renderer.

If the light source is a point light a standard shadow map with bilinear percentage closer filtering is used. If the light source is an area light source, the area light source will be replaced by eight point light sources, one in the centre of the area and the other seven will surround this area. In this case, the agreement will be done between the results of the eight shadow maps.

This algorithm is robust if the shadow map resolution is adequate to the tessellation of the scene. Yet this is difficult to achieve overall unless the scene is carefully modelled using a constant tessellation parameter across all geometric objects. Errors may occur if, despite the fact that the four pixels are in agreement the shadow status reported by the algorithm is incorrect. For instance a pixel may project in a triangle that is not captured by the shadow map because it does not cover the centre of a texel, and the three surrounding texels may also be empty. In this situation all texels agree that the point is lit, yet the point should be in shadow.

2.4.CONCLUSION

Shadow mapping was initially presented at Siggraph 1978 by Williams. It is a very simple technique, easy to implement, hardware friendly, and performance wise very efficient. Yet, it suffers from severe aliasing, which causes severe artefacts in the computed shadows. There are many issues related to sampling issues that may cause very poor results in some circumstances.

The perspective mismatch and projection issues, together with limited hardware precision gave rise to a lot of research to improve this algorithm. Several methods are based on the computation of the light frustum to improve the texel usage of the shadow map. Others such as Cascade Shadow Maps propose the computation of a set of shadow maps to cope with the under-sampling issue. Algorithms such as Perspective Shadow Mapping and Light Image Space Shadow Mapping transform the projection itself to deal with the same issue.

These methods have produced great improvements on the shadow mapping result, producing shadows far more perfect than the original algorithm, without significantly overloading the algorithm performance wise.

The ray-tracing approach is far more capable quality wise, producing pixel perfect shadows. However it requires a much larger number of computations, hence it is computationally more expensive than shadow mapping.

Researchers have combined both methods, in an attempt to get the performance of the shadow map algorithm, and the accuracy of the ray-tracer solution. These approaches initially compute a shadow map and then perform selective ray-tracing for a comparatively small number of pixels.

Although the results are far superior to the standard algorithm, all solutions above are not error free.

3. ALGORITHM DESCRIPTION

As mentioned in chapter 2, shadow maps are highly prone to errors due to all sorts of aliasing. Perspective mismatch, sampling mismatch, projection aliasing and limited precision are the most prominent causes of errors. Ray-tracing on the other hand is pixel perfect, but far more demanding from a computational point of view.

Researchers have developed methods that combine these two approaches in an attempt to improve the shadow mapping quality using ray-tracing selectively to fix potential errors present in the shadow mapping technique.

This chapter will explore the information that is stored in a shadow map to evaluate how far can this information be helpful in fixing the shadow map errors by using ray-tracing in a very selective fashion, to reduce its impact in obtaining the final solution.

The shadow mapping used in here is based on the original algorithm, with adaptive light frustum adapted to the view frustum of the camera as an optimization of the shadow map usage, front face culling to prevent self shadowing and using normals to dismiss all scene points which are not facing the light.

In this work, besides recording the depths, the IDs of the triangles will also be stored in the shadow map texels. Hence for each point it is possible to check if the corresponding light ray really intersects the triangles whose ID is stored on the texel of the shadow map that the point being tested projects upon.

First the location of the errors found with shadow mapping will be discussed. Afterwards, once error location is established, several techniques will explore the shadow map information to discover which pixels are correctly shadowed.

3.1.SHADOW MAPPING ERRORS

3.1.1. Shadow Status and Errors

When performing simple shadow mapping, a pixel is classified as either lit or in shadow. Ray-tracing the corresponding scene points with light rays provides the ground truth. If for a given scene point the shadow mapping provides the same status (lit/shadowed) as the ray-

tracer, then the pixel has been correctly classified. Otherwise the pixel has a wrong status as reported by the shadow mapping algorithm.

Regarding the shadow mapping technique, the status of a scene is determined by the comparison of the distance of the point to the light source and the distance stored in the shadow map texel where the scene point projects. If the distance is larger than the recorded depth the point is classified as in shadow, otherwise it is classified as lit.

If a point is reported as in shadow by the shadow mapping technique, then the pixel projects into a texel that has a recorded depth smaller than the distance from the point to the light source. However the triangle that has its depth recorded in the texel may in fact not intersect a light ray from the scene point to the light source as shown in Figure 15.

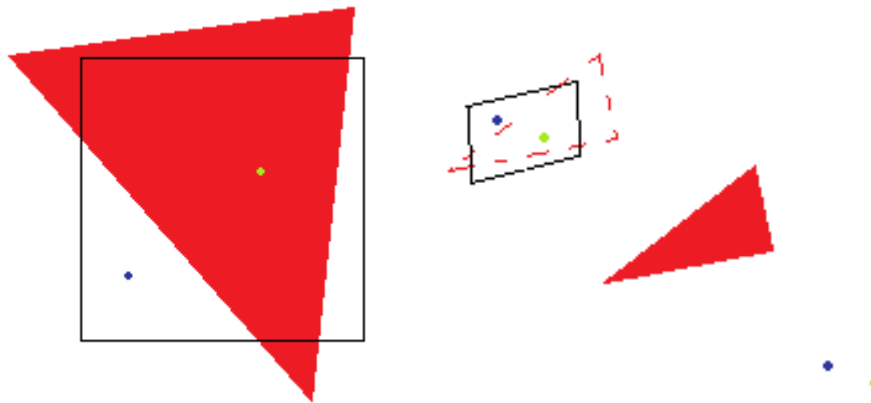


Figure 15: Correctly (in green) and incorrectly (in blue) shadowed points by shadow mapping.

Based on Figure 15, since both points are further away from the light source than the red triangle, both points will be shadowed since both points project upon the texel where the depth of the red triangle is stored. But the triangle doesn't actually shade the blue point, which should be lit, so in this case the point will be incorrectly shadowed when using shadow mapping.

For a lit scene point, as reported by shadow mapping, the depth recorded in the texel is greater than the distance from the point to the light source, be it by the triangle that had its depth recorded being farther away, or by the fact that there was no stored triangle at all. Errors can result if there is a triangle that actually intersects a light ray from the point but the triangle is not registered in the texel where the point projects.

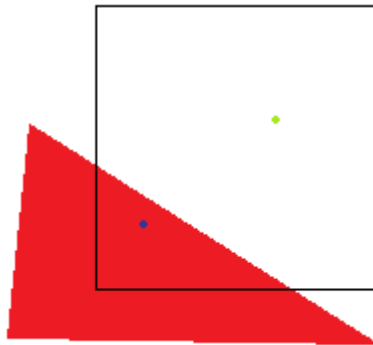


Figure 16: Correctly (in green) and incorrectly (in blue) lit points by shadow mapping.

In Figure 16, the depth stored in the texel is the maximum value possible since there is no triangle that projects upon its centre. Since the depth stored is higher than the depth of the two points, both will be lit when using shadow mapping. But the blue point has another triangle, the red one, which shades it. But as the depth of this triangle isn't stored in the texel, since the triangle doesn't cover the centre of the texel, it won't be able to shadow the point. The same would happen if the stored depth came from a triangle further away than the points being tested.

3.1.2. Error Location

A naked eye comparison between shadow mapping and ray-tracer solutions shows that shadow mapping errors are mostly present in the contours. This can be observed in Figure 17. Figure 17 marks the contours in green, the errors inside the contours in red if the pixel is incorrectly lit and in yellow if the pixel is incorrectly shadowed and in blue if the error is outside the contour. The larger the width of the contour line the more errors are contained in the contour. To create an unbiased contour, i.e. a contour that has roughly 50/50 shadow/light pixels a contour with an even width is used.

The resolution of the shadow map plays a crucial role in the percentage of errors caught in the contours. Higher resolutions have a better definition of the shadowed areas hence require narrower contours, whereas lower resolutions need thicker contour lines to catch a similar percentage of errors.

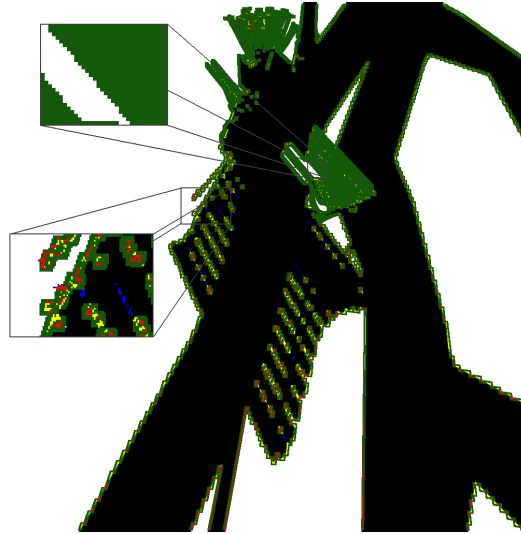


Figure 17: Marked contours and errors of the scene.

As the contours are computed for the rendered image, narrower contours will decrease the amount of tests that will be done as fewer pixels are contained inside the contour.

The tests realized for this work corroborate the above hypothesis, with averages of 90% of incorrect points inside the contours when using a shadow map resolution that is the double of the camera viewport. The remaining errors are caused by lack of shadow map resolution where small holes in the geometry, or small geometry, aren't caught by the shadow map, not being able to correctly shadow some points in the scene.

As there are no clues as to the location of the remaining errors and the vast majority of errors are concentrated on the contours of the shadow/light boundary of the rendered scene, all tests from this point forward will only take into account these points.

In our tests the points in the contours are roughly equally divided between lit and in shadow points, with the percentage of correctly classified points ranging from 68 to almost 100% in each category.

3.2.USING TEXEL INFORMATION

Regarding scene points classified as in shadow two possible outcomes are possible:

- a) the light ray intersects the triangle whose ID is stored in the texel;
- b) the light ray does not intersect the triangle.

In a) it can be concluded that the pixel is correctly classified. However situation b) is not conclusive, as there may be a triangle that really intersects the light ray but its ID is not stored in the shadow map. An example of both these situations can be found in Figure 18.

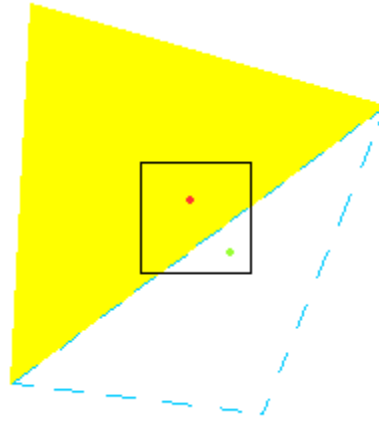


Figure 18: Cases of using texel information.

The yellow triangle is stored in the texel since it covers the centre of the texel. As for the points, both the red point, corresponding to a), and the green point, corresponding to b), project on the texel where the yellow triangle is stored. In the case of the red point, the intersection with the yellow triangle will succeed and the point will be correctly maintained shadowed. But in the case of the green point, the intersection will fail hence the point shadow status cannot be confirmed. The problem here is that there is no way to be sure if the point will be correctly lit due to there being no triangle that shades it, or if the point will be incorrectly lit due to the fact that another triangle shades it, for instance the one represented by the blue dashed line.

Hence for points classified as in shadow a single intersection test will allow finding out that all points in a) are correctly classified and that no further testing is required. For points in b) further tests are required, but there is no more information of use in the texel that treats the shading of the tested point.

Test results below show that the average of points inside a contour of type a) increase with the number of pixels in the contours, as well as with the resolution of the shadow map. According to the tests described in the next chapter, it compensates to use larger shadow maps as more points are confirmed even when using narrower contours. A very significant

percentage of points reported as in shadow by the shadow mapping technique is in case a), the percentage varying from 52.71% to 93.54%, depending on the thickness of the contours and the resolution of the shadow map.

These points are confirmed by this simple test as being correctly classified by the shadow map as in shadow. Taking into account the ground truth of the ray-tracer, and considering all the correctly classified shadow points of the shadow map, this simple test can detect a large number of these points, with percentages varying from 69.20% to 97.96% reported in testing. Unfortunately, when considering the points that, although correctly classified by the shadow map, are not confirmed by this test, a wide range of percentages has been found, ranging from 7.03% to 80.69%.

For points classified as lit by shadow mapping this test may seem useless, as the depth recorded in the texel is larger than the distance from the point to the light source, hence the triangle stored in the texel shouldn't be between the light source and the point being tested. There are however situations where, for a point classified as lit, the light ray actually intersects the triangle whose ID is stored in the shadow map.

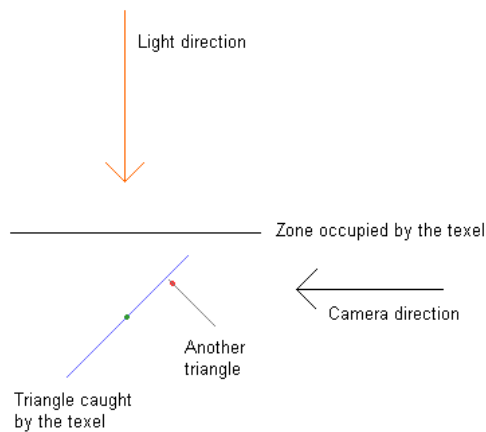


Figure 19: Correcting a point wrongly defined in light with the triangle stored in the projected texel.

In Figure 19, the green point projects upon the centre of the texel of the shadow map, so the blue triangle will be saved in the texel, with the distance saved being the one from the light source to the green point. This is an important observation, since other parts of the triangle are at a different distance from the light source. The camera, for one particular pixel, catches the red point. When testing the red point the shadow map will define this point in light, since

the red point is closer to the light source than the green point, the distance saved in the texel. But when testing for intersection, the ray shooting out of the red point will intersect the blue triangle in a place that is actually closer to the light source than the green point (and the red point), and the point will be shadowed.

Tests show that this case seldom occurs, with an average of 0.09% of pixels being corrected this way. Since the number of lit points is significant, the benefits of performing these tests for lit points can be arguable.

All these cases can be seen in Figure 20. Here, the red and orange pixels are the pixels that started in light and shadow respectively and were corrected to shadow or confirmed in shadow respectively. The green and blue pixels represent pixels that started in light and shadow respectively but still need further testing.

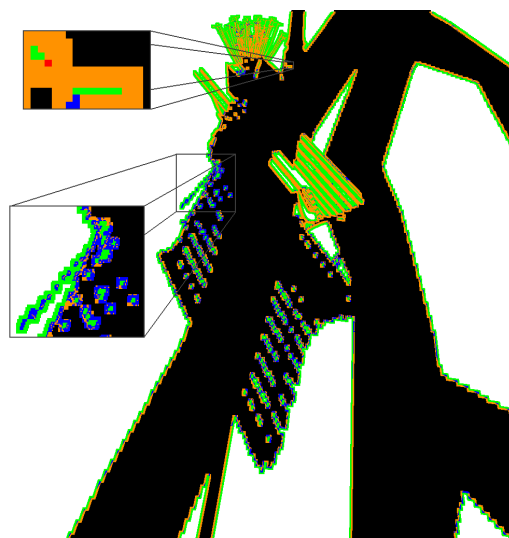


Figure 20: Pixel confirmation using texel information.

Concluding, this test consists of a single intersection test for each point reported as in shadow by the shadow mapping algorithm. The test will assure that all points where an intersection occurs are correctly in shadow hence no further testing is required in this case. Considering all tests, an average of 76.39% of the points in shadow in the contours is confirmed by this test. Still remaining for further testing are all the lit points and the remaining shadow points. From these remaining shadow points, 10.71% should be in light and 12.90% should be in shadow.

3.3.USING THE INFORMATION OF THE NEIGHBOURING TEXELS

As referred above, there are still many pixels that, after testing for intersection with the triangle stored in the texel where the point being tested projects upon, require further testing. The problem is that the texel doesn't always have the information of the triangle that actually shades the point, which may happen if this triangle doesn't project onto the centre of the pixel. So in order to improve the odds of finding the triangle that actually shades the point intersections tests will be performed with nearby triangles. In this section the triangles that are stored in the texels neighbouring the texel that the point projects upon will be checked. Two levels of neighbouring will be detailed. The first, besides verifying the centre texel, will verify the three closest neighbours to the quadrant of the texel where the point being tested projects upon. The second one will verify all of the nine texels surrounding the projected point.

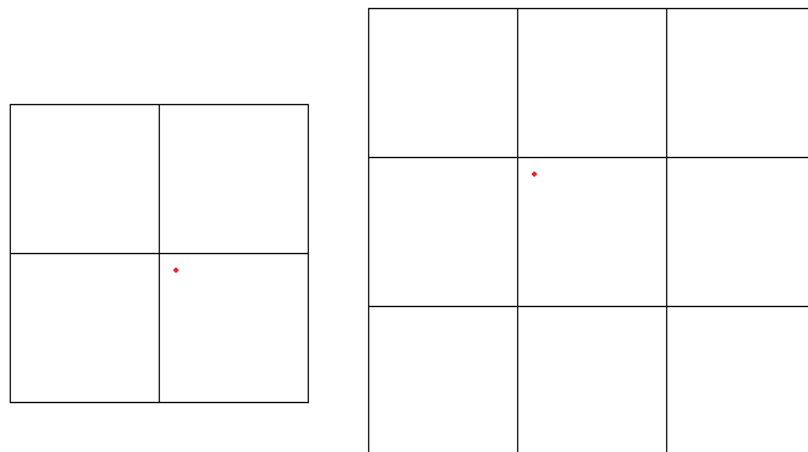


Figure 21: The two cases of neighbouring texels.

The outcomes for points classified as in shadow by the shadow mapping algorithm are similar to the ones when testing with only one texel. So regarding points classified in shadow the outcomes will once again be:

- a) the light ray intersects one of the triangles saved on the neighbouring texels;
- b) the light ray doesn't intersect any of these triangles.

Once again, points in a) can be concluded to be correctly in shadow, while points in b) will need even further testing. An example of both cases can be found in Figure 22.

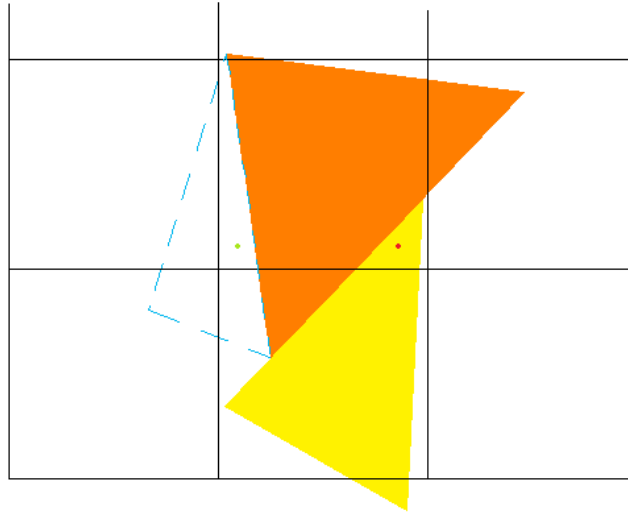


Figure 22: Cases using neighbouring texel information with a triangle stored in the centre texel.

In Figure 22 are the cases referred above, with the red point representing case a) and the green point representing case b). The texel where the points project upon has information of the orange triangle stored and the texel below it has information of the yellow triangle stored. For the red point, intersection with the yellow triangle will succeed and the point will be correctly shadowed. But for the green point, the intersection with the yellow triangle will fail and the point will be defined as lit. But once again, it is unknown if the point is correctly lit or if there is a triangle that shades the point that wasn't stored in any of the neighbouring texels, a possible case represented by the blue dashed lines.

Using only the closest four neighbours tests with this method have confirmed 58.52% to 95.65% of the points classified as in shadow by the shadow map. If only the correctly classified shadowed points are taken into account, then the percentage of confirmed points ranges from 76.82% to 99.86%. Considering the unconfirmed points, the percentage of correctly classified points ranges from 1.65 to 69.75%. When using nine neighbours these percentages are clearly superior, with the range of confirmed points going from 62.77% to 95.74%. Considering only the correctly shadowed points the range of confirmed points is from 79.83% to 99.96%. Finally, amongst the unconfirmed points, between 0.54% and 65.39% are correctly classified as in shadow.

For points classified as lit by shadow mapping, and as opposed to the single texel test, there may be information in the neighbour texels that is helpful in correcting the pixel. So for each

scene point, and considering the neighbour texels, cases a) and b) will be considered again. If a neighbour texel contains a triangle that is intersected by the light ray from the point, case a), then the point was mislabelled as lit by the shadow map algorithm. All scene points that are contained in this case can be safely classified as in shadow and no further testing is needed for these points. As for points in b) these scene points may have no triangle recorded in the neighbour texels as shown for the green point. Hence using this test there is no conclusive information regarding the shadow status of the point.

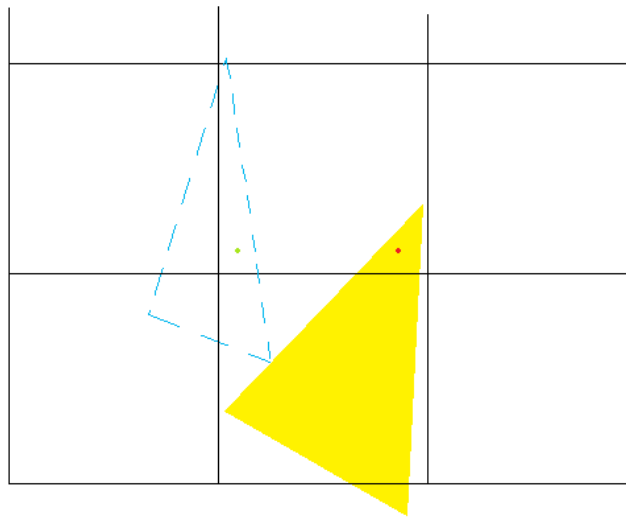


Figure 23: Cases using neighbouring texel information without a triangle stored in the centre texel.

The tests performed report that, when using four neighbours, the percentage of initially lit points that can be corrected ranges from 0.64% to 29.25%. When considering only the misclassified lit points the percentages of corrected pixels range from 29.73% to 97.94%. Regarding points that can't be corrected, because no suitable triangle intersecting the light ray is found on the neighbourhood, 82.86% to 99.91% are correctly classified as lit. As in the shadowed points, these percentages get better with a larger neighbourhood. Using the nine neighbouring texels the percentage of corrected points ranges from 0.81% to 30.03%. Considering only the incorrectly classified points, the percentage of corrected points ranges from 37.07% to 98.97%. Regarding the points that the method is unable to either correct or confirm, the percentage of correctly classified points goes from 84.16% to 99.96%.

All these cases can be seen in Figure 24. Here nine neighbouring texels are used. The red and orange pixels are the pixels that started in light and shadow respectively and were corrected

to shadow or confirmed in shadow respectively. The green and blue pixels represent pixels that started in light and shadow respectively but still need further testing. Basically the same colour scheme that was used with the single texel approach.

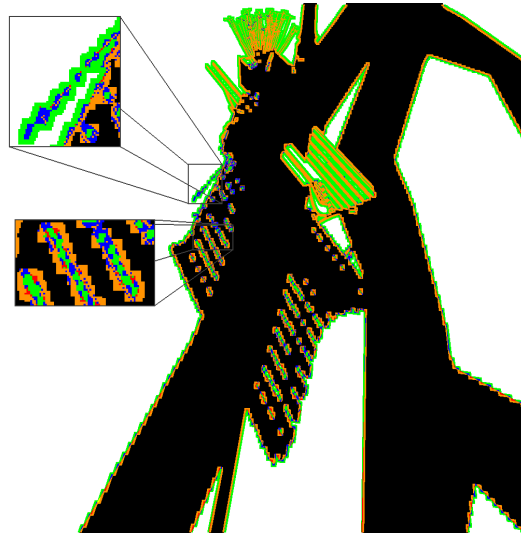


Figure 24: Pixel confirmation using neighbouring texel information with 8 neighbours.

Concluding, this test consists in intersecting the light ray with the triangles stored in the texels neighbouring the texel where the point being tested projects upon. Regarding the points initially classified as in shadow by the shadow mapping algorithm, only those that were not verified by the single texel test should be tested. All points that fall in case a) are confirmed as in shadow. For lit points, as defined by the shadow mapping approach, this test allows the correction of initially incorrectly classified points, and their lighting status can be safely updated from lit to shadow. Results show that a significant number of pixels originally classified as lit are corrected, and also a significant number of points originally in shadow are confirmed.

3.4.USING TEXEL COHERENCE

As seen in (Sen, Cammarano, & Hanrahan, 2003), (Chan & Durand, 2004) and (Beister, Ernst, & Stamminger, 2005), a strong hint for the shadow status of a pixel comes from looking not only at the respective texel, but also to the texel neighbourhood coherency. The approach considers whether the neighbouring texels are coherent regarding the shadow status of the pixel.

It uses the neighbourhood texels to determine whether a scene point is in shadow. For each texel in the neighbourhood the test compares if the depth stored in the shadow map is greater than the distance from the scene point to the light, and classifies it accordingly. If all neighbour texels agree then it can be said that there is coherency regarding the shadow status of a pixel, or scene point.

Note that this differs from the approach from the previous section, as in here only the depths are being tested. There is no intersection test. Therefore this test is faster than the previous ones, where actual intersection tests were used, but it provides no guarantee for the pixel shadow status, it is merely a hint. Miscalculations are possible, i.e. a scene point with texel coherency may in fact be misclassified.

When the neighbourhood includes only four pixels this is equivalent to using Percentage Closer Filtering (PCF) when only results of zero or one, the results that show texel coherency, are considered.

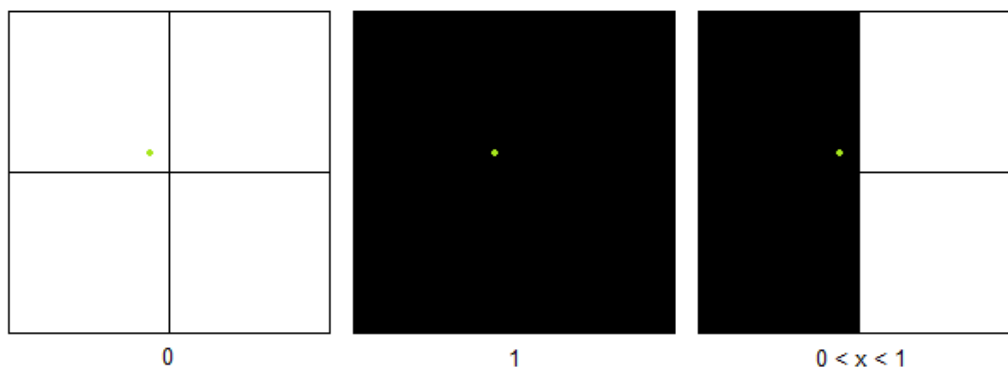


Figure 25: Examples of PCF results.

As mentioned before, tests show that the percentage of miscalculations for scene points where there is texel coherence is fairly small. If the user is willing to accept these small error rates then PCF can be applied and texel coherence can be used to determine which points are likely in shadow or lit. This greatly reduces the number of points which require testing.

In Figure 26 some examples of these cases can be observed. PCF with 4 texels is used to check for texel coherence. The purple pixels represent the pixels of the contour that don't have texel coherence. The pixels in red are pixels that were hinted correctly as being in light, with green pixels being pixels that were incorrectly hinted as in light. Similarly, the pixels in

orange and in blue represent pixels hinted as shadowed and incorrectly hinted as shadowed respectively.



Figure 26: Pixel confirmation using PCF with four texels.

Considering only the points initially classified as in shadow, the percentage of points that have texel coherence goes from 2.37% to 90.15%. Incorrect hints are rare, with percentages up to 0.75%. Regarding points initially classified as in light, the percentage of points that have texel coherence ranges from 2.42% to 91.70%. The range of percentages for incorrect hints is higher though, ranging going up to 7.07% in some scenes.

The test can be expanded to cover a larger adjacency, for instance using 9 texels instead of 4. Testing with larger adjacencies is only useful if the contours are thicker than two points. The larger the adjacency the less points should gather texel coherence, but the result should be more accurate. As expected, tests confirm both these tendencies. Considering points initially classified as shadow, the percentage of points that have texel coherence with 9 texels varies between 0.00% and 80.86%, with incorrect coherence ranging from 0.00% to 0.10%. As for points classified initially as in light, the percentage of pixels that have coherence with nine texels ranges from 0.00% to 82.27% and incorrect coherences range from 0.00% to 1.32%.

Concluding, texel coherence is a good indicator of a point status given the small error margins in average. Note however that the percentage of hinted points has a very wide range of values.

3.5.USING GEOMETRIC ADJACENCY INFORMATION

Another possibility to test the pixel shadow status is to use geometric adjacency information. The goal is to test intersections not only with the triangle whose ID is stored in the texel, but also with all triangles that share an edge or a vertex with the aforementioned triangle.

Unlike the previous tests, the adjacency information isn't readily available in the shadow map, but this information can easily be accessed if lists with the IDs of the adjacent triangles to each triangle of the scene are previously created. These lists can be created as a pre-processing stage since the adjacency of a scene is usually static, even in dynamic scenes. There are effects that may alter the models of the scene, altering the adjacency information, but these effects are rare, and the particular models that are subject to these effects could be left out of this test.

As mentioned before, two levels of adjacency can be considered: edge and vertex, referred in here as first and second level adjacencies. A triangle in the first level is considered to be adjacent if it shares an edge with the triangle stored in the texel. In the second level any triangle that shares a vertex shall be considered adjacent.

Considering only the points originally reported as in shadow by the shadow mapping algorithm, the light ray will either intersect one of the triangles being tested or it won't intersect any of the triangles, resulting in the same a) and b) cases above respectively. And once more, the points in case a) will be correct and will need no further testing, while the points in case b) will need further testing. An example of case a) and b) for this test will be viewed below in Figure 27 and Figure 28 respectively.

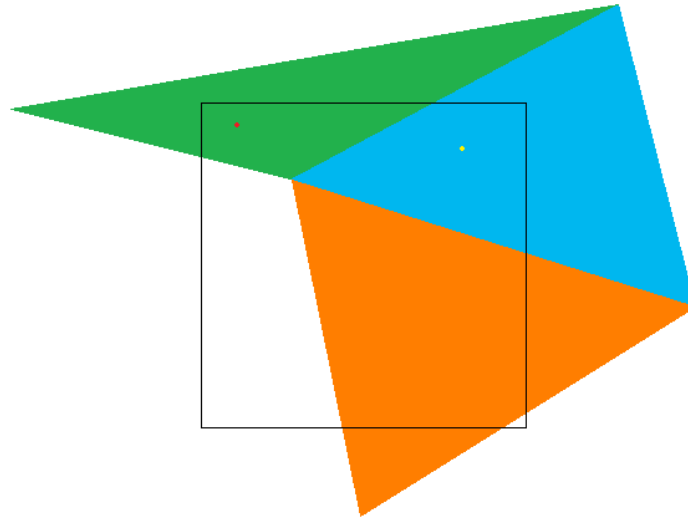


Figure 27: Using adjacent geometry information for case a).

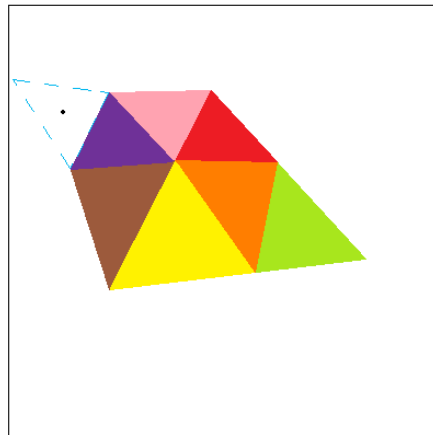


Figure 28: Using adjacent geometry information for case b).

In Figure 27 both points represent case a). The texel has the information of the orange triangle stored. When testing intersection for both points, the yellow point will be shadowed by the blue triangle found in the first level of adjacency of the orange triangle and the red point will be shadowed by the green triangle found in the second level of adjacency. As for case b), this case is represented in Figure 28 by the black point. The texel, the whole box, has the information of the orange triangle stored. When testing the black point for intersection with every adjacent triangle, these intersections will fail, so once more it is unknown if this point should be changed to light due to having no triangles shading it or if there exists a triangle, marked by the dashed blue line, out of the adjacency of the orange triangle that would shade the point.

This method is expected to confirm more points in shadow than the single texel approach, and the tests confirm an average increase in the number of point confirmations. In fact, the results point to this being the strongest method to confirm shadow points, topping even the texel neighbouring approaches both with four and nine neighbours.

Regarding points classified as in shadow, this method confirmed a very significant number of those points, with percentages varying from 64.12% to 96.26% with edge adjacency and 67.92% to 97.76% with vertex adjacency. When considering only the correctly classified points, the confirmation percentages range from 78.84% to 99.80% with edge adjacency and 85.69% to 99.98% with vertex adjacency. Focusing on the unconfirmed points, the percentage of correctly classified points goes from 1.15% to 67.85% with edge adjacency, and 0.30% to 56.20% with vertex adjacency.

As for the points defined as lit by shadow mapping, this test will suffer from the same problem as when using only the centre triangle. A point is lit either if there is no triangle covering the texel it projects onto, or there is a single triangle but the distance stored is larger than the distance of the point to the light.

In the first case the method can't be applied since there is no triangle to get adjacencies from. Regarding the second case it is unlikely that a triangle that is further away than the point being tested, actually has adjacent triangles that are closer to the light than the point.

Nevertheless this is possible as shown in Figure 29.

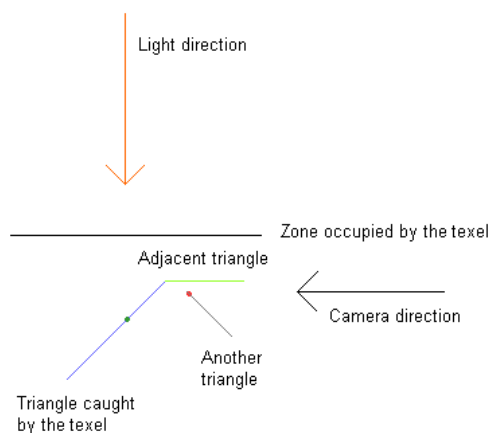


Figure 29: Correcting a point wrongly defined in light using triangle adjacency.

Figure 29 is similar to Figure 19, with the difference that now the ray doesn't intersect the blue triangle. But the ray will intersect the green triangle that is adjacent to the blue triangle, correcting the point that is wrongly defined in light.

But once more, this case rarely happens, so once more the benefits of performing these tests are minimal so this test could be skipped for all lit points.

Figure 30 shows the cases stated above, with the same colouring scheme as seen in previous examples. Red and orange pixels are pixels confirmed that started in light and shadow respectively, where the green and blue pixels are uncertain pixels that started in light and shadow respectively.

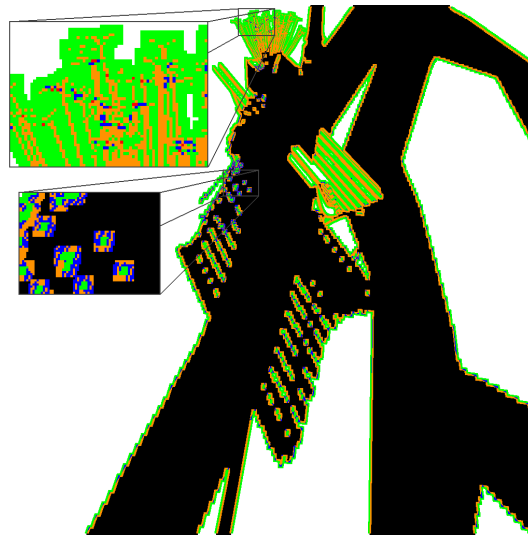


Figure 30: Pixel confirmation using geometry adjacency information with 2 levels of adjacency.

To conclude, this test consists of intersections with the geometric adjacency of the triangle stored in the texel. As mentioned before the benefits of applying it to originally lit points are marginal, hence it could be applied only to points shadowed by the shadow map. And once more, the test will assure that for all points where an intersection with the tested triangles occurs no further testing will be needed since these points will definitely be in shadow.

3.6.PUTTING IT ALL TOGETHER

In the previous sections several approaches were proposed to check the shadow status of a pixel as determined by the shadow map approach. All the work was performed only in contour pixels since these are where the majority of errors are to be found.

It is important to note that a point incorrectly classified as in shadow can never be corrected using only these methods. This is due to the fact that there may be a triangle that shades said point which is not a part of the small subset of triangles tested with these methods. On the other hand it is possible to correct a point initially lit as this operation only requires that a triangle be found which is intersected by the point's light ray. Since only a small subset of triangles is being tested it is likely that some points don't get corrected. Similarly it is not possible to confirm a point as being lit and only points initially classified as in shadow can be confirmed.

Texel coherence is a method that relies solely on the texel neighbourhood, and while not able to confirm or correct points, it provides a strong hint regarding the shadow status of a pixel of a significant average number of points. The remaining methods, although computationally more expensive, can actually confirm/correct the shadow status of a pixel.

A summary of each one of the methods can be seen in below in Figure 31.

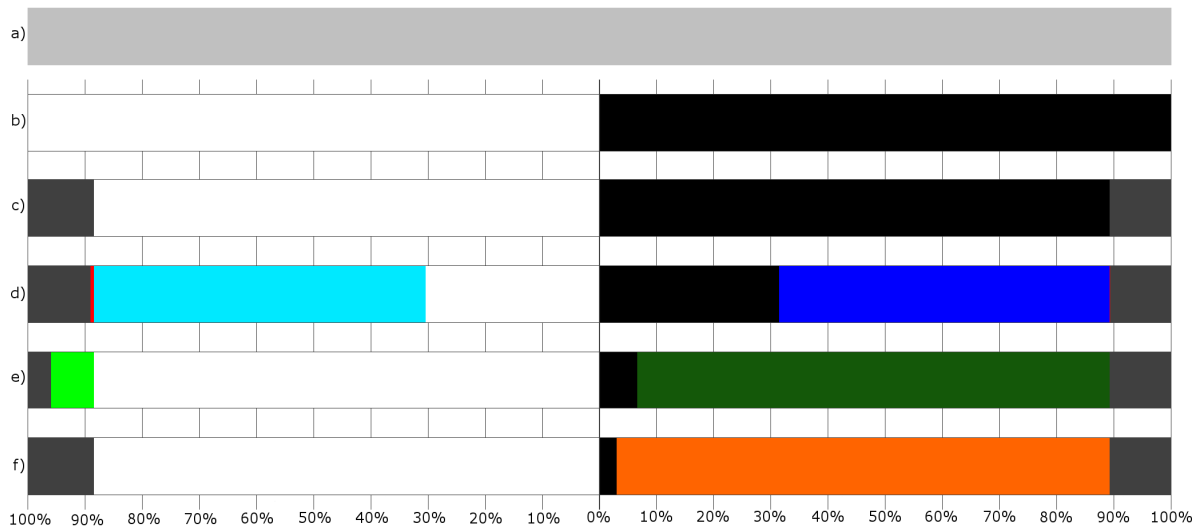


Figure 31: Average of corrected/confirmed/hinted contour pixels by each method: a) contour pixels; b) shadow map results separated in shadow (black) and light (white); c) errors of the shadow map (gray); d) correct (blue) and incorrect (red) hints using texel coherence; e) confirmed shadow (dark green) and corrected light (light green) pixels by neighbouring texels; f) confirmed shadow pixels (orange) by adjacent geometry.

In Figure 31 the first bar represents the amount of pixels in the contour. The second bar represents the amount of shadow (black) and light (white) pixels after shadow mapping. The third bar marks in grey the pixels that the shadow map incorrectly states as in light or as in

shadow. The fourth bar represents the hinted pixels by the texel coherence method, where the blue light and dark blue colours represent the correctly hinted pixels and the red colour represents the incorrectly hinted pixels. The fifth bar represents the results of the neighbouring texel method, where the dark green represents confirmed shadow pixels and the light green represents corrected light pixels. Finally, the sixth bar represents the results of the adjacent geometry method, where the orange colour represents the confirmed shadow pixels. The colour code found above will be used in similar graphics from here on forth.

From all the methods above, only the neighbouring texels method is actually capable of correcting the shadow status of a point. Hence this method could in principle be applied as a standalone method. Although only points initially classified as in light can be corrected the range of improvement can go all the way up 97.94%. However the improvements are not perceptually significant as the incorrectly classified pixels in shadow are too prominent.

Another option is to consider these methods as a step whose goal is to reduce the workload of a regular ray-tracer. In this context, all confirmed/hinted/corrected points would not require further work, hence reducing the burden of the ray-tracer to verify only the remaining points.

In this section some ways of chaining the previous methods together to improve the shadow map result and to reduce the workload of a full ray-tracer to obtain the correct shadows will be proposed.

Texel coherence, as mentioned before, does not correct the shadow status of a pixel, yet it provides a strong hint of its status. It could be used as the first step, to significantly reduce the workload of the remaining steps. In a progressive approach, this method could be used in the first step when the camera is moving to speed things up, and afterwards, when the camera is still, it could be discarded. Another scenario is for this method to kick in when the frame rate drops below a defined threshold.

Texel coherence hints from 2.37% to 90.15% of the points initially classified as in shadow, and 2.42% to 91.70% for those initially classified as lit.

As for the remaining methods these should be applied starting from the least computationally expensive, the texel neighbourhood, followed by the adjacent triangles method. These methods will only be applied on points that have not been resolved in the previous steps.

After applying the texel neighbourhood method (nine neighbours) to the non-hinted points, and considering the shadow map classification, from 63.03% up to 96.77% of the points initially classified as in shadow are confirmed/hinted, and 26.97% - 92.50% of the previously lit points are now either hinted or corrected.

The adjacent triangles approach is only applied to points initially classified as in shadow, and it shall be applied to the points that have not been hinted/confirmed before. The range of hinted/confirmed points goes up to 68.07% to 97.78% after applying all the methods.

These methods combined are able to confirm a very significant number of initially shadowed pixels shadow, and even correct an also significant number of pixels initially reported as in light. As for the pixels that still remain unconfirmed after all the previous steps, (2.22%-31.93% in shadow and 7.50%-73.03% in light), these can be confirmed/corrected by using ray-tracing. This way the amount of pixels that need ray-tracing will be greatly reduced. Figure 32 below represents the average of results of the combination provided above.

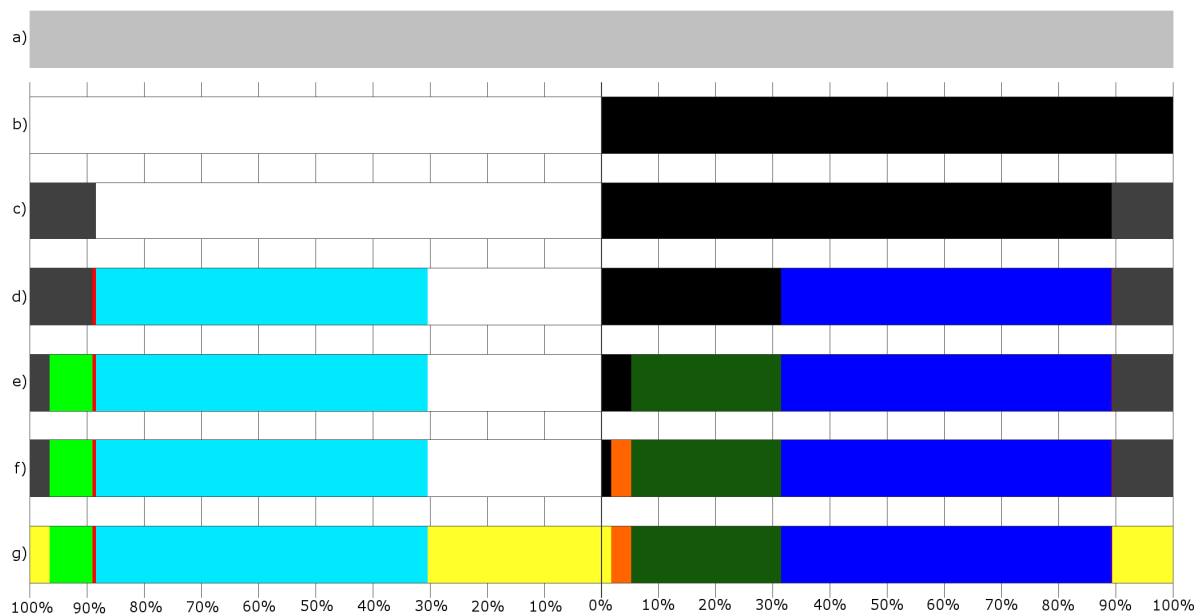


Figure 32: Average of corrected/confirmed/hinted contour pixels by the chaining of methods: a) contour pixels; b) shadow map results separated in shadow (black) and light (white); c) errors of the shadow map (gray); d) correct (blue) and incorrect (red) hints using texel coherence; e) confirmed shadow (dark green) and corrected light (light green) pixels by neighbouring texels; f) confirmed shadow pixels (orange) by adjacent geometry; g) non-hinted/uncorrected/unconfirmed pixels (yellow).

In Figure 32 the first four bars represent the same as in Figure 31. The remaining bars show further steps in the chaining of methods. The fifth bar represents the results after the neighbouring texels method and the sixth bar represents the results after using the adjacent geometry method. The final bar marks in yellow all pixels that remained non-hinted, unconfirmed or uncorrected.

3.7.CONCLUSION

This chapter presented a study on the location and identification of shadow mapping errors. The first goal was to narrow down the location of errors. Shadow map errors can be present in any part of the image, yet the vast majority seems to be located in average on the contours of the shadows. Focusing on this area reduces significantly the search for shadow mapping errors.

The next step was to figure out if it is possible to evaluate the correctness of the shadow mapping shadow or light status. Several methods were proposed that can confirm the correctness of a pixel in the rendered scene for pixels in shadow and some of these methods are even able to determine if a pixel is incorrectly lit.

These methods use information readily available on the shadow map. The adjacency method also requires a table of adjacencies for each triangle. Adjacencies can be vertex or edge based.

One of the methods, texel coherence, is not able to either correct/confirm any pixel, yet it provides a strong hint about its correctness. Few errors are to be found in these hints, and the method is extremely fast, in fact as fast as PCF shadow mapping.

Since each method has its strengths and weaknesses, an algorithm was proposed to chain these methods together. The algorithm starts by identifying the contours of the shadow areas and then proceeds to use each of the methods described in this section. Each method corrects/confirms a set of pixels, and the remaining uncorrected/unconfirmed pixels pass on to the next stage.

The methods are only able to confirm that a pixel in shadow is actually in shadow, i.e. they are unable to determine if a pixel in shadow should be lit. The test is performed with a limited number of triangles hence there is no guarantee that there is not a triangle in the full data set

that covers it. Similarly, for pixels that remain uncorrected in light, these were only tested with a limited number of triangles, so the same reasoning applies.

At the end of the chain, the percentage of uncorrected/unconfirmed pixels is severely reduced. These pixels can be correctly shadowed/lit but the information available on does not allow its verification. To determine the shadow status of these remaining pixels a full ray-tracer is required. However, applying a full ray-tracer to only these pixels severely reduces this last step, making it affordable for real-time shadows.

4. ALGORITHM TESTING

The descriptions of the approaches referred above were put together after an observation of some test results of these approaches. In this chapter some of these tests will be observed in greater detail. These tests consisted in using the proposed approaches to obtain the image viewed by the camera in a scene. Afterwards these images were compared to their ray-tracer and shadow mapping equivalents in order to ascertain the quality of the results of the approach.

This chapter will start by presenting the scenes and viewpoints being tested and the ray-traced shadows of these scenes. Afterwards this chapter will follow the algorithm proposed in the previous chapter, presenting an average of all of the tests and the best and worst case scenarios of the tests of each respective approach when used by itself and also for the proposed algorithm after passing through the specified approach. As for specifics of the tests there will be three contour thicknesses that will be tested. These contours will be two, four and six pixels thick and may also be described by referring to dilations, corresponding to the simple contour and the contours with one and two dilations respectively. Tests will also be done with shadow map resolutions of 1024x1024 and 2048x2048, a viewport resolution of 1024x1024 and three viewpoints for each one of the four scenes. The view frustum will have the minimum size needed to contain the objects being seen by the camera, including also all the geometry that could influence lighting, from each one of the viewpoints. The light used will be a directional light in all cases. In order to not clutter up this chapter with result tables, only some of the results will be displayed here. The results that will be displayed are the best and worst cases for each shadow map resolution for each one of the approaches by itself, the proposed algorithm, which will be observed throughout each algorithm step, and also the average of every result. There will also be an average case that will be followed throughout the chapter, the “with” viewpoint of the “bench” scene (information of scenes and viewpoints tested will be observed in detail below) when using a two pixel thick contour and a 2048x2048 resolution shadow map. This case was chosen due to its results being close to those of the average results. Except if stated otherwise, the results presented here will be the percentage of pixels in relation to the total amount of pixels inside the contour being tested, be it the actual total amount, when nothing is referred, or the total amount of light or shadow

pixels, when the percentage is explicitly related to light or shadow pixels. The remaining results, not presented in this chapter, can be seen in detail in the appendix.

4.1. TEST SCENES

The following images will show the scenes and that will be used for testing and the various viewpoints that will be used for said tests.

The first scene, represented in Figure 33, consists of a simple scene with a plane with a torus, a cylinder, a pyramid and a sphere on top. All this geometry has a total of 4944 triangles. This scene will be called “Primitives”. Information of light, field of view and cameras of each viewpoint can be observed in Table 1.

Viewpoint		Coordinates		
		x	y	z
Side	Position	35.0	50.0	-43.0
	Direction	-1.0	-1.2	1.0
With	Position	-28.0	38.0	-40.0
	Direction	0.4	-0.7	0.6
Against	Position	31.0	54.0	38.0
	Direction	-0.4	-0.7	-0.5
Light Direction		0.528542	-0.376004	0.761095
View Frustum		Far Plane: 250	Near Plane: 20	FoV: 60°

Table 1: Information of the first scene.



Figure 33: The side (left), with (centre) and against (right) viewpoints of the first scene.

The second scene, represented in Figure 34 consists of a scene with two trees, a lamp, a flower box and a bench on a plane. The scene has a total of 55026 triangles. This scene will be called “Bench”. Information of light, camera and field of view of this scene can be observed in Table 2.

Viewpoint		Coordinates		
		x	y	z
Side	Position	-23.277	18.541	30.143
	Direction	0.397	-0.644774	-0.652
With	Position	-37.034573	35.208973	-8.597797
	Direction	0.605439	-0.732089	0.312232
Against	Position	27.214222	27.875109	27.032139
	Direction	-0.560848	-0.777942	-0.283293
Light Direction		0.744	-0.408	0.527
View Frustum		Far Plane: 120	Near Plane: 15	FoV: 60°

Table 2: Information of the second scene.



Figure 34: The side (left), with (centre) and against (right) viewpoints of the second scene.

The third scene, called “Trees”, will use the same models as the second scene, but will focus attention on an area of the ground where only the shadows of the trees will be seen. Since the trees are constituted by big triangles, this will allow the evaluation of the effect of big triangles on the results. Information of cameras of each viewpoint can be observed in Table 3.

Viewpoint		Coordinates		
		x	y	z
With	Position	42.947086	24.103859	-27.831772
	Direction	0.415959	-0.784187	0.460467
Side	Position	76.844704	28.391548	-31.870102
	Direction	-0.232891	-0.79644	0.558073
Against	Position	90.805244	35.846294	24.061787
	Direction	-0.421061	-0.852832	0.350347
Light Direction		0.744	-0.408	0.527
View Frustum		Far Plane: 120	Near Plane: 15	FoV: 60°

Table 3: Information of the third scene.

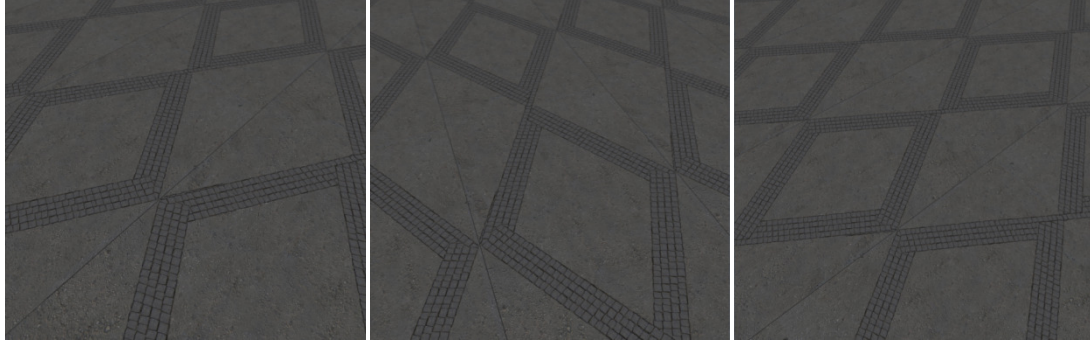


Figure 35: The with (left), side (centre) and against (right) viewpoints of the third scene.

The fourth scene, named “Flowers”, will also use the same models as the second scene, but will closely observe the shadows cast by the flowers. The flowers are modelled with very small triangles, allowing the visualization the effect of small geometry on the algorithm. In Table 4 the information of the camera of each viewpoint can be viewed.

Viewpoint		Coordinates		
		x	y	z
Side	Position	-3.615331	22.376335	2.338565
	Direction	-0.387214	-0.852832	0.350347
Against	Position	-3.263903	24.423452	12.998949
	Direction	-0.239566	-0.958412	-0.155095
With	Position	-17.561422	24.968716	4.010894
	Direction	0.386402	-0.873032	0.297505
Light Direction		0.744	-0.408	0.527
View Frustum		Far Plane: 120	Near Plane: 15	FoV: 60°

Table 4: Information of the fourth scene.



Figure 36: The side (left), against (centre) and with (right) viewpoints of the fourth scene.

4.2.RAY-TRACER

The first step is to show the results for each scene and viewpoint obtained by the implemented ray-tracer. The ray-tracer results are the ground truth that will be used to test

everything else against. The results below will show each scene when shadowed and a binary lit/shadowed image of the shadowing of each scene.

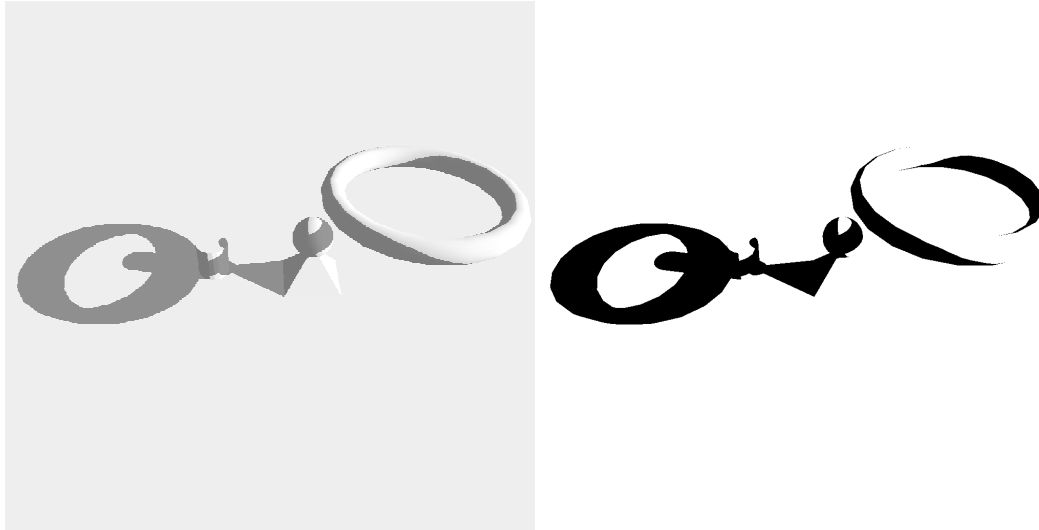


Figure 37: Ray-tracer results for the side viewpoint of the primitives scene.



Figure 38: Ray-tracer results for the with viewpoint of the primitives scene.

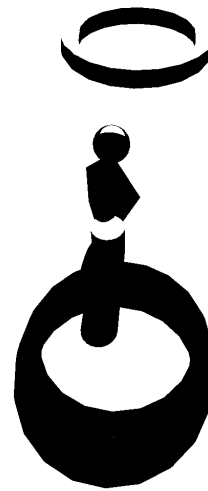


Figure 39: Ray-tracer results for the against viewpoint of the primitives scene.

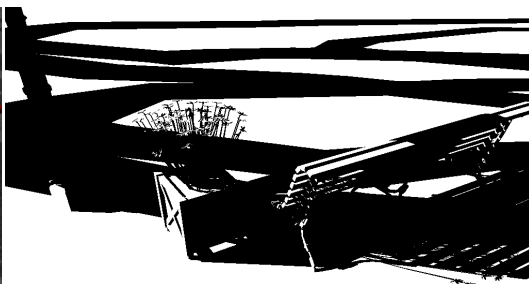
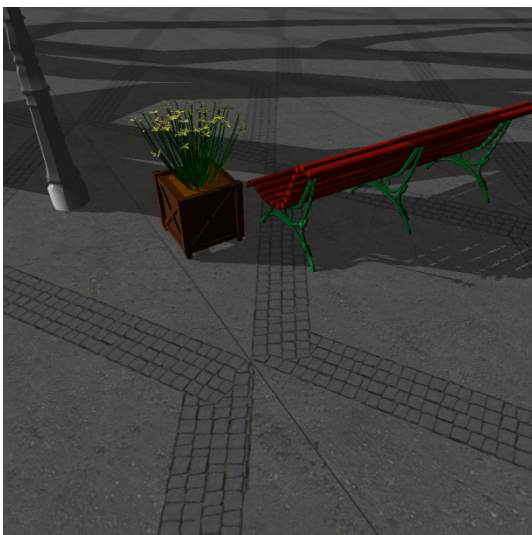


Figure 40: Ray-tracer results for the side viewpoint of the bench scene.



Figure 41: Ray-tracer results for the with viewpoint of the bench scene.

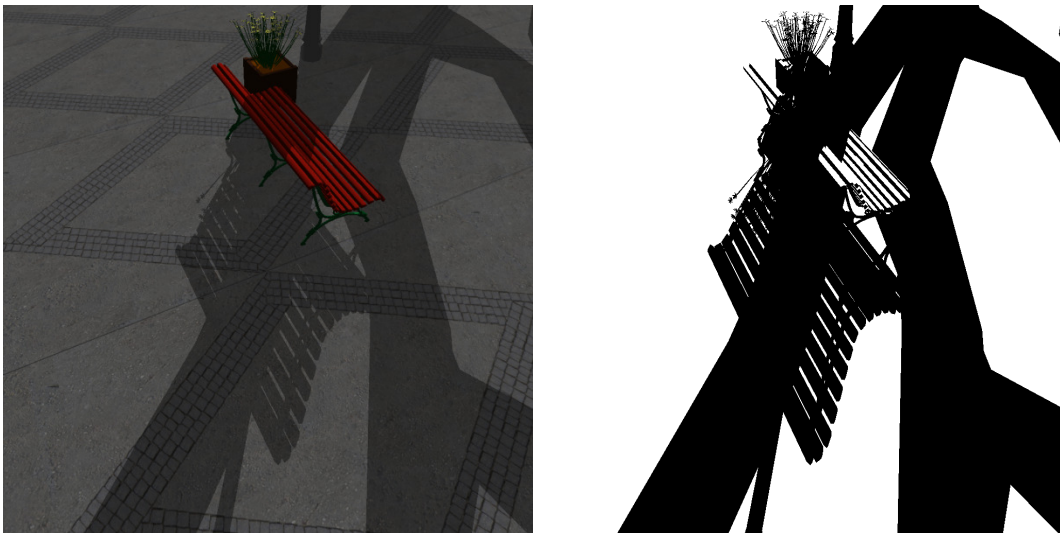


Figure 42: Ray-tracer results for the against viewpoint of the bench scene.

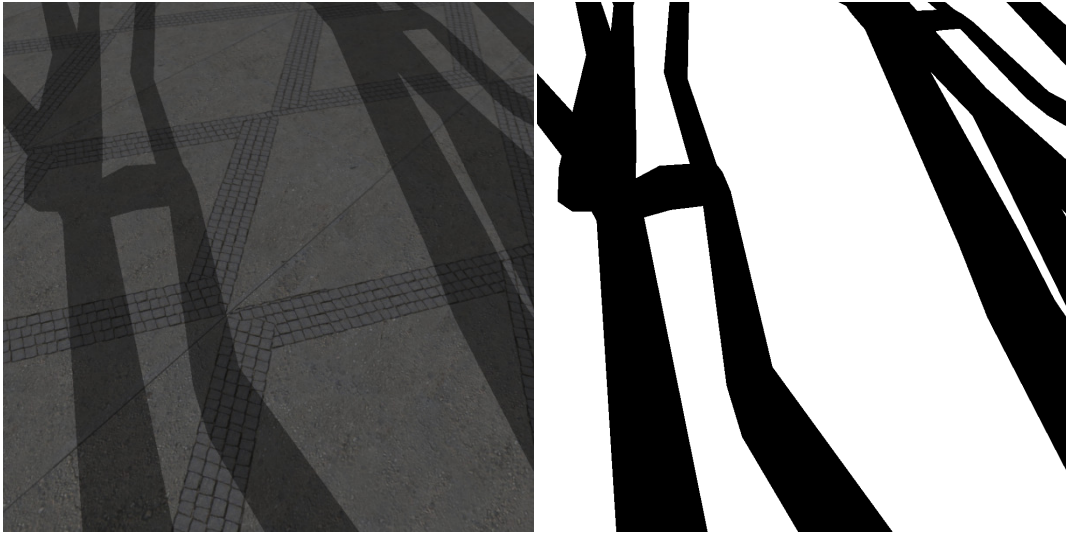


Figure 43: Ray-tracer results for the with viewpoint of the trees scene.

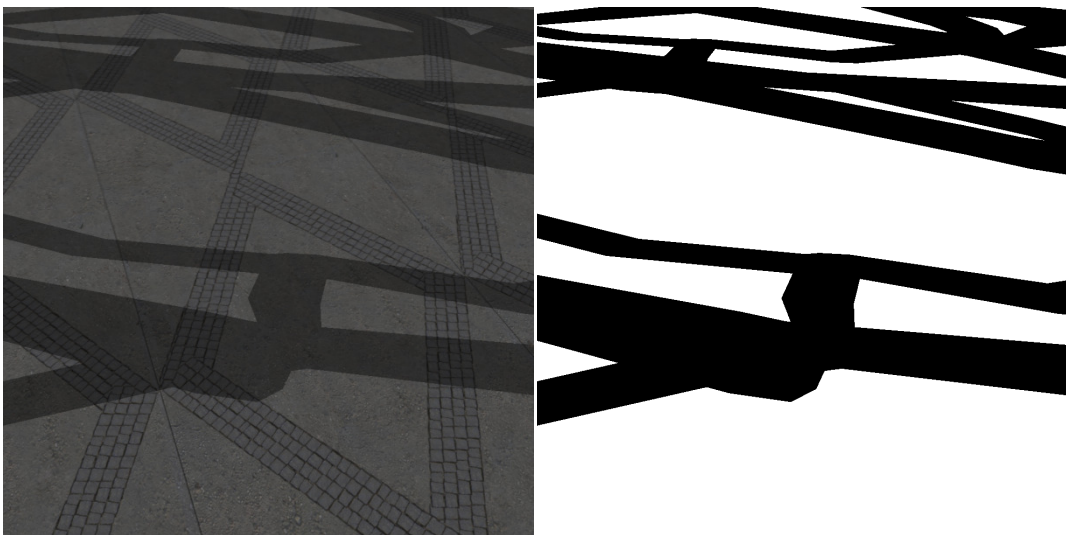


Figure 44: Ray-tracer results for the side viewpoint of the trees scene.

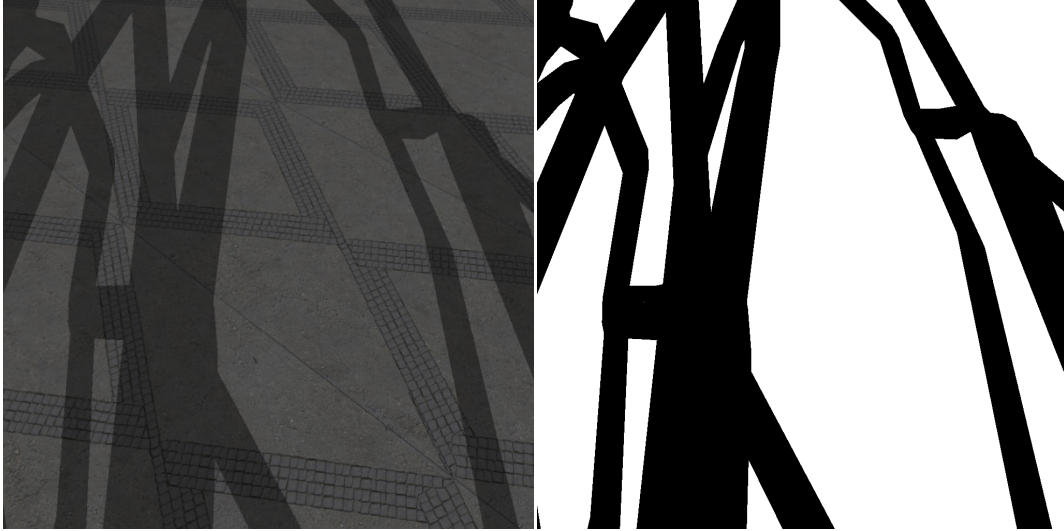


Figure 45: Ray-tracer results for the against viewpoint of the trees scene.

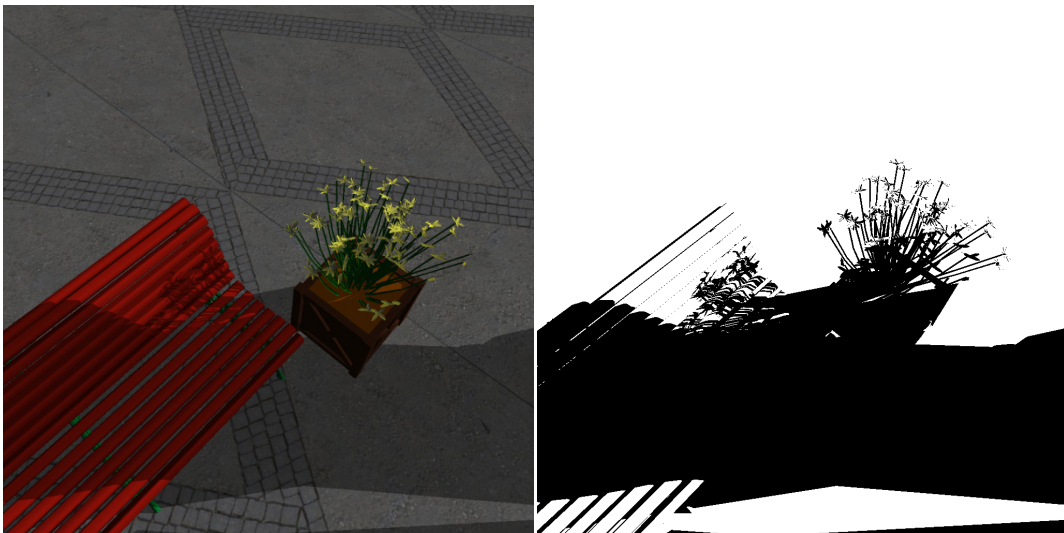


Figure 46: Ray-tracer results for the side viewpoint of the flowers scene.

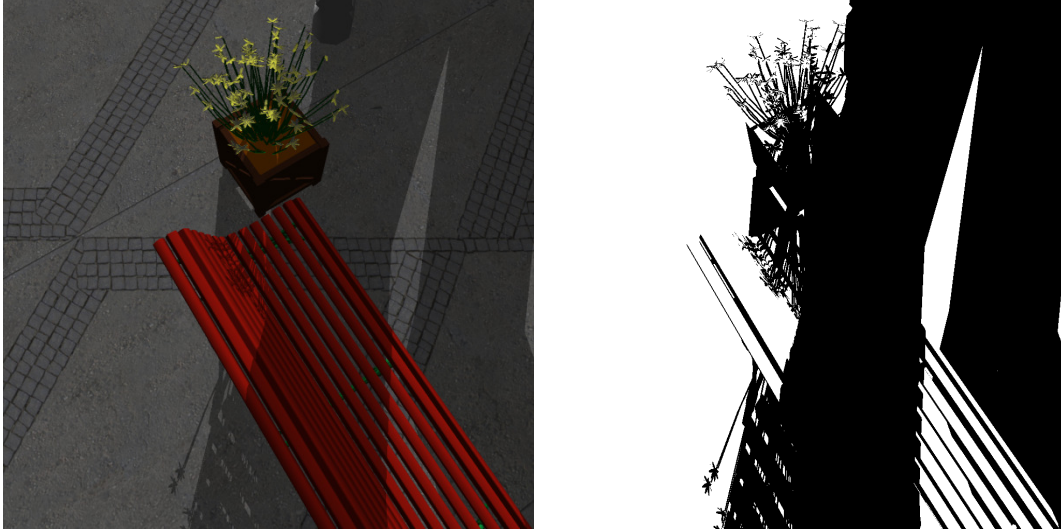


Figure 47: Ray-tracer results for the against viewpoint of the flowers scene.

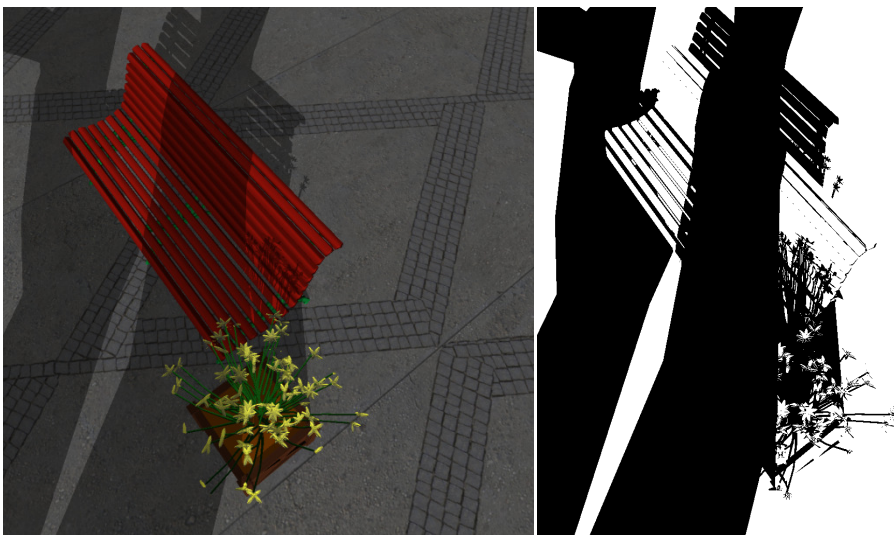


Figure 48: Ray-tracer results for the with viewpoint of the flowers scene.

4.3.SHADOW MAPPING ERRORS

Now the shadow mapping results will be compared against the results of the ray-tracer. With the shadow mapping results calculated the contours can be found and with the errors calculated tests can be made in order to find out if in fact the contours contain the majority of the errors of the shadow mapping approach. In this sub-chapter the percentages of errors caught inside contours will be presented.

	Average	Shadow Map				Average Case
		1024x1024		2048x2048		
		Best Case	Worst Case	Best Case	Worst Case	
Scene	--	Primitives	Primitives	Primitives	Flowers	Bench
Viewpoint	--	Side/With	Against	Side	Side	With
Contour Size	--	6 pixels	2 pixels	6 pixels	2 pixels	2 pixels
Caught Errors (%)	92.41	100.00	57.42	100.00	81.00	97.12

Table 5: Percentages of errors inside the contours.

As seen in Table 5, in average over 90% of the shadow map errors are caught inside the contours. Below are the images of the results of the best, worst and medium case scenarios. The contours are marked with green, the errors outside the contour are in blue and the errors inside the contour are in red and yellow if the pixel is incorrectly in light and shadow respectively.



Figure 49: Best case of shadow map errors being caught inside contours with a 2048x2048 shadow map.

In the best case scenarios seen in above, with both shadow map resolutions the results have a small amount of errors, so by using a 6 pixel thick contour, this small amount of errors will be caught inside the contours.



Figure 50: Worst case of shadow map errors being caught inside contours with a 2048x2048 shadow map.

The worst case scenarios seen above use thinner contours and the big amount of aliasing causes the thin contour to not be able to catch many of the errors of the shadow map. The worst case when using a 1024x1024 shadow map has a lower percentage of errors caught, since with smaller shadow map resolutions bigger aliasing will be present.



Figure 51: Average case of shadow map errors being caught inside contours.

The medium case catches a big amount of the errors inside the contours, even when using a two pixel thick contour. The errors that aren't caught inside the contours can be found in the area shadowed by the small geometry that constitutes the flowers.

Also, to be used as comparison with the proposed approaches, the information of the percentage of incorrect pixels of the contour is presented below.

	Average	Shadow Map				Average Case
		1024x1024		2048x2048		
		Best Case	Worst Case	Best Case	Worst Case	
Scene	--	Primitives	Trees	Primitives	Trees	Bench
Viewpoint	--	With	Against	With	With	With
Contour Size	--	6 pixels	2 pixels	6 pixels	2 pixels	2 pixels
Errors (%)	11.09	3.40	26.68	1.75	20.50	5.06
Errors in Light (%)	11.50	3.06	25.41	1.41	18.93	4.31
Errors in Shadow (%)	10.71	3.89	27.93	2.22	22.07	5.99

Table 6: Percentage of contour pixels that are incorrect.

Figure 52 below presents the average of results for the shadow map separated by contour thickness. Each bar is divided in three smaller bars corresponding, from top to bottom, to the 2, 4 and 6 pixel thick contours.

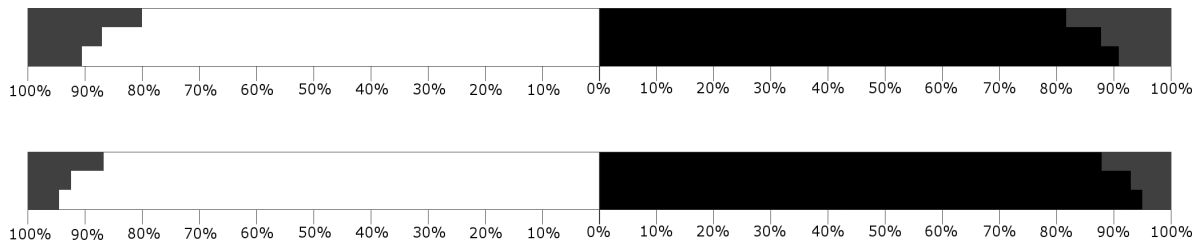


Figure 52: Average shadow map results separated by contour thickness with a 1024x1024 shadow map (top) and a 2048x2048 shadow map (bottom).

4.4. USING TEXEL COHERENCE

Now the results of the texel coherence will be presented. Since this is the first step in the proposed algorithm, the results of using this approach by itself and within the algorithm are the same.

	Average	Shadow Map				Average Case
		1024x1024		2048x2048		
		Best Case	Worst Case	Best Case	Worst Case	
Scene	--	Primitives	Trees	Primitives	Trees	Bench
Viewpoint	--	With	Against	With	With	With
Contour Size	--	6 pixels	2 pixels	6 pixels	2 pixels	2 pixels
Confirmations (%)	58.30	82.80	2.39	91.06	21.24	57.98
Confirmations in Light (%)	58.52	84.26	2.42	91.70	21.13	59.69
Confirmations in Shadow (%)	57.96	80.76	2.37	90.15	21.35	56.25
Wrong Confirmations in Light (%)	0.55	0.04	0.00	0.03	0.00	0.56
Wrong Confirmations in Shadow (%)	0.12	0.00	0.00	0.00	0.00	0.17

Table 7: Percentage of confirmations by PCF with four texels.

As seen in Table 7, in average almost 60% of the pixels inside a contour are confirmed when using texel coherence with four texels. Of the pixels confirmed in light or in shadow the average of incorrect confirmations is less than 1%, so the amount of errors is small. The images of the best and worst cases will be shown below. In these images, the purple pixels are uncertain pixels, the light grey pixels are pixels confirmed as lit, in dark grey are pixels confirmed as shadowed, in red are pixels incorrectly confirmed as lit and in yellow are pixels incorrectly confirmed as shadowed.



Figure 53: Best case of texel coherence confirmation using four texels and a 2048x2048 shadow map.

In the best case scenarios the scene and the viewpoint are the same in both shadow map resolutions. In both cases the amount of confirmed pixels is high because a big amount of the shadowed area appears due to objects facing away from the light source instead of shadowing due to other objects, which helps in the confirmation of a bigger amount of pixels since all approaches use normals to check if an object is facing away from the direction of the light or not.



Figure 54: Worst case of texel coherence confirmation using four texels and a 2048x2048 shadow map.

In the worst case scenarios barely any pixel is confirmed with the use of texel coherence. All of the shadowed area in these images comes from shadows cast by other objects, so the PCF used will not have any shadow confirmed due to surfaces facing away from the light source. Also, it is known that the bigger amount of errors of the shadow map can be found in the contours, so it is logical that all of the indecisions of using texel coherence can be found in the contours. By using such a thin contour, this contour will not be able to catch much more than uncertain pixels.



Figure 55: Average case of texel coherence confirmation using four texels.

In the medium case the uncertain pixels can be found in bigger quantity around the shadows cast by the flowers and the bench. A thin line of uncertain pixels can also be found surrounding the shadows cast by the trees.

	Average	Shadow Map				Average Case
		1024x1024		2048x2048		
		Best Case	Worst Case	Best Case	Worst Case	
Scene	--	Primitives	Trees	Primitives	Trees	Bench
Viewpoint	--	With	With/Against	With	Against	With
Contour Size	--	6 pixels	2 pixels	6 pixels	2 pixels	2 pixels
Confirmations (%)	43.02	73.56	0.00	81.69	2.31	34.23
Confirmations in Light (%)	42.76	75.47	0.00	82.27	2.29	36.00
Confirmations in Shadow (%)	43.15	70.86	0.00	80.86	2.32	32.43
Wrong Confirmations in Light (%)	0.28	0.03	0.00	0.01	0.00	0.29
Wrong Confirmations in Shadow (%)	0.02	0.00	0.00	0.00	0.00	0.00

Table 8: Percentage of confirmations by PCF with nine texels.

When using 9 texels for texel coherence, the amount of confirmations averages a little over 40%. As expected, the amount of confirmations is lower, but also the amount of errors introduced. The best case scenarios are the same as when using texel coherence with four texels. In the worst case scenarios, when using a 2048x2048 shadow map the worst case scenario is different and when using a 1024x1024 shadow map besides the worst case

scenario when using four texels, there is another case that ties with it for worst case, with both these tied cases having no pixel confirmed. The reasoning behind these cases is similar as when using four texels for coherence, so no need to repeat the explanation again.



Figure 56: Best case of texel coherence confirmation using nine texels and a 2048x2048 shadow map.



Figure 57: Worst case of texel coherence confirmation using nine texels and a 2048x2048 shadow map.



Figure 58: Average case of texel coherence confirmation using nine texels.

As observed above, when using four texels for coherence the amount of confirmations is in average 15% more than when using nine texels, with the amount of confirmation errors still staying below 1%. So in the proposed algorithms four texels will be used for coherence.

Below is a graphic with the averages of results of texel coherence with four texels.

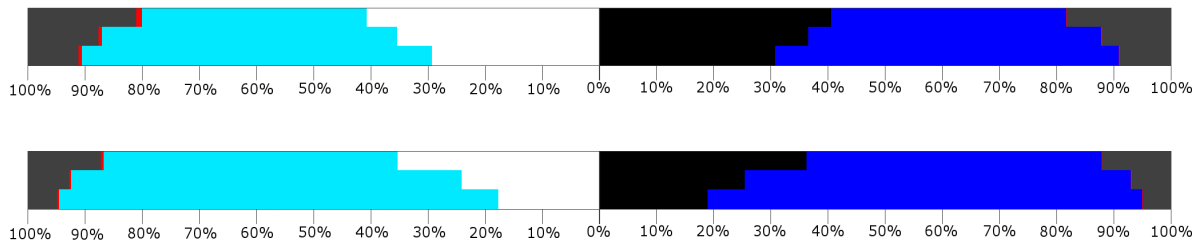


Figure 59: Average results of texel coherence with four texels separated by contour thickness with a 1024x1024 shadow map (top) and a 2048x2048 shadow map (bottom).

4.5.USING TEXEL INFORMATION

Following below are the results when using the triangle stored in the centre texel. The tables below will show the results of exclusively using this approach. The results of using this approach in the proposed algorithm won't be shown as these results are included in the neighbouring texels step. The results of the algorithm used alone will display two percentages. The first percentage is the percentage of errors in the contour after using the approach, since in this case rays that don't intersect the triangle being tested will be

considered in light instead of uncertain. As observed in the previous chapter, all of the errors are pixels that should be in shadow but will be in light due to the fact that the triangle that actually shades the point being tested isn't the one stored in the texel. The second percentage, between parentheses, presents the percentage of light pixels that were corrected in relation to the total amount of incorrect light pixels or the percentage of shadow pixels that were confirmed in relation to the total amount of correct shadow pixels, depending if the pixel started as lit or as shadowed.

	Average	Shadow Map				Average Case
		1024x1024		2048x2048		
		Best Case	Worst Case	Best Case	Worst Case	
Scene	--	Trees	Flowers	Trees	Flowers	Bench
Viewpoint	--	Side	With	Side	With	With
Contour Size	--	6 pixels	2 pixels	6 pixels	2 pixels	2 pixels
Errors (%)	12.06	5.72	24.78	3.11	21.37	13.09
Light Pixels Corrected (%)	0.09 (0.77)	0.00 (0.00)	0.33 (1.31)	0.00 (0.06)	0.59 (3.09)	0.11 (1.02)
Shadow Pixels Confirmed (%)	76.39 (85.50)	87.38 (95.33)	57.03 (70.13)	93.54 (97.65)	62.72 (72.01)	75.38 (82.79)

Table 9: Percentage of errors by only using the information of the centre texel.

As observed in Table 9, the amount of pixels that should be in shadow instead of light is a bit over 12% in average. Also as observed in this table, the amount of light pixels corrected is in average 0.09%, which is a really small amount. This is the reason why in the previous chapter it was stated that it wouldn't be worthwhile to apply this approach on light pixels. The image results of the best and worst cases can be seen below.



Figure 60: Best case of only using centre texel information with a 2048x2048 shadow map.

Observing the images of the best cases, which are results from the same scene and viewpoint, it can be observed that the image isn't as aliased as when using shadow mapping. But there is some light leaking in the areas of the contour, due to the fact that the triangle covering these points wasn't the one stored in the centre texel.

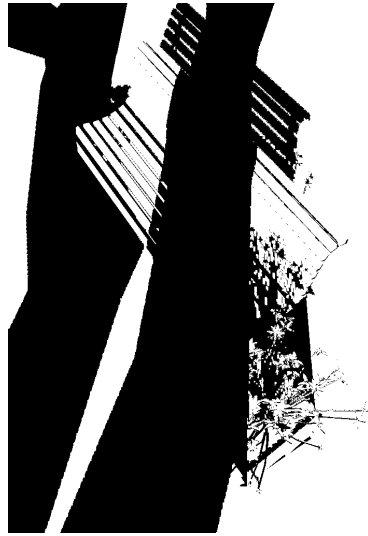


Figure 61: Worst case of using centre texel information by itself with a 2048x2048 shadow map.

In the worst cases images, also from the both scene and viewpoint, it can be observed that there is still a lot of aliasing. By using a thin contour many of the errors were not caught and were not corrected. This aliasing is most visible in the shadows cast by the flowers.



Figure 62: Average case of using centre texel information by itself.

In the medium case the shadow cast by the trees seems a little bit aliased, but the shadow cast by the flowers and the bench seem to have more errors.

4.6.USING THE INFORMATION OF THE NEIGHBOURS OF THE TEXEL

Here the results of using the information stored in the neighbouring texels will be displayed. As before, when using this approach by itself the result will be a binary shadow/lit image, where the errors will all be in the lit area.

Number of Neighbours		Average	Shadow Map				Average Case
			1024x1024		2048x2048		
			Best Case	Worst Case	Best Case	Worst Case	
4 neighbours	Scene	--	Trees	Flowers	Trees	Flowers	Bench
	Viewpoint	--	Side	With	Side	With	With
	Contour Size	--	6 pixels	2 pixels	6 pixels	2 pixels	2 pixels
	Errors (%)	6.39	0.38	16.99	0.11	14.03	7.04
	Light Pixels	6.80	6.92	10.02	3.92	7.83	6.47
	Corrected (%)	(58.20)	(95.74)	(39.82)	(97.94)	(43.48)	(61.62)
	Shadow Pixels	81.03	91.21	62.64	95.65	69.69	81.03
	Confirmed (%)	(90.68)	(99.51)	(77.02)	(99.86)	(80.01)	(89.00)
9 neighbours	Scene	--	Trees	Flowers	Trees	Flowers	Bench
	Viewpoint	--	Side	With	Side	With	With
	Contour Size	--	6 pixels	2 pixels	4/6 pixels	2 pixels	2 pixels
	Errors (%)	5.30	0.15	15.17	0.05	11.96	5.74
	Light Pixels	7.46	7.08	11.41	3.96	9.13	7.07
	Corrected (%)	(64.25)	(97.96)	(45.24)	(98.97)	(49.84)	(67.21)
	Shadow Pixels	82.61	91.51	64.93	95.74	72.65	83.03
	Confirmed (%)	(92.46)	(99.83)	(79.83)	(99.95)	(83.41)	(91.20)

Table 10: Percentage of errors by only using the information of the centre and neighbouring texels.

The cases above are the same as when using only the centre texel (with the exception of one of the best cases sharing its status when using only 4 pixel thick contours), but with better results. The average of errors here are below 7% and 6% when using four and nine neighbours respectively. The results also show that using nine neighbours offers better results than when using only four, so in the algorithm nine neighbours will be used. Below follow the images of these cases. Since the reasoning in this cases is the same as when using only the centre texel, there will be no need to repeat what was said before.



Figure 63: Best case of only using information of four neighbouring texels with a 2048x2048 shadow map.



Figure 64: Best case of only using information of nine neighbouring texels with a 2048x2048 shadow map.

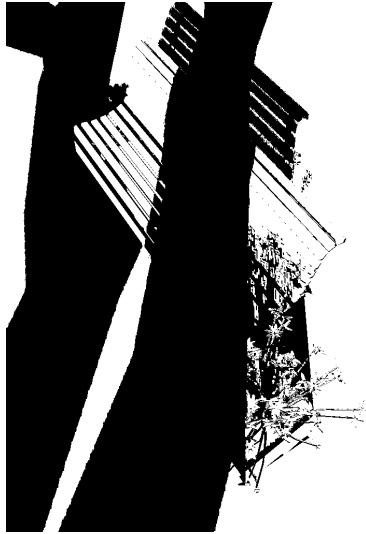


Figure 65: Worst case of only using information of four neighbouring texels with a 2048x2048 shadow map.



Figure 66: Worst case of only information of nine neighbouring texels with a 2048x2048 shadow map.



Figure 67: Average case of only using information of four neighbouring texels.



Figure 68: Average case of only using information of nine neighbouring texels.

Below is Figure 69 that displays the averages of results when using the neighbouring texels method with nine texels.

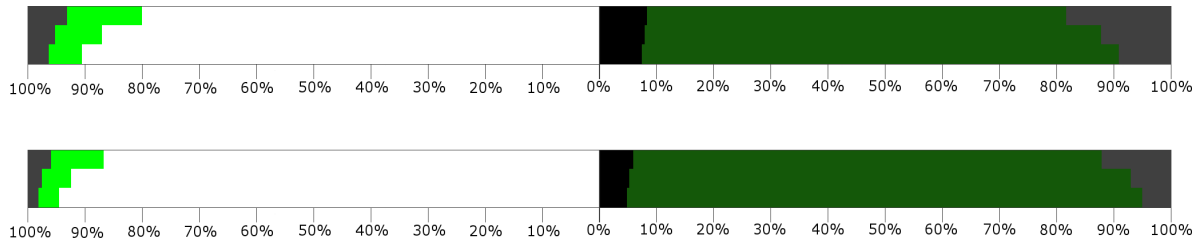


Figure 69: Average results of neighbouring texels with nine texels separated by contour thickness with a 1024x1024 shadow map (top) and a 2048x2048 shadow map (bottom).

4.7.USING GEOMETRIC ADJACENCY INFORMATION

In this section the results of using the information of the adjacent geometry will be displayed.

Adjacency Levels		Average	Shadow Map				Average Case
			1024x1024		2048x2048		
			Best Case	Worst Case	Best Case	Worst Case	
1 level	Scene	--	Primitives	Flowers	Primitives	Flowers	Bench
	Viewpoint	--	With	With	With	With	With
	Contour Size	--	6 pixels	2 pixels	6 pixels	2 pixels	2 pixels
	Errors (%)	8.93	3.38	21.17	1.46	16.27	9.64
	Light Pixels Corrected (%)	0.17 (1.42)	0.00 (0.00)	0.68 (2.66)	0.00 (0.00)	1.12 (5.91)	0.22 (2.03)
	Shadow Pixels Confirmed (%)	82.71 (92.59)	92.27 (96.00)	64.12 (78.84)	96.26 (98.44)	72.53 (83.27)	82.21 (90.29)
2 levels	Scene	--	Primitives	Flowers	Primitives	Flowers	Bench
	Viewpoint	--	With	With	With	With	With
	Contour Size	--	6 pixels	2 pixels	6 pixels	2 pixels	2 pixels
	Errors (%)	7.19	1.85	18.25	0.84	12.28	7.29
	Light Pixels Corrected (%)	0.25 (2.14)	0.00 (0.00)	1.11 (4.33)	0.00 (0.00)	1.55 (8.13)	0.28 (2.64)
	Shadow Pixels Confirmed (%)	86.19 (96.51)	95.97 (99.86)	69.69 (85.69)	97.76 (99.97)	80.21 (92.09)	86.87 (95.41)

Table 11: Percentage of errors by only using the information of the centre texel and the adjacent geometry.

As observed in the previous chapter, the average percentage of errors when using adjacent geometry is higher than when using neighbouring texel information, due to the fact that this case isn't very effective in correcting pixels that are incorrectly in light. Also, as what happened when using the information of the centre texel only, the percentage of light pixels corrected by this approach is extremely low, so this approach won't be used on light pixels in the algorithm. As also observed in the table, by using two levels of adjacency the results are better, so this is what will be used in the algorithm. The observation of the best, worst and middle cases are below.

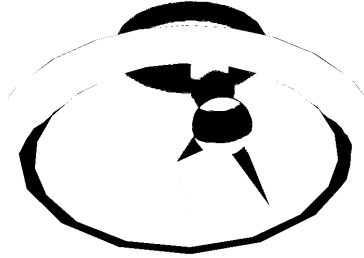


Figure 70: Best case of only using centre and first level of adjacent geometry information with a 2048x2048 shadow map.

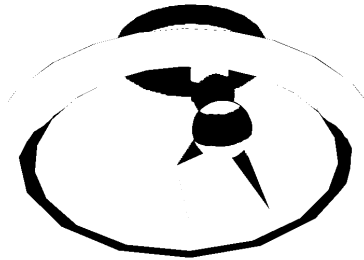


Figure 71: Best case of only using centre and second level of adjacent geometry information with a 2048x2048 shadow map.

The best case here has changed in relation to the previous approaches. This may be due to the fact that the “trees” scene has many overlapping branches and this approach isn’t very effective in getting information of triangles from another branch. On the other hand, in the best case presented here there is barely any object overlap, with almost all of the shadows seen being from the torus, so getting nearby triangles here is much more effective.

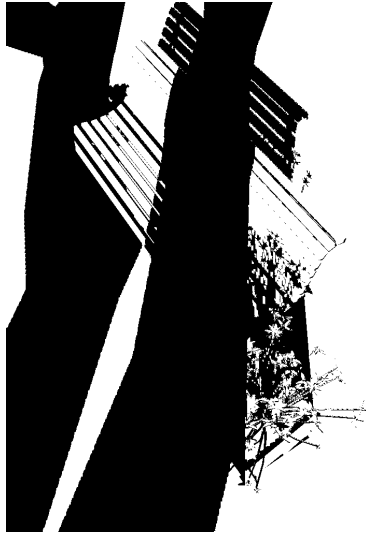


Figure 72: Worst case of only using centre and first level of adjacent geometry information with a 2048x2048 shadow map.

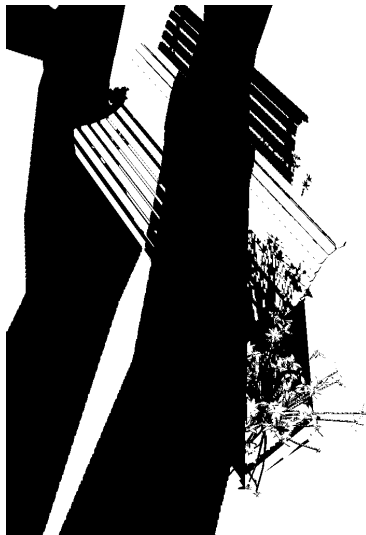


Figure 73: Worst case of only using centre and second level of adjacent geometry information with a 2048x2048 shadow map.

The worst cases are still the same, with the same reasoning as before behind the problems found.



Figure 74: Average case of only using centre and first level of adjacent geometry information.



Figure 75: Average case of only using centre and second level of adjacent geometry information.

In the medium case the aliasing in the shadows cast by the trees is slightly visible, where in the neighbouring texel results it has practically disappeared. The shadows cast by the bench seem good, but in the shadows cast by the flowers some errors can still be observed.

And below Figure 76 shows the average results for the adjacent geometry approach when used with two levels of adjacency.

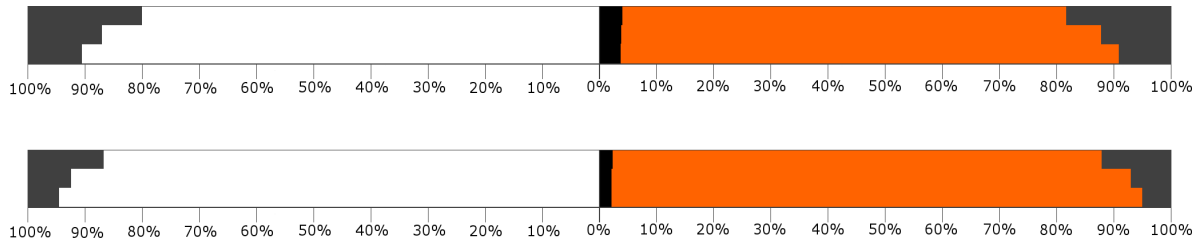


Figure 76: Average results of adjacent geometry with two levels of adjacency separated by contour thickness with a 1024x1024 shadow map (top) and a 2048x2048 shadow map (bottom).

4.8.PUTTING IT ALL TOGETHER

Here the results of chaining the methods will be presented. Since the texel coherence step is the first one the result of using it by itself in this chaining will be the same, so the information will not be repeated here.

Below follows the table of the next step of the algorithm that uses the neighbouring texels to confirm extra shadow pixels and correct some of the light pixels. The percentage of the light pixels that will be corrected will be added to the confirmations in light of the texel coherence step to attain the total percentage of light pixels that don't need confirmation or correcting.

	Average	Shadow Map				Average Case
		1024x1024		2048x2048		
		Best Case	Worst Case	Best Case	Worst Case	
Scene	--	Primitives	Trees	Primitives	Trees	Bench
Viewpoint	--	With	Against	With	With	With
Contour Size	--	6 pixels	2 pixels	6 pixels	2 pixels	2 pixels
Confirmations (%)	75.04	88.16	49.09	94.27	58.71	76.36
Confirmations/Corrections in Light (%)	65.98	85.43	26.97	92.50	39.68	66.79
Confirmations in Shadow (%)	84.13	92.00	71.13	96.77	77.68	86.04

Table 12: Percentage of confirmations by algorithm after using neighbouring texel information.

The average percentages of confirmations have risen about 5% each in relation to the previous step. Now the pixels that are confirmed average 75% of the total amount of pixels in the contours, so only 25% pixels remain for confirmation. The best, worst and middle case scenario images are shown below.



Figure 77: Best case of algorithm pixel confirmation after using information of the neighbouring texels with a 2048x2048 shadow map.

The best case scenarios still are the same, with a slight increase of percentage of confirmed pixels, between a 1% and 2% increase.



Figure 78: Worst case of algorithm pixel confirmation after using information of the neighbouring texels with a 2048x2048 shadow map.

The worst cases seen above have an increase of confirmations of over 10% in relation to the previous step. Now even the worst cases have almost or even over 50% of pixel confirmations, depending in the resolution of the shadow map.



Figure 79: Average case of algorithm pixel confirmation after using information of the neighbouring texels.

The amount of confirmed pixels in the medium case has increased by approximately 5%, with light pixels seeing a 7% confirmation increase and shadow pixels seeing an increase of over 3% of pixels confirmed. By observing Figure 79, the shadows cast by the trees are steadily losing unconfirmed pixels, and even in the shadows cast by the flowers and the bench the grey pixels demarking confirmed pixels are starting to be more visible.

The graphics below present the average of results of the algorithm after the neighbouring texel step.

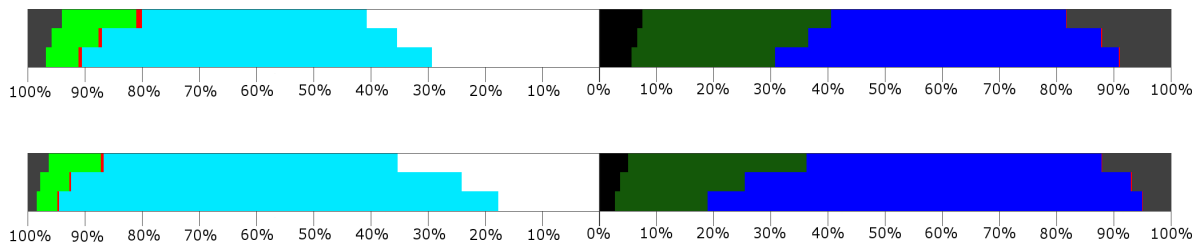


Figure 80: Average results of the algorithm after the neighbouring texel step separated by contour thickness with a 1024x1024 shadow map (top) and a 2048x2048 shadow map (bottom).

Following below are the results of the algorithm after passing through the adjacent geometry step.

	Average	Shadow Map				Average Case
		1024x1024		2048x2048		
		Best Case	Worst Case	Best Case	Worst Case	
Scene	--	Primitives	Trees	Primitives	Trees	Bench
Viewpoint	--	With	Against	With	With	With
Contour Size	--	6 pixels	2 pixels	6 pixels	2 pixels	2 pixels
Confirmations (%)	76.74	89.81	49.52	94.68	58.82	78.00
Confirmations in Shadow (%)	87.63	96.00	71.98	97.78	85.63	89.34

Table 13: Percentage of confirmations by algorithm after using adjacent geometry information.

As seen above, the average of confirmations has risen almost 2%, with the confirmations in shadow increasing 3% in average. The best, worst and middle cases will be seen below.



Figure 81: Best case of algorithm pixel confirmation after using information of the adjacent geometry with a 2048x2048 shadow map.

The best cases see a slight increase in confirmations, with a 1% increase when using a 1024x1024 shadow map and an under 0.5% increase when using a 2048x2048 shadow map.



Figure 82: Worst case of algorithm pixel confirmation after using information of the adjacent geometry with a 2048x2048 shadow map.

The worst cases have increases in confirmation of less than 1%, so in these cases this step didn't change the result much.



Figure 83: Average case of algorithm pixel confirmation after using information of the adjacent geometry.

In the medium case result the increase of pixel confirmation is over 1%, with the confirmation of shadow pixels increasing over 3%, almost reaching a 90% pixel confirmation. This is visible in Figure 83 with the increase of grey pixels in the shadows cast by the flowers.

The graphics seen in Figure 84 below show the average of results of the algorithm after the adjacent geometry step.

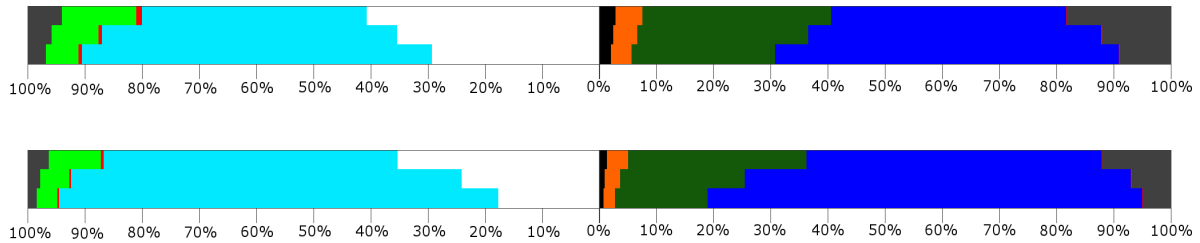


Figure 84: Average results of the algorithm after the adjacent geometry step separated by contour thickness with a 1024x1024 shadow map (top) and a 2048x2048 shadow map (bottom).

And finally below the graphics will mark with yellow the pixels that remained not hinted, uncorrected or unconfirmed.

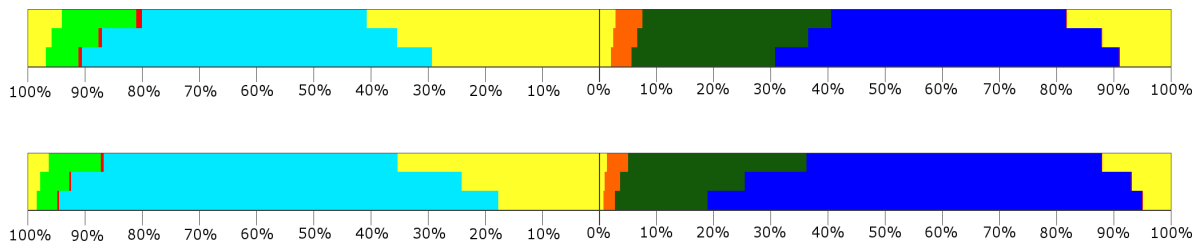


Figure 85: Average results of the algorithm after the adjacent geometry step with pixels that were not confirmed, corrected or hinted marked, separated by contour thickness with a 1024x1024 shadow map (top) and a 2048x2048 shadow map (bottom).

4.9.FINAL OBSERVATIONS

As seen above, after the proposed algorithm an average of 75% of the pixels in the contours is confirmed, leaving around 25% unconfirmed pixels. These pixels can then be passed to a ray-tracer to be tested, effectively decreasing the pixels in the contour that need ray-tracing to an average of one fourth of the total amount of contour pixels. After using ray-tracing, the errors that the contours will have will only be those introduced in the texel coherence step.

	Average	Shadow Map				Average Case
		1024x1024		2048x2048		
		Best Case	Worst Case	Best Case	Worst Case	
Scene	--	Trees	Flowers	Trees	Flowers	Bench
Viewpoint	--	Side	With	Side	With	With
Contour Size	--	2/4 pixels	2 pixels	2/4/6 pixels	2 pixels	2 pixels
Wrong Confirmations (%)	0.33	0.00	1.59	0.00	0.93	0.37
Wrong Confirmations in Light (%)	0.55	0.04	0.00	0.03	0.00	0.56
Wrong Confirmations in Shadow (%)	0.12	0.00	0.00	0.00	0.00	0.17

Table 14: Percentage of wrong confirmations after applying the algorithm and ray-tracing uncertain pixels.

The best cases are only an example, as the other viewpoints of the “trees” scene also have examples where the amount of confirmation errors is zero. The best cases come from the scene where the triangles are bigger and the worst cases come from the scene where the triangles are smaller and the viewpoint captures much of the shadows of these small triangles. This might imply that bigger triangles allow for fewer errors in the results of the algorithm.

But as it has also been observed throughout the chapter, the amount of shadow pixels that remain unconfirmed and that should be in light seems bigger than those that are also unconfirmed but should stay in shadow. To better observe this, following below are the percentages of incorrect pixels if uncertain pixels are left in light.

	Average	Shadow Map				Average Case
		1024x1024		2048x2048		
		Best Case	Worst Case	Best Case	Worst Case	
Scene	--	Trees	Flowers	Trees	Flowers	Bench
Viewpoint	--	Side	With	Side	With	With
Contour Size	--	6 pixels	2 pixels	6 pixels	2 pixels	2 pixels
Wrong Confirmations (%)	2.98	0.08	11.19	0.02	7.15	2.80
Wrong Confirmations in Light (%)	4.05	0.15	14.16	0.04	9.81	3.55
Wrong Confirmations in Shadow (%)	1.89	0.01	8.03	0.00	4.40	2.05

Table 15: Percentage of wrongly defined pixels if uncertain pixels after algorithm are left in light.

The scenes and viewpoints here are the same as in the previous table, so the introduction of errors by letting all of the uncertain pixels stay in light doesn’t seem to change much in the difference of quality between scenes. As observed above, if unconfirmed pixels are changed

to light, the average of errors is less than 3%, which presents a better result than the 11% average of the shadow mapping results. Although this result is better, it isn't totally sure that the quality increase is actually perceptible when observing the image. Below are the images of the cases shown in the tables above. The orange pixels are pixels that were incorrectly confirmed by texel coherence and the red pixels are pixels that are incorrectly lit if the uncertain pixels are left as lit. Besides this, there are also blue pixels that mark errors that weren't caught inside the contours. There isn't any information of these pixels in the two previous tables but this allows the visualization of all of the errors that remained in each case.



Figure 86: Marked errors of the best case when using a 2048x2048 shadow map.



Figure 87: Marked errors of the worst case when using a 2048x2048 shadow map.



Figure 88: Marked errors of the average case.

5. CONCLUSIONS AND FUTURE WORK

Shadow mapping is probably the most used algorithm to compute shadows in real time. The performance of the algorithm is very high, but it has severe issues that cause aliased shadow contours.

Ray-tracer on the other hand is capable of producing pixel perfect shadows. Yet, from a performance point of view is not as friendly.

Shadow mapping has been a deeply studied algorithm, with many researchers proposing improvements to its quality without compromising its efficiency. Most of the new approaches focus only on the original method, or variations thereof.

Nevertheless some researchers have developed hybrid methods, combining shadow mapping with ray-tracing. The main goal of these hybrid methods is to obtain visual results that closely match ray-traced shadows, while not fully compromising performance. The main approach is therefore to use a first pass with shadow mapping and use this information to determine which pixels should be ray-traced. Ideally this set of pixels should be a small subset of the original rendered image.

One of these methods focuses on the contours of the shadows, and uses texel coherence to determine if a pixel should be ray-traced. Pixels that have texel coherence are those that project onto a texel which has an identical shadow status to the neighbouring texels. For instance if a pixel projects onto a texel which indicates a shadow, and the neighbouring texels also indicate a shadow, then said pixel has texel coherence.

This work established the theme for this thesis. The main goals are to quantify the assumptions being made on the referred work, and to discover other methods to reduce the subset of pixels that require ray-tracing, i.e. those whose shadow status can't be determined for sure using only the shadow map information.

As for the first goal, it was verified that in average the vast majority of shadow mapping errors are indeed in the contour areas of the shadows in the rendered image. As for using texel coherence as a hint for the shadow status it was verified that in average roughly half of the contour pixels have texel coherence, with only a small percentage of those being

incorrectly hinted. However it was also found that the percentage varies wildly with the scene, achieving values as low as less than 3% of the contour pixels.

The second goal was to reduce the subset of pixels that require ray-tracing. To achieve this a number of techniques that significantly reduce the size of this subset have been developed. These methods rely solely on the information about which triangles are recorded on the shadow map, and one of them also uses geometric adjacency information.

The techniques are able to confirm pixels in shadow and/or detect incorrect pixels in light. Note that it is not possible to correct a pixel in shadow with this limited information, since that would imply a guarantee that there is no triangle in the scene that causes a shadow to the said pixel. The methods work on very limited information, having access to only the triangles that are recorded on the shadow map, and geometric adjacency information, hence no assurances can be made regarding the remaining triangles. Similarly, for a pixel originally in light it is not possible to confirm it, as that would imply a guarantee that no triangle in the scene intersects the light ray.

The first technique is to determine if the light ray for that pixel intersects the triangle which covered the respective texel. For pixels in shadow if an intersection occurs then the pixel is definitely in shadow, otherwise the test is not conclusive. For pixels in light, it is usually the case that the triangle that covers the texel is further away from the light than the said pixel. Special situations where this is not the case have been properly identified but their occurrence is too rare to compensate the effort.

Extending this test to neighbouring texels provides potentially more triangles to test, with the upper limit of as many triangles as neighbouring texels. With this approach not only a larger set of confirmed pixels in shadow can be obtained but also a good amount of pixels erroneously in light can be corrected.

The adjacency information allows to further confirmation of pixels in shadow, but it is not very successful at correcting pixels originally in light.

Since each method has its strengths, a pipeline was proposed where in each stage the input are the pixels that were not confirmed/correct in the previous stages. The lightest methods

were placed on the beginning of the pipeline to limit the heavier methods to as few pixels as possible.

While texel coherence is not capable of actually confirming/correcting pixels it does provide a strong hint regarding the shadow status, and the number of pixels hinted can be very significant. Under this context, and since this method is as fast as shadow mapping itself, texel coherence could be used in a dynamic approach when the frame rate drops below a certain threshold.

The final number of pixels that remain unconfirmed/uncorrected is significantly reduced with this pipeline when compared to texel coherence per se hence the goals of this work have been achieved.

As further work we would like to implement the above mentioned pipeline as a GPU solution, using only shaders, and evaluate its performance. Ray-tracing the unconfirmed/uncorrected pixels could be performed for instance with OptiX. A full evaluation performance could then be completed to evaluate the merits of the proposed solution.

6. BIBLIOGRAPHY

Agrawala, M., Ramamoorthi, R., Heirich, A., & Moll, L. (2000). Efficient Image-Based Methods for Rendering Soft Shadows. *Proceedings of SIGGRAPH, Computer Graphics Proceedings, Annual Conference Series* (pp. 375-384). ACM.

Annen, T., Mertens, T., Bekaert, P., Seidel, H., & Kautz, J. (2007). Convolution Shadow Maps. *Rendering Techniques 2007, volume 1 of Eurographics/ACMSIGGRAPH Symposium Proceedings* (pp. 51-60). Eurographics.

Annen, T., Mertens, T., Seidel, H., Flerackers, E., & Kautz, J. (2008). Exponential Shadow Maps. *Proceedings of Graphics Interface 2008* (pp. 155-161). Ontario, Canada: Canadian Information Processing Society.

Barbec, S., Annen, T., & Seidel, H. (2002). *Practical Shadow Mapping*.

Beister, M., Ernst, M., & Stamminger, M. (2005). A Hybrid GPU-CPU Renderer. *VMV 2005*.

Chan, E., & Durand, F. (2004). An Efficient Hybrid Shadow Rendering Algorithm. *Proceedings of the Eurographics Symposium on Rendering* (pp. 185-195). Norrköping, Sweden: Eurographics Association.

Dempski, K., & Viale, E. (2004). *Advanced Lighting and Materials with Shaders*. Wordware Publishing Inc.

Donnelly, W., & Lauritzen, A. (2006). *Variance Shadow Maps*. ID3.

Fernando, R., Fernandez, S., Bala, K., & Greenberg, D. P. (2001). Adaptive Shadow Maps. *Proceedings of ACM SIGGRAPH 2001, ACM Press/ACM SIGGRAPH, Computer Graphics Proceedings, Annual Conference Series* (pp. 387-390). ACM.

Hertel, S., Hormann, K., & Westermann, R. (2009). A hybrid GPU rendering for alias-free hard shadows. In D. Ebert, & J. Krüger (Ed.), *Eurographics 2009 Areas Papers* (pp. 59-66). München, Germany: Eurographics Association.

Jensen, H. W. (2001). *Realistic Image Synthesis Using Photon Mapping*. A. K. Peters.

- Lafortune, E. P., & Willems, Y. D. (1993). Bidirectional Path Tracing. *Compugraphics '93*, (pp. 95-104).
- Martin, T., & Tanin, T. (2004). Anti-aliasing and Continuity with Trapezoidal Shadow Maps. *Proceedings of Eurographics Symposium on Rendering*.
- Möller, T., & Trumbore, B. (1997). Fast, Minimum Storage Ray/Triangle Intersection. *journal of graphics, gpu, and game tools* , 2, 21-28.
- Reeves, W. T., Salesin, D. H., & Cook, R. L. (1987). Rendering antialiased shadows with depth maps. *Proceedings of the 14th annual conference on Computer graphics and interactive techniques* (pp. 283-291). New York: ACM.
- Sen, P., Cammarano, M., & Hanrahan, P. (2003, July). Shadow Silhouette Maps. *ACM Transactions on Graphics (TOG) - Proceedings of ACM SIGGRAPH 2003* , 521-526.
- Stamminger, M., & Drettakis, G. (2002). Perspective Shadow Maps. *Proceedings of ACM SIGGRAPH 2002*.
- Tadamura, K., Qin, X., Jiao, G., & Nakamae, E. (2001). *The Visual Computer* (Vol. 17). Springer.
- Whitted, T. (1980). *An Improved Illumination Model for Shaded Display* (6 ed., Vol. 23). New York, NY, USA: ACM.
- Williams, L. (1978). Casting Curved Shadows on Curved Surfaces. *Computer Graphics (SIGGRAPH 1978 Proceedings)*, (pp. 270-274).
- Wimmer, M., Scherzer, D., & Purgathofer, W. (2004). Light Space Perspective Shadow Maps. *Proceedings of the 2nd EG Symposium on Rendering*. Springer Computer Science, Eurographics.
- Xie, F., Tabellion, E., & Pearce, A. (2007). Soft Shadows by Ray Tracing Multilayer Transparent Shadow Maps. *Proceedings of the Eurographics Symposium on Rendering*.
- Zhang, F., Sun, H., Xu, L., & Lun, L. K. (2006). Parallel-split Shadow Maps for Large-scale Virtual Environments. *Proceedings of the 2006 ACM International Conference on Virtual Reality Continuum and its Applications* (pp. 311-318). New York: VRCIA '06, ACM.

APPENDIX

This appendix will display results for the tested scenes that weren't presented in chapter 4. The results being presented for these viewpoints will be the same as in the viewpoints displayed in the referred sub-chapters.

The results of the "side" viewpoint of the "primitives" scene follow below.



Figure 89: Result of the ray-tracing approach for the side viewpoint of the primitives scene.



Figure 90: Result of the shadow mapping approach for the side viewpoint of the primitives scene.



Figure 91: Result of texel coherence with four texels for the side viewpoint of the primitives scene.



Figure 92: Result of texel coherence with nine texels for the side viewpoint of the primitives scene.



Figure 93: Result of the single texel approach on the side viewpoint of the primitives scene.



Figure 94: Result of the neighbour texels approach using four neighbours for the side viewpoint of the primitives scene.



Figure 95: Result of the neighbour texels approach using nine neighbours for the side viewpoint of the primitives scene.



Figure 96: Result of the adjacent geometry approach with one level of adjacency for the side viewpoint of the primitives scene.



Figure 97: Result of the adjacent geometry approach with two levels of adjacency for the side viewpoint of the primitives scene.



Figure 98: Result of the algorithm with a six pixel thick contour and a 2048x2048 resolution shadow map for the side viewpoint of the primitives scene.

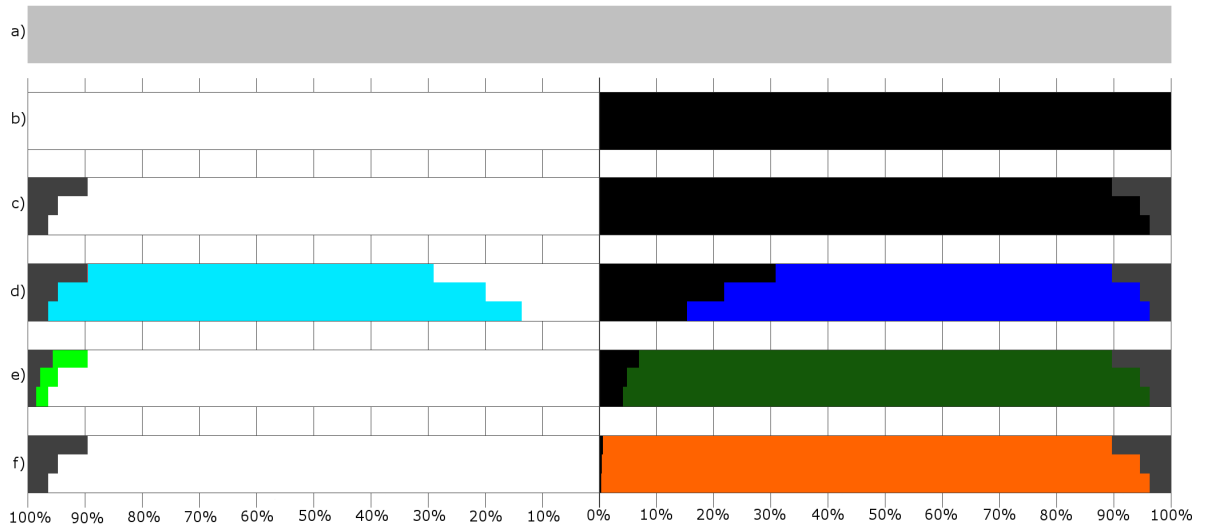
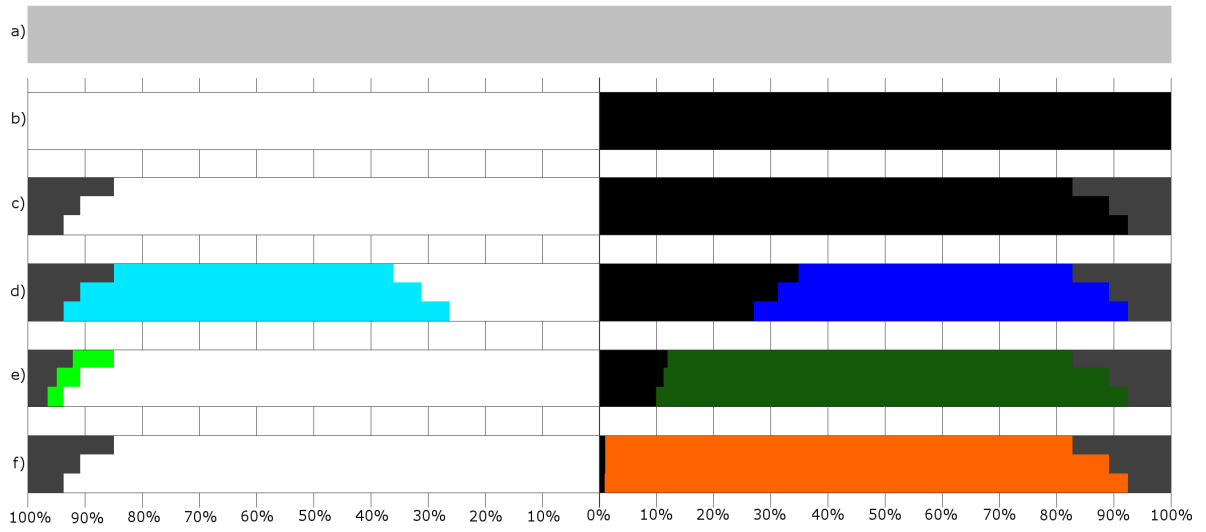


Figure 99: Corrected/confirmed/hinted contour pixels by each method for the side viewpoint of the primitives scene using a 1024x1024 (top) and a 2048x2048 (bottom) resolution shadow map.

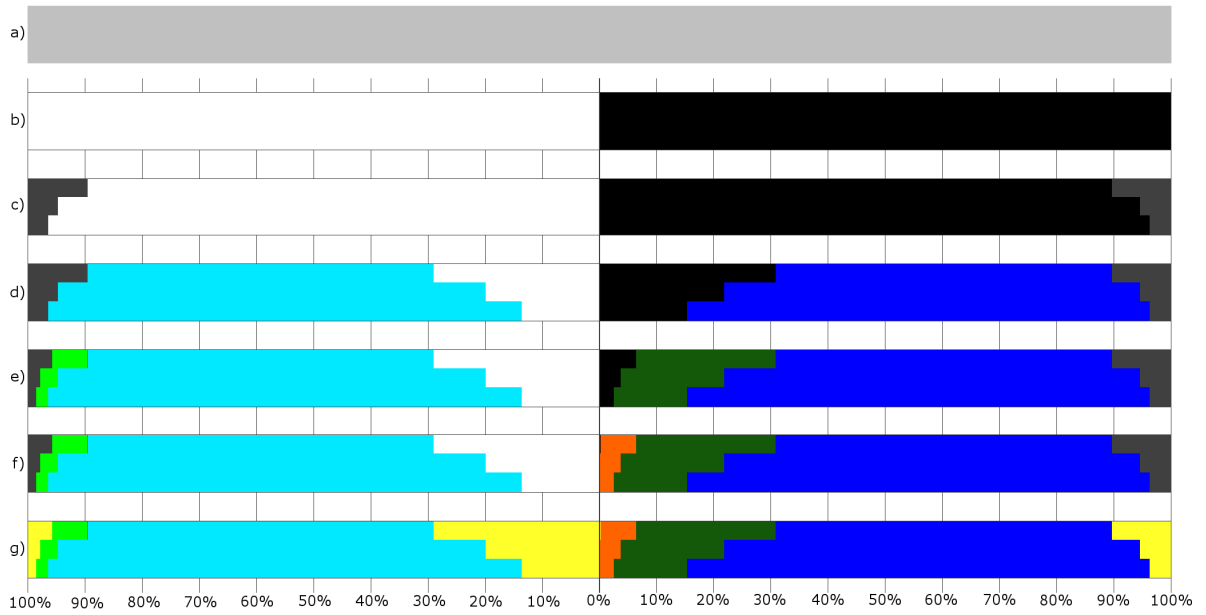
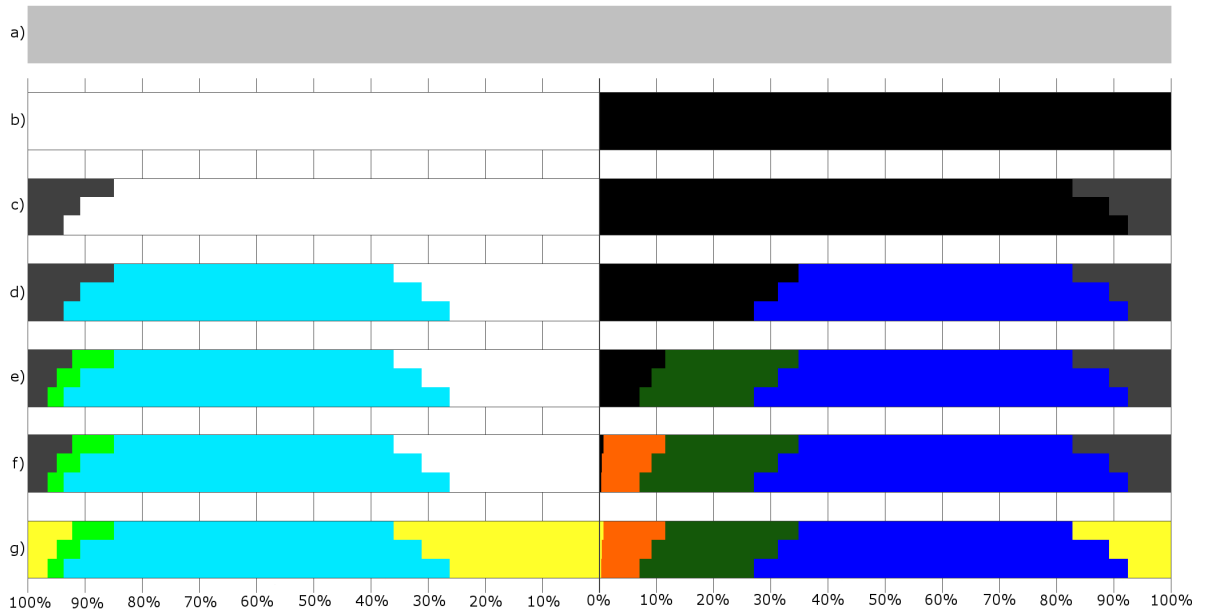


Figure 100: Corrected/confirmed/hinted contour pixels by the chaining of methods for the side viewpoint of the primitives scene using a 1024x1024 (top) and a 2048x2048 (bottom) resolution shadow map.

Shadow Map Resolution	Approach	Contour Thickness			
		Two Pixels	Four Pixels	Six Pixels	Whole Image
1024x1024	Pixels in Contour	11000	21482	31683	1048576
	Shadow Map	1769 (16.08%)	2138 (9.95%)	2164 (6.83%)	2164 (0.21%)
	Single Texel	1973 (17.94%)	3418 (15.91%)	4458 (14.07%)	17500 (1.67%)
	Neighbour Texels (4Neighbours)	1384 (12.58%)	2256 (10.50%)	2790 (8.81%)	7345 (0.70%)
	Neighbour Texels (9 Neighbours)	1086 (9.87%)	1729 (8.05%)	2077 (6.56%)	5004 (0.48%)
	Adjacent Geometry (One Level)	1401 (12.74%)	2068 (9.63%)	2403 (7.58%)	4812 (0.46%)
	Adjacent Geometry (Two Level)	903 (8.21%)	1129 (5.26%)	1184 (3.74%)	1290 (0.12%)
2048x2048	Pixels in Contour	10750	21022	31047	1048576
	Shadow Map	1111 (10.33%)	1123 (5.34%)	1123 (3.62%)	1123 (0.11%)
	Single Texel	1452 (13.51%)	2136 (10.16%)	2833 (9.12%)	9989 (0.95%)
	Neighbour Texels (4 Neighbours)	796 (7.40%)	1027 (4.89%)	1231 (3.96%)	2486 (0.24%)
	Neighbour Texels (9 Neighbours)	608 (5.66%)	733 (3.49%)	858 (2.76%)	1620 (0.15%)
	Adjacent Geometry (One Level)	855 (7.95%)	990 (4.71%)	1115 (3.59%)	1754 (0.17%)
	Adjacent Geometry (Two Level)	609 (5.67%)	630 (3.00%)	638 (2.05%)	682 (0.07%)

Table 16: Difference between the approaches that use ray-tracing and the actual ray-tracer for the side viewpoint of the primitives scene.

Shadow Map Resolution	Contour Thickness		
	Two Pixels	Four Pixels	Six Pixels
1024x1024	1769 of 2164 (81.75%)	2138 of 2164 (98.80%)	2164 of 2164 (100.00%)
2048x2048	1111 of 1123 (98.93%)	1123 of 1123 (100.00%)	1123 of 1123 (100.00%)

Table 17: Wrongly defined pixels in the shadow mapping result which are inside the contour in the side viewpoint of the primitives scene.

Shadow Map Resolution	Contour Thickness	Pixel Shading	
		Light	Shadow
1024x1024	Two Pixels	845 of 5633	924 of 5367
	Four Pixels	1022 of 11189	1116 of 10293
	Six Pixels	1034 of 16711	1130 of 14972
	Whole Image	1034 of 979478	1130 of 69098
2048x2048	Two Pixels	575 of 5541	536 of 5209
	Four Pixels	580 of 11067	543 of 9955
	Six Pixels	580 of 16564	543 of 14483
	Whole Image	580 of 979611	543 of 68965

Table 18: Pixels that the shadow map defines wrongly in the side viewpoint of the primitives scene, separated in pixels defined in light and in shadow, compared to the total amount of pixels lighted in the same way.

Shadow Map Resolution	Contour Thickness	Texel Coherence					
		Light			Shadow		
		Confirmed	Incorrectly Confirmed	Undecided	Confirmed	Incorrectly Confirmed	Undecided
1024x1024	Two Pixels	2755 (48.91%)	3 (0.05%)	2878 (51.09%)	2570 (47.89%)	0 (0.00%)	2797 (52.11%)
	Four Pixels	6674 (59.65%)	3 (0.03%)	4515 (40.35%)	5953 (57.84%)	0 (0.00%)	4340 (42.16%)
	Six Pixels	11288 (67.55%)	3 (0.02%)	5423 (32.45%)	9787 (65.37%)	0 (0.00%)	5185 (34.63%)
	Whole Image	973603 (99.40%)	3 (0.00%)	5875 (0.60%)	63578 (92.01%)	0 (0.00%)	5520 (7.99%)
2048x2048	Two Pixels	3356 (60.57%)	3 (0.05%)	2185 (39.43%)	3064 (58.82%)	0 (0.00%)	2145 (41.18%)
	Four Pixels	8276 (74.78%)	3 (0.03%)	2791 (25.22%)	7233 (72.66%)	0 (0.00%)	2722 (27.34%)
	Six Pixels	13713 (82.79%)	3 (0.02%)	2851 (17.21%)	11715 (80.89%)	0 (0.00%)	2768 (19.11%)
	Whole Image	976720 (99.70%)	3 (0.00%)	2891 (0.30%)	66193 (95.98%)	0 (0.00%)	2772 (4.02%)

Table 19: Pixel confirmation when using texel coherence with four texels for the side viewpoint of the primitives scene.

Shadow Map Resolution	Contour Thickness	Texel Shadowing							
		Light				Shadow			
		3 shadow/1 light	3 shadow/1 light in ray-tracer shadow	1 shadow/3 light	1 shadow/3 light in ray-tracer light	3 shadow/1 light	3 shadow/1 light in ray-tracer shadow	1 shadow/3 light	1 shadow/3 light in ray-tracer light
1024x1024	Two Pixels	629	437	1038	1004	922	892	666	462
	Four Pixels	675	454	1671	1630	1461	1428	717	489
	Six Pixels	675	454	2028	1987	1763	1728	717	489
	Whole Image	675	454	2377	2336	1992	1957	717	489
2048x2048	Two Pixels	310	229	774	737	718	698	326	227
	Four Pixels	310	229	1046	1009	952	932	326	227
	Six Pixels	310	229	1103	1066	994	974	326	227
	Whole Image	310	229	1143	1106	998	978	326	227

Table 20: Pixel shadowing for pixels that don't achieve texel coherence with four texels for the side viewpoint of the primitives scene.

Shadow Map Resolution	Contour Thickness	Texel Coherence					
		Light			Shadow		
		Confirmed	Incorrectly Confirmed	Undecided	Confirmed	Incorrectly Confirmed	Undecided
1024x1024	Two Pixels	2572 (45.66%)	1 (0.02%)	3061 (54.34%)	2505 (46.67%)	0 (0.00%)	2862 (53.33%)
	Four Pixels	5358 (47.89%)	1 (0.01%)	5831 (52.11%)	4820 (46.83%)	0 (0.00%)	5473 (53.17%)
	Six Pixels	8677(51.92%)	1 (0.01%)	8034(48.08%)	7512(50.17%)	0 (0.00%)	7460(49.83%)
	Whole Image	967426(98.77%)	1 (0.00%)	12052(1.23%)	58152(84.16%)	0 (0.00%)	10946(15.84%)
2048x2048	Two Pixels	2719 (49.07%)	2 (0.04%)	2822 (50.93%)	2564 (49.22%)	0 (0.00%)	2645 (50.78%)
	Four Pixels	6400 (57.83%)	2 (0.02%)	4667 (42.17%)	5577 (56.02%)	0 (0.00%)	4378 (43.98%)
	Six Pixels	11034 (66.61%)	2 (0.01%)	5530 (33.39%)	9290 (64.14%)	0 (0.00%)	5193 (35.86%)
	Whole Image	973682 (99.39%)	2 (0.00%)	5929 (0.61%)	63477 (92.04%)	0 (0.00%)	5488 (7.96%)

Table 21: Pixel confirmation when using texel coherence with nine texels for the side viewpoint of the primitives scene.

Shadow Map Lighting	Texel Shadowing	Shadow Map							
		1024x1024				2048x2048			
		Two Pixels	Four Pixels	Six Pixels	Whole Image	Two Pixels	Four Pixels	Six Pixels	Whole Image
Light	8 S-1 L	0	0	0	0	0	0	0	0
	8 S-1 L in RT Shadow	0	0	0	0	0	0	0	0
	7 S-2 L	14	22	22	22	2	2	2	2
	7 S-2 L in RT Shadow	14	18	18	18	2	2	2	2
	6 S-3 L	35	42	42	42	5	5	5	5
	6 S-3 L in RT Shadow	18	19	19	19	2	2	2	2
	5 S-4 L	52	91	99	99	23	23	23	23
	5 S-4 L in RT Shadow	13	15	15	15	5	5	5	5
	4 S-5 L	952	1581	1739	1742	763	842	842	842
	4 S-5 L in RT Light	466	999	1157	1160	462	540	540	540
	3 S-6 L	1219	2280	3069	4455	1265	2026	2378	2443
	3 S-6 L in RT Light	925	1914	2691	4077	1005	1762	2114	2179
	2 S-7 L	455	892	1337	2226	398	737	916	1021
	2 S-7 L in RT Light	437	872	1317	2206	397	736	915	1020
1 S-8 L	334	923	1726	3466	366	1032	1364	1593	
1 S-8 L in RT Light	333	922	1725	3465	364	1030	1362	1591	
Shadow	8 S-1 L	146	593	1233	2637	246	852	1139	1308
	8 S-1 L in RT Shadow	145	591	1230	2634	246	852	1139	1308
	7 S-2 L	428	839	1217	1922	347	647	821	880
	7 S-2 L in RT Shadow	409	817	1192	1897	337	637	811	870
	6 S-3 L	1174	2230	3054	4431	1251	2008	2362	2429
	6 S-3 L in RT Shadow	834	1811	2625	4002	1022	1774	2128	2195
	5 S-4 L	1025	1694	1832	1832	756	825	825	825
	5 S-4 L in RT Shadow	541	1116	1254	1254	495	562	562	562
	4 S-5 L	23	37	44	44	22	23	23	23
	4 S-5 L in RT Light	16	20	20	20	13	13	13	13
	3 S-6 L	27	28	28	28	11	11	11	11
	3 S-6 L in RT Light	25	25	25	25	11	11	11	11
	2 S-7 L	11	11	11	11	4	4	4	4
	2 S-7 L in RT Light	11	11	11	11	4	4	4	4
1 S-8 L	28	41	41	41	8	8	8	8	
1 S-8 L in RT Light	28	39	39	39	8	8	8	8	

Table 22: Pixel shadowing for pixels that don't achieve texel coherence with nine texels for the side viewpoint of the primitives scene.

Shadow Map Resolution	Contour Thickness	Corrected		Turned Bad		Maintained Correct		Maintained Incorrect	
		L→S	S→L	L→S	S→L	L→L	S→S	L→L	S→S
1024x1024	Two Pixels	3	924	0	1131	4966	3312	842	0
	Four Pixels	3	1116	0	2399	10487	6778	1019	0
	Six Pixels	3	1130	0	3427	15984	10415	1031	0
	Whole Image	3	1130	0	16469	978444	51499	1031	0
2048x2048	Two Pixels	1	536	0	878	4966	3795	574	0
	Four Pixels	1	543	0	1557	10487	7855	579	0
	Six Pixels	1	543	0	2254	15984	11686	579	0
	Whole Image	1	543	0	9410	979031	59012	579	0

Table 23: Pixel correction between the single texel approach and the shadow mapping approach for the side viewpoint of the primitives scene.

Shadow Map Resolution	Number of Neighbours	Contour Thickness	Corrected		Turned Bad		Maintained Correct		Maintained Incorrect	
			L→S	S→L	L→S	S→L	L→L	S→S	L→L	S→S
1024x1024	3	Two Pixels	311	924	0	850	4788	3593	534	0
		Four Pixels	334	1116	0	1568	10167	7609	688	0
		Six Pixels	334	1130	0	2090	15677	11752	700	0
		Whole Image	334	1130	0	6645	978444	61323	700	0
	8	Two Pixels	401	924	0	642	4788	3801	444	0
		Four Pixels	453	1116	0	1160	10167	8017	569	0
		Six Pixels	453	1130	0	1496	15677	12346	581	0
		Whole Image	453	1130	0	4423	978444	63545	581	0
2048x2048	3	Two Pixels	259	536	0	480	4966	4193	316	0
		Four Pixels	259	543	0	706	10487	8706	321	0
		Six Pixels	259	543	0	910	15984	13030	321	0
		Whole Image	259	543	0	2165	979031	66257	321	0
	8	Two Pixels	333	536	0	366	4966	4307	242	0
		Four Pixels	334	543	0	487	10487	8925	246	0
		Six Pixels	334	543	0	612	15984	13328	246	0
		Whole Image	334	543	0	1374	979031	67048	246	0

Table 24: Pixel correction between the neighbour texels approach and the shadow mapping approach for the side viewpoint of the primitives scene.

Shadow Map Resolution	Number of Neighbours	Triangle Average	Two Pixels	Four Pixels	Six Pixels	Whole Image
1024x1024	3	Used	1.7095	1.6777	1.6571	0.2447
		Available	1.9614	2.0321	2.0965	2.3679
	8	Used	3.1852	3.1525	3.1125	0.4395
		Available	3.6357	3.6266	3.6446	4.0428
2048x2048	3	Used	1.5052	1.4487	1.4053	0.1923
		Available	1.8179	1.8994	1.9452	1.9112
	8	Used	2.5110	2.4245	2.3448	0.3018
		Available	2.8848	2.8997	2.9437	2.9213

Table 25: Average of triangle intersections when using the neighbour texels approach for the side viewpoint of the primitives scene.

Shadow Map Resolution	Adjacency Level	Contour Thickness	Corrected		Turned Bad		Maintained Correct		Maintained Incorrect	
			L→S	S→L	L→S	S→L	L→L	S→S	L→L	S→S
1024x1024	One Level	Two Pixels	3	924	0	559	4788	3884	842	0
		Four Pixels	3	1116	0	1049	10167	8128	1019	0
		Six Pixels	3	1130	0	1372	15677	12470	1031	0
		Whole Image	3	1130	0	3781	978444	64187	1031	0
	Two Levels	Two Pixels	3	924	0	61	4788	4382	842	0
		Four Pixels	3	1116	0	110	10167	9067	1019	0
		Six Pixels	3	1130	0	153	15677	13689	1031	0
		Whole Image	3	1130	0	259	978444	67709	1031	0
2048x2048	One Level	Two Pixels	2	536	0	282	4966	4391	573	0
		Four Pixels	2	543	0	412	10487	9000	578	0
		Six Pixels	2	543	0	537	15984	13403	578	0
		Whole Image	2	543	0	1176	979031	67246	578	0
	Two Levels	Two Pixels	3	536	0	37	4966	4636	572	0
		Four Pixels	3	543	0	53	10487	9359	577	0
		Six Pixels	3	543	0	61	15984	13879	577	0
		Whole Image	3	543	0	105	979031	68317	577	0

Table 26: Pixel correction between the adjacent geometry approach and the shadow mapping approach for the side viewpoint of the primitives scene.

Shadow Map Resolution	Adjacency Level	Triangle Average	Two Pixels	Four Pixels	Six Pixels	Whole Image
1024x1024	One Level	Used	2.2647	2.2824	2.2937	0.3773
		Available	4.0000	4.0000	4.0000	4.0000
	Two Levels	Used	6.9370	6.9552	6.9672	1.1357
		Available	12.2542	12.1869	12.1500	12.03966
2048x2048	One Level	Used	2.3289	2.3423	2.3510	0.3811
		Available	4.0000	4.0000	4.0000	4.0000
	Two Levels	Used	7.0945	7.0956	7.1057	1.1476
		Available	12.1850	12.1172	12.0896	12.0434

Table 27: Average of triangle intersections when using the adjacent geometry approach for the side viewpoint of the primitives scene.

Contour Thickness		Two Pixels		Four Pixels		Six Pixels		Whole Image		
Lighting		L→S	S→L	L→S	S→L	L→S	S→L	L→S	S→L	
Shadow Map Resolution	1024x1024	Corrected by Both	3	924	3	1116	3	1130	3	1130
		Turned Bad by Both	0	45	0	69	0	82	0	116
		Corrected by Neighbour Texels Only	398	0	450	0	450	0	450	0
		Corrected by Adjacent Geometry Only	0	0	0	0	0	0	0	0
		Turned Bad by Neighbour Texels Only	0	597	0	1091	0	1414	0	4307
		Turned Bad by Adjacent Geometry Only	0	16	0	41	0	71	0	143
	2048x2048	Corrected by Both	3	536	3	543	3	543	3	543
		Turned Bad by Both	0	14	0	14	0	14	0	21
		Corrected by Neighbour Texels Only	330	0	331	0	331	0	331	0
		Corrected by Adjacent Geometry Only	0	0	0	0	0	0	0	0
		Turned Bad by Neighbour Texels Only	0	352	0	473	0	598	0	1353
		Turned Bad by Adjacent Geometry Only	0	23	0	39	0	47	0	84

Table 28: Pixel correction by the neighbour texels (9 texels) and the adjacent geometry (2 levels) approaches separated by lighting change for the side viewpoint of the primitives scene.

Algorithm Step	Confirmations and Errors	1024x1024			2048x2048		
		Two Pixels	Four Pixels	Six Pixel	Two Pixels	Four Pixels	Six Pixel
Shadow Map	Total Contour Pixels	11000	21482	31683	10750	21022	31047
	Correct Light Pixels	4788 (85.00%)	10167 (90.87%)	15677 (93.81%)	4966 (89.62%)	10487 (94.76%)	15984 (96.50%)
	Correct Shadow Pixels	4443 (82.78%)	9177 (89.16%)	13842 (92.45%)	4673 (89.71%)	9412 (94.55%)	13940 (96.25%)
	Incorrect Light Pixels	845 (15.00%)	1022 (9.13%)	1034 (6.19%)	575 (10.38%)	580 (5.24%)	580 (3.50%)
	Incorrect Shadow Pixels	924 (17.22%)	1116 (10.84%)	1130 (7.55%)	536 (10.29%)	543 (5.45%)	543 (3.75%)
Texel Coherence	Confirmations in Light	2755 (48.91%)	6674 (59.65%)	11288 (67.55%)	3356 (60.57%)	8276 (74.78%)	13713 (82.79%)
	Confirmations in Shadow	2570 (47.89%)	5953 (57.84%)	9787 (65.37%)	3064 (58.82%)	7233 (72.66%)	11715 (80.89%)
	Wrong Confirmations in Light	3 (0.05%)	3 (0.03%)	3 (0.02%)	3 (0.05%)	3 (0.03%)	3 (0.02%)
	Wrong Confirmations in Shadow	0 (0.00%)	0 (0.00%)	0 (0.00%)	0 (0.00%)	0 (0.00%)	0 (0.00%)
Neighbouring Texels	Corrections from Light	400 (7.10%)	452 (4.04%)	452 (2.70%)	333 (6.01%)	334 (3.02%)	334 (2.02%)
	Confirmations in Shadow	3823 (71.23%)	8228 (79.94%)	12776 (85.33%)	4335 (83.22%)	9032 (90.73%)	13559 (93.62%)
Adjacent Geometry	Confirmations in Shadow	4398 (81.95%)	9125 (88.65%)	13790 (92.11%)	4659 (89.44%)	9398 (94.40%)	13926 (96.15%)
Final Lighting	Wrong Confirmations in Light	445 (7.90%)	570 (5.09%)	582 (3.48%)	242 (4.37%)	246 (2.22%)	246 (1.49%)
	Wrong Confirmations in Shadow	45 (0.84%)	52 (0.51%)	52 (0.35%)	14 (0.27%)	14 (0.14%)	14 (0.10%)

Table 29: Algorithm results of the side viewpoint of the primitives scene.

The results of the “with” viewpoint of the “primitives” scene are presented below.

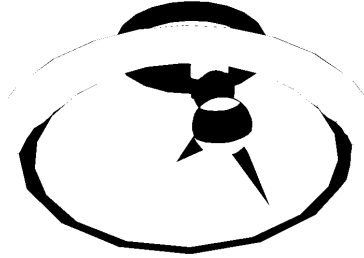


Figure 101: Result of the ray-tracing approach for the with viewpoint of the primitives scene.

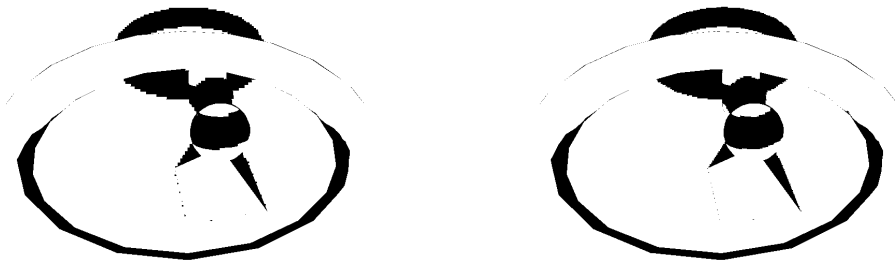


Figure 102: Result of the shadow mapping approach for the with viewpoint of the primitives scene.

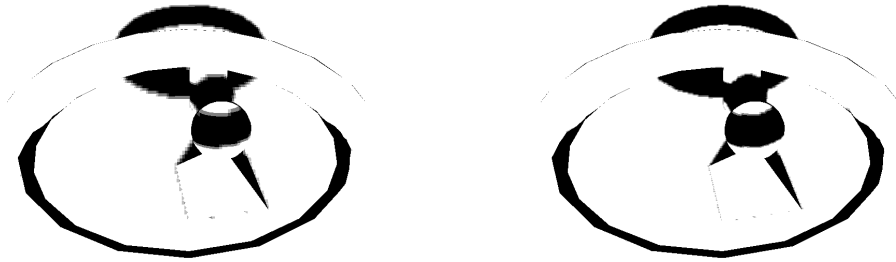


Figure 103: Result of texel coherence with four texels for the with viewpoint of the primitives scene.

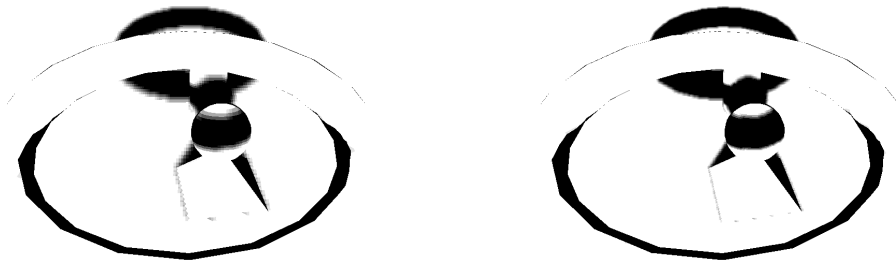


Figure 104: Result of texel coherence with nine texels for the with viewpoint of the primitives scene.

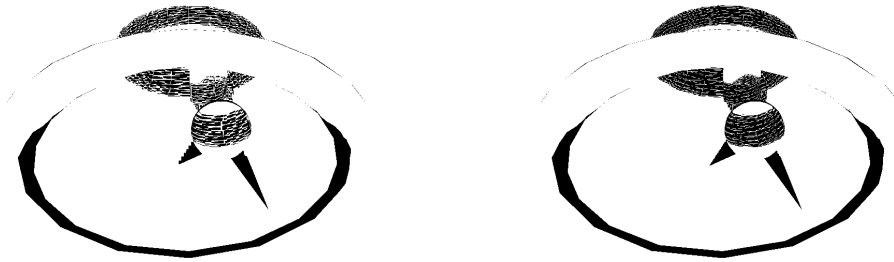


Figure 105: Result of the single texel approach for the with viewpoint of the primitives scene.

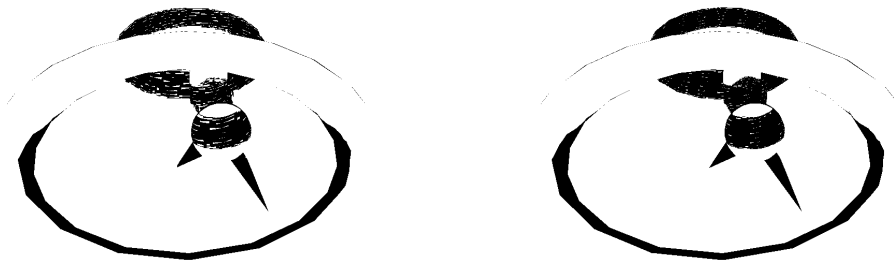


Figure 106: Result of the neighbour texels approach using four neighbours for the with viewpoint of the primitives scene.

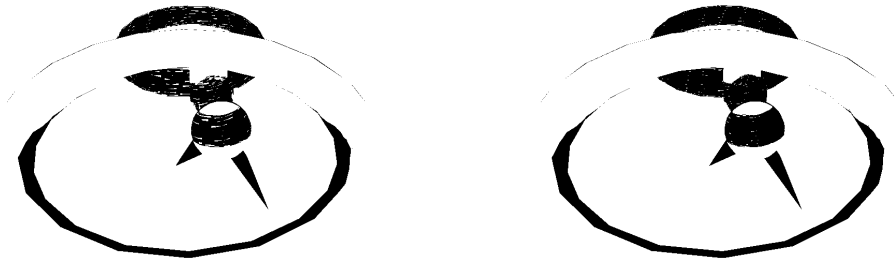


Figure 107: Result of the neighbour texels approach using nine neighbours for the with viewpoint of the primitives scene.

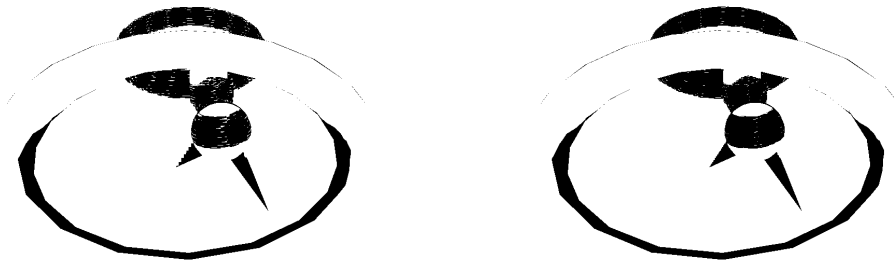


Figure 108: Result of the adjacent geometry approach with one level of adjacency for the with viewpoint of the primitives scene.

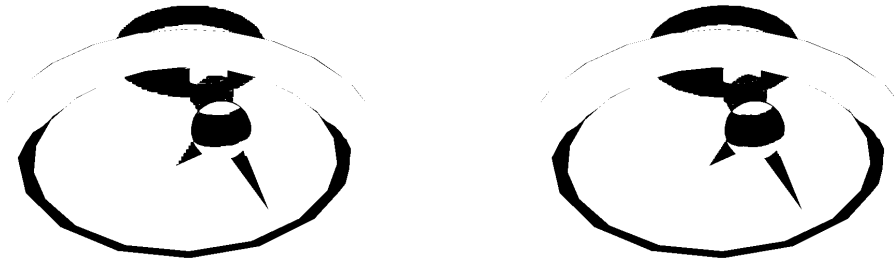


Figure 109: Result of the adjacent geometry approach with two levels of adjacency for the with viewpoint of the primitives scene.



Figure 110: Result of the algorithm with a six pixel thick contour and a 2048x2048 resolution shadow map for the with viewpoint of the primitives scene.

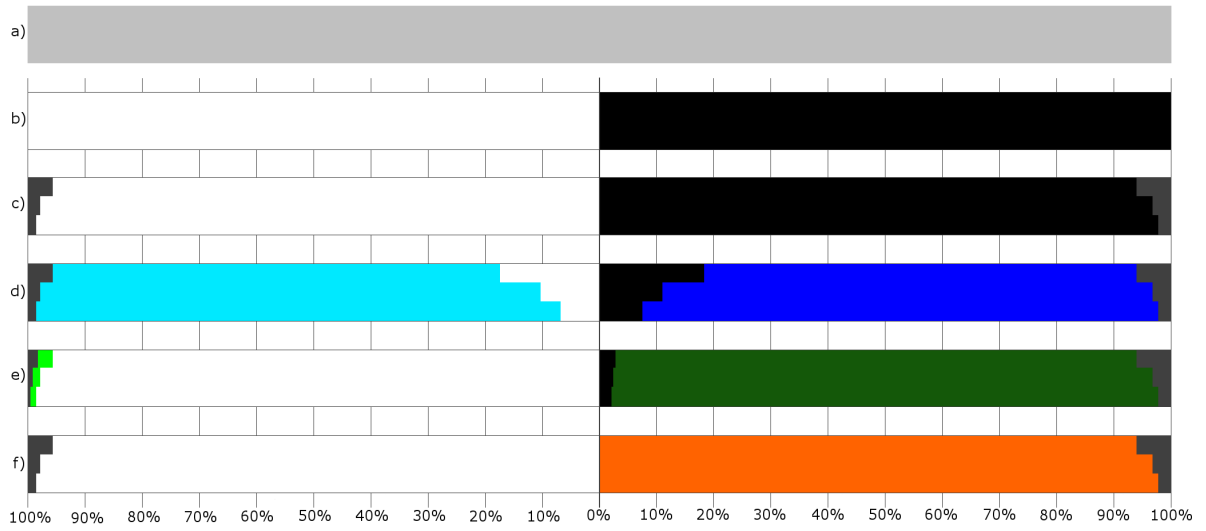
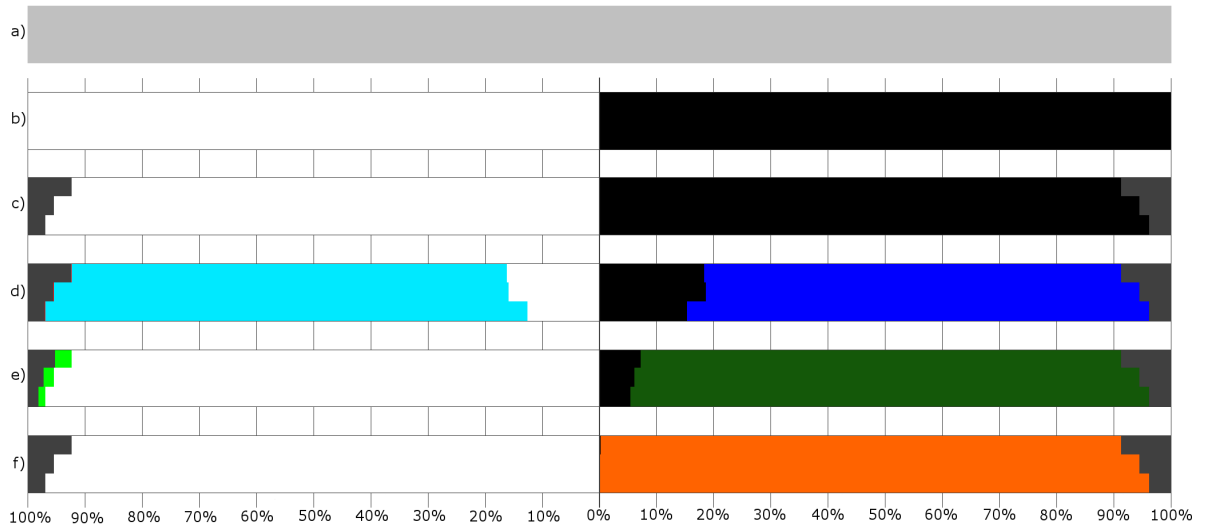


Figure 111: Corrected/confirmed/hinted contour pixels by each method for the with viewpoint of the primitives scene using a 1024x1024 (top) and a 2048x2048 (bottom) resolution shadow map.

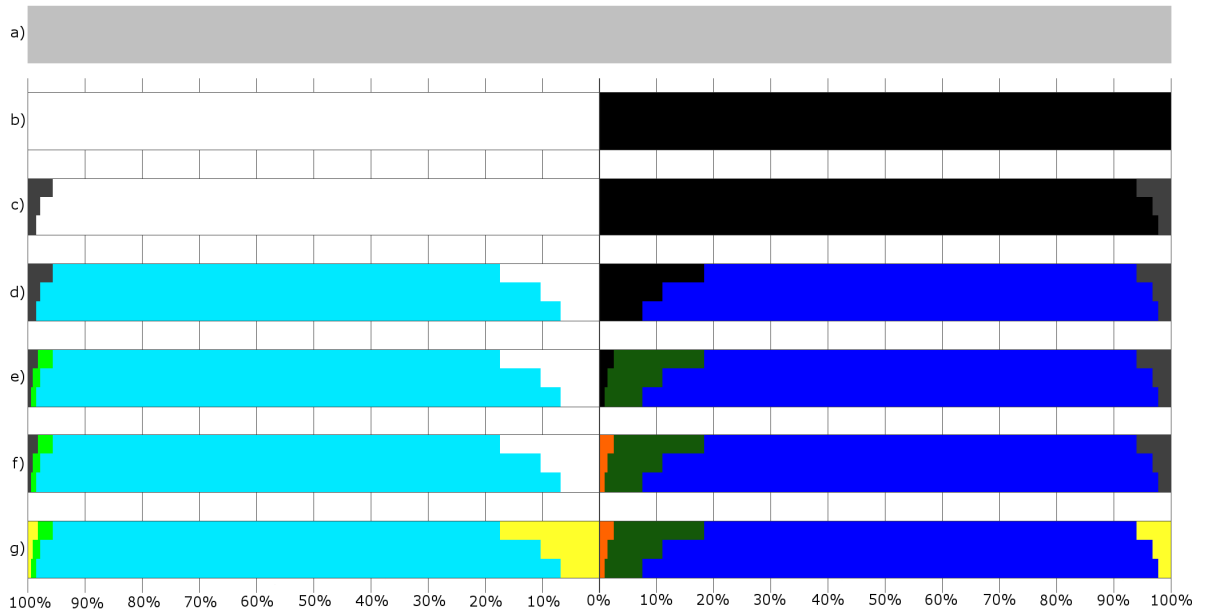
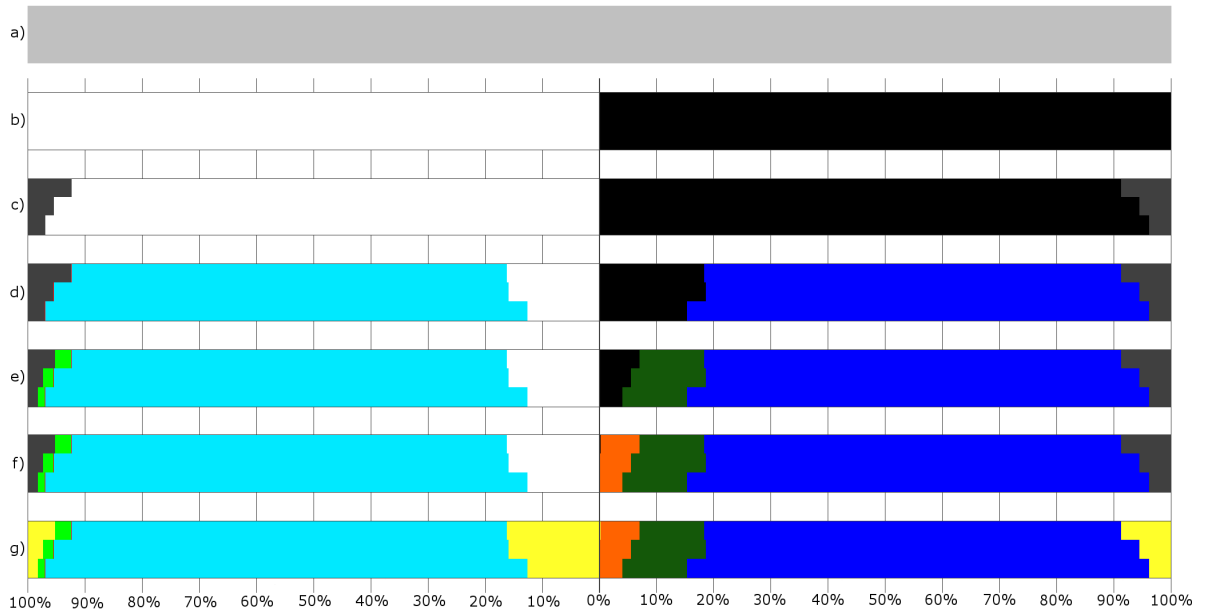


Figure 112: Corrected/confirmed/hinted contour pixels by the chaining of methods for the with viewpoint of the primitives scene using a 1024x1024 (top) and a 2048x2048 (bottom) resolution shadow map.

Shadow Map Resolution	Approach	Contour Thickness			
		Two Pixels	Four Pixels	Six Pixels	Whole Image
1024x1024	Pixels in Contour	12244	24077	35874	1048576
	Shadow Map	1004 (8.20%)	1211 (5.03%)	1221 (3.40%)	1221 (0.12%)
	Single Texel	1310 (10.7%)	2087 (8.67%)	2759 (7.69%)	9815 (0.94%)
	Neighbour Texels (4 Neighbours)	892 (7.29%)	1296 (5.38%)	1563 (4.36%)	3583 (0.34%)
	Neighbour Texels (9 Neighbours)	729 (5.95%)	1023 (4.25%)	1211 (3.38%)	2517 (0.24%)
	Adjacent Geometry (One Level)	818 (6.68%)	1069 (4.44%)	1213 (3.38%)	2166 (0.21%)
	Adjacent Geometry (Two Level)	533 (4.35%)	651 (2.70%)	662 (1.85%)	695 (0.07%)
2048x2048	Pixels in Contour	12249	24119	35959	1048576
	Shadow Map	620 (5.06%)	626 (2.60%)	628 (1.75%)	628 (0.06%)
	Single Texel	725 (5.92%)	1210 (5.02%)	1677 (4.66%)	5208 (0.50%)
	Neighbour Texels (4 Neighbours)	367 (3.00%)	523 (2.17%)	649 (1.80%)	1105 (0.11%)
	Neighbour Texels (9 Neighbours)	279 (2.28%)	379 (1.57%)	449 (1.25%)	692 (0.07%)
	Adjacent Geometry (One Level)	381 (3.11%)	445 (1.85%)	525 (1.46%)	728 (0.07%)
	Adjacent Geometry (Two Level)	293 (2.39%)	300 (1.24%)	302 (0.84%)	314 (0.03%)

Table 30: Difference between the approaches that use ray-tracing and the actual ray-tracer for the with viewpoint of the primitives scene.

Shadow Map Resolution	Contour Thickness		
	Two Pixels	Four Pixels	Six Pixels
1024x1024	1004 of 1221 (82.23%)	1211 of 1221 (99.18%)	1221 of 1221 (100.00%)
2048x2048	620 of 628 (98.73%)	626 of 628 (99.68%)	628 of 628 (100.00%)

Table 31: Wrongly defined pixels in the shadow mapping result which are inside the contour in the with viewpoint of the primitives scene.

Shadow Map Resolution	Contour Thickness	Pixel Shading	
		Light	Shadow
1024x1024	Two Pixels	518 of 6752	486 of 5492
	Four Pixels	634 of 13807	577 of 10270
	Six Pixels	642 of 21006	579 of 14868
	Whole Image	642 of 1001569	579 of 47007
2048x2048	Two Pixels	292 of 6771	328 of 5478
	Four Pixels	296 of 13854	330 of 10265
	Six Pixels	298 of 21081	330 of 14878
	Whole Image	298 of 1001474	330 of 47102

Table 32: Pixels that the shadow map defines wrongly in the with viewpoint of the primitives scene, separated in pixels defined in light and in shadow, compared to the total amount of pixels lighted in the same way.

Shadow Map Resolution	Contour Thickness	Texel Coherence					
		Light			Shadow		
		Confirmed	Incorrectly Confirmed	Undecided	Confirmed	Incorrectly Confirmed	Undecided
1024x1024	Two Pixels	5137 (76.08%)	3 (0.04%)	1615 (23.92%)	3995 (72.74%)	0 (0.00%)	1497 (27.26%)
	Four Pixels	10965 (79.42%)	6 (0.04%)	2842 (20.58%)	7773 (75.69%)	0 (0.00%)	2497 (24.31%)
	Six Pixels	17697 (84.25%)	8 (0.04%)	3309 (15.75%)	12007 (80.76%)	0 (0.00%)	2861 (19.24%)
	Whole Image	998128 (99.66%)	8 (0.00%)	3441 (0.34%)	44126 (93.87%)	0 (0.00%)	2881 (6.13%)
2048x2048	Two Pixels	5294 (78.19%)	2 (0.03%)	1477 (21.81%)	4143 (75.63%)	0 (0.00%)	1335 (24.37%)
	Four Pixels	12124 (87.51%)	4 (0.03%)	1730 (12.49%)	8800 (85.73%)	0 (0.00%)	1465 (14.27%)
	Six Pixels	19331 (91.70%)	6 (0.03%)	1750 (8.30%)	13413 (90.15%)	0 (0.00%)	1465 (9.85%)
	Whole Image	999672 (99.82%)	6 (0.00%)	1802 (0.18%)	45637 (96.89%)	0 (0.00%)	1465 (3.11%)

Table 33: Pixel confirmation when using texel coherence with four texels for the with viewpoint of the primitives scene.

Shadow Map Resolution	Contour Thickness	Texel Shadowing							
		Light				Shadow			
		3 shadow/1 light	3 shadow/1 light in ray-tracer shadow	1 shadow/3 light	1 shadow/3 light in ray-tracer light	3 shadow/1 light	3 shadow/1 light in ray-tracer shadow	1 shadow/3 light	1 shadow/3 light in ray-tracer light
1024x1024	Two Pixels	246	211	593	563	414	408	318	236
	Four Pixels	314	254	1172	1135	795	789	394	266
	Six Pixels	319	256	1430	1393	941	935	399	267
	Whole Image	319	256	1553	1516	956	950	399	267
2048x2048	Two Pixels	156	114	627	612	420	407	214	158
	Four Pixels	159	114	790	775	486	473	217	159
	Six Pixels	159	114	810	795	486	473	217	159
	Whole Image	159	114	857	842	486	473	217	159

Table 34: Pixel shadowing for pixels that don't achieve texel coherence with four texels for the with viewpoint of the primitives scene.

Shadow Map Resolution	Contour Thickness	Texel Coherence					
		Light			Shadow		
		Confirmed	Incorrectly Confirmed	Undecided	Confirmed	Incorrectly Confirmed	Undecided
1024x1024	Two Pixels	4948 (73.28%)	2 (0.03%)	1804 (26.72%)	3906 (71.12%)	0 (0.00%)	1586 (28.88%)
	Four Pixels	10267 (74.36%)	5 (0.04%)	3540 (25.64%)	7245 (70.55%)	0 (0.00%)	3025 (29.45%)
	Six Pixels	15853(75.47%)	6 (0.03%)	5153(24.53%)	10536(70.86%)	0 (0.00%)	4332(29.14%)
	Whole Image	994244(99.27%)	6 (0.00%)	7325(0.73%)	41372(88.01%)	0 (0.00%)	5635(11.99%)
2048x2048	Two Pixels	4945 (73.03%)	0 (0.00%)	1826 (26.97%)	3989 (72.82%)	0 (0.00%)	1489 (27.18%)
	Four Pixels	10628 (76.71%)	1 (0.01%)	3226 (23.29%)	7755 (75.55%)	0 (0.00%)	2510 (24.45%)
	Six Pixels	17344 (82.27%)	3 (0.01%)	3737 (17.73%)	12030 (80.86%)	0 (0.00%)	2848 (19.14%)
	Whole Image	997546 (99.61%)	3 (0.00%)	3928 (0.39%)	44238 (93.92%)	0 (0.00%)	2864 (6.08%)

Table 35: Pixel confirmation when using texel coherence with nine texels for the with viewpoint of the primitives scene.

Shadow Map Lighting	Texel Shadowing	Shadow Map							
		1024x1024				2048x2048			
		Two Pixels	Four Pixels	Six Pixels	Whole Image	Two Pixels	Four Pixels	Six Pixels	Whole Image
Light	8 S-1 L	0	0	0	0	0	0	0	0
	8 S-1 L in RT Shadow	0	0	0	0	0	0	0	0
	7 S-2 L	0	0	0	0	0	0	0	0
	7 S-2 L in RT Shadow	0	0	0	0	0	0	0	0
	6 S-3 L	0	0	0	0	0	0	0	0
	6 S-3 L in RT Shadow	0	0	0	0	0	0	0	0
	5 S-4 L	21	35	42	44	7	10	10	10
	5 S-4 L in RT Shadow	12	12	12	12	4	4	4	4
	4 S-5 L	363	594	711	756	329	413	418	418
	4 S-5 L in RT Light	147	323	439	484	190	273	278	278
	3 S-6 L	762	1466	2088	2716	719	1209	1344	1358
	3 S-6 L in RT Light	479	1125	1742	2370	575	1064	1199	1213
	2 S-7 L	374	708	1007	1404	329	552	633	700
	2 S-7 L in RT Light	371	705	1004	1401	328	551	632	699
	1 S-8 L	284	737	1305	2405	442	1042	1332	1442
1 S-8 L in RT Light	282	735	1302	2402	438	1037	1327	1437	
Shadow	8 S-1 L	111	382	753	1235	174	484	607	617
	8 S-1 L in RT Shadow	111	382	753	1235	172	482	605	615
	7 S-2 L	248	475	689	892	230	387	437	441
	7 S-2 L in RT Shadow	244	471	685	888	224	381	431	435
	6 S-3 L	751	1428	2013	2573	693	1148	1308	1310
	6 S-3 L in RT Shadow	570	1214	1799	2359	584	1039	1199	1201
	5 S-4 L	394	651	788	846	338	436	441	441
	5 S-4 L in RT Shadow	175	381	516	574	180	277	282	282
	4 S-5 L	36	41	41	41	19	19	19	19
	4 S-5 L in RT Light	36	41	41	41	19	19	19	19
	3 S-6 L	38	40	40	40	19	19	19	19
	3 S-6 L in RT Light	38	40	40	40	19	19	19	19
	2 S-7 L	8	8	8	8	6	6	6	6
	2 S-7 L in RT Light	8	8	8	8	6	6	6	6
	1 S-8 L	0	0	0	0	10	11	11	11
1 S-8 L in RT Light	0	0	0	0	9	10	10	10	

Table 36: Pixel shadowing for pixels that don't achieve texel coherence with nine texels for the with viewpoint of the primitives scene.

Shadow Map Resolution	Contour Thickness	Corrected		Turned Bad		Maintained Correct		Maintained Incorrect	
		L→S	S→L	L→S	S→L	L→L	S→S	L→L	S→S
1024x1024	Two Pixels	0	486	0	792	6234	4214	518	0
	Four Pixels	0	577	0	1453	13173	8240	634	0
	Six Pixels	0	579	0	2117	20364	12172	642	0
	Whole Image	0	579	0	9173	1000927	37255	642	0
2048x2048	Two Pixels	0	328	0	433	6479	4717	292	0
	Four Pixels	0	330	0	914	13558	9021	296	0
	Six Pixels	0	330	0	1379	20783	13169	298	0
	Whole Image	0	330	0	4910	1001176	41862	298	0

Table 37: Pixel correction between the single texel approach and the shadow mapping approach for the with viewpoint of the primitives scene.

Shadow Map Resolution	Contour Thickness	Corrected		Turned Bad		Maintained Correct		Maintained Incorrect	
		L→S	S→L	L→S	S→L	L→L	S→S	L→L	S→S
1024x1024	Two Pixels	154	486	0	528	6234	4478	364	0
	Four Pixels	191	577	0	853	13173	8840	443	0
	Six Pixels	192	579	0	1113	20364	13176	450	0
	Whole Image	192	579	0	3133	1000927	43295	450	0
2048x2048	Two Pixels	135	328	0	210	6479	4940	157	0
	Four Pixels	135	330	0	362	13558	9573	161	0
	Six Pixels	135	330	0	486	20783	14062	163	0
	Whole Image	135	330	0	942	1001176	45830	163	0

Table 38: Pixel correction between the neighbour texels approach using four neighbours and the shadow mapping approach for the with viewpoint of the primitives scene.

Shadow Map Resolution	Contour Thickness	Corrected		Turned Bad		Maintained Correct		Maintained Incorrect	
		L→S	S→L	L→S	S→L	L→L	S→S	L→L	S→S
1024x1024	Two Pixels	192	486	0	403	6234	4603	326	0
	Four Pixels	248	577	0	637	13173	9056	386	0
	Six Pixels	249	579	0	818	20364	13471	393	0
	Whole Image	249	579	0	2124	1000927	44304	393	0
2048x2048	Two Pixels	169	328	0	156	6479	4994	123	0
	Four Pixels	171	330	0	254	13558	9681	125	0
	Six Pixels	171	330	0	322	20783	14226	127	0
	Whole Image	171	330	0	565	1001176	46207	127	0

Table 39: Pixel correction between the neighbour texels approach using nine neighbours and the shadow mapping approach for the with viewpoint of the primitives scene.

Shadow Map Resolution	Number of Neighbours	Triangle Average	Two Pixels	Four Pixels	Six Pixels	Whole Image
1024x1024	3	Used	1.8071	1.7945	1.7747	0.5350
		Available	2.1849	2.2240	2.2695	2.3858
	8	Used	3.1873	3.1604	3.1373	0.9273
		Available	3.8373	3.8433	3.8414	4.0719
2048x2048	3	Used	1.6202	1.5841	1.5555	0.4183
		Available	1.9882	2.0587	2.0774	1.8785
	8	Used	2.6189	2.5901	2.5436	0.6416
		Available	3.1642	3.2022	3.2462	2.8590

Table 40: Average of triangle intersections when using the neighbour texels approach for the with viewpoint of the primitives scene.

Shadow Map Resolution	Contour Thickness	Corrected		Turned Bad		Maintained Correct		Maintained Incorrect	
		L→S	S→L	L→S	S→L	L→L	S→S	L→L	S→S
1024x1024	Two Pixels	0	486	0	300	6234	4706	518	0
	Four Pixels	0	577	0	435	13173	9258	634	0
	Six Pixels	0	579	0	571	20364	13718	642	0
	Whole Image	0	579	0	1524	1000927	44904	642	0
2048x2048	Two Pixels	0	328	0	89	6479	5061	292	0
	Four Pixels	0	330	0	149	13558	9786	296	0
	Six Pixels	0	330	0	227	20783	14321	298	0
	Whole Image	0	330	0	430	1001176	46342	298	0

Table 41: Pixel correction between the adjacent geometry approach with one level of adjacency and the shadow mapping approach for the with viewpoint of the primitives scene.

Shadow Map Resolution	Contour Thickness	Corrected		Turned Bad		Maintained Correct		Maintained Incorrect	
		L→S	S→L	L→S	S→L	L→L	S→S	L→L	S→S
1024x1024	Two Pixels	0	486	0	15	6234	4991	518	0
	Four Pixels	0	577	0	17	13173	9676	634	0
	Six Pixels	0	579	0	20	20364	14269	642	0
	Whole Image	0	579	0	53	1000927	46375	642	0
2048x2048	Two Pixels	0	328	0	1	6479	5149	292	0
	Four Pixels	0	330	0	4	13558	9931	296	0
	Six Pixels	0	330	0	4	20783	14544	298	0
	Whole Image	0	330	0	16	1001176	46756	298	0

Table 42: Pixel correction between the adjacent geometry approach with two levels of adjacency and the shadow mapping approach for the with viewpoint of the primitives scene.

Shadow Map Resolution	Adjacency Level	Triangle Average	Two Pixels	Four Pixels	Six Pixels	Whole Image
1024x1024	One Level	Used	2.4802	2.5010	2.5125	0.8570
		Available	4.0000	4.0000	4.0000	4.0000
	Two Levels	Used	7.5215	7.1057	7.6283	2.6583
		Available	12.1303	12.1380	12.1448	12.4070
2048x2048	One Level	Used	2.5974	2.6077	2.6164	0.8670
		Available	4.0000	4.0000	4.0000	4.0000
	Two Levels	Used	7.9256	7.1057	7.9950	2.6924
		Available	12.2053	12.2097	12.2229	12.4218

Table 43: Average of triangle intersections when using the adjacent geometry approach for the with viewpoint of the primitives scene.

Contour Thickness		Two Pixels		Four Pixels		Six Pixels		Whole Image		
Lighting		L→S	S→L	L→S	S→L	L→S	S→L	L→S	S→L	
Shadow Map Resolution	1024x1024	Corrected by Both	0	486	0	577	0	579	0	579
		Turned Bad by Both	0	14	0	16	0	18	0	33
		Corrected by Neighbour Texels Only	192	0	248	0	249	0	249	0
		Corrected by Adjacent Geometry Only	0	0	0	0	0	0	0	0
		Turned Bad by Neighbour Texels Only	0	389	0	621	0	800	0	2091
		Turned Bad by Adjacent Geometry Only	0	1	0	1	0	2	0	20
	2048x2048	Corrected by Both	0	328	0	330	0	330	0	330
		Turned Bad by Both	0	1	0	2	0	2	0	3
		Corrected by Neighbour Texels Only	169	0	171	0	171	0	171	0
		Corrected by Adjacent Geometry Only	0	0	0	0	0	0	0	0
		Turned Bad by Neighbour Texels Only	0	155	0	252	0	320	0	562
		Turned Bad by Adjacent Geometry Only	0	0	0	2	0	2	0	13

Table 44: Pixel correction by the neighbour texels (9 texels) and the adjacent geometry (2 levels) approaches separated by lighting change for the with viewpoint of the primitives scene.

Algorithm Step	Confirmations and Errors	1024x1024			2048x2048		
		Two Pixels	Four Pixels	Six Pixel	Two Pixels	Four Pixels	Six Pixel
Shadow Map	Total Contour Pixels	12244	24077	35874	12249	24119	35959
	Correct Light Pixels	6234 (92.33%)	13173 (95.41%)	20364 (96.94%)	6479 (95.69%)	13558 (97.86%)	20783 (98.59%)
	Correct Shadow Pixels	5006 (91.15%)	9693 (94.38%)	14289 (96.11%)	5150 (94.01%)	9935 (96.79%)	14548 (97.78%)
	Incorrect Light Pixels	518 (7.67%)	634 (4.59%)	642 (3.06%)	292 (4.31%)	296 (2.14%)	298 (1.41%)
	Incorrect Shadow Pixels	486 (8.85%)	577 (5.62%)	579 (3.89%)	328 (5.99%)	330 (3.21%)	330 (2.22%)
Texel Coherence	Confirmations in Light	5137 (76.08%)	10965 (79.42%)	17697 (84.25%)	5294 (78.19%)	12124 (87.51%)	19331 (91.70%)
	Confirmations in Shadow	3995 (72.74%)	7773 (75.69%)	12007 (80.76%)	4143 (75.63%)	8800 (85.73%)	13413 (90.15%)
	Wrong Confirmations in Light	3 (0.04%)	6 (0.04%)	8 (0.04%)	2 (0.03%)	4 (0.03%)	6 (0.03%)
	Wrong Confirmations in Shadow	0 (0.00%)	0 (0.00%)	0 (0.00%)	0 (0.00%)	0 (0.00%)	0 (0.00%)
Neighbouring Texels	Corrections from Light	192 (2.84%)	248 (1.80%)	249 (1.19%)	168 (2.48%)	169 (1.22%)	169 (0.80%)
	Confirmations in Shadow	4614 (84.01%)	9117 (88.77%)	13679 (92.00%)	5006 (91.38%)	9784 (95.31%)	14397 (96.77%)
Adjacent Geometry	Confirmations in Shadow	4992 (90.90%)	9678 (94.24%)	14274 (96.00%)	5149 (93.99%)	9934 (96.78%)	14547 (97.78%)
Final Lighting	Wrong Confirmations in Light	323 (4.78%)	380 (2.75%)	385 (1.83%)	122 (1.80%)	123 (0.89%)	123 (0.58%)
	Wrong Confirmations in Shadow	14 (0.25%)	15 (0.15%)	15 (0.10%)	1 (0.02%)	1 (0.01%)	1 (0.01%)

Table 45: Algorithm results of the with viewpoint of the primitives scene.

Following are the results of the “against” viewpoint of the “primitives” scene.

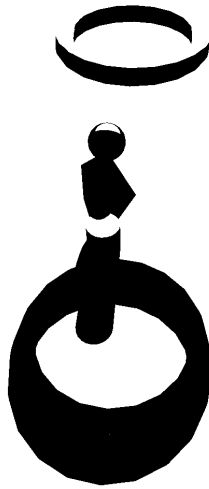


Figure 113: Result of the ray-tracing approach for the against viewpoint of the primitives scene.

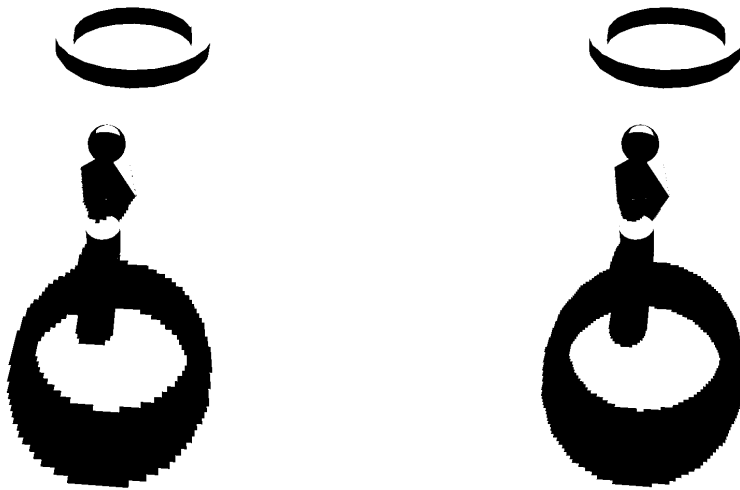


Figure 114: Result of the shadow mapping approach for the against viewpoint of the primitives scene.

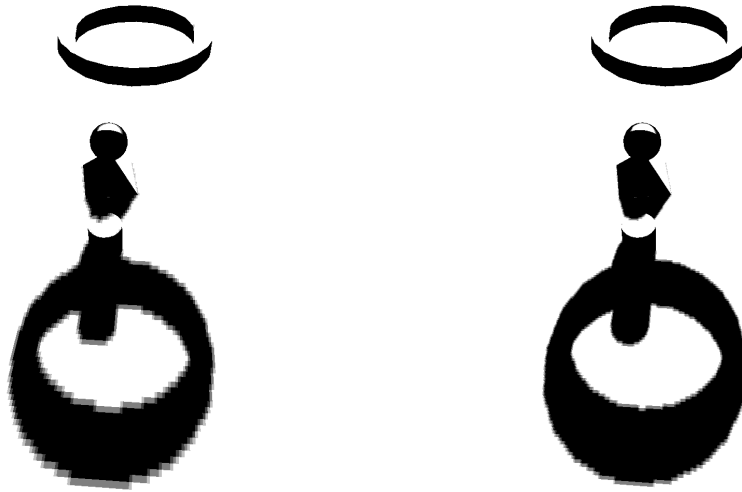


Figure 115: Result of texel coherence with four texels for the against viewpoint of the primitives scene.

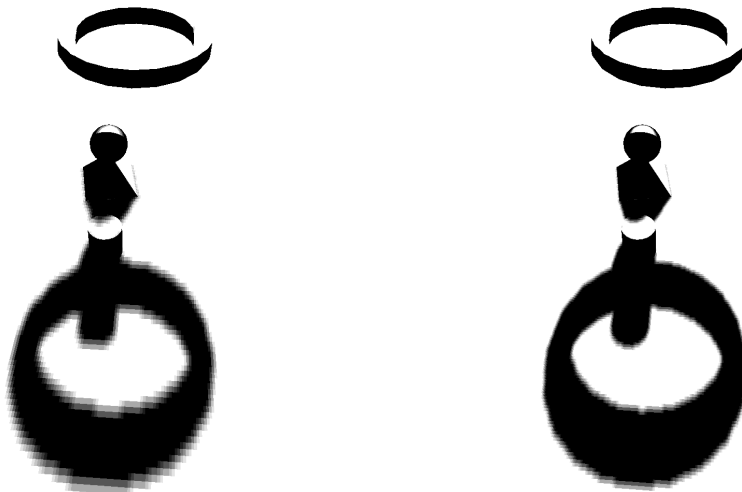


Figure 116: Result of texel coherence with nine texels for the against viewpoint of the primitives scene.



Figure 117: Result of the single texel approach for the against viewpoint of the primitives scene.

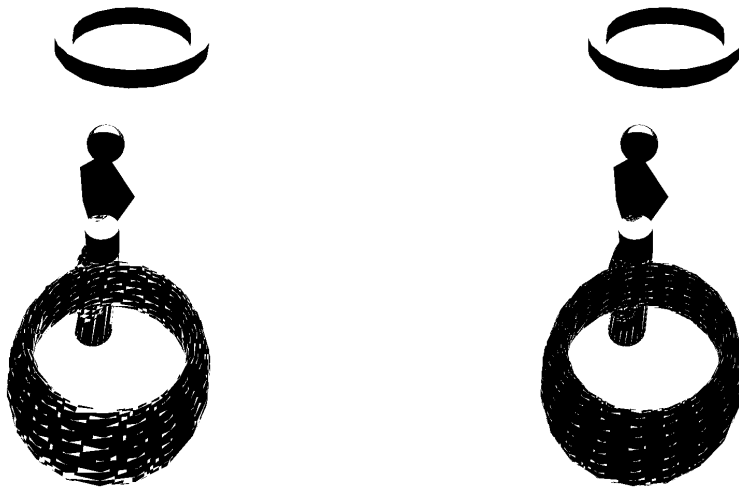


Figure 118: Result of the neighbour texels approach using three pixels for the against viewpoint of the primitives scene.

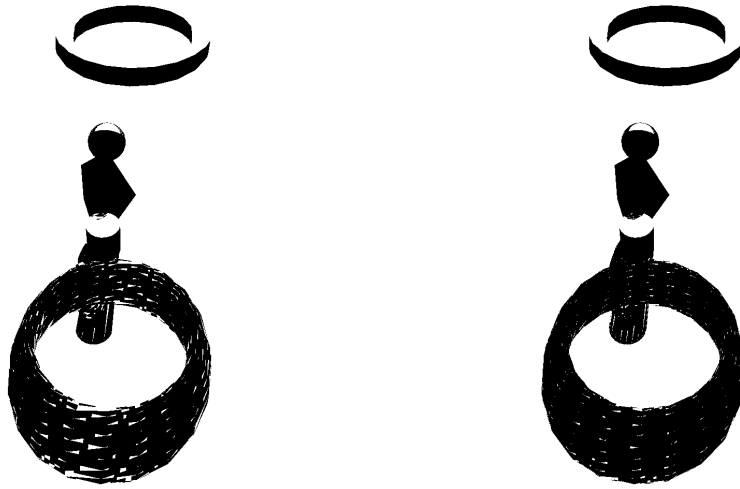


Figure 119: Result of the neighbour texels approach using eight pixels for the against viewpoint of the primitives scene.

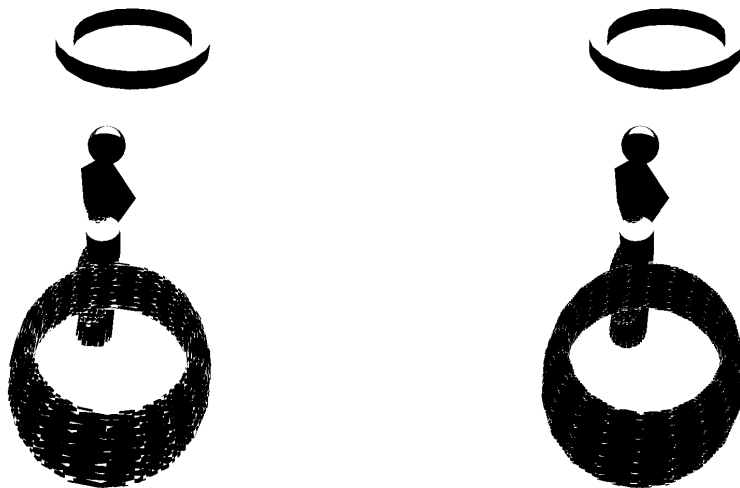


Figure 120: Result of the adjacent geometry approach with one level of adjacency for the against viewpoint of the primitives scene.

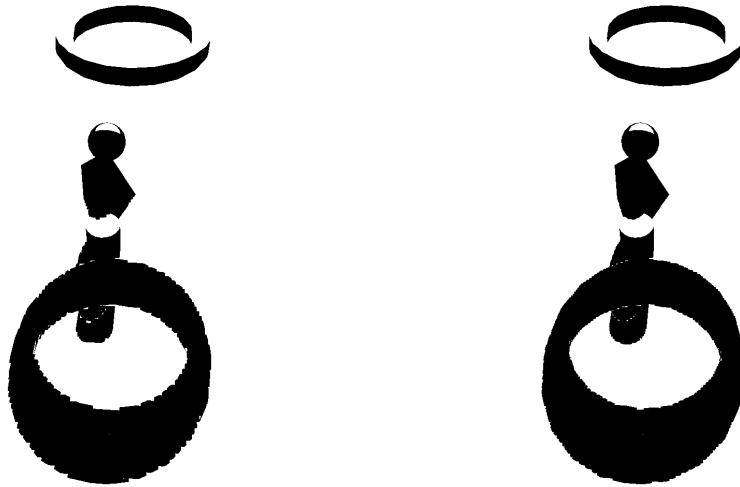


Figure 121: Result of the adjacent geometry approach with two levels of adjacency for the against viewpoint of the primitives scene.

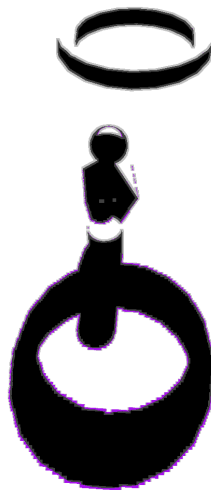


Figure 122: Result of the algorithm with a six pixel thick contour and a 2048x2048 resolution shadow map for the against viewpoint of the primitives scene.

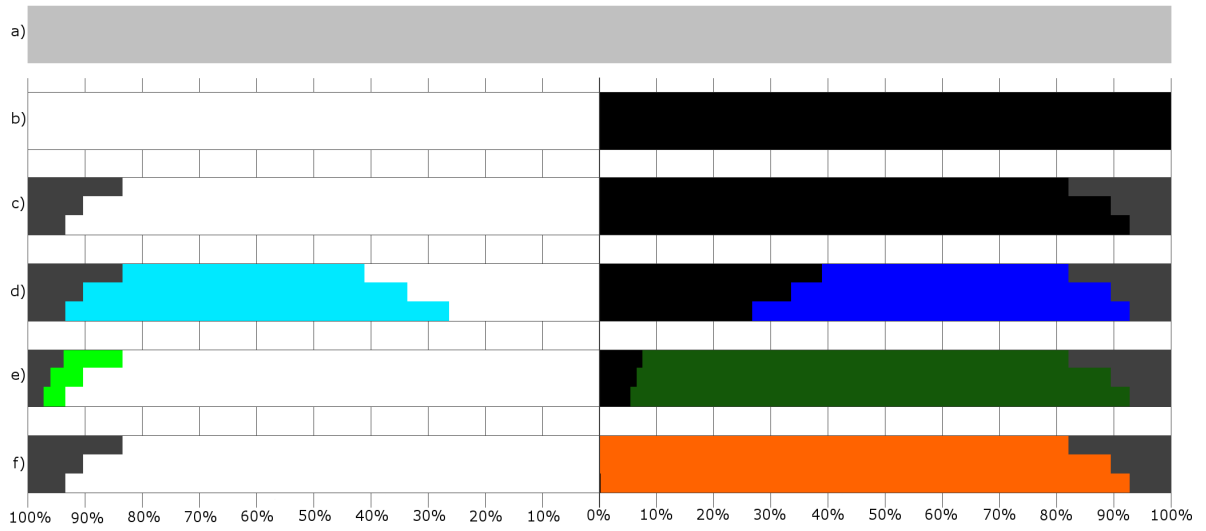
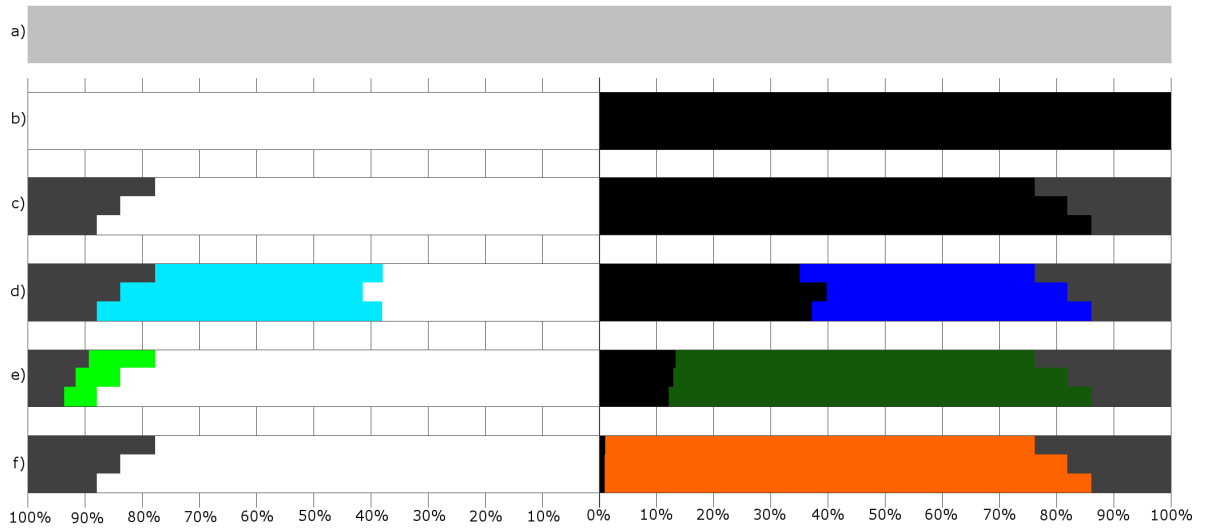


Figure 123: Corrected/confirmed/hinted contour pixels by each method for the against viewpoint of the primitives scene using a 1024x1024 (top) and a 2048x2048 (bottom) resolution shadow map.

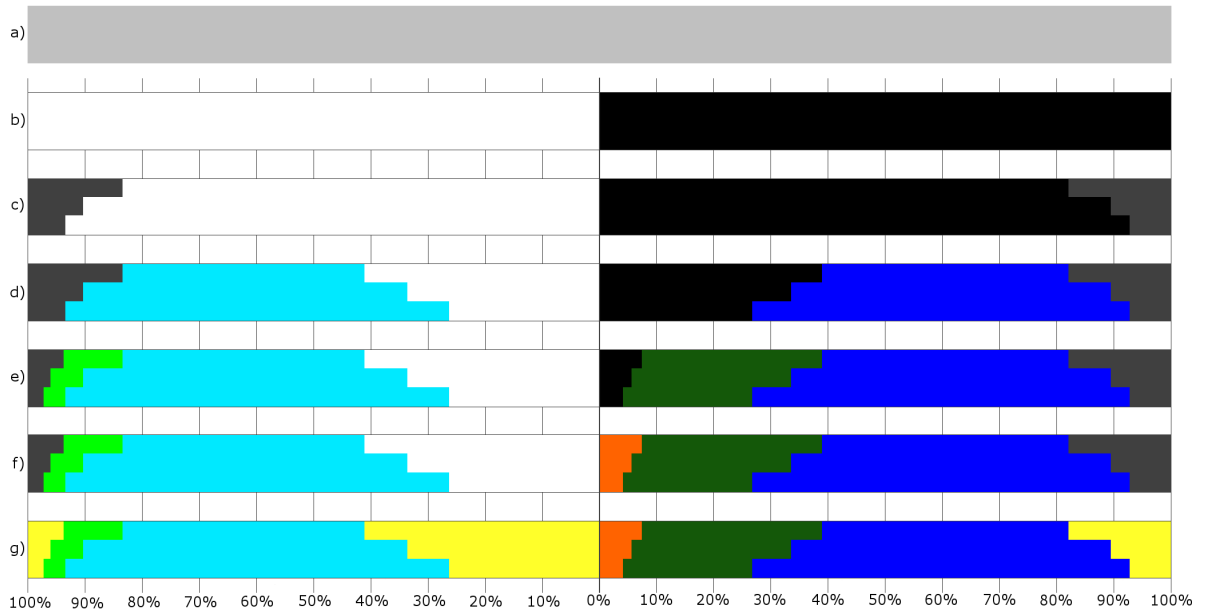
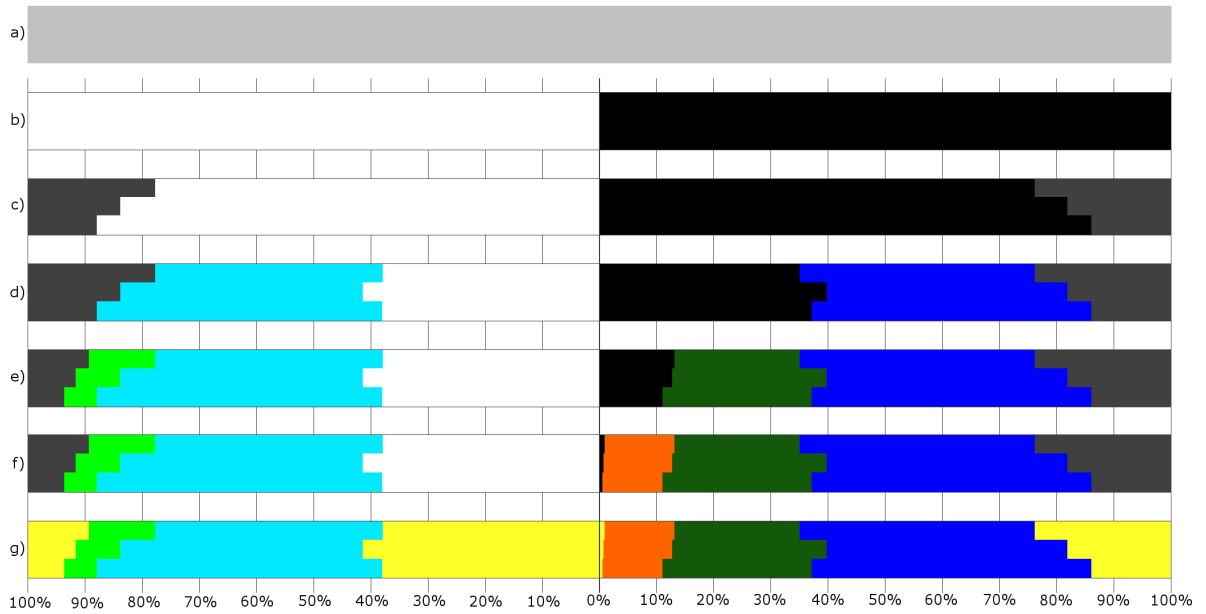


Figure 124: Corrected/confirmed/hinted contour pixels by the chaining of methods for the against viewpoint of the primitives scene using a 1024x1024 (top) and a 2048x2048 (bottom) resolution shadow map.

Shadow Map Resolution	Approach	Contour Thickness			
		Two Pixels	Four Pixels	Six Pixels	Whole Image
1024x1024	Pixels in Contour	11229	22196	32998	1048576
	Shadow Map	2582 (22.99%)	3799 (17.12%)	4272 (12.95%)	4497 (0.43%)
	Single Texel	2559 (22.79%)	4499 (20.27%)	6021 (18.25%)	36323 (3.46%)
	Neighbour Texels (4 Neighbours)	1747 (15.56%)	3066 (13.81%)	3969 (12.03%)	12958 (1.24%)
	Neighbour Texels (9 Neighbours)	1352 (12.04%)	2367 (10.66%)	3048 (9.24%)	8768 (0.84%)
	Adjacent Geometry (One Level)	1882 (16.76%)	2956 (13.32%)	3602 (10.92%)	8643 (0.82%)
	Adjacent Geometry (Two Level)	1311 (11.68%)	1931 (8.70%)	2194 (6.65%)	2548 (0.24%)
2048x2048	Pixels in Contour	11186	22079	32776	1048576
	Shadow Map	1922 (17.18%)	2222 (10.06%)	2251 (6.87%)	2252 (0.21%)
	Single Texel	1915 (17.12%)	3118 (14.12%)	3976 (12.13%)	20399 (1.95%)
	Neighbour Texels (4 Neighbours)	1000 (8.94%)	1561 (7.07%)	1832 (5.59%)	4181 (0.40%)
	Neighbour Texels (9 Neighbours)	776 (6.94%)	1169 (5.29%)	1340 (4.09%)	2731 (0.26%)
	Adjacent Geometry (One Level)	1235 (11.04%)	1634 (7.40%)	1816 (5.54%)	3167 (0.30%)
	Adjacent Geometry (Two Level)	940 (8.40%)	1103 (5.00%)	1135 (3.46%)	1237 (0.12%)

Table 46: Difference between the approaches that use ray-tracing and the actual ray-tracer for the against viewpoint of the primitives scene.

Shadow Map Resolution	Contour Thickness		
	Two Pixels	Four Pixels	Six Pixels
1024x1024	2582 of 4497 (57.42%)	3799 of 4497 (84.48%)	4272 of 4497 (95.00%)
2048x2048	1922 of 2252 (85.35%)	2222 of 2252 (98.67%)	2251 of 2252 (99.96%)

Table 47: Wrongly defined pixels in the shadow mapping result which are inside the contour in the against viewpoint of the primitives scene.

Shadow Map Resolution	Contour Thickness	Pixel Shading	
		Light	Shadow
1024x1024	Two Pixels	1256 of 5663	1326 of 5566
	Four Pixels	1827 of 11300	1972 of 10896
	Six Pixels	2035 of 16905	2237 of 16093
	Whole Image	2118 of 918386	2379 of 130190
2048x2048	Two Pixels	932 of 5650	990 of 5536
	Four Pixels	1082 of 11267	1140 of 10812
	Six Pixels	1100 of 16833	1151 of 15943
	Whole Image	1100 of 918595	1152 of 129981

Table 48: Pixels that the shadow map defines wrongly in the against viewpoint of the primitives scene, separated in pixels defined in light and in shadow, compared to the total amount of pixels lighted in the same way.

Shadow Map Resolution	Contour Thickness	Texel Coherence					
		Light			Shadow		
		Confirmed	Incorrectly Confirmed	Undecided	Confirmed	Incorrectly Confirmed	Undecided
1024x1024	Two Pixels	2257 (39.86%)	1 (0.02%)	3406 (60.14%)	2289 (41.12%)	0 (0.00%)	3277 (58.88%)
	Four Pixels	4788 (42.37%)	1 (0.01%)	6512 (57.63%)	4588 (42.11%)	0 (0.00%)	6308 (57.89%)
	Six Pixels	8433 (49.88%)	1 (0.01%)	8472 (50.12%)	7873 (48.92%)	0 (0.00%)	8220 (51.08%)
	Whole Image	907090 (98.77%)	1 (0.00%)	11296 (1.23%)	119227 (91.58%)	1 (0.00%)	10963 (8.42%)
2048x2048	Two Pixels	2392 (42.34%)	1 (0.02%)	3258 (57.66%)	2387 (43.12%)	0 (0.00%)	3149 (56.88%)
	Four Pixels	6390 (56.71%)	1 (0.01%)	4877 (43.29%)	6036 (55.83%)	0 (0.00%)	4776 (44.17%)
	Six Pixels	11298 (67.12%)	1 (0.01%)	5535 (32.88%)	10524 (66.01%)	0 (0.00%)	5419 (33.99%)
	Whole Image	912949 (99.39%)	1 (0.00%)	5646 (0.61%)	124459 (95.75%)	1 (0.00%)	5522 (4.25%)

Table 49: Pixel confirmation when using texel coherence with four texels for the against viewpoint of the primitives scene.

Shadow Map Resolution	Contour Thickness	Texel Shadowing							
		Light				Shadow			
		3 shadow/1 light	3 shadow/1 light in ray-tracer shadow	1 shadow/3 light	1 shadow/3 light in ray-tracer light	3 shadow/1 light	3 shadow/1 light in ray-tracer shadow	1 shadow/3 light	1 shadow/3 light in ray-tracer light
1024x1024	Two Pixels	812	646	1236	1140	1084	982	856	675
	Four Pixels	1302	919	2577	2456	2354	2220	1352	972
	Six Pixels	1384	956	3472	3346	3186	3041	1438	1015
	Whole Image	1384	956	4466	4340	4104	3956	1438	1015
2048x2048	Two Pixels	640	463	1279	1216	1156	1111	675	480
	Four Pixels	678	479	1968	1904	1839	1794	712	496
	Six Pixels	678	479	2173	2109	2033	1988	712	496
	Whole Image	678	479	2200	2136	2068	2023	712	496

Table 50: Pixel shadowing for pixels that don't achieve texel coherence with four texels for the against viewpoint of the primitives scene.

Shadow Map Resolution	Contour Thickness	Texel Coherence					
		Light			Shadow		
		Confirmed	Incorrectly Confirmed	Undecided	Confirmed	Incorrectly Confirmed	Undecided
1024x1024	Two Pixels	2103 (37.14%)	1 (0.02%)	3560 (62.86%)	2266 (40.71%)	0 (0.00%)	3300 (59.29%)
	Four Pixels	4376 (38.73%)	1 (0.01%)	6924 (61.27%)	4449 (40.83%)	0 (0.00%)	6447 (59.17%)
	Six Pixels	6749 (39.92%)	1 (0.01%)	10156 (60.08%)	6575 (40.86%)	0 (0.00%)	9518 (59.14%)
	Whole Image	895539 (97.51%)	1 (0.00%)	22847 (2.49%)	108429 (83.29%)	1 (0.00%)	21761 (16.71%)
2048x2048	Two Pixels	2220 (39.29%)	1 (0.02%)	3430 (60.71%)	2295 (41.46%)	0 (0.00%)	3241 (58.54%)
	Four Pixels	4711 (41.81%)	1 (0.01%)	6556 (58.19%)	4595 (42.50%)	0 (0.00%)	6217 (57.50%)
	Six Pixels	8118 (48.23%)	1 (0.01%)	8715 (51.77%)	7632 (47.87%)	0 (0.00%)	8311 (52.13%)
	Whole Image	907160 (98.76%)	1 (0.00%)	11435 (1.24%)	118950 (91.51%)	1 (0.00%)	11031 (8.49%)

Table 51: Pixel confirmation when using texel coherence with nine texels for the against viewpoint of the primitives scene.

Shadow Map Lighting	Texel Shadowing	Shadow Map							
		1024x1024				2048x2048			
		Two Pixels	Four Pixels	Six Pixels	Whole Image	Two Pixels	Four Pixels	Six Pixels	Whole Image
Light	8 S-1 L	1	1	1	1	0	0	0	0
	8 S-1 L in RT Shadow	1	1	1	1	0	0	0	0
	7 S-2 L	3	3	3	3	4	4	4	4
	7 S-2 L in RT Shadow	3	3	3	3	4	4	4	4
	6 S-3 L	0	0	0	0	0	0	0	0
	6 S-3 L in RT Shadow	0	0	0	0	0	0	0	0
	5 S-4 L	37	66	88	99	31	46	46	46
	5 S-4 L in RT Shadow	9	9	9	9	15	15	15	15
	4 S-5 L	1108	2019	2749	3559	1005	1652	1776	1776
	4 S-5 L in RT Light	437	1015	1631	2405	488	1059	1179	1179
	3 S-6 L	1513	2880	4092	9150	1412	2532	3262	4525
	3 S-6 L in RT Light	955	2086	3204	8215	1025	2071	2787	4050
	2 S-7 L	580	1103	1607	3924	570	1071	1480	2014
	2 S-7 L in RT Light	567	1088	1592	3909	562	1063	1472	2006
	1 S-8 L	318	852	1616	6111	408	1251	2147	3070
1 S-8 L in RT Light	318	852	1616	6111	408	1251	2147	3070	
Shadow	8 S-1 L	128	510	1142	5420	256	990	1846	2752
	8 S-1 L in RT Shadow	126	508	1140	5417	256	990	1846	2752
	7 S-2 L	500	987	1472	3670	500	974	1349	1882
	7 S-2 L in RT Shadow	467	941	1418	3614	485	959	1334	1867
	6 S-3 L	1448	2748	3927	8893	1379	2472	3172	4453
	6 S-3 L in RT Shadow	949	2016	3078	7961	977	2000	2693	3974
	5 S-4 L	1176	2154	2929	3730	1084	1757	1920	1920
	5 S-4 L in RT Shadow	431	1009	1644	2390	533	1126	1285	1285
	4 S-5 L	16	16	16	16	9	11	11	11
	4 S-5 L in RT Light	15	15	15	15	9	9	9	9
	3 S-6 L	17	17	17	17	9	9	9	9
	3 S-6 L in RT Light	17	17	17	17	9	9	9	9
	2 S-7 L	12	12	12	12	3	3	3	3
	2 S-7 L in RT Light	12	12	12	12	3	3	3	3
	1 S-8 L	3	3	3	3	1	1	1	1
1 S-8 L in RT Light	3	3	3	3	1	1	1	1	

Table 52: Pixel shadowing for pixels that don't achieve texel coherence with nine texels for the against viewpoint of the primitives scene.

Shadow Map Resolution	Contour Thickness	Corrected		Turned Bad		Maintained Correct		Maintained Incorrect	
		L→S	S→L	L→S	S→L	L→L	S→S	L→L	S→S
1024x1024	Two Pixels	3	1326	0	1306	4407	2934	1253	0
	Four Pixels	3	1972	0	2675	9473	6249	1824	0
	Six Pixels	3	2237	0	3989	14870	9867	2032	0
	Whole Image	3	2379	0	34208	916268	93603	2115	0
2048x2048	Two Pixels	3	990	0	986	4718	3560	929	0
	Four Pixels	3	1140	0	2039	10185	7633	1079	0
	Six Pixels	3	1151	0	2879	15733	11913	1097	0
	Whole Image	3	1152	0	19302	917495	109527	1097	0

Table 53: Pixel correction between the single texel approach and the shadow mapping approach for the against viewpoint of the primitives scene.

Shadow Map Resolution	Contour Thickness	Corrected		Turned Bad		Maintained Correct		Maintained Incorrect	
		L→S	S→L	L→S	S→L	L→L	S→S	L→L	S→S
1024x1024	Two Pixels	492	1326	0	983	4407	3257	764	0
	Four Pixels	654	1972	0	1893	9473	7031	1173	0
	Six Pixels	692	2237	0	2626	14870	11230	1343	0
	Whole Image	697	2379	0	11537	916268	116274	1421	0
2048x2048	Two Pixels	496	990	0	564	4718	3982	436	0
	Four Pixels	526	1140	0	1005	10185	8667	556	0
	Six Pixels	526	1151	0	1258	15733	13534	574	0
	Whole Image	526	1152	0	3607	917495	125222	574	0

Table 54: Pixel correction between the neighbour texels approach using four neighbours and the shadow mapping approach for the against viewpoint of the primitives scene.

Shadow Map Resolution	Contour Thickness	Corrected		Turned Bad		Maintained Correct		Maintained Incorrect	
		L→S	S→L	L→S	S→L	L→L	S→S	L→L	S→S
1024x1024	Two Pixels	650	1326	0	746	4407	3494	606	0
	Four Pixels	880	1972	0	1420	9473	7504	947	0
	Six Pixels	951	2237	0	1964	14870	11892	1084	0
	Whole Image	973	2379	0	7623	916268	120188	1145	0
2048x2048	Two Pixels	574	990	0	418	4718	4128	358	0
	Four Pixels	631	1140	0	718	10185	8954	451	0
	Six Pixels	634	1151	0	874	15733	13918	466	0
	Whole Image	634	1152	0	2265	917495	126564	466	0

Table 55: Pixel correction between the neighbour texels approach using nine neighbours and the shadow mapping approach for the against viewpoint of the primitives scene.

Shadow Map Resolution	Number of Neighbours	Triangle Average	Two Pixels	Four Pixels	Six Pixels	Whole Image
1024x1024	3	Used	1.6412	1.6300	1.6140	0.3340
		Available	1.8256	1.8301	1.8905	2.3087
	8	Used	2.9919	2.9659	2.9501	0.5905
		Available	3.3178	3.2965	3.2863	3.8000
2048x2048	3	Used	1.4886	1.3992	1.3600	0.2555
		Available	1.6243	1.7016	1.7675	1.8358
	8	Used	2.3250	2.2859	2.2285	0.3950
		Available	2.5855	2.5631	2.5890	2.7329

Table 56: Average of triangle intersections when using the neighbour texels approach for the against viewpoint of the primitives scene.

Shadow Map Resolution	Contour Thickness	Corrected		Turned Bad		Maintained Correct		Maintained Incorrect	
		L→S	S→L	L→S	S→L	L→L	S→S	L→L	S→S
1024x1024	Two Pixels	6	1326	0	632	4407	3608	1250	0
	Four Pixels	6	1972	0	1135	9473	7789	1821	0
	Six Pixels	6	2237	0	1573	14870	12283	2029	0
	Whole Image	6	2379	0	6531	916268	121280	2112	0
2048x2048	Two Pixels	5	990	0	308	4718	4238	927	0
	Four Pixels	5	1140	0	557	10185	9115	1077	0
	Six Pixels	5	1151	0	721	15733	14071	1095	0
	Whole Image	5	1152	0	2072	917495	126757	1095	0

Table 57: Pixel correction between the adjacent geometry approach with one level of adjacency and the shadow mapping approach for the against viewpoint of the primitives scene.

Shadow Map Resolution	Contour Thickness	Corrected		Turned Bad		Maintained Correct		Maintained Incorrect	
		L→S	S→L	L→S	S→L	L→L	S→S	L→L	S→S
1024x1024	Two Pixels	6	1326	0	61	4407	4179	1250	0
	Four Pixels	6	1972	0	110	9473	8814	1821	0
	Six Pixels	6	2237	0	165	14870	13691	2029	0
	Whole Image	6	2379	0	436	916268	127375	2112	0
2048x2048	Two Pixels	5	990	0	13	4718	4533	927	0
	Four Pixels	5	1140	0	26	10185	9646	1077	0
	Six Pixels	5	1151	0	40	15733	14752	1095	0
	Whole Image	5	1152	0	142	917495	128687	1095	0

Table 58: Pixel correction between the adjacent geometry approach with two levels of adjacency and the shadow mapping approach for the against viewpoint of the primitives scene.

Shadow Map Resolution	Adjacency Level	Triangle Average	Two Pixels	Four Pixels	Six Pixels	Whole Image
1024x1024	One Level	Used	2.2196	2.2274	2.2412	0.5277
		Available	4.0000	4.0000	4.0000	4.0000
	Two Levels	Used	6.7627	7.1057	6.8057	1.6326
		Available	12.1871	12.1625	12.1464	12.3744
2048x2048	One Level	Used	2.2410	2.2581	2.2689	0.5292
		Available	4.0000	4.0000	4.0000	4.0000
	Two Levels	Used	6.7846	7.1057	6.8511	1.6362
		Available	12.1098	12.0856	12.0785	12.3665

Table 59: Average of triangle intersections when using the adjacent geometry approach for the against viewpoint of the primitives scene.

Contour Thickness		Two Pixels		Four Pixels		Six Pixels		Whole Image		
Lighting		L→S	S→L	L→S	S→L	L→S	S→L	L→S	S→L	
Shadow Map Resolution	1024x1024	Corrected by Both	5	1326	5	1972	5	2237	5	2379
		Turned Bad by Both	0	54	0	92	0	130	0	241
		Corrected by Neighbour Texels Only	645	0	875	0	946	0	968	0
		Corrected by Adjacent Geometry Only	1	0	1	0	1	0	1	0
		Turned Bad by Neighbour Texels Only	0	692	0	1328	0	1834	0	7382
		Turned Bad by Adjacent Geometry Only	0	7	0	18	0	35	0	195
	2048x2048	Corrected by Both	5	990	5	1140	5	1151	5	1152
		Turned Bad by Both	0	10	0	11	0	13	0	29
		Corrected by Neighbour Texels Only	569	0	626	0	629	0	629	0
		Corrected by Adjacent Geometry Only	0	0	0	0	0	0	0	0
		Turned Bad by Neighbour Texels Only	0	408	0	707	0	861	0	2236
		Turned Bad by Adjacent Geometry Only	0	3	0	15	0	27	0	113

Table 60: Pixel correction by the neighbour texels (9 texels) and the adjacent geometry (2 levels) approaches separated by lighting change for the against viewpoint of the primitives scene.

Algorithm Step	Confirmations and Errors	1024x1024			2048x2048		
		Two Pixels	Four Pixels	Six Pixel	Two Pixels	Four Pixels	Six Pixel
Shadow Map	Total Contour Pixels	11229	22196	32998	11186	22079	32776
	Correct Light Pixels	4407 (77.82%)	9473 (83.83%)	14870 (87.96%)	4718 (83.50%)	10185 (90.40%)	15733 (93.47%)
	Correct Shadow Pixels	4240 (76.18%)	8924 (81.90%)	13856 (86.10%)	4546 (82.12%)	9672 (89.46%)	14792 (92.78%)
	Incorrect Light Pixels	1256 (22.18%)	1827 (16.17%)	2035 (12.04%)	932 (16.50%)	1082 (9.60%)	1100 (6.53%)
	Incorrect Shadow Pixels	1326 (23.82%)	1972 (18.10%)	2237 (13.90%)	990 (17.88%)	1140 (10.54%)	1151 (7.22%)
Texel Coherence	Confirmations in Light	2257 (39.86%)	4788 (42.37%)	8433 (49.88%)	2392 (42.34%)	6390 (56.71%)	11298 (67.12%)
	Confirmations in Shadow	2289 (41.12%)	4588 (42.11%)	7873 (48.92%)	2387 (43.12%)	6036 (55.83%)	10524 (66.01%)
	Wrong Confirmations in Light	10 (0.00%)	10 (0.00%)	10 (0.00%)	10 (0.00%)	10 (0.00%)	10 (0.00%)
	Wrong Confirmations in Shadow	0 (0.00%)	0 (0.00%)	0 (0.00%)	0 (0.00%)	0 (0.00%)	0 (0.00%)
Neighbouring Texels	Corrections from Light	650 (11.48%)	880 (7.79%)	951 (5.63%)	574 (10.16%)	631 (5.60%)	634 (3.77%)
	Confirmations in Shadow	3508 (63.03%)	7534 (69.14%)	12078 (75.05%)	4131 (74.62%)	9051 (83.71%)	14118 (88.55%)
Adjacent Geometry	Confirmations in Shadow	4186 (75.21%)	8832 (81.06%)	13753 (85.46%)	4536 (81.94%)	9662 (89.36%)	14782 (92.72%)
Final Lighting	Wrong Confirmations in Light	606 (10.70%)	947 (8.38%)	1084 (6.41%)	358 (6.34%)	451 (4.00%)	466 (2.77%)
	Wrong Confirmations in Shadow	54 (0.97%)	92 (0.84%)	103 (0.64%)	10 (0.18%)	10 (0.09%)	10 (0.06%)

Table 61: Algorithm results of the against viewpoint of the primitives scene.

Below are the results for the “side” viewpoint of the “bench” scene.

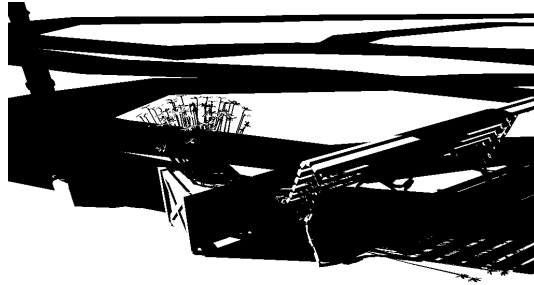


Figure 125: Result of the ray-tracing approach for the side viewpoint of the bench scene.

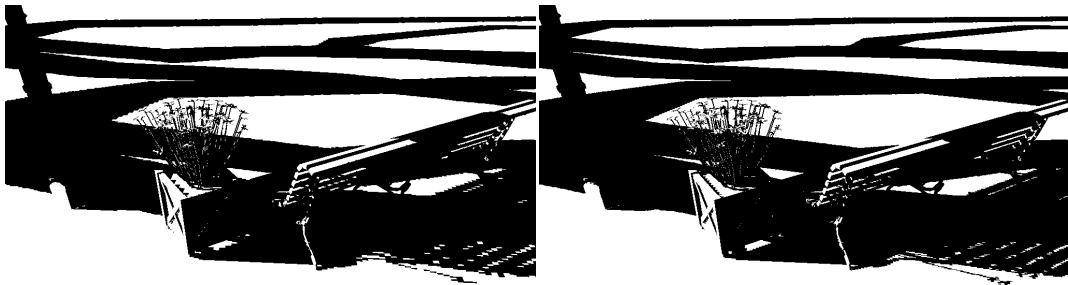


Figure 126: Result of the shadow mapping approach for the side viewpoint of the bench scene.



Figure 127: Result of texel coherence with four texels for the side viewpoint of the bench scene.

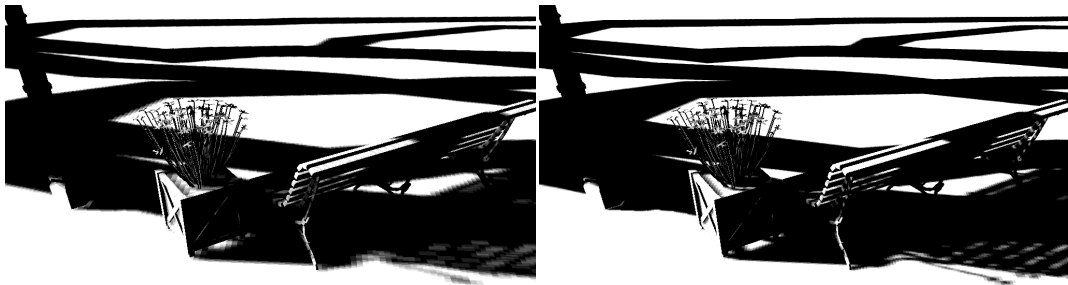


Figure 128: Result of texel coherence with nine texels for the side viewpoint of the bench scene.

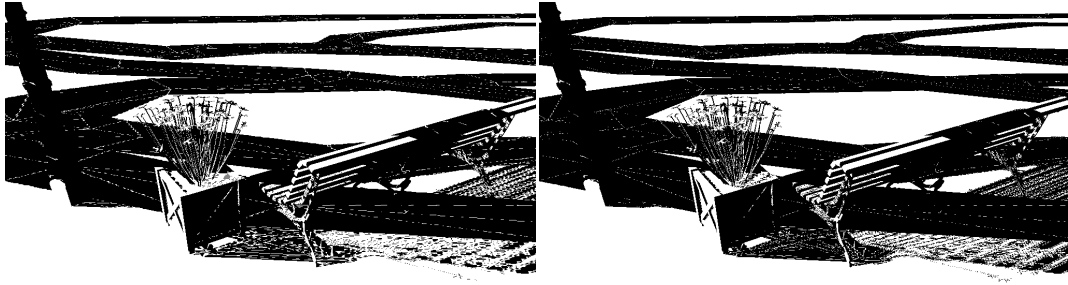


Figure 129: Result of the single texel approach for the side viewpoint of the bench scene.

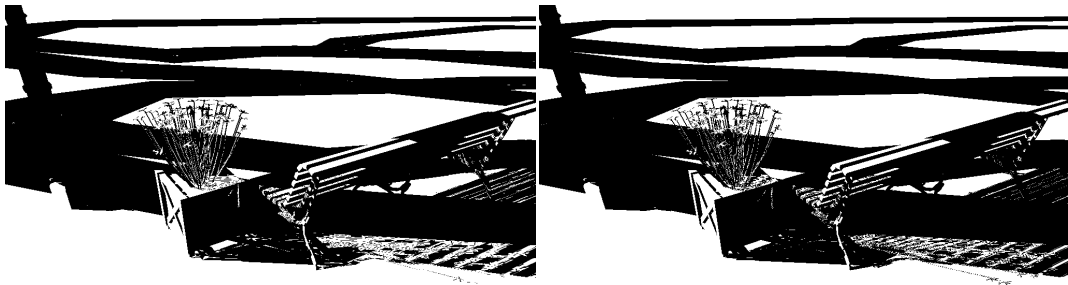


Figure 130: Result of the neighbour texels approach with four neighbours for the side viewpoint of the bench scene.

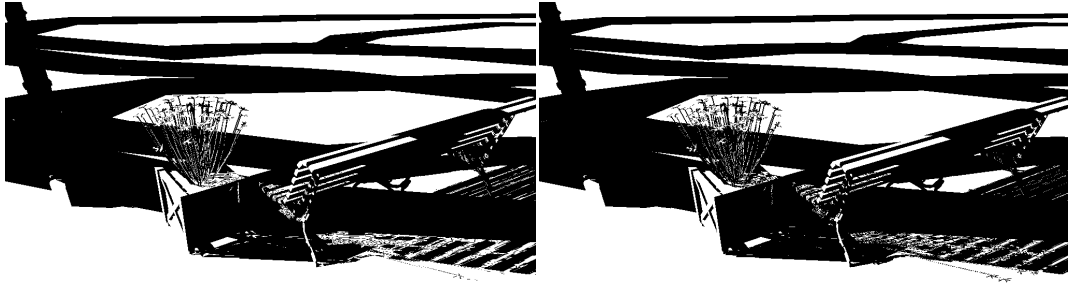


Figure 131: Result of the neighbour texels approach with nine neighbours for the side viewpoint of the bench scene.

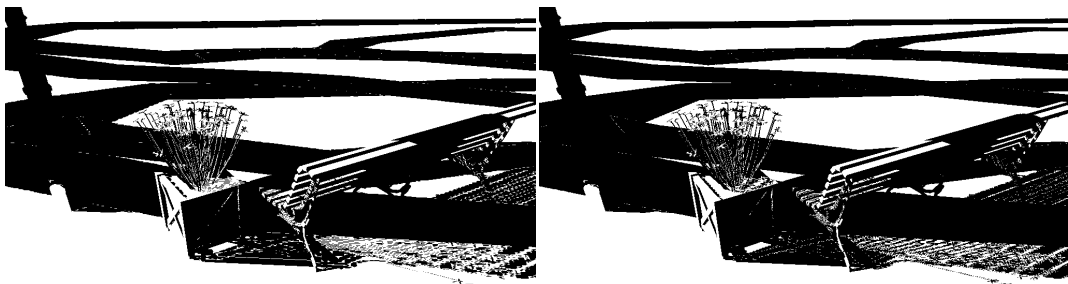


Figure 132: Result of the adjacent geometry approach with one level of adjacency for the side viewpoint of the bench scene.

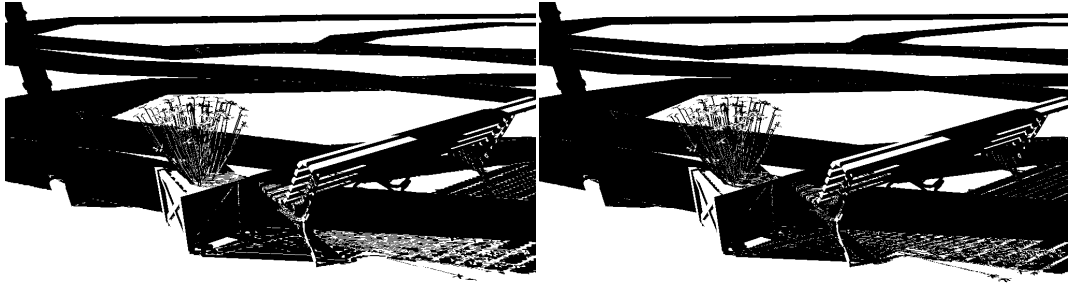


Figure 133: Result of the adjacent geometry approach with two levels of adjacency for the side viewpoint of the bench scene.

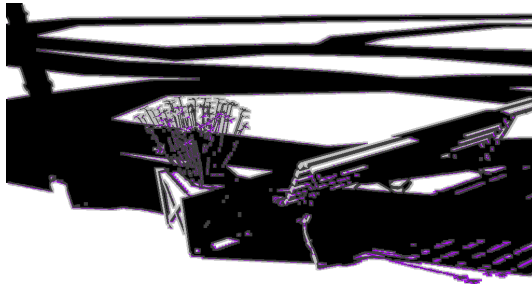


Figure 134: Result of the algorithm with a six pixel thick contour and a 2048x2048 resolution shadow map for the side viewpoint of the bench scene.

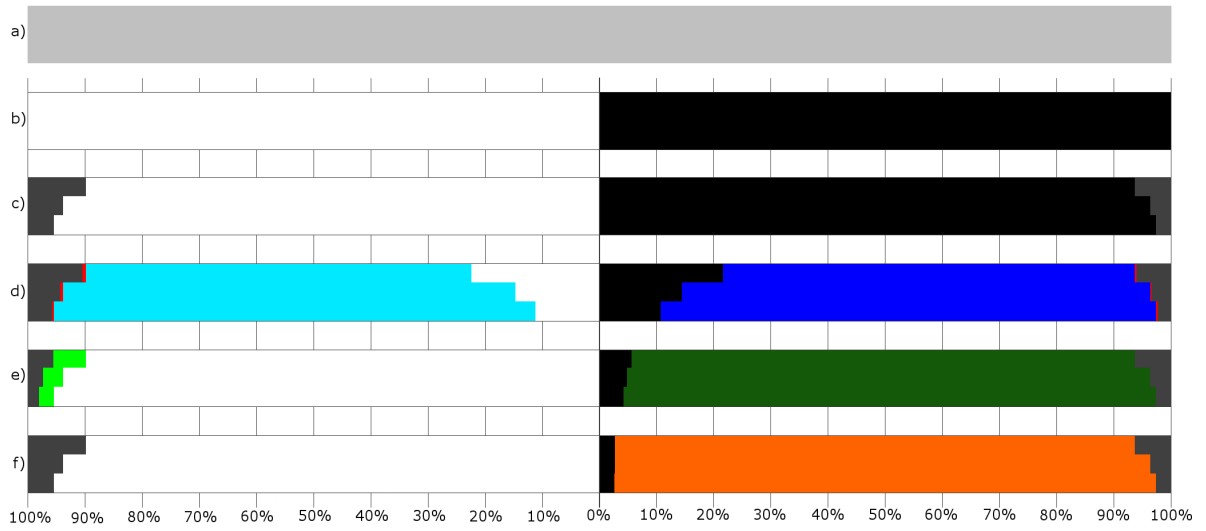
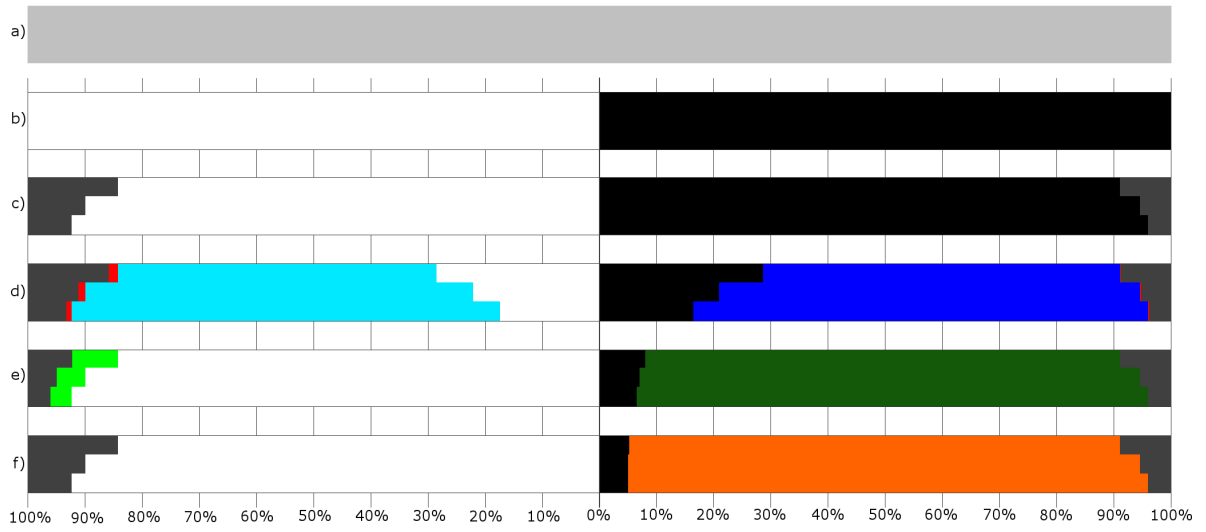


Figure 135: Corrected/confirmed/hinted contour pixels by each method for the side viewpoint of the bench scene using a 1024x1024 (top) and a 2048x2048 (bottom) resolution shadow map.

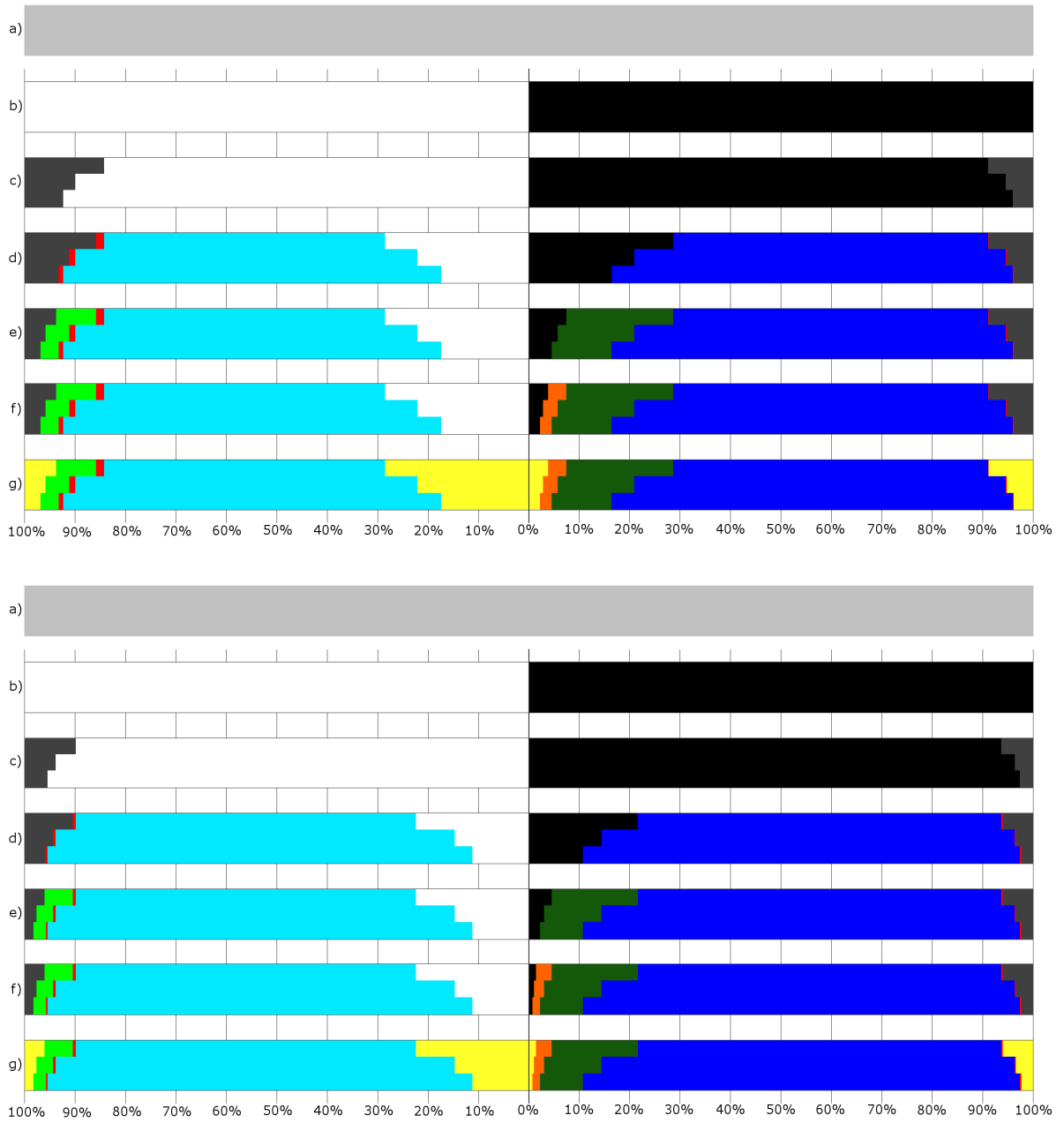


Figure 136: Corrected/confirmed/hinted contour pixels by the chaining of methods for the side viewpoint of the bench scene using a 1024x1024 (top) and a 2048x2048 (bottom) resolution shadow map.

Shadow Map Resolution	Approach	Contour Thickness			
		Two Pixels	Four Pixels	Six Pixels	Whole Image
1024x1024	Pixels in Contour	47615	85277	117574	1048576
	Shadow Map	5775 (12.13%)	6361 (7.46%)	6540 (5.56%)	6847 (0.65%)
	Single Texel	6475 (13.60%)	9321 (10.93%)	11605 (9.87%)	33965 (3.24%)
	Neighbour Texels (4 Neighbours)	4157 (8.73%)	6007 (7.04%)	7265 (6.18%)	16861 (1.61%)
	Neighbour Texels (9 Neighbours)	3772 (7.92%)	5395 (6.33%)	6445 (5.48%)	13606 (1.30%)
	Adjacent Geometry (One Level)	5492 (11.53%)	7417 (8.70%)	8953 (7.61%)	21151 (2.02%)
	Adjacent Geometry (Two Level)	4732 (9.94%)	6062 (7.11%)	7137 (6.07%)	15923 (1.52%)
2048x2048	Pixels in Contour	48096	85741	118318	1048576
	Shadow Map	3885 (8.08%)	4033 (4.70%)	4058 (3.43%)	4128 (0.39%)
	Single Texel	4928 (10.25%)	7120 (8.30%)	8732 (7.38%)	23592 (2.25%)
	Neighbour Texels (4 Neighbours)	2885 (6.00%)	4030 (4.70%)	4815 (4.07%)	10769 (1.03%)
	Neighbour Texels (9 Neighbours)	2464 (5.12%)	3347 (3.90%)	3935 (3.33%)	7839 (0.75%)
	Adjacent Geometry (One Level)	3728 (7.75%)	4985 (5.81%)	5897 (4.98%)	13244 (1.26%)
	Adjacent Geometry (Two Level)	2896 (6.02%)	3527 (4.11%)	4031 (3.41%)	8084 (0.77%)

Table 62: Difference between the approaches that use ray-tracing and the actual ray-tracer for the side viewpoint of the bench scene.

Shadow Map Resolution	Contour Thickness		
	Two Pixels	Four Pixels	Six Pixels
1024x1024	5775 of 6847 (84.34%)	6361 of 6847 (92.90%)	6540 of 6847 (95.52%)
2048x2048	3885 of 4128 (94.11%)	4033 of 4128 (97.70%)	4058 of 4128 (98.30%)

Table 63: Wrongly defined pixels in the shadow mapping result which are inside the contour in the side viewpoint of the bench scene.

Shadow Map Resolution	Contour Thickness	Pixel Shading	
		Light	Shadow
1024x1024	Two Pixels	3536 of 22450	2239 of 25165
	Four Pixels	3837 of 38495	2524 of 46782
	Six Pixels	3910 of 51325	2630 of 66249
	Whole Image	3954 of 727189	2893 of 321387
2048x2048	Two Pixels	2286 of 22566	1599 of 25530
	Four Pixels	2321 of 38321	1712 of 47420
	Six Pixels	2324 of 51024	1734 of 67294
	Whole Image	2333 of 726666	1795 of 321910

Table 64: Pixels that the shadow map defines wrongly in the side viewpoint of the bench scene, separated in pixels defined in light and in shadow, compared to the total amount of pixels lighted in the same way.

Shadow Map Resolution	Contour Thickness	Texel Coherence					
		Light			Shadow		
		Confirmed	Incorrectly Confirmed	Undecided	Confirmed	Incorrectly Confirmed	Undecided
1024x1024	Two Pixels	12382 (55.15%)	347 (1.55%)	10068 (44.85%)	15717 (62.46%)	15 (0.06%)	9448 (37.54%)
	Four Pixels	26537 (68.94%)	412 (1.07%)	11958 (31.06%)	34515 (73.78%)	72 (0.15%)	12267(26.2 2%)
	Six Pixels	38867 (75.73%)	440 (0.86%)	12458 (24.27%)	52837 (79.76%)	116 (0.18%)	13412 (20.24%)
	Whole Image	714366 (98.24%)	451 (0.06%)	12823 (1.76%)	306506 (95.37%)	310 (0.10%)	14881 (4.63%)
2048x2048	Two Pixels	15340 (67.98%)	129 (0.57%)	7226 (32.02%)	18418 (72.14%)	33 (0.13%)	7112 (27.86%)
	Four Pixels	30465 (79.50%)	144 (0.38%)	7856 (20.50%)	38912 (82.06%)	71 (0.15%)	8508 (17.94%)
	Six Pixels	43081 (84.43%)	145 (0.28%)	7943 (15.57%)	58399 (86.78%)	86 (0.13%)	8895 (13.22%)
	Whole Image	718661 (98.90%)	145 (0.02%)	8005 (1.10%)	312737 (97.15%)	131 (0.04%)	9173 (2.85%)

Table 65: Pixel confirmation when using texel coherence with four texels for the side viewpoint of the bench scene.

Shadow Map Resolution	Contour Thickness	Texel Shadowing							
		Light				Shadow			
		3 shadow/1 light	3 shadow/1 light in ray-tracer shadow	1 shadow/3 light	1 shadow/3 light in ray-tracer light	3 shadow/1 light	3 shadow/1 light in ray-tracer shadow	1 shadow/3 light	1 shadow/3 light in ray-tracer light
1024x1024	Two Pixels	2524	1590	3912	3414	4327	3895	1593	960
	Four Pixels	2718	1659	4945	4403	6166	5610	1766	984
	Six Pixels	2718	1659	5291	4739	7041	6440	1799	989
	Whole Image	2734	1670	5545	4980	8255	7595	1810	991
2048x2048	Two Pixels	1544	985	3003	2672	3327	3060	1226	713
	Four Pixels	1547	987	3431	3092	4265	3960	1263	715
	Six Pixels	1548	988	3495	3155	4531	4223	1279	716
	Whole Image	1556	993	3522	3182	4687	4373	1293	718

Table 66: Pixel shadowing for pixels that don't achieve texel coherence with four texels for the side viewpoint of the bench scene.

Shadow Map Resolution	Contour Thickness	Texel Coherence					
		Light			Shadow		
		Confirmed	Incorrectly Confirmed	Undecided	Confirmed	Incorrectly Confirmed	Undecided
1024x1024	Two Pixels	8247 (36.73%)	174 (0.78%)	14203 (63.27%)	12715 (50.53%)	2 (0.01%)	12450 (49.47%)
	Four Pixels	19626 (50.98%)	183 (0.48%)	18869 (49.02%)	28276 (60.44%)	8 (0.02%)	18506 (39.56%)
	Six Pixels	30488 (59.40%)	187 (0.36%)	20837 (40.60%)	44458 (67.11%)	16 (0.02%)	21791 (32.89%)
	Whole Image	704625 (96.90%)	198 (0.03%)	22564 (3.10%)	293499 (91.32%)	174 (0.05%)	27888 (8.68%)
2048x2048	Two Pixels	11762 (52.12%)	67 (0.30%)	10804 (47.88%)	15032 (58.88%)	4 (0.02%)	10498 (41.12%)
	Four Pixels	25588 (66.77%)	75 (0.20%)	12733 (33.23%)	33488 (70.62%)	12 (0.03%)	13932 (29.38%)
	Six Pixels	37864 (74.21%)	75 (0.15%)	13160 (25.79%)	52038 (77.33%)	18 (0.03%)	15256 (22.67%)
	Whole Image	713215 (98.15%)	75 (0.01%)	13451 (1.85%)	305286 (94.84%)	52 (0.02%)	16624 (5.16%)

Table 67: Pixel confirmation when using texel coherence with nine texels for the side viewpoint of the bench scene.

Shadow Map Lighting	Texel Shadowing	Shadow Map							
		1024x1024				2048x2048			
		Two Pixels	Four Pixels	Six Pixels	Whole Image	Two Pixels	Four Pixels	Six Pixels	Whole Image
Light	8 S-1 L	567	607	607	607	159	159	159	162
	8 S-1 L in RT Shadow	352	362	362	362	93	93	93	93
	7 S-2 L	663	804	822	823	379	382	382	382
	7 S-2 L in RT Shadow	341	392	402	402	187	187	187	187
	6 S-3 L	857	1072	1104	1127	662	693	693	699
	6 S-3 L in RT Shadow	402	461	470	475	298	298	298	299
	5 S-4 L	502	620	651	664	679	770	770	780
	5 S-4 L in RT Shadow	209	231	237	239	250	251	251	253
	4 S-5 L	2323	2775	2850	2874	1998	2153	2159	2168
	4 S-5 L in RT Light	1425	1828	1897	1914	1344	1492	1497	1504
	3 S-6 L	3800	4915	5266	5466	2832	3176	3246	3271
	3 S-6 L in RT Light	3157	4227	4559	4752	2360	2697	2767	2790
	2 S-7 L	2618	3494	3877	4147	1803	2137	2216	2287
	2 S-7 L in RT Light	2310	3155	3529	3787	1624	1954	2032	2103
	1 S-8 L	2873	4582	5660	6856	2292	3263	3535	3702
1 S-8 L in RT Light	2664	4348	5416	6612	2206	3169	3440	3607	
Shadow	8 S-1 L	2307	4570	6393	10973	2180	3932	4741	5574
	8 S-1 L in RT Shadow	2205	4414	6194	10719	2122	3854	4654	5478
	7 S-2 L	2810	4248	4979	6062	2226	3031	3348	3644
	7 S-2 L in RT Shadow	2541	3902	4615	5658	2056	2821	3135	3426
	6 S-3 L	3664	5022	5457	5707	2996	3477	3581	3723
	6 S-3 L in RT Shadow	3099	4427	4847	5092	2575	3037	3139	3272
	5 S-4 L	2406	3037	3232	3363	2094	2297	2336	2380
	5 S-4 L in RT Shadow	1544	2118	2298	2427	1493	1687	1725	1765
	4 S-5 L	465	577	606	634	449	541	558	583
	4 S-5 L in RT Light	160	181	181	184	139	145	145	145
	3 S-6 L	465	612	653	670	319	373	393	412
	3 S-6 L in RT Light	149	168	170	170	96	103	103	103
	2 S-7 L	265	349	371	377	178	224	241	250
	2 S-7 L in RT Light	103	120	124	124	86	90	90	90
	1 S-8 L	68	91	100	102	56	57	58	58
1 S-8 L in RT Light	27	31	32	32	24	24	25	25	

Table 68: Pixel shadowing for pixels that don't achieve texel coherence with nine texels for the side viewpoint of the bench scene.

Shadow Map Resolution	Contour Thickness	Corrected		Turned Bad		Maintained Correct		Maintained Incorrect	
		L→S	S→L	L→S	S→L	L→L	S→S	L→L	S→S
1024x1024	Two Pixels	64	2239	0	3003	18914	19923	3472	0
	Four Pixels	64	2524	0	5548	34658	38710	3773	0
	Six Pixels	64	2630	0	7759	47415	55860	3846	0
	Whole Image	64	2893	0	30075	723235	288419	3890	0
2048x2048	Two Pixels	56	1599	0	2698	20280	21233	2230	0
	Four Pixels	56	1712	0	4855	36000	40853	2265	0
	Six Pixels	56	1734	0	6464	48700	59096	2268	0
	Whole Image	56	1795	0	21315	724333	298800	2277	0

Table 69: Pixel correction between the single texel approach and the shadow mapping approach for the side viewpoint of the bench scene.

Shadow Map Resolution	Contour Thickness	Corrected		Turned Bad		Maintained Correct		Maintained Incorrect	
		L→S	S→L	L→S	S→L	L→L	S→S	L→L	S→S
1024x1024	Two Pixels	1622	2239	0	2243	18914	20683	1914	0
	Four Pixels	1661	2524	0	3831	34658	40427	2176	0
	Six Pixels	1669	2630	0	5024	47415	58595	2241	0
	Whole Image	1681	2893	0	14588	723235	303906	2273	0
2048x2048	Two Pixels	1127	1599	0	1726	20280	22205	1159	0
	Four Pixels	1133	1712	0	2842	36000	42866	1188	0
	Six Pixels	1134	1734	0	3625	48700	61935	1190	0
	Whole Image	1140	1795	0	9576	724333	310539	1193	0

Table 70: Pixel correction between the neighbour texels approach using four neighbours and the shadow mapping approach for the side viewpoint of the bench scene.

Shadow Map Resolution	Contour Thickness	Corrected		Turned Bad		Maintained Correct		Maintained Incorrect	
		L→S	S→L	L→S	S→L	L→L	S→S	L→L	S→S
1024x1024	Two Pixels	1795	2239	0	2031	18914	20895	1741	0
	Four Pixels	1854	2524	0	3412	34658	40846	1983	0
	Six Pixels	1863	2630	0	4398	47415	59221	2047	0
	Whole Image	1879	2893	0	11531	723235	306963	2075	0
2048x2048	Two Pixels	1266	1599	0	1444	20280	22487	1020	0
	Four Pixels	1276	1712	0	2302	36000	43406	1045	0
	Six Pixels	1277	1734	0	2888	48700	62672	1047	0
	Whole Image	1284	1795	0	6790	724333	313325	1049	0

Table 71: Pixel correction between the neighbour texels approach using nine neighbours and the shadow mapping approach for the side viewpoint of the bench scene.

Shadow Map Resolution	Number of Neighbours	Triangle Average	Two Pixels	Four Pixels	Six Pixels	Whole Image
1024x1024	3	Used	1.6106	1.4925	1.4168	0.5363
		Available	1.9790	1.9579	1.9221	1.6291
	8	Used	2.8643	2.6245	2.4574	0.8287
		Available	3.2868	3.2068	3.1183	2.4649
2048x2048	3	Used	1.4633	1.3589	1.2932	0.4819
		Available	1.9108	1.8710	1.8228	1.4787
	8	Used	2.4907	2.2582	2.1095	0.6899
		Available	3.0470	2.9452	2.8457	2.0924

Table 72: Average of triangle intersections when using the neighbour texels approach for the side viewpoint of the bench scene.

Shadow Map Resolution	Contour Thickness	Corrected		Turned Bad		Maintained Correct		Maintained Incorrect	
		L→S	S→L	L→S	S→L	L→L	S→S	L→L	S→S
1024x1024	Two Pixels	99	2239	0	2055	18914	20871	3437	0
	Four Pixels	99	2524	0	3679	34658	40579	3738	0
	Six Pixels	99	2630	0	5142	47415	58477	3811	0
	Whole Image	99	2893	0	17296	723235	301198	3855	0
2048x2048	Two Pixels	82	1599	0	1524	20280	22407	2204	0
	Four Pixels	86	1712	0	2750	36000	42958	2235	0
	Six Pixels	86	1734	0	3659	48700	61901	2238	0
	Whole Image	86	1795	0	10997	724333	309118	2247	0

Table 73: Pixel correction between the adjacent geometry approach with one level of adjacency and the shadow mapping approach for the side viewpoint of the bench scene.

Shadow Map Resolution	Contour Thickness	Corrected		Turned Bad		Maintained Correct		Maintained Incorrect	
		L→S	S→L	L→S	S→L	L→L	S→S	L→L	S→S
1024x1024	Two Pixels	140	2239	0	1336	18914	21590	3396	0
	Four Pixels	148	2524	0	2373	34658	41885	3689	0
	Six Pixels	148	2630	0	3375	47415	60244	3762	0
	Whole Image	148	2893	0	12117	723235	306377	3806	0
2048x2048	Two Pixels	109	1599	0	719	20280	23212	2177	0
	Four Pixels	116	1712	0	1322	36000	44386	2205	0
	Six Pixels	116	1734	0	1823	48700	63737	2208	0
	Whole Image	116	1795	0	5867	724333	314248	2217	0

Table 74: Pixel correction between the adjacent geometry approach with two levels of adjacency and the shadow mapping approach for the side viewpoint of the bench scene.

Shadow Map Resolution	Adjacency Level	Triangle Average	Two Pixels	Four Pixels	Six Pixels	Whole Image
1024x1024	One Level	Used	2.4328	2.4567	2.4731	1.2381
		Available	3.8549	3.8641	3.8724	3.9006
	Two Levels	Used	7.8846	7.9396	8.0098	4.0985
		Available	12.4934	12.4881	12.5415	12.9121
2048x2048	One Level	Used	2.4726	2.5012	2.5187	1.2440
		Available	3.8447	3.8582	3.8682	3.8978
	Two Levels	Used	7.8913	7.9598	8.0509	4.1005
		Available	12.2702	12.2784	12.3648	12.8484

Table 75: Average of triangle intersections when using the adjacent geometry approach for the side viewpoint of the bench scene.

Contour Thickness		Two Pixels		Four Pixels		Six Pixels		Whole Image		
Lighting		L→S	S→L	L→S	S→L	L→S	S→L	L→S	S→L	
Shadow Map Resolution	1024x1024	Corrected by Both	82	2239	86	2524	86	2630	86	2893
		Turned Bad by Both	0	1072	0	1793	0	2386	0	6359
		Corrected by Neighbour Texels Only	1713	0	1768	0	1777	0	1793	0
		Corrected by Adjacent Geometry Only	58	0	62	0	62	0	62	0
		Turned Bad by Neighbour Texels Only	0	959	0	1619	0	2012	0	5172
		Turned Bad by Adjacent Geometry Only	0	264	0	580	0	989	0	5758
	2048x2048	Corrected by Both	76	1599	78	1712	78	1734	78	1795
		Turned Bad by Both	0	487	0	831	0	1085	0	2575
		Corrected by Neighbour Texels Only	1190	0	1198	0	1199	0	1206	0
		Corrected by Adjacent Geometry Only	33	0	38	0	38	0	38	0
		Turned Bad by Neighbour Texels Only	0	957	0	1471	0	1803	0	4215
		Turned Bad by Adjacent Geometry Only	0	232	0	491	0	738	0	3292

Table 76: Pixel correction by the neighbour texels (9 texels) and the adjacent geometry (2 levels) approaches separated by lighting change for the side viewpoint of the bench scene.

Algorithm Step	Confirmations and Errors	1024x1024			2048x2048		
		Two Pixels	Four Pixels	Six Pixel	Two Pixels	Four Pixels	Six Pixel
Shadow Map	Total Contour Pixels	47615	85277	117574	48096	85741	118318
	Correct Light Pixels	18914 (84.25%)	34658 (90.03%)	47415 (92.38%)	20280 (89.87%)	36000 (93.94%)	48700 (95.45%)
	Correct Shadow Pixels	22926 (91.10%)	44258 (94.60%)	63619 (96.03%)	23931 (93.74%)	45708 (96.39%)	65560 (97.42%)
	Incorrect Light Pixels	3536 (15.75%)	3837 (9.97%)	3910 (7.62%)	2286 (10.13%)	2321 (6.06%)	2324 (4.55%)
	Incorrect Shadow Pixels	2239 (8.90%)	2524 (5.40%)	2630 (3.97%)	1599 (6.26%)	1712 (3.61%)	1734 (2.58%)
Texel Coherence	Confirmations in Light	12382 (55.15%)	26537 (68.94%)	38867 (75.73%)	15340 (67.98%)	30465 (79.50%)	43081 (84.43%)
	Confirmations in Shadow	15717 (62.46%)	34515 (73.78%)	52837 (79.76%)	18418 (72.14%)	38912 (82.06%)	58399 (86.78%)
	Wrong Confirmations in Light	347 (1.55%)	412 (1.07%)	440 (0.86%)	129 (0.57%)	144 (0.38%)	145 (0.28%)
	Wrong Confirmations in Shadow	15 (0.06%)	72 (0.15%)	116 (0.18%)	33 (0.13%)	71 (0.15%)	86 (0.13%)
Neighbouring Texels	Corrections from Light	1765 (7.86%)	1818 (4.72%)	1827 (3.56%)	1248 (5.53%)	1256 (3.28%)	1257 (2.46%)
	Confirmations in Shadow	21056 (83.67%)	41606 (88.94%)	60672 (91.58%)	22796 (89.29%)	44303 (93.43%)	64076 (95.22%)
Adjacent Geometry	Confirmations in Shadow	21969 (87.30%)	42965 (91.84%)	62186 (93.87%)	23570 (92.32%)	45277 (95.48%)	65109 (96.75%)
Final Lighting	Wrong Confirmations in Light	1782 (7.94%)	2030 (5.27%)	2094 (4.08%)	1059 (4.69%)	1086 (2.83%)	1088 (2.13%)
	Wrong Confirmations in Shadow	987 (3.92%)	1437 (3.07%)	1665 (2.51%)	427 (1.67%)	573 (1.21%)	623 (0.93%)

Table 77: Algorithm results of the side viewpoint of the bench scene.

And below are the results of the “with” viewpoint of the “bench” scene.



Figure 137: Result of the ray-tracing approach for the with viewpoint of the bench scene.

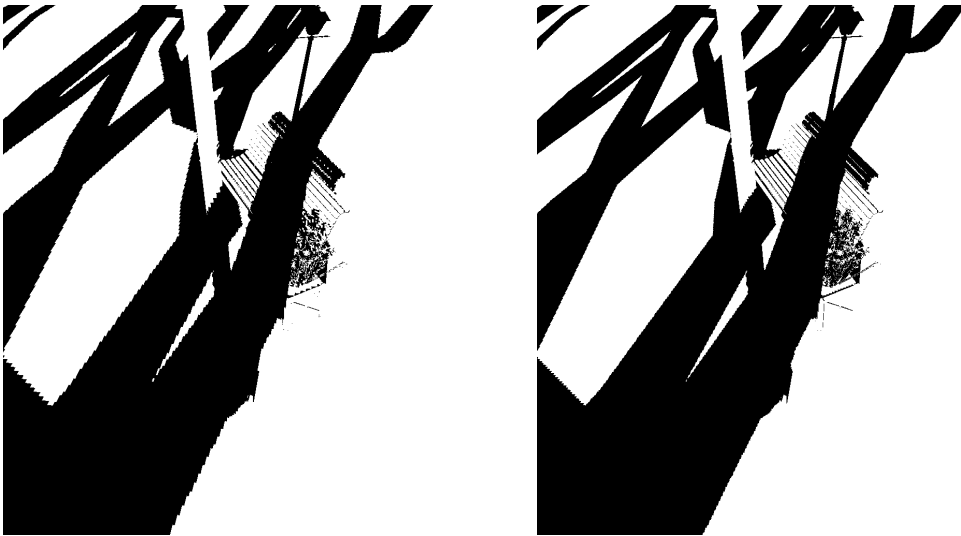


Figure 138: Result of the shadow mapping approach for the with viewpoint of the bench scene.

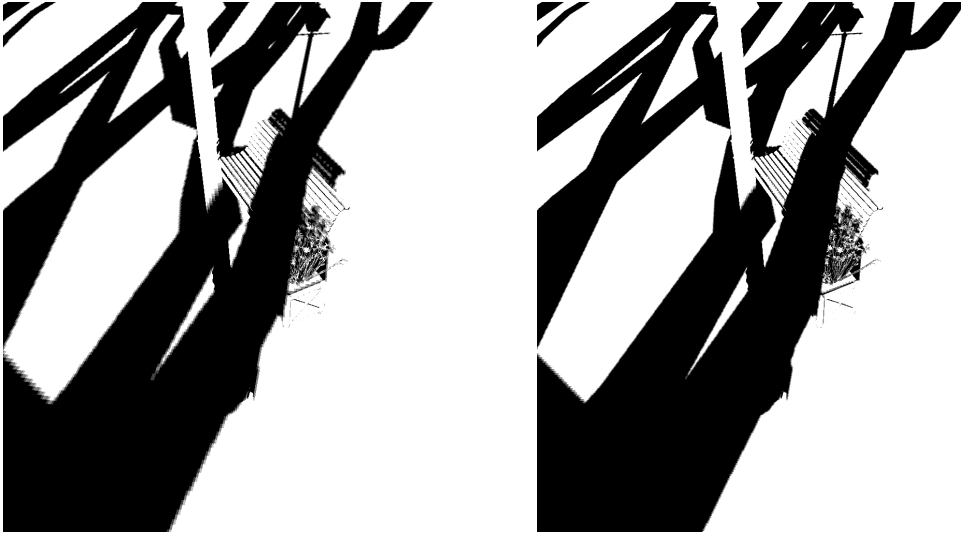


Figure 139: Result of texel coherence with four texels for the with viewpoint of the bench scene.

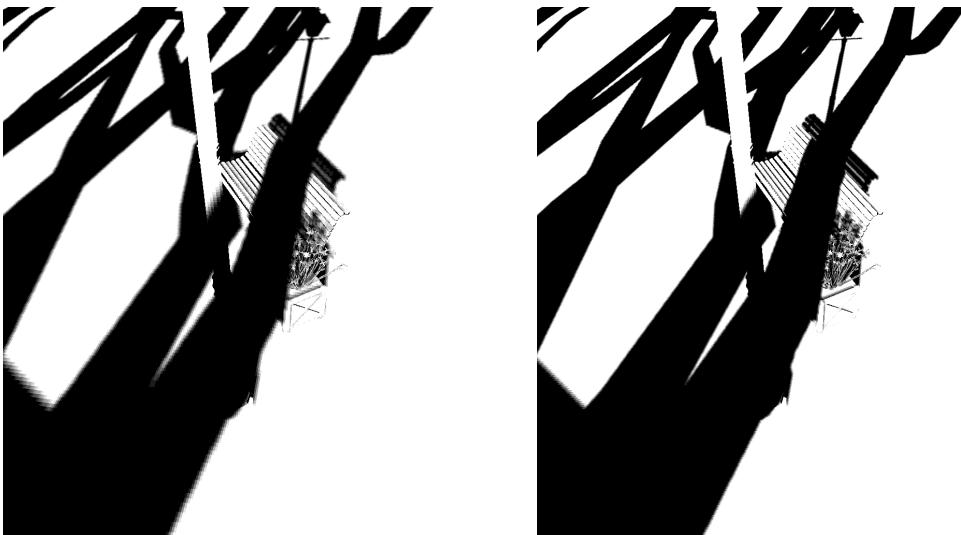


Figure 140: Result of texel coherence with nine texels for the with viewpoint of the bench scene.

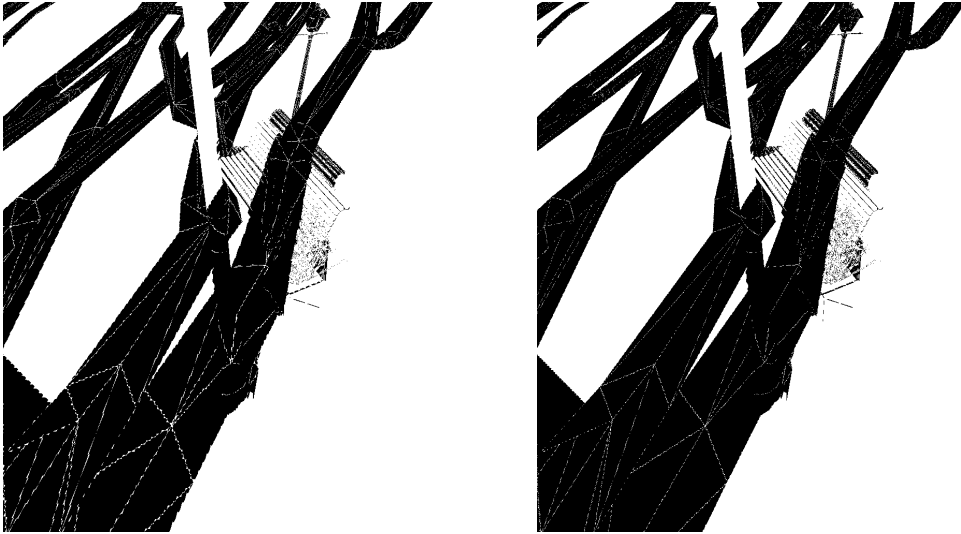


Figure 141: Result of the single texel approach for the with viewpoint of the bench scene.

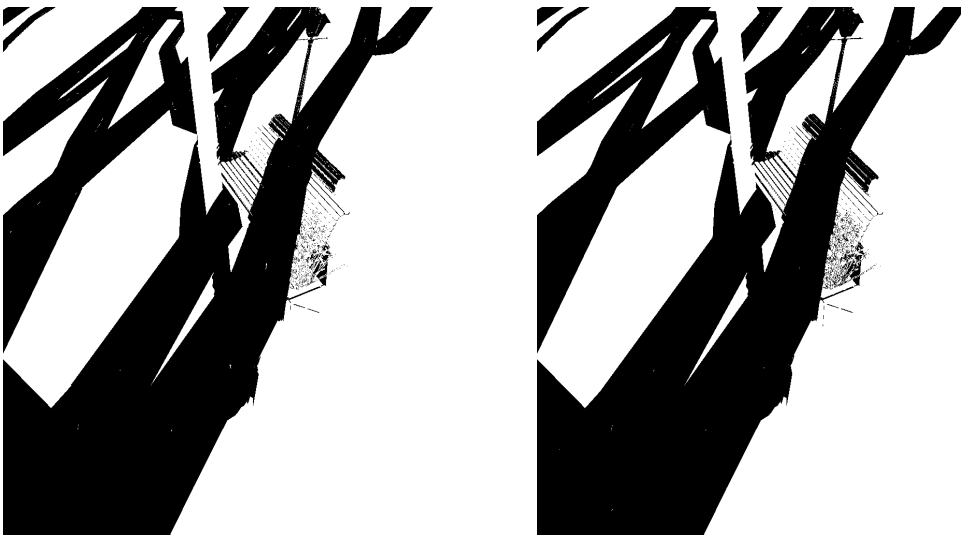


Figure 142: Result of the neighbour texels approach with four neighbours for the with viewpoint of the bench scene.

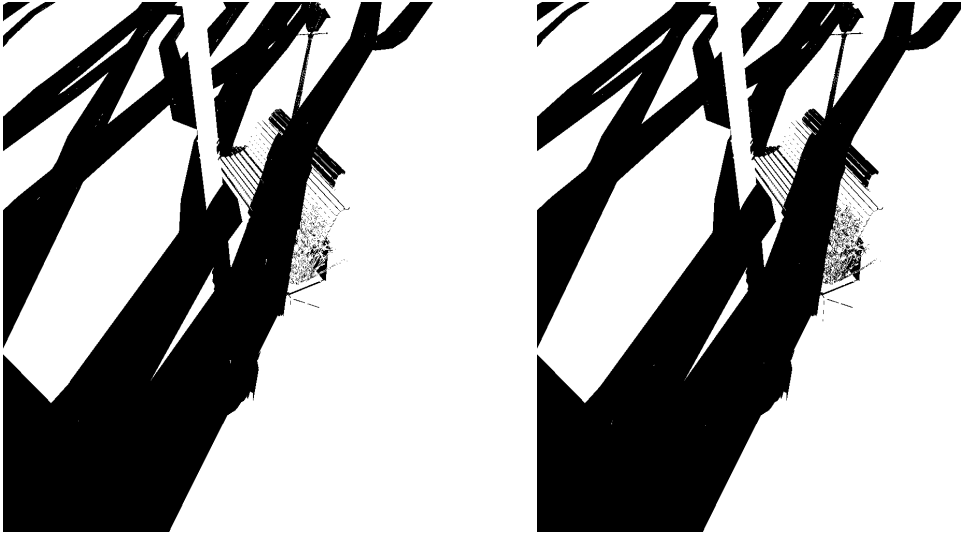


Figure 143: Result of the neighbour texels approach with nine neighbours for the with viewpoint of the bench scene.

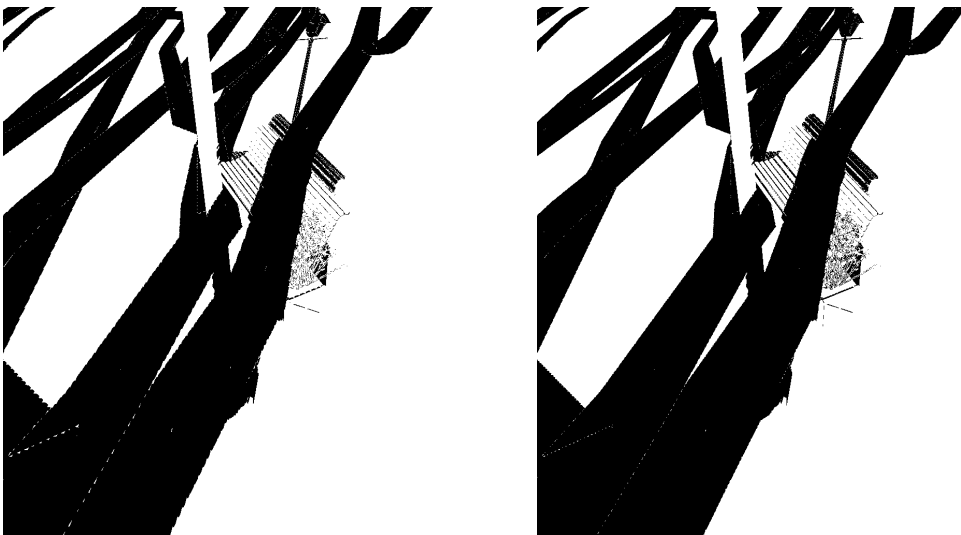


Figure 144: Result of the adjacent geometry approach with one level of adjacency for the with viewpoint of the bench scene.

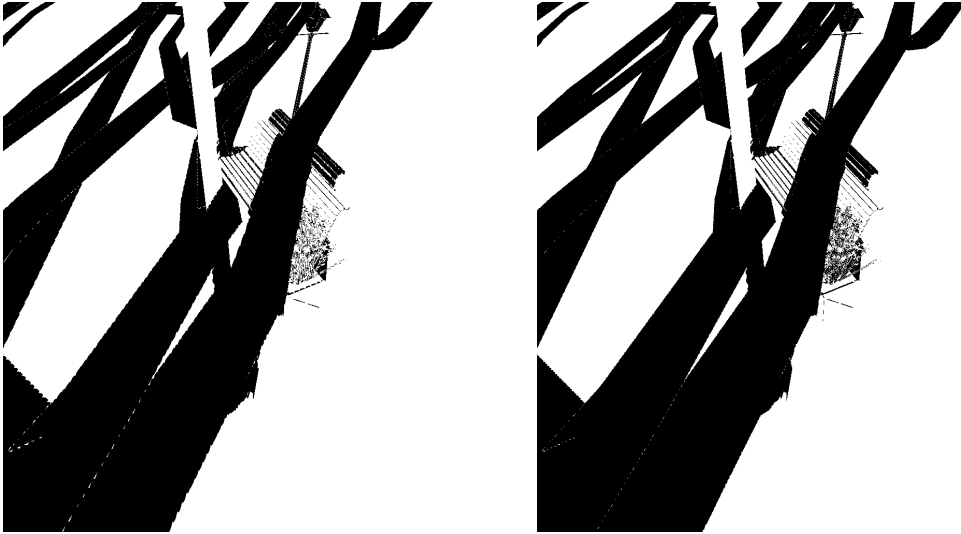


Figure 145: Result of the adjacent geometry approach with two levels of adjacency for the with viewpoint of the bench scene.



Figure 146: Result of the algorithm with a six pixel thick contour and a 2048x2048 resolution shadow map for the with viewpoint of the bench scene.

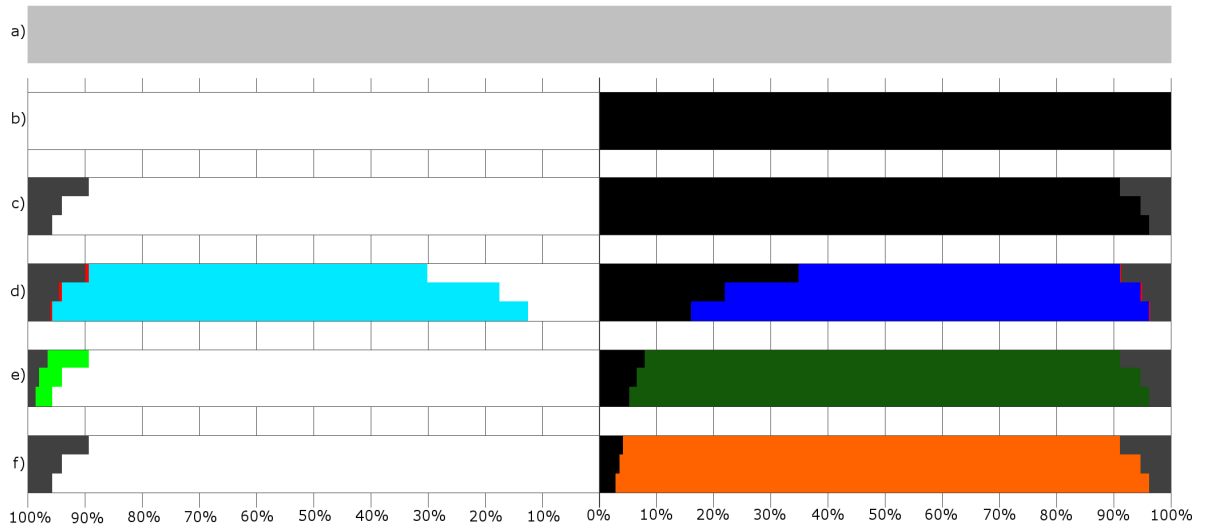
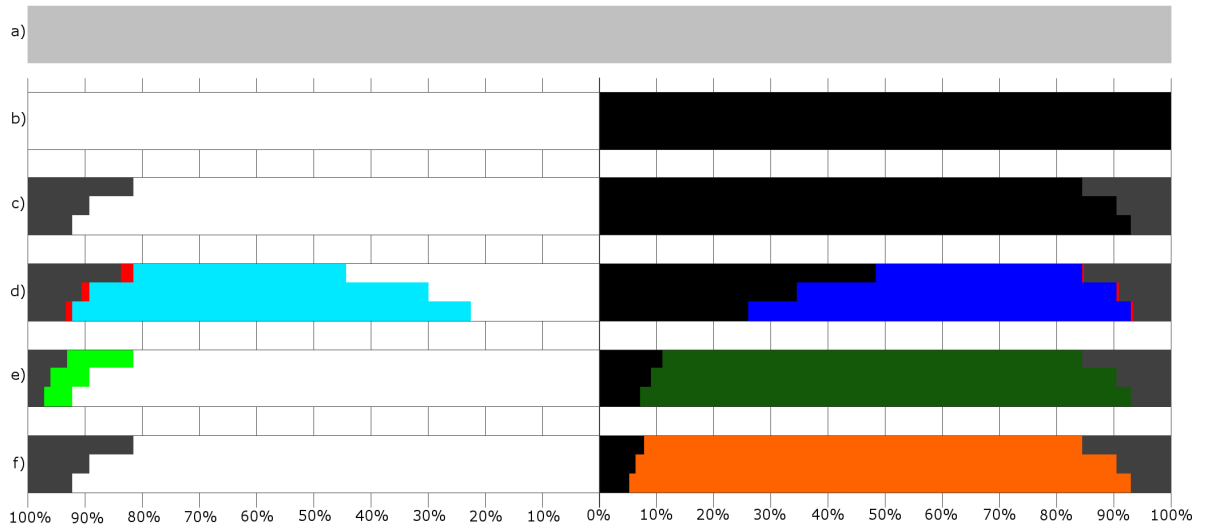


Figure 147: Corrected/confirmed/hinted contour pixels by each method for the with viewpoint of the bench scene using a 1024x1024 (top) and a 2048x2048 (bottom) resolution shadow map.

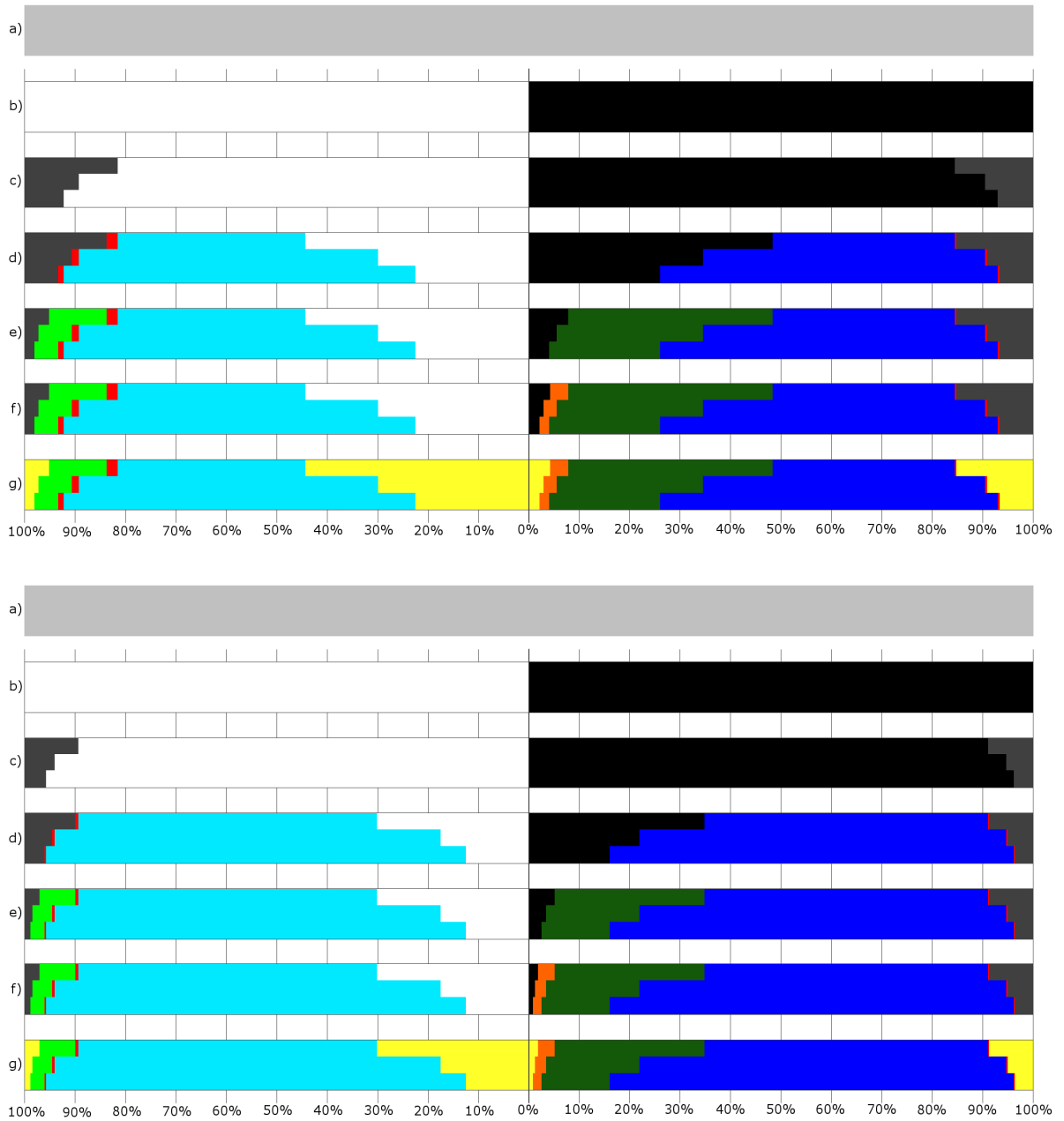


Figure 148: Corrected/confirmed/hinted contour pixels by the chaining of methods for the with viewpoint of the bench scene using a 1024x1024 (top) and a 2048x2048 (bottom) resolution shadow map.

Shadow Map Resolution	Approach	Contour Thickness			
		Two Pixels	Four Pixels	Six Pixels	Whole Image
1024x1024	Pixels in Contour	36910	65811	91380	1048576
	Shadow Map	6268 (16.98%)	6664 (10.13%)	6721 (7.36%)	6799 (0.65%)
	Single Texel	6643 (18.00%)	8439 (12.82%)	9284 (10.16%)	20216 (1.93%)
	Neighbour Texels (4 Neighbours)	3783 (10.25%)	4853 (7.37%)	5179 (5.67%)	5591 (0.53%)
	Neighbour Texels (9 Neighbours)	3298 (8.94%)	4247 (6.45%)	4535 (4.96%)	4801 (0.46%)
	Adjacent Geometry (One Level)	5546 (15.03%)	6669 (10.13%)	7076 (7.74%)	8278 (0.79%)
	Adjacent Geometry (Two Level)	4833 (13.09%)	5619 (8.54%)	5911 (6.47%)	6800 (0.65%)
2048x2048	Pixels in Contour	36758	65457	91013	1048576
	Shadow Map	3603 (9.80%)	3674 (5.61%)	3684 (4.05%)	3710 (0.35%)
	Single Texel	4811 (13.09%)	6084 (9.29%)	6629 (7.28%)	12081 (1.15%)
	Neighbour Texels (4 Neighbours)	2586 (7.04%)	3376 (5.16%)	3629 (3.99%)	3754 (0.36%)
	Neighbour Texels (9 Neighbours)	2110 (5.74%)	2760 (4.22%)	2985 (3.28%)	3063 (0.29%)
	Adjacent Geometry (One Level)	3543 (9.64%)	4288 (6.55%)	4577 (5.03%)	5101 (0.49%)
	Adjacent Geometry (Two Level)	2679 (7.29%)	3079 (4.70%)	3231 (3.55%)	3639 (0.35%)

Table 78: Difference between the approaches that use ray-tracing and the actual ray-tracer for the with viewpoint of the bench scene.

Shadow Map Resolution	Contour Thickness		
	Two Pixels	Four Pixels	Six Pixels
1024x1024	6268 of 6799 (92.19%)	6664 of 6799 (98.01%)	6721 of 6799 (98.85%)
2048x2048	3603 of 3710 (97.12%)	3674 of 3710 (99.03%)	3684 of 3710 (99.30%)

Table 79: Wrongly defined pixels in the shadow mapping result which are inside the contour in the with viewpoint of the bench scene.

Shadow Map Resolution	Contour Thickness	Pixel Shading	
		Light	Shadow
1024x1024	Two Pixels	3464 of 18814	2804 of 18096
	Four Pixels	3648 of 34230	3016 of 31581
	Six Pixels	3663 of 47648	3058 of 43732
	Whole Image	3710 of 681367	3089 of 367209
2048x2048	Two Pixels	1967 of 18481	1636 of 18277
	Four Pixels	1987 of 33605	1687 of 31852
	Six Pixels	1991 of 46917	1693 of 44096
	Whole Image	2010 of 681056	1700 of 367520

Table 80: Pixels that the shadow map defines wrongly in the with viewpoint of the bench scene, separated in pixels defined in light and in shadow, compared to the total amount of pixels lighted in the same way.

Shadow Map Resolution	Contour Thickness	Texel Coherence					
		Light			Shadow		
		Confirmed	Incorrectly Confirmed	Undecided	Confirmed	Incorrectly Confirmed	Undecided
1024x1024	Two Pixels	7381 (39.23%)	390 (2.07%)	11433 (60.77%)	6585 (36.39%)	43 (0.24%)	11511 (63.61%)
	Four Pixels	20741 (60.59%)	438 (1.28%)	13489 (39.41%)	17755 (56.22%)	111 (0.35%)	13826 (43.78%)
	Six Pixels	33681 (70.69%)	449 (0.94%)	13967 (29.31%)	29414 (67.26%)	140 (0.32%)	14318 (32.74%)
	Whole Image	667121 (97.91%)	456 (0.07%)	14246 (2.09%)	352645 (96.03%)	143 (0.04%)	14564 (3.97%)
2048x2048	Two Pixels	11032 (59.69%)	104 (0.56%)	7449 (40.31%)	10280 (56.25%)	31 (0.17%)	7997 (43.75%)
	Four Pixels	25827 (76.85%)	122 (0.36%)	7778 (23.15%)	23227 (72.92%)	74 (0.23%)	8625 (27.08%)
	Six Pixels	39120 (83.38%)	126 (0.27%)	7797 (16.62%)	35399 (80.28%)	78 (0.18%)	8697 (19.72%)
	Whole Image	673171 (98.84%)	127 (0.02%)	7885 (1.16%)	358774 (97.62%)	78 (0.02%)	8746 (2.38%)

Table 81: Pixel confirmation when using texel coherence with four texels for the with viewpoint of the bench scene.

Shadow Map Resolution	Contour Thickness	Texel Shadowing							
		Light				Shadow			
		3 shadow/1 light	3 shadow/1 light in ray-tracer shadow	1 shadow/3 light	1 shadow/3 light in ray-tracer light	3 shadow/1 light	3 shadow/1 light in ray-tracer shadow	1 shadow/3 light	1 shadow/3 light in ray-tracer light
1024x1024	Two Pixels	1960	1347	4325	3839	4304	3999	1903	1222
	Four Pixels	2082	1387	5594	5067	5746	5392	2030	1257
	Six Pixels	2084	1387	5943	5413	6089	5729	2032	1257
	Whole Image	2100	1399	6105	5571	6233	5871	2051	1271
2048x2048	Two Pixels	1150	789	3022	2754	3203	3052	1161	733
	Four Pixels	1150	789	3273	3003	3584	3428	1168	734
	Six Pixels	1150	789	3290	3020	3619	3462	1168	734
	Whole Image	1161	797	3336	3066	3635	3478	1170	735

Table 82: Pixel shadowing for pixels that don't achieve texel coherence with four texels for the with viewpoint of the bench scene.

Shadow Map Resolution	Contour Thickness	Texel Coherence					
		Light			Shadow		
		Confirmed	Incorrectly Confirmed	Undecided	Confirmed	Incorrectly Confirmed	Undecided
1024x1024	Two Pixels	3771 (20.04%)	189 (1.00%)	15043 (79.96%)	3666 (20.26%)	5 (0.03%)	14430 (79.74%)
	Four Pixels	12006 (35.07%)	201 (0.59%)	22224 (64.93%)	9663 (30.60%)	12 (0.04%)	21918 (69.40%)
	Six Pixels	22729 (47.70%)	206 (0.43%)	24919 (52.30%)	18954 (43.34%)	21 (0.05%)	24778 (56.66%)
	Whole Image	654010 (95.98%)	211 (0.03%)	27357 (4.02%)	340196 (92.64%)	24 (0.01%)	27013 (7.36%)
2048x2048	Two Pixels	6653 (36.00%)	53 (0.29%)	11828 (64.00%)	5928 (32.43%)	0 (0.00%)	12349 (67.57%)
	Four Pixels	19631 (58.42%)	64 (0.19%)	13974 (41.58%)	16770 (52.65%)	18 (0.06%)	15082 (47.35%)
	Six Pixels	32460 (69.19%)	67 (0.14%)	14457 (30.81%)	28473 (64.57%)	20 (0.05%)	15623 (35.43%)
	Whole Image	666300 (97.83%)	68 (0.01%)	14756 (2.17%)	351707 (95.70%)	20 (0.01%)	15813 (4.30%)

Table 83: Pixel confirmation when using texel coherence with nine texels for the with viewpoint of the bench scene.

Shadow Map Lighting	Texel Shadowing	Shadow Map							
		1024x1024				2048x2048			
		Two Pixels	Four Pixels	Six Pixels	Whole Image	Two Pixels	Four Pixels	Six Pixels	Whole Image
Light	8 S-1 L	147	153	153	153	49	49	49	49
	8 S-1 L in RT Shadow	105	107	107	107	31	31	31	31
	7 S-2 L	332	345	345	346	148	148	148	148
	7 S-2 L in RT Shadow	177	178	178	179	77	77	77	77
	6 S-3 L	460	513	513	517	258	258	258	259
	6 S-3 L in RT Shadow	211	219	219	222	137	137	137	138
	5 S-4 L	377	438	446	458	333	341	341	341
	5 S-4 L in RT Shadow	149	161	161	161	114	115	115	115
	4 S-5 L	3595	4766	5092	5181	2689	2887	2887	2911
	4 S-5 L in RT Light	2048	3133	3458	3534	1780	1978	1978	1990
	3 S-6 L	4325	5837	6250	6680	3341	3699	3760	3816
	3 S-6 L in RT Light	3743	5237	5650	6060	2950	3307	3368	3419
	2 S-7 L	3349	5135	5711	6135	2563	2976	3069	3113
	2 S-7 L in RT Light	3090	4848	5423	5847	2395	2804	2897	2941
	1 S-8 L	2458	5037	6409	7887	2447	3616	3945	4119
1 S-8 L in RT Light	2213	4775	6139	7612	2360	3526	3854	4028	
Shadow	8 S-1 L	1943	4567	6074	7518	2342	3755	4088	4178
	8 S-1 L in RT Shadow	1859	4445	5947	7391	2302	3705	4035	4125
	7 S-2 L	3191	5009	5619	6009	2656	3129	3221	3253
	7 S-2 L in RT Shadow	3023	4809	5406	5795	2578	3041	3133	3165
	6 S-3 L	4436	6130	6563	6844	3561	4010	4086	4141
	6 S-3 L in RT Shadow	3778	5440	5864	6141	3143	3584	3660	3710
	5 S-4 L	3650	4847	5142	5259	2720	2988	3012	3022
	5 S-4 L in RT Shadow	2131	3235	3525	3620	1833	2098	2121	2129
	4 S-5 L	462	536	547	549	393	446	453	454
	4 S-5 L in RT Light	145	148	149	150	74	75	75	75
	3 S-6 L	346	401	404	405	407	476	485	487
	3 S-6 L in RT Light	96	103	103	103	77	78	78	78
	2 S-7 L	262	282	283	283	225	231	231	231
	2 S-7 L in RT Light	92	92	92	92	46	46	46	46
	1 S-8 L	140	146	146	146	45	47	47	47
1 S-8 L in RT Light	37	37	37	37	16	16	16	16	

Table 84: Pixel shadowing for pixels that don't achieve texel coherence with nine texels for the with viewpoint of the bench scene.

Shadow Map Resolution	Contour Thickness	Corrected		Turned Bad		Maintained Correct		Maintained Incorrect	
		L→S	S→L	L→S	S→L	L→L	S→S	L→L	S→S
1024x1024	Two Pixels	4	2804	0	3183	15350	12109	3460	0
	Four Pixels	5	3016	0	4796	30582	23769	3643	0
	Six Pixels	5	3058	0	5626	43985	35048	3658	0
	Whole Image	6	3089	0	16512	677657	347608	3704	0
2048x2048	Two Pixels	20	1636	0	2864	16514	13777	1947	0
	Four Pixels	21	1687	0	4118	31618	26047	1966	0
	Six Pixels	21	1693	0	4659	44926	37744	1970	0
	Whole Image	21	1700	0	10092	679046	355728	1989	0

Table 85: Pixel correction between the single texel approach and the shadow mapping approach for the with viewpoint of the bench scene.

Shadow Map Resolution	Contour Thickness	Corrected		Turned Bad		Maintained Correct		Maintained Incorrect	
		L→S	S→L	L→S	S→L	L→L	S→S	L→L	S→S
1024x1024	Two Pixels	2004	2804	0	2323	15350	12969	1460	0
	Four Pixels	2088	3016	0	3293	30582	25272	1560	0
	Six Pixels	2093	3058	0	3609	43985	37065	1570	0
	Whole Image	2124	3089	0	4005	677657	360115	1586	0
2048x2048	Two Pixels	1212	1636	0	1831	16514	14810	755	0
	Four Pixels	1214	1687	0	2603	31618	27562	773	0
	Six Pixels	1214	1693	0	2852	44926	39551	777	0
	Whole Image	1231	1700	0	2975	679046	362845	779	0

Table 86: Pixel correction between the neighbour texels approach using four neighbours and the shadow mapping approach for the with viewpoint of the bench scene.

Shadow Map Resolution	Contour Thickness	Corrected		Turned Bad		Maintained Correct		Maintained Incorrect	
		L→S	S→L	L→S	S→L	L→L	S→S	L→L	S→S
1024x1024	Two Pixels	2174	2804	0	2008	15350	13284	1290	0
	Four Pixels	2264	3016	0	2863	30582	25702	1384	0
	Six Pixels	2269	3058	0	3141	43985	37533	1394	0
	Whole Image	2300	3089	0	3391	677657	360729	1410	0
2048x2048	Two Pixels	1322	1636	0	1465	16514	15176	645	0
	Four Pixels	1325	1687	0	2098	31618	28067	662	0
	Six Pixels	1325	1693	0	2319	44926	40084	666	0
	Whole Image	1342	1700	0	2395	679046	363425	668	0

Table 87: Pixel correction between the neighbour texels approach using nine neighbours and the shadow mapping approach for the with viewpoint of the bench scene.

Shadow Map Resolution	Number of Neighbours	Triangle Average	Two Pixels	Four Pixels	Six Pixels	Whole Image
1024x1024	3	Used	1.7403	1.5169	1.3771	0.5181
		Available	1.8936	1.8295	1.7593	1.3163
	8	Used	2.9387	2.5643	2.2880	0.6783
		Available	2.9997	2.7842	2.6401	1.6848
2048x2048	3	Used	1.5417	1.3238	1.1987	0.4675
		Available	1.8342	1.7206	1.6283	1.2018
	8	Used	2.5304	2.1126	1.8500	0.5646
		Available	2.7415	2.5288	2.3489	1.4341

Table 88: Average of triangle intersections when using the neighbour texels approach for the with viewpoint of the bench scene.

Shadow Map Resolution	Contour Thickness	Corrected		Turned Bad		Maintained Correct		Maintained Incorrect	
		L→S	S→L	L→S	S→L	L→L	S→S	L→L	S→S
1024x1024	Two Pixels	20	2804	0	2102	15350	13190	3444	0
	Four Pixels	23	3016	0	3044	30582	25521	3625	0
	Six Pixels	24	3058	0	3437	43985	37237	3639	0
	Whole Image	25	3089	0	4593	677657	359527	3685	0
2048x2048	Two Pixels	40	1636	0	1616	16514	15025	1927	0
	Four Pixels	41	1687	0	2342	31618	27823	1946	0
	Six Pixels	41	1693	0	2627	44926	39776	1950	0
	Whole Image	41	1700	0	3132	679046	362688	1969	0

Table 89: Pixel correction between the adjacent geometry approach with one level of adjacency and the shadow mapping approach for the with viewpoint of the bench scene.

Shadow Map Resolution	Contour Thickness	Corrected		Turned Bad		Maintained Correct		Maintained Incorrect	
		L→S	S→L	L→S	S→L	L→L	S→S	L→L	S→S
1024x1024	Two Pixels	51	2804	0	1420	15350	13872	3413	0
	Four Pixels	55	3016	0	2026	30582	26539	3593	0
	Six Pixels	56	3058	0	2304	43985	38370	3607	0
	Whole Image	57	3089	0	3147	677657	360973	3653	0
2048x2048	Two Pixels	52	1636	0	764	16514	15877	1915	0
	Four Pixels	53	1687	0	1145	31618	29020	1934	0
	Six Pixels	53	1693	0	1293	44926	41110	1938	0
	Whole Image	53	1700	0	1682	679046	364138	1957	0

Table 90: Pixel correction between the adjacent geometry approach with two levels of adjacency and the shadow mapping approach for the with viewpoint of the bench scene.

Shadow Map Resolution	Adjacency Level	Triangle Average	Two Pixels	Four Pixels	Six Pixels	Whole Image
1024x1024	One Level	Used	2.6226	2.5888	2.5643	1.5079
		Available	3.8788	3.8798	3.8819	3.9437
	Two Levels	Used	8.3600	8.2441	8.1693	5.2342
		Available	12.3645	12.3552	12.3670	13.6896
2048x2048	One Level	Used	2.6600	2.6235	2.5947	1.5098
		Available	3.8605	3.8669	3.8715	3.9412
	Two Levels	Used	8.4322	8.3126	8.2318	5.2390
		Available	12.2375	12.2524	12.2826	13.6755

Table 91: Average of triangle intersections when using the adjacent geometry approach for the with viewpoint of the bench scene.

Contour Thickness		Two Pixels		Four Pixels		Six Pixels		Whole Image		
Lighting		L→S	S→L	L→S	S→L	L→S	S→L	L→S	S→L	
Shadow Map Resolution	1024x1024	Corrected by Both	7	2804	9	3016	9	3058	10	3089
		Turned Bad by Both	0	1137	0	1602	0	1780	0	1846
		Corrected by Neighbour Texels Only	2167	0	2255	0	2260	0	2290	0
		Corrected by Adjacent Geometry Only	44	0	46	0	47	0	47	0
		Turned Bad by Neighbour Texels Only	0	871	0	1261	0	1361	0	1545
		Turned Bad by Adjacent Geometry Only	0	283	0	424	0	524	0	1301
	2048x2048	Corrected by Both	39	1636	40	1687	40	1693	40	1700
		Turned Bad by Both	0	533	0	804	0	894	0	916
		Corrected by Neighbour Texels Only	1283	0	1285	0	1285	0	1302	0
		Corrected by Adjacent Geometry Only	13	0	13	0	13	0	13	0
		Turned Bad by Neighbour Texels Only	0	932	0	1294	0	1425	0	1479
		Turned Bad by Adjacent Geometry Only	0	231	0	341	0	399	0	766

Table 92: Pixel correction by the neighbour texels (9 texels) and the adjacent geometry (2 levels) approaches separated by lighting change for the with viewpoint of the bench scene.

Algorithm Step	Confirmations and Errors	1024x1024			2048x2048		
		Two Pixels	Four Pixels	Six Pixel	Two Pixels	Four Pixels	Six Pixel
Shadow Map	Total Contour Pixels	36910	65811	91380	96758	65457	91013
	Correct Light Pixels	15350 (81.59%)	30582 (89.34%)	43985 (92.31%)	16514 (89.36%)	31618 (94.09%)	44926 (95.76%)
	Correct Shadow Pixels	15292 (84.50%)	28565 (90.45%)	40674 (93.01%)	16641 (91.05%)	30165 (94.70%)	42403 (96.16%)
	Incorrect Light Pixels	3464 (18.41%)	3648 (10.66%)	3663 (7.69%)	1967 (10.64%)	1987 (5.91%)	1991 (4.24%)
	Incorrect Shadow Pixels	2804 (15.50%)	3016 (9.55%)	3058 (6.99%)	1636 (8.95%)	1687 (5.30%)	1693 (3.84%)
Texel Coherence	Confirmations in Light	7381 (39.23%)	20741 (60.59%)	33681 (70.69%)	11032 (59.69%)	25827 (76.85%)	39120 (83.38%)
	Confirmations in Shadow	6585 (36.39%)	17755 (56.22%)	29414 (67.26%)	10280 (56.25%)	23227 (72.92%)	35399 (80.28%)
	Wrong Confirmations in Light	390 (2.07%)	438 (1.28%)	449 (0.94%)	104 (0.56%)	122 (0.36%)	126 (0.27%)
	Wrong Confirmations in Shadow	43 (0.24%)	111 (0.35%)	140 (0.32%)	31 (0.17%)	74 (0.23%)	78 (0.18%)
Neighbouring Texels	Corrections from Light	2148 (11.42%)	2233 (6.52%)	2237 (4.69%)	1311 (7.09%)	1311 (3.90%)	1311 (2.79%)
	Confirmations in Shadow	13900 (76.81%)	26902 (85.18%)	39021 (89.23%)	15726 (86.05%)	29138 (91.48%)	41358 (93.79%)
Adjacent Geometry	Confirmations in Shadow	14553 (80.42%)	27724 (87.79%)	39854 (91.13%)	16328 (89.34%)	29842 (93.69%)	42082 (95.44%)
Final Lighting	Wrong Confirmations in Light	929 (7.01%)	980 (4.14%)	980 (3.00%)	565 (3.62%)	567 (2.05%)	567 (1.48%)
	Wrong Confirmations in Shadow	782 (4.56%)	952 (3.37%)	960 (2.52%)	344 (2.05%)	397 (1.48%)	399 (1.08%)

Table 93: Algorithm results of the with viewpoint of the bench scene.

Following below are the results of the “against” viewpoint of the “bench” scene.



Figure 149: Result of the ray-tracing approach for the against viewpoint of the bench scene.

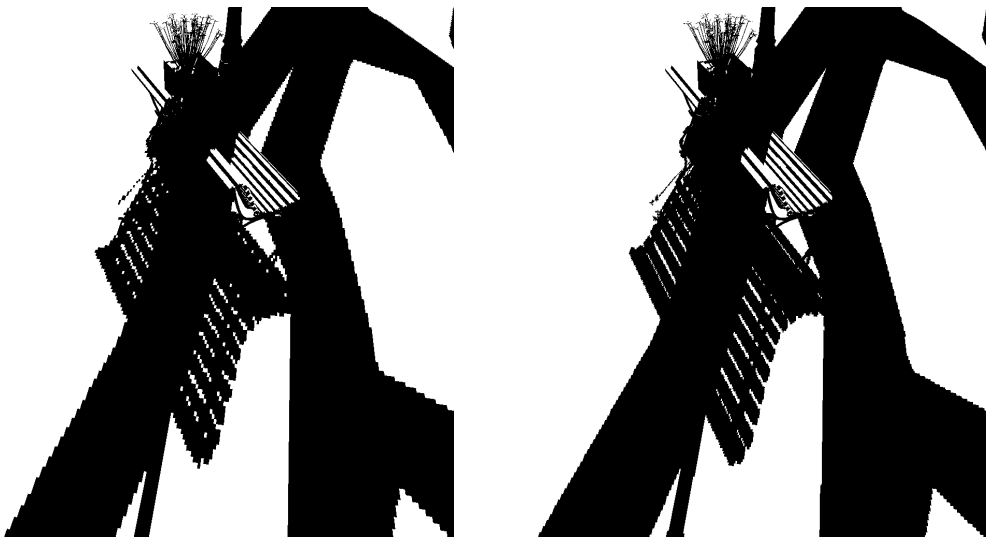


Figure 150: Result of the shadow mapping approach for the against viewpoint of the bench scene.

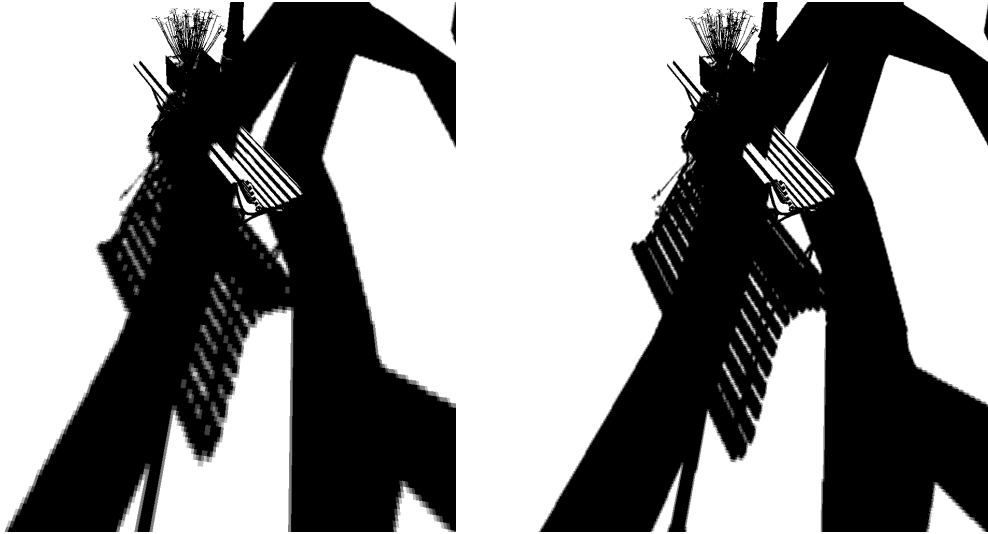


Figure 151: Result of texel coherence with four texels for the against viewpoint of the bench scene.



Figure 152: Result of texel coherence with nine texels for the against viewpoint of the bench scene.

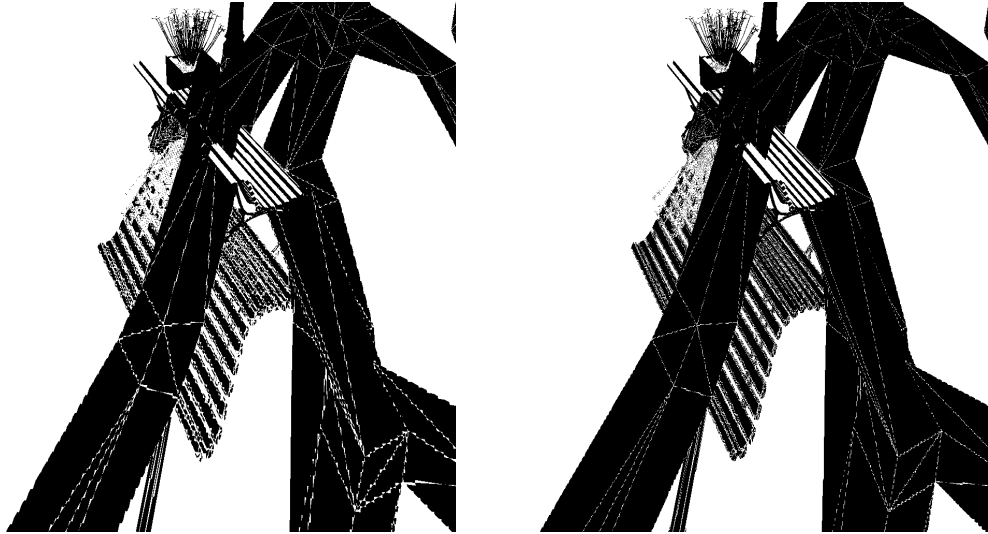


Figure 153: Result of the single texel approach for the against viewpoint of the bench scene.

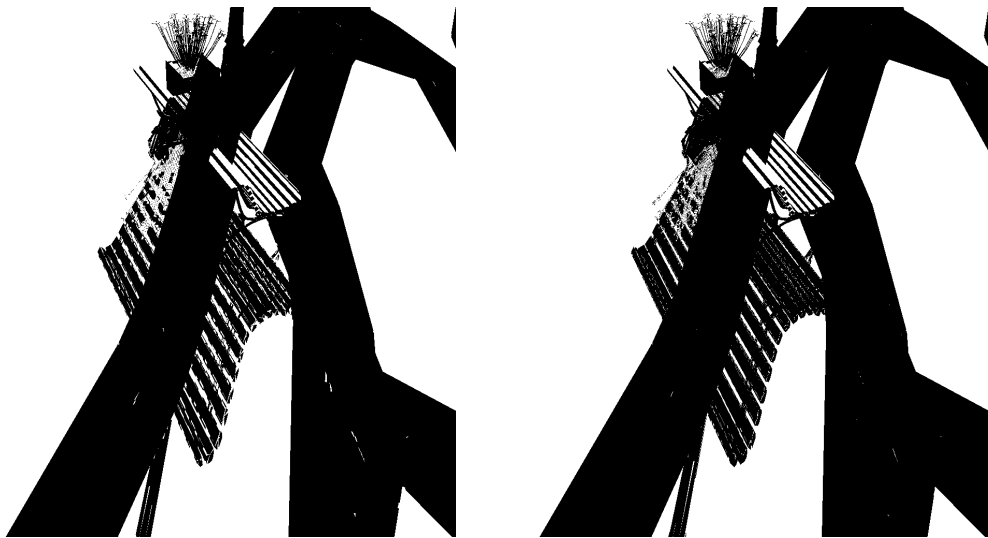


Figure 154: Result of the neighbour texels approach using four neighbours for the against viewpoint of the bench scene.



Figure 155: Result of the neighbour texels approach using nine neighbours for the against viewpoint of the bench scene.

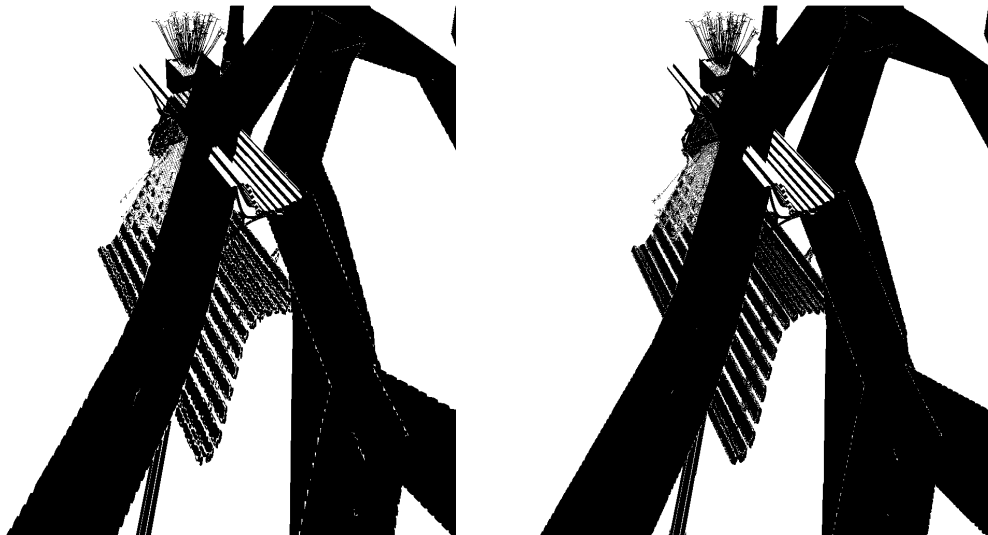


Figure 156: Result of the adjacent geometry approach with one level of adjacency for the against viewpoint of the bench scene.

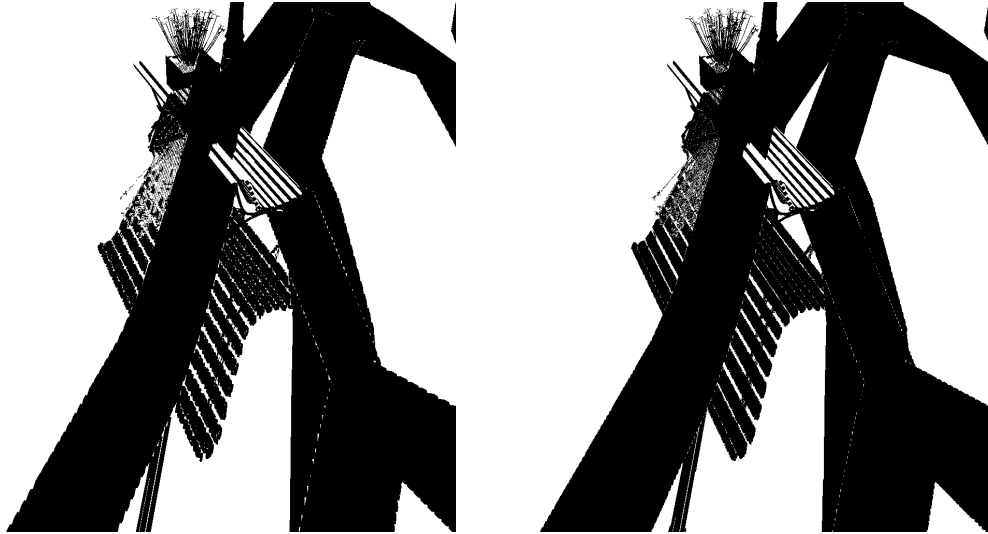


Figure 157: Result of the adjacent geometry approach with two levels of adjacency for the against viewpoint of the bench scene.



Figure 158: Result of the algorithm with a six pixel thick contour and a 2048x2048 resolution shadow map for the against viewpoint of the bench scene.

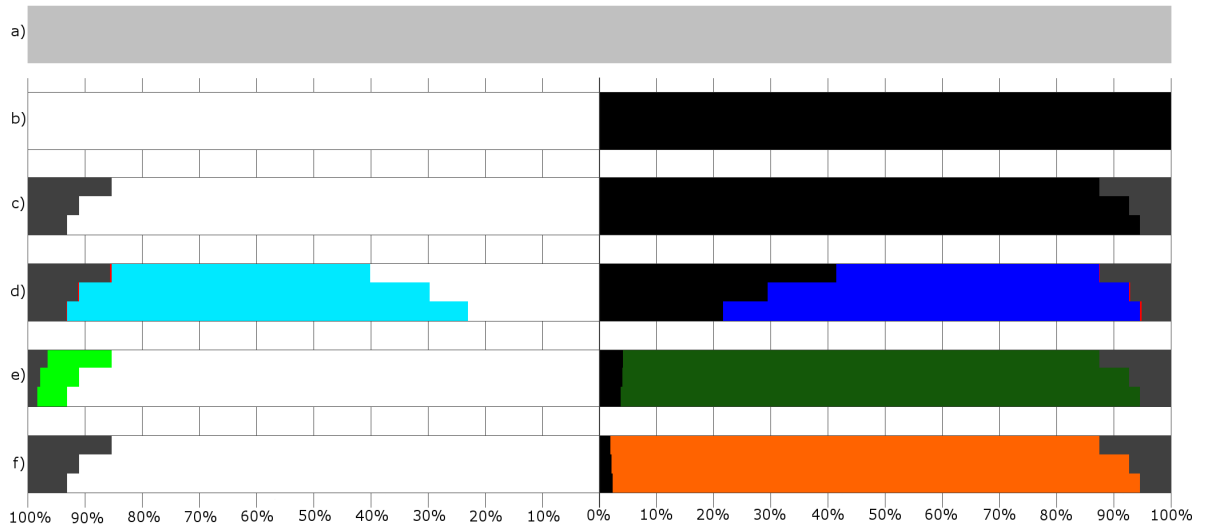
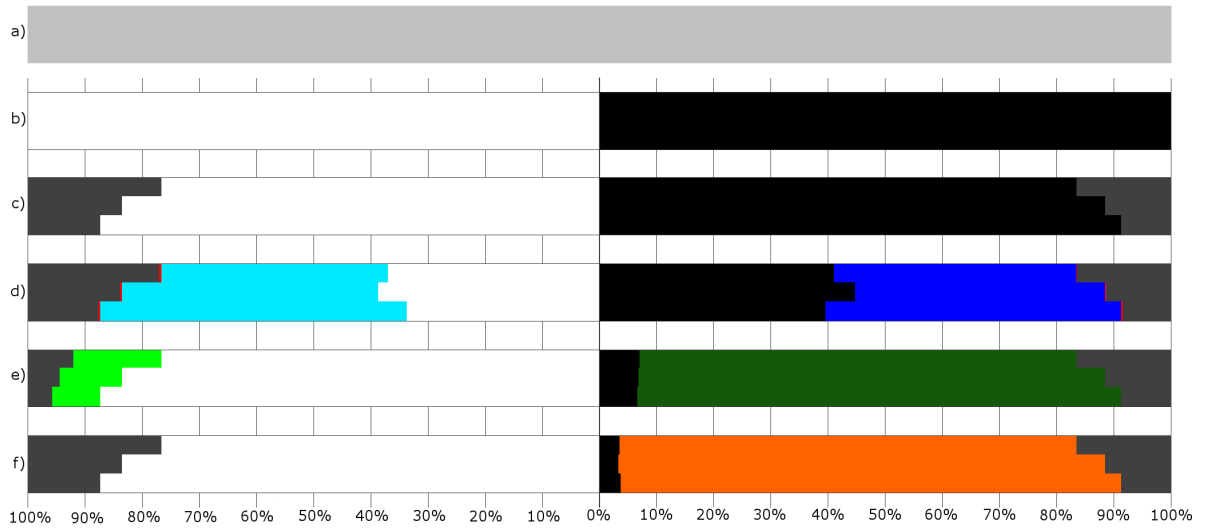


Figure 159: Corrected/confirmed/hinted contour pixels by each method for the against viewpoint of the bench scene using a 1024x1024 (top) and a 2048x2048 (bottom) resolution shadow map.

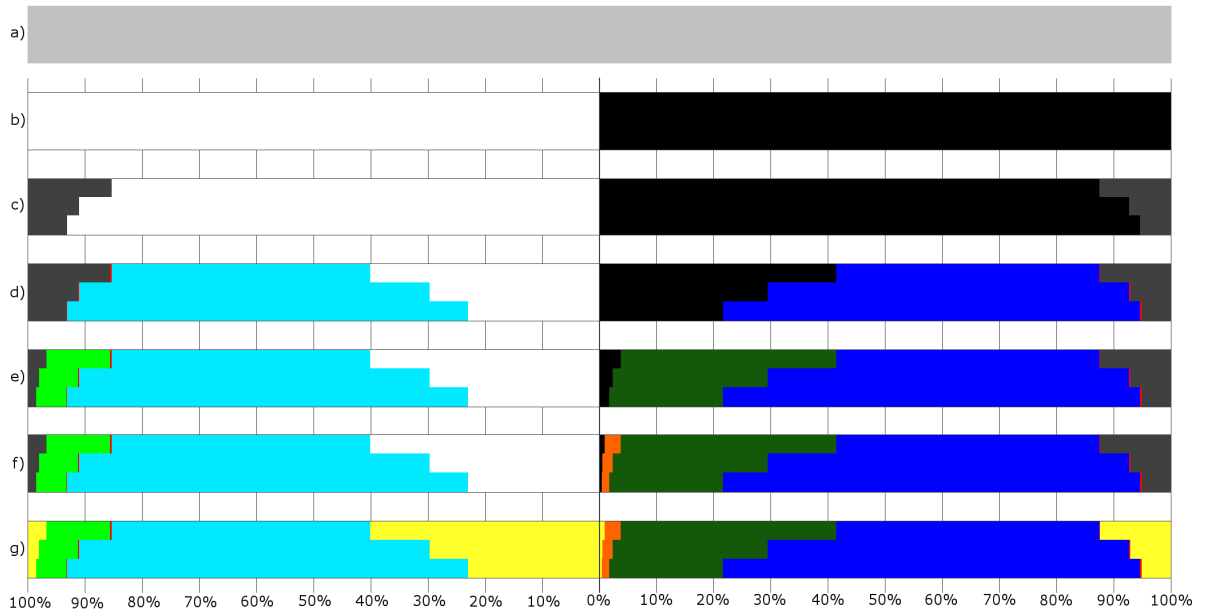
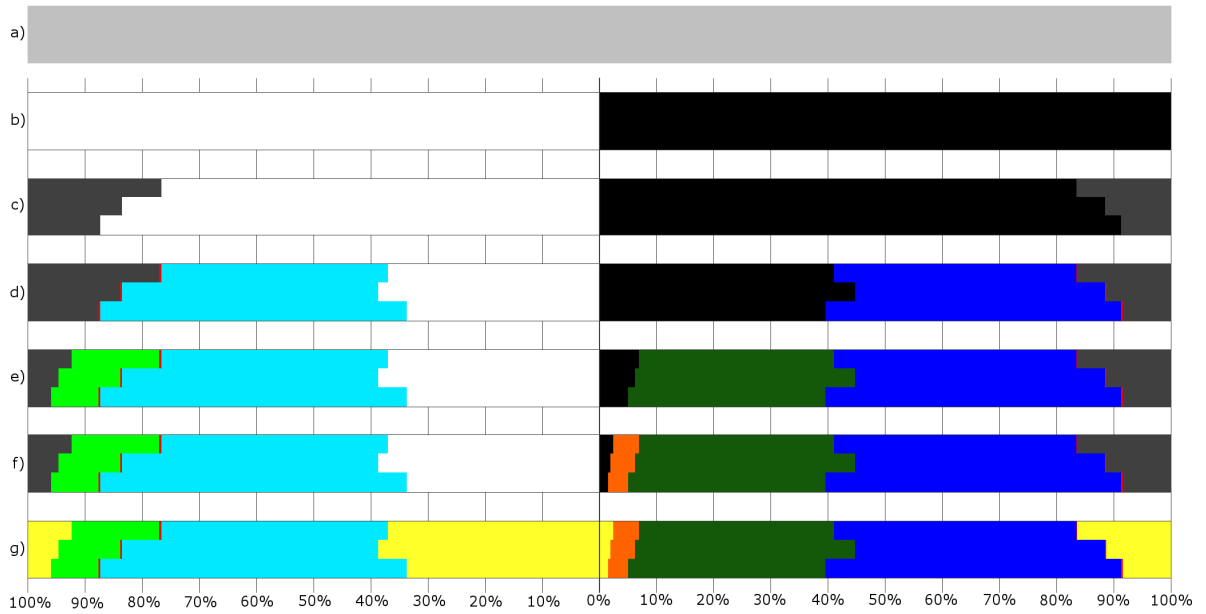


Figure 160: Corrected/confirmed/hinted contour pixels by the chaining of methods for the against viewpoint of the bench scene using a 1024x1024 (left) and a 2048x2048 (bottom) resolution shadow map.

Shadow Map Resolution	Approach	Contour Thickness			
		Two Pixels	Four Pixels	Six Pixels	Whole Image
1024x1024	Pixels in Contour	36248	64370	86929	1048576
	Shadow Map	7171 (19.78%)	8887 (13.81%)	9130 (10.50%)	9542 (0.91%)
	Single Texel	6661 (18.38%)	10005 (15.54%)	12383 (14.24%)	40722 (3.88%)
	Neighbour Texels (4 Neighbours)	3390 (9.35%)	5246 (8.15%)	6496 (7.47%)	14574 (1.39%)
	Neighbour Texels (9 Neighbours)	2731 (7.53%)	4048 (6.29%)	4859 (5.59%)	10272 (0.98%)
	Adjacent Geometry (One Level)	5480 (15.12%)	7526 (11.69%)	8816 (10.14%)	19608 (1.87%)
	Adjacent Geometry (Two Level)	4708 (12.99%)	6107 (9.49%)	6803 (7.83%)	13372 (1.28%)
2048x2048	Pixels in Contour	37821	65950	88864	1048576
	Shadow Map	5113 (13.52%)	5315 (8.06%)	5338 (6.01%)	5392 (0.51%)
	Single Texel	4881 (12.91%)	7234 (10.97%)	9191 (10.34%)	25404 (2.42%)
	Neighbour Texels (4 Neighbours)	1969 (5.21%)	2880 (4.37%)	3470 (3.90%)	7371 (0.70%)
	Neighbour Texels (9 Neighbours)	1465 (3.87%)	2097 (3.18%)	2494 (2.81%)	5022 (0.48%)
	Adjacent Geometry (One Level)	3648 (9.65%)	4722 (7.16%)	5560 (6.26%)	11058 (1.05%)
	Adjacent Geometry (Two Level)	3015 (7.97%)	3486 (5.29%)	3872 (4.36%)	6987 (0.67%)

Table 94: Difference between the approaches that use ray-tracing and the actual ray-tracer for the against viewpoint of the bench scene.

Shadow Map Resolution	Contour Thickness		
	Two Pixels	Four Pixels	Six Pixels
1024x1024	7171 of 9542 (75.15%)	8887 of 9542 (93.14%)	9130 of 9542 (95.68%)
2048x2048	5113 of 5392 (94.83%)	5315 of 5392 (98.57%)	5338 of 5392 (99.00%)

Table 95: Wrongly defined pixels in the shadow mapping result which are inside the contour in the against viewpoint of the bench scene.

Shadow Map Resolution	Contour Thickness	Pixel Shading	
		Light	Shadow
1024x1024	Two Pixels	4063 of 17429	3108 of 18819
	Four Pixels	4966 of 30268	3921 of 34102
	Six Pixels	5037 of 40012	4093 of 46917
	Whole Image	5080 of 604815	4462 of 443761
2048x2048	Two Pixels	2647 of 18100	2466 of 19721
	Four Pixels	2719 of 30480	2596 of 35470
	Six Pixels	2720 of 39980	2618 of 48884
	Whole Image	2745 of 604295	2647 of 444281

Table 96: Pixels that the shadow map defines wrongly in the against viewpoint of the bench scene, separated in pixels defined in light and in shadow, compared to the total amount of pixels lighted in the same way.

Shadow Map Resolution	Contour Thickness	Texel Coherence					
		Light			Shadow		
		Confirmed	Incorrectly Confirmed	Undecided	Confirmed	Incorrectly Confirmed	Undecided
1024x1024	Two Pixels	6944 (39.84%)	50 (0.29%)	10485 (60.16%)	7988 (42.45%)	7 (0.04%)	10831 (57.55%)
	Four Pixels	13631 (45.03%)	65 (0.21%)	16637 (54.97%)	14920 (43.75%)	30 (0.09%)	19182 (56.25%)
	Six Pixels	21521 (53.79%)	79 (0.20%)	18491 (46.21%)	24345 (51.89%)	102 (0.22%)	22572 (48.11%)
	Whole Image	585401 (96.79%)	85 (0.01%)	19414 (3.21%)	419750 (94.59%)	425 (0.10%)	24011 (5.41%)
2048x2048	Two Pixels	8223 (45.43%)	43 (0.24%)	9877 (54.57%)	9084 (46.06%)	19 (0.10%)	10637 (53.94%)
	Four Pixels	18729 (61.45%)	52 (0.17%)	11751 (38.55%)	22499 (63.43%)	79 (0.22%)	12971 (36.57%)
	Six Pixels	28097 (70.28%)	53 (0.13%)	11883 (29.72%)	35753 (73.14%)	99 (0.20%)	13131 (26.86%)
	Whole Image	592322 (98.02%)	53 (0.01%)	11973 (1.98%)	431064 (97.03%)	115 (0.03%)	13217 (2.97%)

Table 97: Pixel confirmation when using texel coherence with four texels for the against viewpoint of the bench scene.

Shadow Map Resolution	Contour Thickness	Texel Shadowing							
		Light				Shadow			
		3 shadow/1 light	3 shadow/1 light in ray-tracer shadow	1 shadow/3 light	1 shadow/3 light in ray-tracer light	3 shadow/1 light	3 shadow/1 light in ray-tracer shadow	1 shadow/3 light	1 shadow/3 light in ray-tracer light
1024x1024	Two Pixels	3234	2256	2869	2660	5015	4465	1514	1098
	Four Pixels	4451	2785	4963	4709	10038	9205	2024	1308
	Six Pixels	4519	2802	5850	5590	12459	11573	2068	1315
	Whole Image	4526	2807	6459	6199	13524	12626	2088	1332
2048x2048	Two Pixels	2348	1463	3823	3666	5269	4930	1710	1095
	Four Pixels	2375	1472	5045	4884	6954	6596	1741	1100
	Six Pixels	2375	1472	5153	4992	7087	6728	1741	1100
	Whole Image	2388	1483	5183	5020	7125	6764	1747	1103

Table 98: Pixel shadowing for pixels that don't achieve texel coherence with four texels for the against viewpoint of the bench scene.

Shadow Map Resolution	Contour Thickness	Texel Coherence					
		Light			Shadow		
		Confirmed	Incorrectly Confirmed	Undecided	Confirmed	Incorrectly Confirmed	Undecided
1024x1024	Two Pixels	5632 (32.31%)	25 (0.14%)	11797 (67.69%)	7863 (41.78%)	1 (0.01%)	10956 (58.22%)
	Four Pixels	10052 (33.21%)	26 (0.09%)	20216 (66.79%)	12616 (36.99%)	4 (0.01%)	21486 (63.01%)
	Six Pixels	14305(35.75%)	31 (0.08%)	25707(64.25%)	16202(34.53%)	12 (0.03%)	30715(65.47%)
	Whole Image	570571 (94.34%)	34 (0.01%)	34244 (5.66%)	394495 (88.90%)	242 (0.05%)	49266 (11.10)
2048x2048	Two Pixels	6740 (37.24%)	25 (0.14%)	11360 (62.76%)	7940 (40.26%)	1 (0.01%)	11781 (59.74%)
	Four Pixels	13285 (43.59%)	29 (0.10%)	17195 (56.41%)	14598 (41.16%)	12 (0.03%)	20872 (58.84%)
	Six Pixels	20940 (52.38%)	30 (0.08%)	19040 (47.62%)	23838 (48.76%)	23 (0.05%)	25046 (51.24%)
	Whole Image	584340 (96.70%)	30 (0.00%)	19955 (3.30%)	417827 (94.05%)	39 (0.01%)	26454 (5.95%)

Table 99: Pixel confirmation when using texel coherence with nine texels for the against viewpoint of the bench scene.

Shadow Map Lighting	Texel Shadowing	Shadow Map							
		1024x1024				2048x2048			
		Two Pixels	Four Pixels	Six Pixels	Whole Image	Two Pixels	Four Pixels	Six Pixels	Whole Image
Light	8 S-1 L	449	604	608	608	81	81	81	81
	8 S-1 L in RT Shadow	279	338	340	340	51	51	51	51
	7 S-2 L	1145	1653	1691	1692	511	515	515	515
	7 S-2 L in RT Shadow	620	774	777	777	231	232	232	232
	6 S-3 L	1268	1876	1991	2005	620	653	653	653
	6 S-3 L in RT Shadow	530	643	653	653	226	226	226	226
	5 S-4 L	655	1087	1288	1347	710	829	830	830
	5 S-4 L in RT Shadow	313	389	397	397	222	223	223	223
	4 S-5 L	2134	3539	4343	5019	3330	4530	4615	4670
	4 S-5 L in RT Light	986	2126	2901	3569	2189	3363	3448	3482
	3 S-6 L	2746	4919	6603	9006	3002	4875	5392	5512
	3 S-6 L in RT Light	1735	3715	5390	7765	2323	4163	4680	4796
	2 S-7 L	1618	3020	4143	5770	1675	2856	3217	3412
	2 S-7 L in RT Light	1520	2890	4012	5638	1626	2801	3162	3357
	1 S-8 L	1782	3518	5040	8797	1431	2856	3737	4282
1 S-8 L in RT Light	1743	3469	4987	8741	1408	2832	3713	4258	
Shadow	8 S-1 L	1950	5340	9495	21727	2155	6236	9129	10128
	8 S-1 L in RT Shadow	1713	4953	9020	21155	2075	6110	8994	9992
	7 S-2 L	3142	5992	8131	10962	2840	4660	5286	5552
	7 S-2 L in RT Shadow	2599	5273	7383	10206	2548	4346	4972	5238
	6 S-3 L	3121	5739	7722	10410	3888	6070	6617	6727
	6 S-3 L in RT Shadow	2323	4796	6768	9450	3105	5265	5810	5914
	5 S-4 L	2208	3706	4597	5367	2450	3430	3537	3570
	5 S-4 L in RT Shadow	982	2179	3037	3779	1362	2313	2420	2447
	4 S-5 L	239	358	407	437	253	279	279	279
	4 S-5 L in RT Light	121	147	149	149	91	91	91	91
	3 S-6 L	103	140	150	150	82	83	84	84
	3 S-6 L in RT Light	56	63	64	64	44	44	44	44
	2 S-7 L	145	161	163	163	80	81	81	81
	2 S-7 L in RT Light	89	93	93	93	61	61	61	61
	1 S-8 L	48	50	50	50	33	33	33	33
1 S-8 L in RT Light	37	38	38	38	26	26	26	26	

Table 100: Pixel shadowing for pixels that don't achieve texel coherence with nine texels for the against viewpoint of the bench scene.

Shadow Map Resolution	Contour Thickness	Corrected		Turned Bad		Maintained Correct		Maintained Incorrect	
		L→S	S→L	L→S	S→L	L→L	S→S	L→L	S→S
1024x1024	Two Pixels	12	3108	0	2610	13366	13101	4051	0
	Four Pixels	12	3921	0	5051	25302	25130	4954	0
	Six Pixels	12	4093	0	7358	34975	35466	5025	0
	Whole Image	12	4462	0	35654	599735	403645	5068	0
2048x2048	Two Pixels	7	2466	0	2241	15453	15014	2640	0
	Four Pixels	7	2596	0	4522	27761	28352	2712	0
	Six Pixels	7	2618	0	6478	37260	39788	2713	0
	Whole Image	7	2647	0	22666	601550	418968	2738	0

Table 101: Pixel correction between the single texel approach and the shadow mapping approach for the against viewpoint of the bench scene.

Shadow Map Resolution	Number of Neighbours	Contour Thickness	Corrected		Turned Bad		Maintained Correct		Maintained Incorrect	
			L→S	S→L	L→S	S→L	L→L	S→S	L→L	S→S
1024x1024	3	Two Pixels	2417	3108	0	1744	13366	13967	1646	0
		Four Pixels	2891	3921	0	3171	25302	27010	2075	0
		Six Pixels	2931	4093	0	4390	34975	38434	2106	0
		Whole Image	2952	4462	0	12446	599735	426853	2128	0
	8	Two Pixels	2676	3108	0	1344	13366	14367	1387	0
		Four Pixels	3271	3921	0	2353	25302	27828	1695	0
		Six Pixels	3320	4093	0	3142	34975	39682	1717	0
		Whole Image	3341	4462	0	8533	599735	430766	1739	0
2048x2048	3	Two Pixels	1812	2466	0	1134	15453	16121	835	0
		Four Pixels	1855	2596	0	2016	27761	30858	864	0
		Six Pixels	1855	2618	0	2605	37260	43661	865	0
		Whole Image	1880	2647	0	6506	601550	435128	865	0
	8	Two Pixels	2010	2466	0	828	15453	16427	637	0
		Four Pixels	2058	2596	0	1436	27761	31438	661	0
		Six Pixels	2058	2618	0	1832	37260	44434	662	0
		Whole Image	2083	2647	0	4360	601550	437274	662	0

Table 102: Pixel correction between the neighbour texels approach and the shadow mapping approach for the against viewpoint of the bench scene.

Shadow Map Resolution	Number of Neighbours	Triangle Average	Two Pixels	Four Pixels	Six Pixels	Whole Image
1024x1024	3	Used	1.7530	1.7171	1.6463	0.6616
		Available	1.9611	1.9479	1.9498	1.4692
	8	Used	3.0846	3.0216	2.8933	0.9510
		Available	3.4369	3.3241	3.2028	2.0564
2048x2048	3	Used	1.5666	1.4929	1.4331	0.5852
		Available	1.7942	1.8355	1.8413	1.3176
	8	Used	2.6181	2.4955	2.3712	0.7686
		Available	2.9150	2.8159	2.7842	1.7037

Table 103: Average of triangle intersections when using the neighbour texels approach for the against viewpoint of the bench scene.

Shadow Map Resolution	Adjacency Level	Contour Thickness	Corrected		Turned Bad		Maintained Correct		Maintained Incorrect	
			L→S	S→L	L→S	S→L	L→L	S→S	L→L	S→S
1024x1024	One Level	Two Pixels	15	3108	0	1432	13366	14279	4048	0
		Four Pixels	16	3921	0	2576	25302	27605	4950	0
		Six Pixels	16	4093	0	3795	34975	39029	5021	0
		Whole Image	16	4462	0	14544	599735	424755	5064	0
	Two Levels	Two Pixels	24	3108	0	669	13366	15042	4039	0
		Four Pixels	25	3921	0	1166	25302	29015	4941	0
		Six Pixels	25	4093	0	1791	34975	41033	5012	0
		Whole Image	25	4462	0	8317	599735	430982	5055	0
2048x2048	One Level	Two Pixels	14	2466	0	1015	15453	16240	2633	0
		Four Pixels	16	2596	0	2019	27761	30855	2703	0
		Six Pixels	16	2618	0	2856	37260	43410	2704	0
		Whole Image	16	2647	0	8329	601550	433305	2729	0
	Two Levels	Two Pixels	17	2466	0	385	15453	16870	2630	0
		Four Pixels	20	2596	0	787	27761	32087	2699	0
		Six Pixels	20	2618	0	1172	37260	45094	2700	0
		Whole Image	20	2647	0	4262	601550	437372	2725	0

Table 104: Pixel correction between the adjacent geometry approach and the shadow mapping approach for the against viewpoint of the bench scene.

Shadow Map Resolution	Adjacency Level	Triangle Average	Two Pixels	Four Pixels	Six Pixels	Whole Image
1024x1024	One Level	Used	2.3801	2.4430	2.4713	1.7130
		Available	3.9118	3.9188	3.9197	3.9682
	Two Levels	Used	7.1309	7.2522	7.3577	5.7876
		Available	11.7199	11.6330	11.6702	13.4077
2048x2048	One Level	Used	2.3990	2.4839	2.5223	1.7168
		Available	3.9140	3.9165	3.9187	3.9682
	Two Levels	Used	7.1897	7.3627	7.4857	5.7982
		Available	11.7304	11.6090	11.6297	13.4022

Table 105: Average of triangle intersections when using the adjacent geometry approach for the against viewpoint of the bench scene.

Contour Thickness		Two Pixels		Four Pixels		Six Pixels		Whole Image		
Lighting		L→S	S→L	L→S	S→L	L→S	S→L	L→S	S→L	
Shadow Map Resolution	1024x1024	Corrected by Both	12	3108	12	3921	12	4093	12	4462
		Turned Bad by Both	0	477	0	793	0	1143	0	3701
		Corrected by Neighbour Texels Only	2664	0	3259	0	3308	0	3329	0
		Corrected by Adjacent Geometry Only	12	0	13	0	13	0	13	0
		Turned Bad by Neighbour Texels Only	0	867	0	1560	0	1999	0	4832
		Turned Bad by Adjacent Geometry Only	0	192	0	373	0	648	0	4616
	2048x2048	Corrected by Both	10	2466	11	2596	11	2618	11	2647
		Turned Bad by Both	0	220	0	428	0	566	0	1637
		Corrected by Neighbour Texels Only	2000	0	2047	0	2047	0	2072	0
		Corrected by Adjacent Geometry Only	7	0	9	0	9	0	9	0
		Turned Bad by Neighbour Texels Only	0	608	0	1008	0	1266	0	2723
		Turned Bad by Adjacent Geometry Only	0	165	0	359	0	606	0	2625

Table 106: Pixel correction by the neighbour texels (9 texels) and the adjacent geometry (2 levels) approaches separated by lighting change for the against viewpoint of the bench scene.

Algorithm Step	Confirmations and Errors	1024x1024			2048x2048		
		Two Pixels	Four Pixels	Six Pixel	Two Pixels	Four Pixels	Six Pixel
Shadow Map	Total Contour Pixels	36248	64370	86929	37821	65950	88864
	Correct Light Pixels	13366 (76.69%)	25302 (83.59%)	34975 (87.41%)	15453 (85.38%)	27761 (91.08%)	37260 (93.20%)
	Correct Shadow Pixels	15711 (83.48%)	30181 (88.50%)	42824 (91.28%)	17255 (87.50%)	32874 (92.68%)	46266 (94.64%)
	Incorrect Light Pixels	4063 (23.31%)	4966 (16.41%)	5037 (12.59%)	2647 (14.62%)	2719 (8.92%)	2720 (6.80%)
	Incorrect Shadow Pixels	3108 (16.52%)	3921 (11.50%)	4093 (8.72%)	2466 (12.50%)	2596 (7.32%)	2618 (5.36%)
Texel Coherence	Confirmations in Light	6944 (39.84%)	13631 (45.03%)	21521 (53.79%)	8223 (45.43%)	18729 (61.45%)	28097 (70.28%)
	Confirmations in Shadow	7988 (42.45%)	14920 (43.75%)	24345 (51.89%)	9084 (46.06%)	22499 (63.43%)	35753 (73.14%)
	Wrong Confirmations in Light	50 (0.29%)	65 (0.21%)	79 (0.20%)	43 (0.24%)	52 (0.17%)	53 (0.13%)
	Wrong Confirmations in Shadow	7 (0.04%)	30 (0.09%)	102 (0.22%)	19 (0.10%)	79 (0.22%)	99 (0.20%)
Neighbouring Texels	Corrections in Light	2676 (15.35%)	3271 (10.81%)	3319 (8.30%)	2008 (11.09%)	2055 (6.74%)	2055 (5.14%)
	Confirmations in Shadow	14399 (76.51%)	28071 (82.31%)	40551 (86.43%)	16518 (83.76%)	32100 (90.50%)	45509 (93.10%)
Adjacent Geometry	Confirmations in Shadow	15256 (81.07%)	29526 (86.58%)	42194 (89.93%)	17069 (86.55%)	32731 (92.28%)	46142 (94.39%)
Final Lighting	Wrong Confirmations in Light	1393 (7.99%)	1701 (5.62%)	1724 (4.31%)	641 (3.54%)	666 (2.19%)	667 (1.67%)
	Wrong Confirmations in Shadow	469 (2.49%)	715 (2.10%)	834 (1.78%)	224 (1.14%)	301 (0.85%)	322 (0.66%)

Table 107: Algorithm results of the against viewpoint of the bench scene.

Below come the results for the “with” viewpoint of the “trees” scene.



Figure 161: Result of the ray-tracing approach for the with viewpoint of the trees scene.



Figure 162: Result of the shadow mapping approach for the with viewpoint of the trees scene.



Figure 163: Result of texel coherence with four texels for the with viewpoint of the trees scene.



Figure 164: Result of texel coherence with nine texels for the with viewpoint of the trees scene.

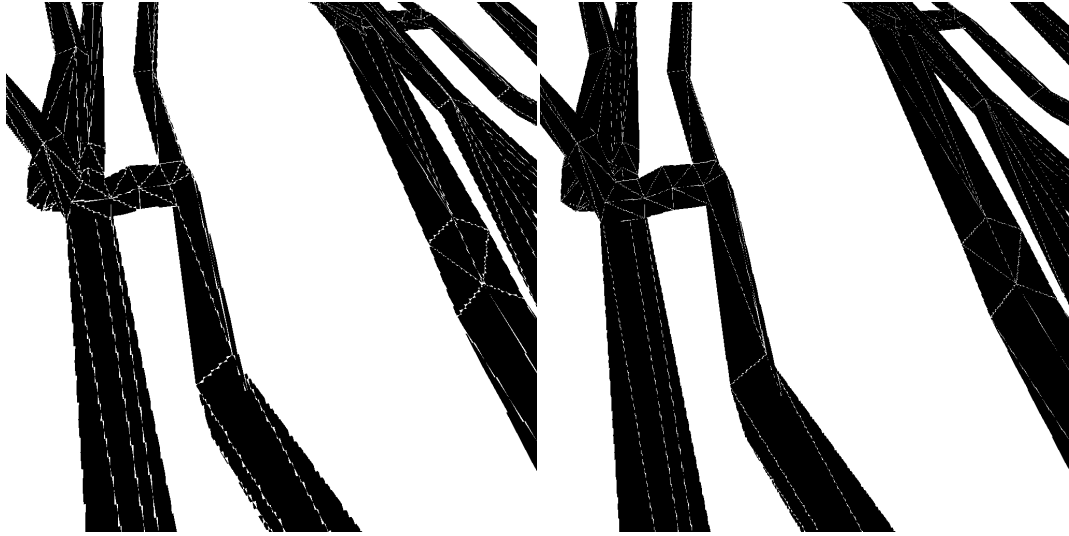


Figure 165: Result of the single texel approach for the with viewpoint of the trees scene.



Figure 166: Result of the neighbour texels approach using four neighbours for the with viewpoint of the trees scene.



Figure 167: Result of the neighbour texels approach using nine neighbours for the with viewpoint of the trees scene.



Figure 168: Result of the adjacent geometry approach with one level of adjacency for the with viewpoint of the trees scene.



Figure 169: Result of the adjacent geometry approach with two levels of adjacency for the with viewpoint of the trees scene.



Figure 170: Result of the algorithm with a six pixel thick contour and a 2048x2048 resolution shadow map for the with viewpoint of the trees scene.

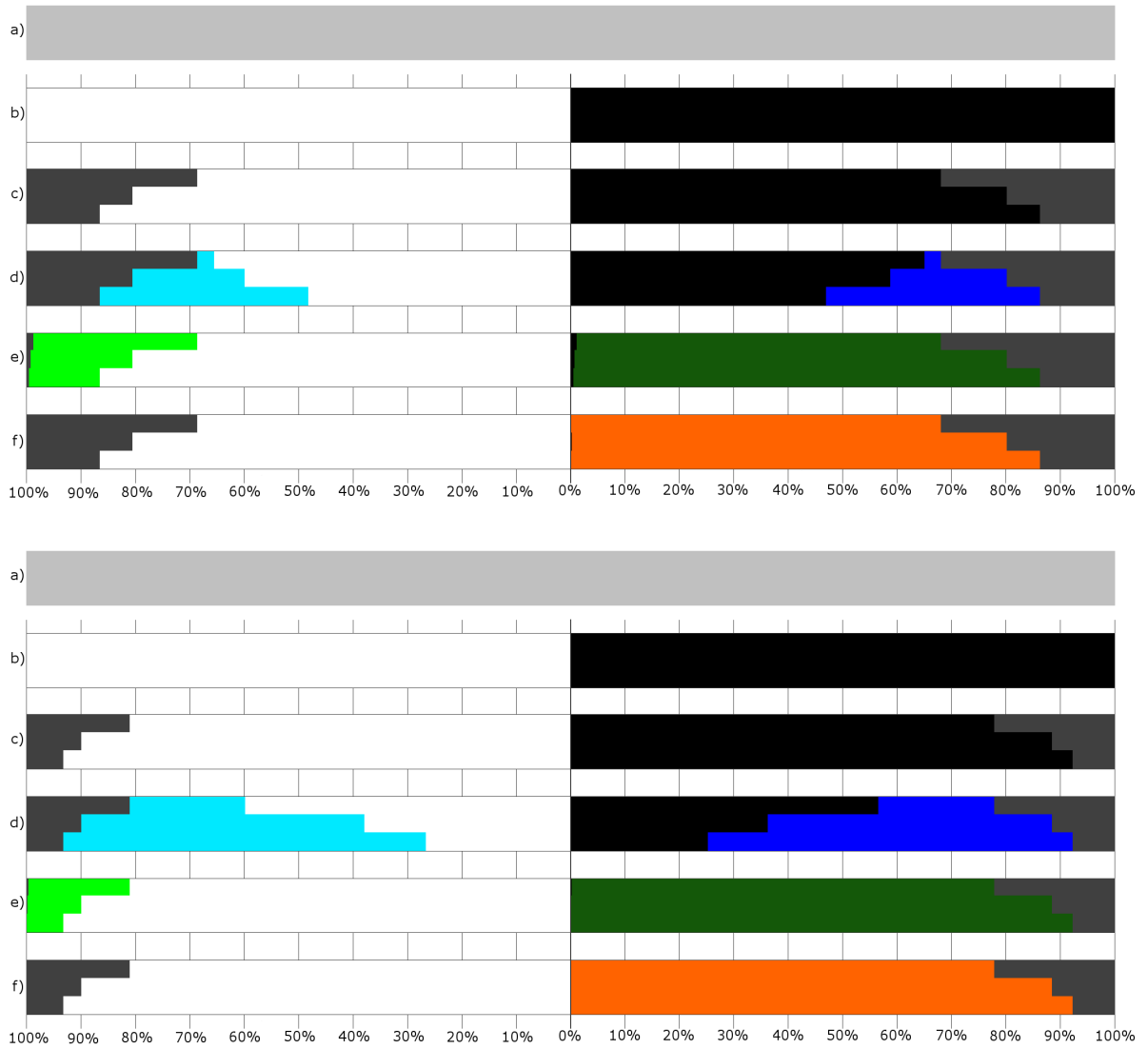


Figure 171: Corrected/confirmed/hinted contour pixels by each method for the with viewpoint of the trees scene using a 1024x1024 (top) and a 2048x2048 (bottom) resolution shadow map.

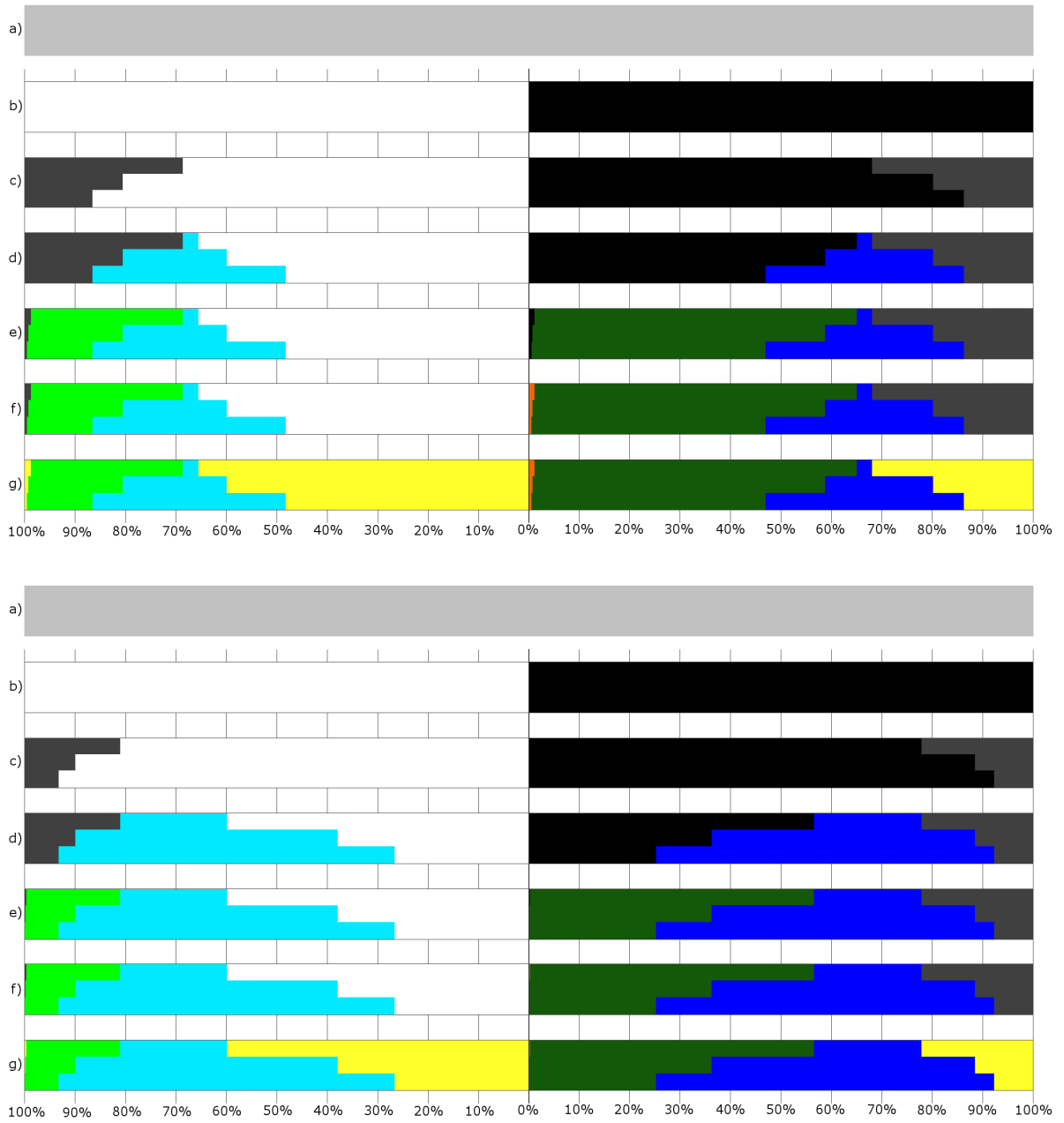


Figure 172: Corrected/confirmed/hinted contour pixels by the chaining of methods for the with viewpoint of the trees scene using a 1024x1024 (top) and a 2048x2048 (bottom) resolution shadow map.

Shadow Map Resolution	Approach	Contour Thickness			
		Two Pixels	Four Pixels	Six Pixels	Whole Image
1024x1024	Pixels in Contour	21562	42323	62580	1048576
	Shadow Map	6812 (31.59%)	8289 (19.59%)	8484 (13.56%)	8599 (0.82%)
	Single Texel	3797 (16.61%)	4903 (11.58%)	5451 (8.71%)	20569 (1.96%)
	Neighbour Texels (4 Neighbours)	436 (2.02%)	567 (1.34%)	609 (0.97%)	1222 (0.12%)
	Neighbour Texels (9 Neighbours)	267 (1.24%)	342 (0.81%)	360 (0.58%)	798 (0.08%)
	Adjacent Geometry (One Level)	3440 (15.95%)	4199 (9.92%)	4330 (6.92%)	5350 (0.51%)
	Adjacent Geometry (Two Level)	3387 (15.71%)	4108 (9.71%)	4207 (6.72%)	4808 (0.46%)
2048x2048	Pixels in Contour	21064	41215	61184	1048576
	Shadow Map	4319 (20.50%)	4431 (10.75%)	4431 (7.24%)	4486 (0.43%)
	Single Texel	2165 (10.28%)	2478 (6.01%)	2773 (4.53%)	10650 (1.02%)
	Neighbour Texels (4 Neighbours)	134 (0.64%)	150 (0.36%)	160 (0.26%)	356 (0.03%)
	Neighbour Texels (9 Neighbours)	69 (0.33%)	78 (0.19%)	85 (0.14%)	230 (0.02%)
	Adjacent Geometry (One Level)	2016 (9.57%)	2089 (5.07%)	2106 (3.44%)	2673 (0.25%)
	Adjacent Geometry (Two Level)	2005 (9.52%)	2066 (5.01%)	2069 (3.38%)	2464 (0.23%)

Table 108: Difference between the approaches that use ray-tracing and the actual ray-tracer for the with viewpoint of the trees scene.

Shadow Map Resolution	Contour Thickness		
	Two Pixels	Four Pixels	Six Pixels
1024x1024	6812 of 8599 (79.22%)	8289 of 8599 (96.39%)	8484 of 8599 (98.66%)
2048x2048	4319 of 4486 (96.28%)	4431 of 4486 (98.77%)	4431 of 4486 (98.77%)

Table 109: Wrongly defined pixels in the shadow mapping result which are inside the contour in the with viewpoint of the trees scene.

Shadow Map Resolution	Contour Thickness	Pixel Shading	
		Light	Shadow
1024x1024	Two Pixels	3369 of 10766	3443 of 10796
	Four Pixels	4080 of 21077	4209 of 21246
	Six Pixels	4162 of 31085	4322 of 31495
	Whole Image	4218 of 655181	4381 of 393395
2048x2048	Two Pixels	1991 of 10515	2328 of 10549
	Four Pixels	2043 of 20511	2388 of 20704
	Six Pixels	2043 of 30352	2388 of 30832
	Whole Image	2074 of 655006	2412 of 393570

Table 110: Pixels that the shadow map defines wrongly in the with viewpoint of the trees scene, separated in pixels defined in light and in shadow, compared to the total amount of pixels lighted in the same way.

Shadow Map Resolution	Contour Thickness	Texel Coherence					
		Light			Shadow		
		Confirmed	Incorrectly Confirmed	Undecided	Confirmed	Incorrectly Confirmed	Undecided
1024x1024	Two Pixels	331 (3.07%)	0 (0.00%)	10435 (96.93%)	327 (3.03%)	0 (0.00%)	10469 (96.97%)
	Four Pixels	4356 (20.67%)	0 (0.00%)	16721 (79.33%)	4555 (21.44%)	2 (0.01%)	16691 (78.56%)
	Six Pixels	11909 (38.31%)	0 (0.00%)	19176 (61.69%)	12365 (39.26%)	4 (0.01%)	19130 (60.74%)
	Whole Image	634459 (96.84%)	0 (0.00%)	20722 (3.16%)	372685 (94.74%)	13 (0.00%)	20710 (5.26%)
2048x2048	Two Pixels	2222 (21.13%)	0 (0.00%)	8293 (78.87%)	2252 (21.35%)	0 (0.00%)	8297 (78.65%)
	Four Pixels	10672 (52.03%)	0 (0.00%)	9839 (47.97%)	10802 (52.17%)	2 (0.01%)	9902 (47.83%)
	Six Pixels	20221 (66.62%)	0 (0.00%)	10131 (33.38%)	20658 (67.00%)	2 (0.01%)	10174 (33.00%)
	Whole Image	644692 (98.43%)	0 (0.00%)	10314 (1.57%)	383204 (97.37%)	2 (0.00%)	10366 (2.63%)

Table 111: Pixel confirmation when using texel coherence with four texels for the with viewpoint of the trees scene.

Shadow Map Resolution	Contour Thickness	Texel Shadowing							
		Light				Shadow			
		3 shadow/1 light	3 shadow/1 light in ray-tracer shadow	1 shadow/3 light	1 shadow/3 light in ray-tracer light	3 shadow/1 light	3 shadow/1 light in ray-tracer shadow	1 shadow/3 light	1 shadow/3 light in ray-tracer light
1024x1024	Two Pixels	1422	1207	2021	1931	2064	1992	1409	1131
	Four Pixels	1976	1527	3971	3865	4026	3931	1964	1452
	Six Pixels	2150	1575	5139	5022	5173	5066	2142	1518
	Whole Image	2195	1607	6447	6327	6542	6429	2180	1542
2048x2048	Two Pixels	960	711	1919	1873	1949	1884	978	747
	Four Pixels	1033	735	2824	2771	2879	2805	1061	779
	Six Pixels	1033	735	3166	3063	3151	3077	1061	779
	Whole Image	1049	748	3216	3159	3259	3185	1079	792

Table 112: Pixel shadowing for pixels that don't achieve texel coherence with four texels for the with viewpoint of the trees scene.

Shadow Map Resolution	Contour Thickness	Texel Coherence					
		Light			Shadow		
		Confirmed	Incorrectly Confirmed	Undecided	Confirmed	Incorrectly Confirmed	Undecided
1024x1024	Two Pixels	0 (0.00%)	0 (0.00%)	10766 (100.00%)	0 (0.00%)	0 (0.00%)	10796 (100.00%)
	Four Pixels	590 (2.80)	0 (0.00%)	20487 (97.20%)	614 (2.89%)	0 (0.00%)	20632 (97.11%)
	Six Pixels	3241(10.43 %)	0 (0.00%)	27844(89.57%)	3404(10.81 %)	1 (0.00%)	28091(89.19%)
	Whole Image	613994 (93.71%)	0 (0.00%)	41187 (6.29%)	351763 (89.42%)	5 (0.00%)	41632 (10.58%)
2048x2048	Two Pixels	280 (2.66%)	0 (0.00%)	10235 (97.34%)	327 (3.10%)	0 (0.00%)	10222 (96.90%)
	Four Pixels	3976 (19.38%)	0 (0.00%)	16535 (80.62%)	4097 (19.79%)	0 (0.00%)	16607 (80.21%)
	Six Pixels	11202 (36.91%)	0 (0.00%)	19150 (63.09%)	11582 (37.56%)	0 (0.00%)	19250 (62.44%)
	Whole Image	634337 (96.84%)	0 (0.00%)	20669 (3.16%)	372782 (94.72%)	0 (0.00%)	20788 (5.28%)

Table 113: Pixel confirmation when using texel coherence with nine texels for the with viewpoint of the trees scene.

Shadow Map Lighting	Texel Shadowing	Shadow Map							
		1024x1024				2048x2048			
		Two Pixels	Four Pixels	Six Pixels	Whole Image	Two Pixels	Four Pixels	Six Pixels	Whole Image
Light	8 S-1 L	0	0	0	0	0	0	0	0
	8 S-1 L in RT Shadow	0	0	0	0	0	0	0	0
	7 S-2 L	17	18	18	18	1	1	1	1
	7 S-2 L in RT Shadow	10	10	10	10	0	0	0	0
	6 S-3 L	52	56	56	56	21	21	21	21
	6 S-3 L in RT Shadow	15	15	15	15	10	10	10	10
	5 S-4 L	67	99	119	156	24	27	27	27
	5 S-4 L in RT Shadow	27	30	30	34	5	5	5	5
	4 S-5 L	2307	3879	4743	5646	1892	2529	2724	2756
	4 S-5 L in RT Light	727	1856	2648	3532	897	1498	1693	1715
	3 S-6 L	6495	12258	16326	21275	6249	9651	10617	10802
	3 S-6 L in RT Light	4761	10259	14317	19233	5270	8656	9622	9786
	2 S-7 L	1565	3029	4123	5522	1512	2391	2740	2791
	2 S-7 L in RT Light	1562	3026	4120	5519	1510	2389	2738	2789
	1 S-8 L	263	1148	2459	8514	536	1915	3020	4271
1 S-8 L in RT Light	263	1148	2459	8514	536	1915	3020	4271	
Shadow	8 S-1 L	283	1204	2590	8845	550	1960	3048	4319
	8 S-1 L in RT Shadow	281	1199	2585	8840	547	1955	3043	4314
	7 S-2 L	1662	3208	4351	5896	1543	2480	2856	2907
	7 S-2 L in RT Shadow	1635	3169	4309	5848	1537	2474	2850	2901
	6 S-3 L	6565	12399	16491	21340	6230	9646	10622	10795
	6 S-3 L in RT Shadow	4708	10265	14345	19166	4942	8342	9318	9481
	5 S-4 L	2286	3821	4659	5551	1895	2516	2719	2762
	5 S-4 L in RT Shadow	729	1790	2531	3402	867	1446	1649	1678
	4 S-5 L	0	0	0	0	4	5	5	5
	4 S-5 L in RT Light	0	0	0	0	3	3	3	3
	3 S-6 L	0	0	0	0	0	0	0	0
	3 S-6 L in RT Light	0	0	0	0	0	0	0	0
	2 S-7 L	0	0	0	0	0	0	0	0
	2 S-7 L in RT Light	0	0	0	0	0	0	0	0
	1 S-8 L	0	0	0	0	0	0	0	0
1 S-8 L in RT Light	0	0	0	0	0	0	0	0	

Table 114: Pixel shadowing for pixels that don't achieve texel coherence with nine texels for the with viewpoint of the trees scene.

Shadow Map Resolution	Contour Thickness	Corrected		Turned Bad		Maintained Correct		Maintained Incorrect	
		L→S	S→L	L→S	S→L	L→L	S→S	L→L	S→S
1024x1024	Two Pixels	2	3443	0	430	7397	6923	3367	0
	Four Pixels	2	4209	0	825	16997	16212	4078	0
	Six Pixels	2	4322	0	1291	26923	25882	4160	0
	Whole Image	2	4381	0	16353	650963	372661	4216	0
2048x2048	Two Pixels	2	2328	0	176	8524	8045	1989	0
	Four Pixels	2	2388	0	437	18468	17879	2041	0
	Six Pixels	2	2388	0	732	28309	27712	2041	0
	Whole Image	2	2412	0	8578	652932	382580	2072	0

Table 115: Pixel correction between the single texel approach and the shadow mapping approach for the with viewpoint of the trees scene.

Shadow Map Resolution	Number of Neighbours	Contour Thickness	Corrected		Turned Bad		Maintained Correct		Maintained Incorrect	
			L→S	S→L	L→S	S→L	L→L	S→S	L→L	S→S
1024x1024	3	Two Pixels	3149	3443	0	216	7397	7137	220	0
		Four Pixels	3807	4209	0	294	16997	16743	273	0
		Six Pixels	3879	4322	0	326	26923	26847	283	0
		Whole Image	3930	4381	0	934	650963	388080	288	0
	8	Two Pixels	3233	3443	0	131	7397	7222	136	0
		Four Pixels	3915	4209	0	177	16997	16860	165	0
		Six Pixels	3997	4322	0	195	26923	26978	165	0
		Whole Image	4050	4381	0	630	650963	388384	168	0
2048x2048	3	Two Pixels	1914	2328	0	57	8524	8164	77	0
		Four Pixels	1963	2388	0	70	18468	18246	80	0
		Six Pixels	1963	2388	0	80	28309	28364	80	0
		Whole Image	1922	2412	0	274	652932	390884	82	0
	8	Two Pixels	1950	2328	0	28	8524	8193	41	0
		Four Pixels	2001	2388	0	36	18468	18280	42	0
		Six Pixels	2001	2388	0	43	28309	28401	42	0
		Whole Image	2030	2412	0	186	652932	390972	44	0

Table 116: Pixel correction between the neighbour texels approach and the shadow mapping approach for the with viewpoint of the trees scene.

Shadow Map Resolution	Number of Neighbours	Triangle Average	Two Pixels	Four Pixels	Six Pixels	Whole Image
1024x1024	3	Used	1.0619	0.9836	0.9045	0.4759
		Available	1.0785	1.0965	1.1170	1.2050
	8	Used	1.2298	1.2151	1.1792	0.5812
		Available	1.2298	1.2323	1.2436	1.4024
2048x2048	3	Used	0.9371	0.7933	0.7265	0.4267
		Available	1.0476	1.0705	1.0851	1.1079
	8	Used	1.1089	1.0251	0.9417	0.4798
		Available	1.1238	1.1346	1.1528	1.2145

Table 117: Average of triangle intersections when using the neighbour texels approach for the with viewpoint of the trees scene.

Shadow Map Resolution	Adjacency Level	Contour Thickness	Corrected		Turned Bad		Maintained Correct		Maintained Incorrect	
			L→S	S→L	L→S	S→L	L→L	S→S	L→L	S→S
1024x1024	One Level	Two Pixels	2	3443	0	73	7397	7280	3367	0
		Four Pixels	2	4209	0	121	16997	16916	4078	0
		Six Pixels	2	4322	0	170	26923	27003	4160	0
		Whole Image	2	4381	0	1134	650963	387880	4216	0
	Two Levels	Two Pixels	2	3443	0	20	7397	7333	3367	0
		Four Pixels	2	4209	0	30	16997	17007	4078	0
		Six Pixels	2	4322	0	47	26923	27126	4160	0
		Whole Image	2	4381	0	592	650963	388422	4216	0
2048x2048	One Level	Two Pixels	2	2328	0	27	8524	8194	1989	0
		Four Pixels	2	2388	0	48	18468	18268	2041	0
		Six Pixels	2	2388	0	65	28309	28379	2041	0
		Whole Image	2	2412	0	601	652932	390557	2072	0
	Two Levels	Two Pixels	2	2328	0	16	8524	8205	1989	0
		Four Pixels	2	2388	0	25	18468	18291	2041	0
		Six Pixels	2	2388	0	28	28309	28416	2041	0
		Whole Image	2	2412	0	392	652932	390766	2072	0

Table 118: Pixel correction between the adjacent geometry approach and the shadow mapping approach for the with viewpoint of the trees scene.

Shadow Map Resolution	Adjacency Level	Triangle Average	Two Pixels	Four Pixels	Six Pixels	Whole Image
1024x1024	One Level	Used	2.0024	2.0078	2.1030	1.5007
		Available	4.0000	4.0000	4.0000	4.0000
	Two Levels	Used	7.1536	7.1787	7.2008	5.3309
		Available	14.2899	14.3016	14.3087	14.2094
2048x2048	One Level	Used	2.0032	2.0094	2.0157	1.5014
		Available	4.0000	4.0000	4.0000	4.0000
	Two Levels	Used	7.1638	7.1943	7.2195	5.3332
		Available	14.3045	14.3216	14.3265	14.2090

Table 119: Average of triangle intersections when using the adjacent geometry approach for the with viewpoint of the trees scene.

Contour Thickness		Two Pixels		Four Pixels		Six Pixels		Whole Image		
Lighting		L→S	S→L	L→S	S→L	L→S	S→L	L→S	S→L	
Shadow Map Resolution	1024x1024	Corrected by Both	2	3443	2	4209	2	4322	2	4381
		Turned Bad by Both	0	4	0	4	0	4	0	13
		Corrected by Neighbour Texels Only	3231	0	3913	0	3995	0	4048	0
		Corrected by Adjacent Geometry Only	0	0	0	0	0	0	0	0
		Turned Bad by Neighbour Texels Only	0	127	0	173	0	191	0	617
		Turned Bad by Adjacent Geometry Only	0	16	0	26	0	43	0	579
	2048x2048	Corrected by Both	2	2328	2	2388	2	2388	2	2412
		Turned Bad by Both	0	3	0	3	0	3	0	3
		Corrected by Neighbour Texels Only	1948	0	1999	0	1999	0	2028	0
		Corrected by Adjacent Geometry Only	0	0	0	0	0	0	0	0
		Turned Bad by Neighbour Texels Only	0	25	0	33	0	40	0	183
		Turned Bad by Adjacent Geometry Only	0	13	0	22	0	25	0	389

Table 120: Pixel correction by the neighbour texels (9 texels) and the adjacent geometry (2 levels) approaches separated by lighting change for the with viewpoint of the trees scene.

Algorithm Step	Confirmations and Errors	1024x1024			2048x2048		
		Two Pixels	Four Pixels	Six Pixel	Two Pixels	Four Pixels	Six Pixel
Shadow Map	Total Contour Pixels	21562	42323	62580	21064	41215	61184
	Correct Light Pixels	7397 (68.71%)	16997 (80.64%)	26923 (86.61%)	8524 (81.07%)	18468 (90.04%)	28309 (93.27%)
	Correct Shadow Pixels	7353 (68.11%)	17037 (80.19%)	27173 (86.28%)	8221 (77.93%)	18316 (88.47%)	28444 (92.25%)
	Incorrect Light Pixels	3369 (31.29%)	4080 (19.36%)	4162 (13.39%)	1991 (18.93%)	2043 (9.96%)	2043 (6.73%)
	Incorrect Shadow Pixels	3443 (31.89%)	4209 (19.81%)	4322 (13.72%)	2328 (22.07%)	2388 (11.53%)	2388 (7.75%)
Texel Coherence	Confirmations in Light	331 (3.07%)	4356 (20.67%)	11909 (38.31%)	2222 (21.13%)	10672 (52.03%)	20221 (66.62%)
	Confirmations in Shadow	327 (3.03%)	4555 (21.44%)	12365 (39.26%)	2252 (21.35%)	10802 (52.17%)	20658 (67.00%)
	Wrong Confirmations in Light	0 (0.00%)	0 (0.00%)	0 (0.00%)	0 (0.00%)	0 (0.00%)	0 (0.00%)
	Wrong Confirmations in Shadow	0 (0.00%)	2 (0.01%)	4 (0.01%)	0 (0.00%)	2 (0.01%)	2 (0.01%)
Neighbouring Texels	Corrections in Light	3233 (30.03%)	3915 (18.57%)	3997 (12.86%)	1950 (18.54%)	2001 (9.76%)	2001 (6.59%)
	Confirmations in Shadow	7222 (66.90%)	16867 (79.39%)	27001 (85.73%)	8194 (77.68%)	18290 (88.34%)	28418 (92.17%)
Adjacent Geometry	Confirmations in Shadow	7349 (68.07%)	17035 (80.18%)	27173 (86.28%)	8218 (77.90%)	18315 (88.46%)	28443 (92.25%)
Final Lighting	Wrong Confirmations in Light	136 (1.26%)	165 (0.78%)	165 (0.53%)	41 (0.39%)	42 (0.20%)	42 (0.14%)
	Wrong Confirmations in Shadow	4 (0.04%)	6 (0.03%)	8 (0.03%)	3 (0.03%)	5 (0.02%)	5 (0.02%)

Table 121: Algorithm results of the with viewpoint of the trees scene.

Below are the results of the “side” viewpoint of the “trees” scene.



Figure 173: Result of the ray-tracing approach for the side viewpoint of the trees scene.

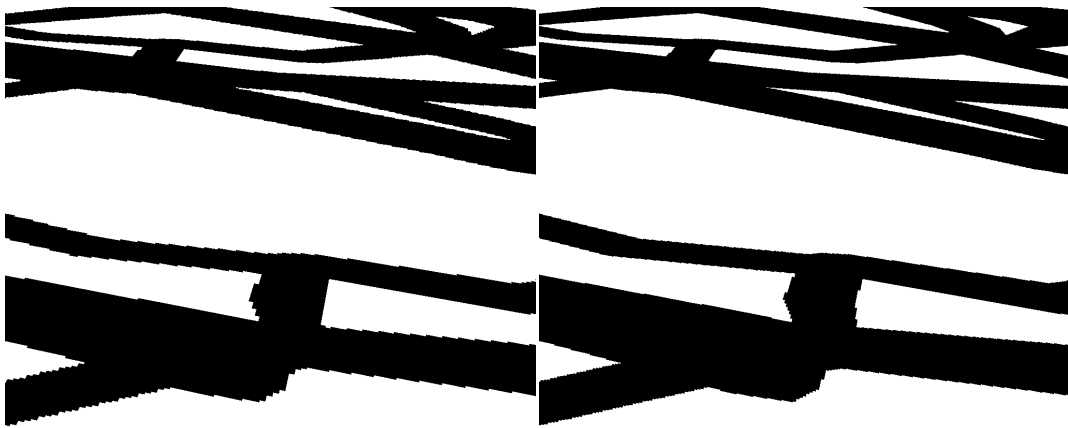


Figure 174: Result of the shadow mapping approach for the side viewpoint of the trees scene.



Figure 175: Result of texel coherence with four texels for the side viewpoint of the trees scene.



Figure 176: Result of texel coherence with nine texels for the side viewpoint of the trees scene.

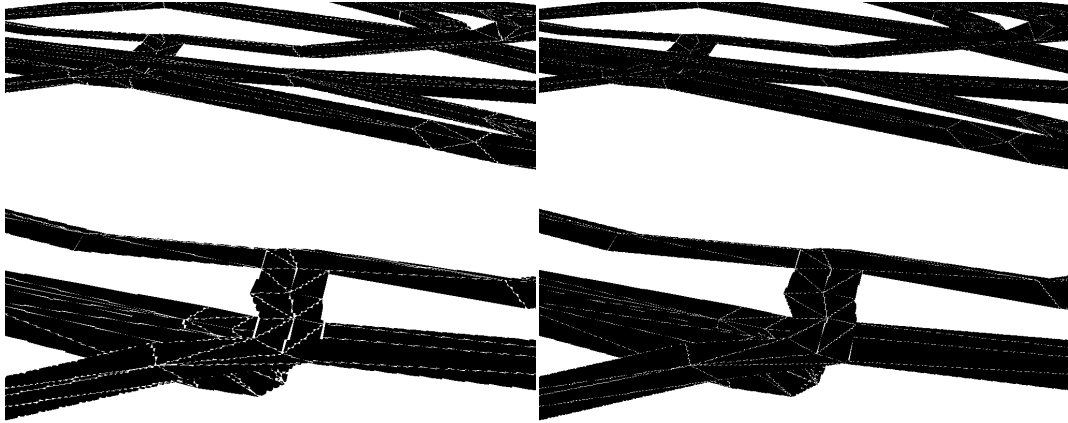


Figure 177: Result of the single texel approach for the side viewpoint of the trees scene.



Figure 178: Result of the neighbour texels approach with four neighbours for the side viewpoint of the trees scene.

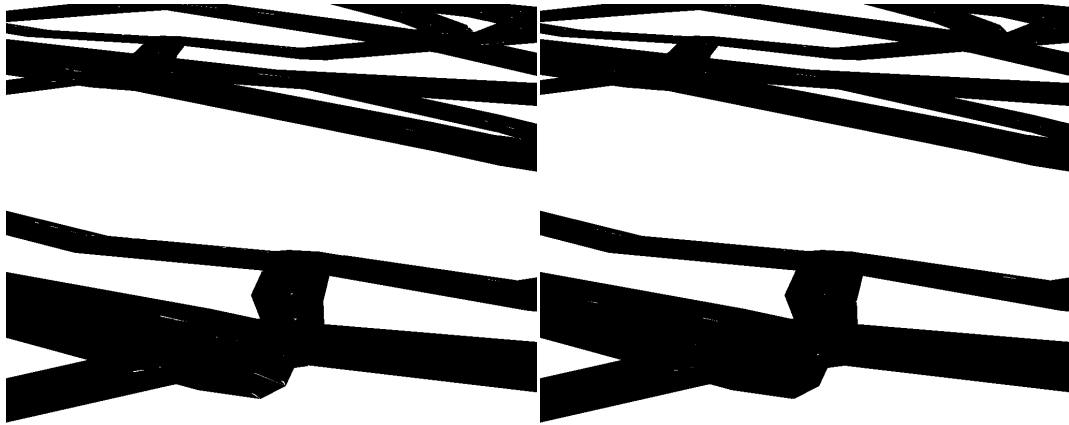


Figure 179: Result of the neighbour texels approach with nine neighbours for the side viewpoint of the trees scene.

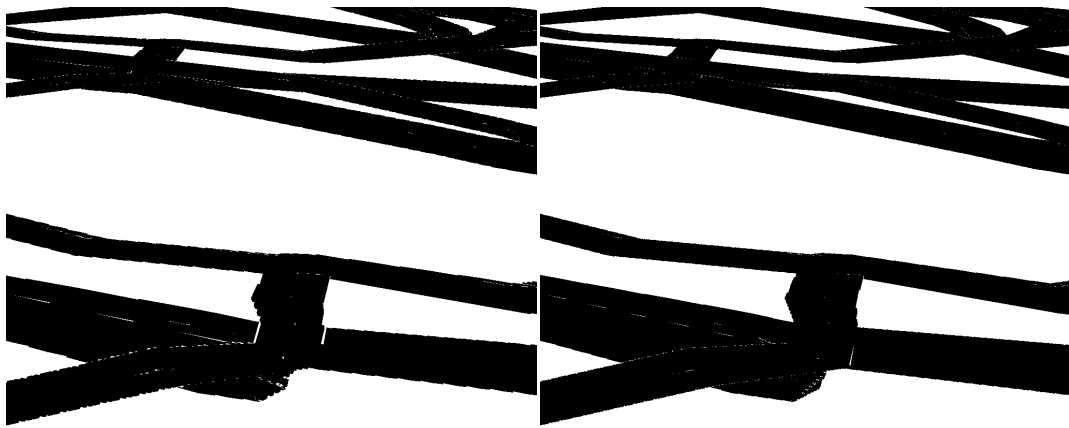


Figure 180: Result of the adjacent geometry approach with one level of adjacency for the side viewpoint of the trees scene.

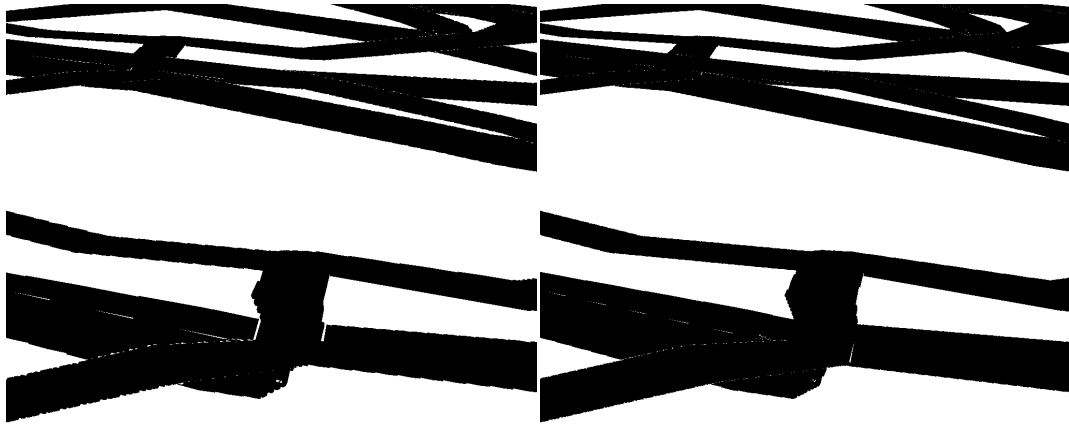


Figure 181: Result of the adjacent geometry approach with two levels of adjacency for the side viewpoint of the trees scene.



Figure 182: Result of the algorithm with a six pixel thick contour and a 2048x2048 resolution shadow map for the side viewpoint of the trees scene.

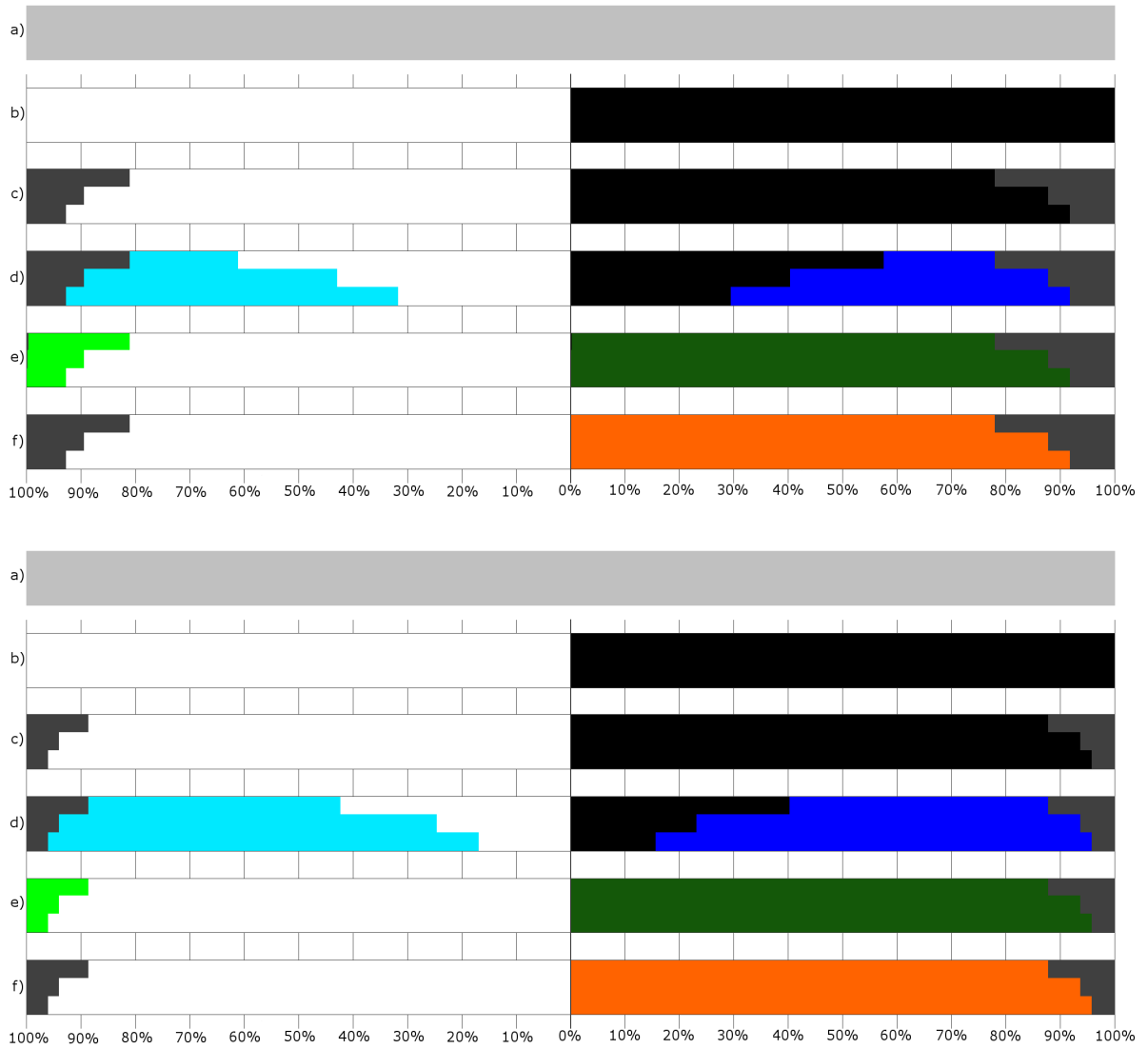


Figure 183: Corrected/confirmed/hinted contour pixels by each method for the side viewpoint of the trees scene using a 1024x1024 (top) and a 2048x2048 (bottom) resolution shadow map.

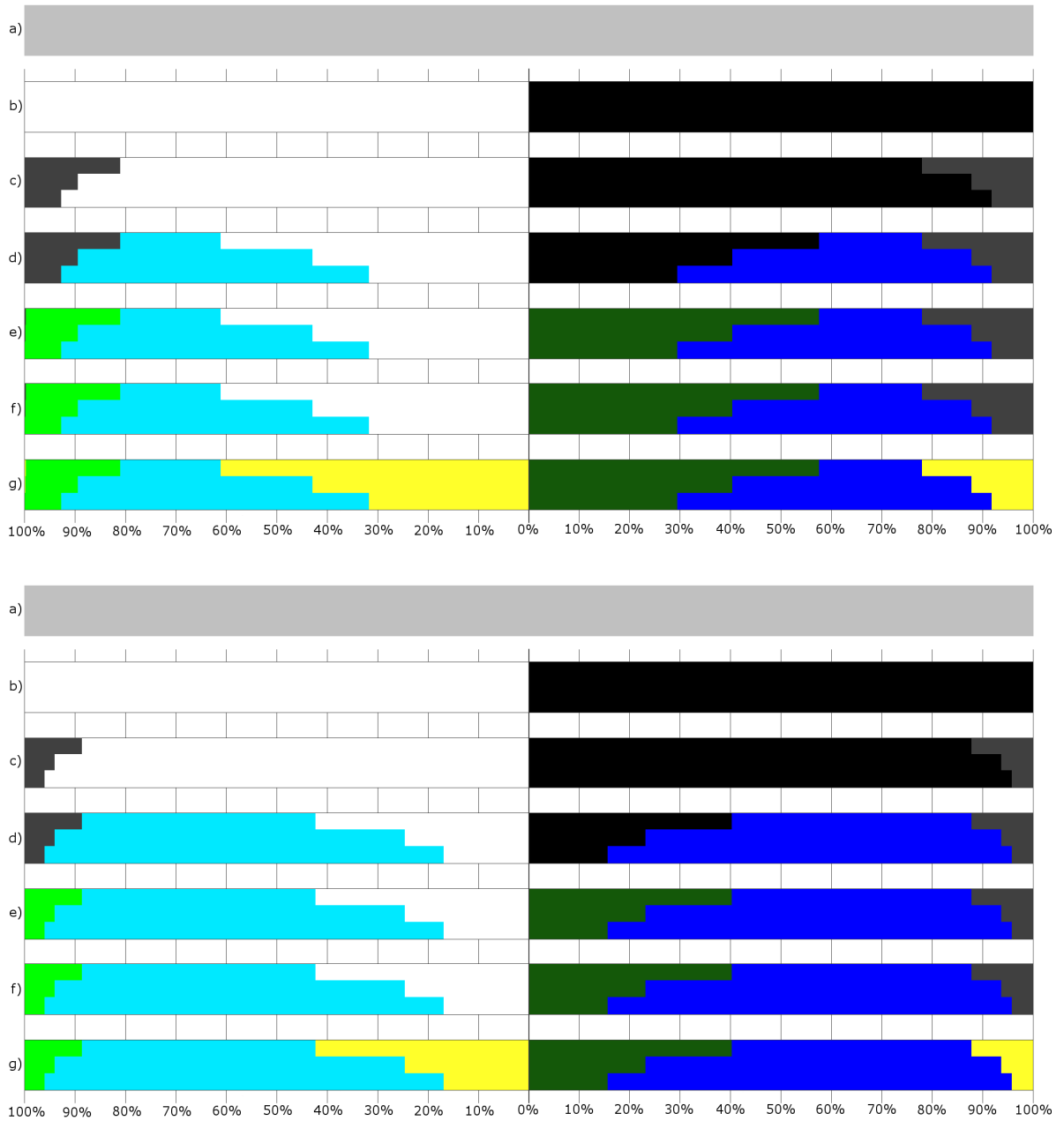


Figure 184: Corrected/confirmed/hinted contour pixels by the chaining of methods for the side viewpoint of the trees scene using a 1024x1024 (top) and a 2048x2048 (bottom) resolution shadow map.

Shadow Map Resolution	Approach	Contour Thickness			
		Two Pixels	Four Pixels	Six Pixels	Whole Image
1024x1024	Pixels in Contour	27414	54182	80266	1048576
	Shadow Map	5602 (20.43%)	6161 (11.37%)	6254 (7.79%)	6349 (0.61%)
	Single Texel	3021 (11.02%)	3831 (7.07%)	4594 (5.72%)	20004 (1.91%)
	Neighbour Texels (4 Neighbours)	215 (0.78%)	257 (0.47%)	306 (0.38%)	984 (0.09%)
	Neighbour Texels (9 Neighbours)	90 (0.33%)	101 (0.19%)	121 (0.15%)	503 (0.05%)
	Adjacent Geometry (One Level)	2640 (9.63%)	2928 (5.40%)	3027 (3.77%)	4635 (0.44%)
	Adjacent Geometry (Two Level)	2601 (9.49%)	2852 (5.26%)	2906 (3.62%)	4127 (0.39%)
2048x2048	Pixels in Contour	27267	53603	79206	1048576
	Shadow Map	3198 (11.73%)	3256 (6.07%)	3257 (4.11%)	3283 (0.31%)
	Single Texel	1788 (6.56%)	2135 (3.98%)	2460 (3.11%)	10338 (0.99%)
	Neighbour Texels (4 Neighbours)	60 (0.22%)	70 (0.13%)	87 (0.11%)	264 (0.03%)
	Neighbour Texels (9 Neighbours)	25 (0.09%)	26 (0.05%)	36 (0.05%)	153 (0.01%)
	Adjacent Geometry (One Level)	1553 (5.70%)	1601 (2.99%)	1628 (2.06%)	2292 (0.22%)
	Adjacent Geometry (Two Level)	1545 (5.67%)	1581 (2.95%)	1589 (2.01%)	2114 (0.20%)

Table 122: Difference between the approaches that use ray-tracing and the actual ray-tracer for the side viewpoint of the trees scene.

Shadow Map Resolution	Contour Thickness		
	Two Pixels	Four Pixels	Six Pixels
1024x1024	5602 of 6349 (88.23%)	6161 of 6349 (97.04%)	6254 of 6349 (98.50%)
2048x2048	3198 of 3283 (97.41%)	3256 of 3283 (99.18%)	3257 of 3283 (99.21%)

Table 123: Wrongly defined pixels in the shadow mapping result which are inside the contour in the side viewpoint of the trees scene.

Shadow Map Resolution	Contour Thickness	Pixel Shading	
		Light	Shadow
1024x1024	Two Pixels	2579 of 13645	3023 of 13769
	Four Pixels	2811 of 26799	3350 of 27383
	Six Pixels	2843 of 39347	3411 of 40919
	Whole Image	2884 of 675205	3465 of 373371
2048x2048	Two Pixels	1528 of 13557	1670 of 13710
	Four Pixels	1552 of 26440	1704 of 27163
	Six Pixels	1552 of 38742	1705 of 40464
	Whole Image	1564 of 675631	1719 of 372945

Table 124: Pixels that the shadow map defines wrongly in the side viewpoint of the trees scene, separated in pixels defined in light and in shadow, compared to the total amount of pixels lighted in the same way.

Shadow Map Resolution	Contour Thickness	Texel Coherence					
		Light			Shadow		
		Confirmed	Incorrectly Confirmed	Undecided	Confirmed	Incorrectly Confirmed	Undecided
1024x1024	Two Pixels	2722 (19.95%)	0 (0.00%)	10923 (80.05%)	2813 (20.43%)	0 (0.00%)	10956 (79.57%)
	Four Pixels	12457 (46.48%)	0 (0.00%)	14342 (53.52%)	12960 (47.33%)	0 (0.00%)	14423 (52.67%)
	Six Pixels	24007 (61.01%)	0 (0.00%)	15340 (38.99%)	25434 (62.16%)	1 (0.00%)	15485 (37.84%)
	Whole Image	659046 (97.61%)	0 (0.00%)	16159 (2.39%)	357046 (95.63%)	11 (0.00%)	16325 (4.37%)
2048x2048	Two Pixels	6288 (46.38%)	0 (0.00%)	7269 (53.62%)	6514 (47.51%)	0 (0.00%)	7196 (52.49%)
	Four Pixels	18358 (69.43%)	0 (0.00%)	8082 (30.57%)	19155 (70.52%)	0 (0.00%)	8008 (29.48%)
	Six Pixels	30604 (78.99%)	0 (0.00%)	8138 (21.01%)	32399 (80.07%)	0 (0.00%)	8065 (19.93%)
	Whole Image	667411 (98.78%)	0 (0.00%)	8220 (1.22%)	364797 (97.82%)	0 (0.00%)	8148 (2.18%)

Table 125: Pixel confirmation when using texel coherence with four texels for the side viewpoint of the trees scene.

Shadow Map Resolution	Contour Thickness	Texel Shadowing							
		Light				Shadow			
		3 shadow/1 light	3 shadow/1 light in ray-tracer shadow	1 shadow/3 light	1 shadow/3 light in ray-tracer light	3 shadow/1 light	3 shadow/1 light in ray-tracer shadow	1 shadow/3 light	1 shadow/3 light in ray-tracer light
1024x1024	Two Pixels	1654	1219	2842	2727	2889	2796	1559	1159
	Four Pixels	1909	1318	4492	4364	4606	4493	1809	1279
	Six Pixels	1909	1318	5134	5006	5308	5188	1809	1279
	Whole Image	1935	1337	5539	5410	5740	5619	1827	1294
2048x2048	Two Pixels	957	679	2289	2236	2282	2228	909	649
	Four Pixels	957	679	2793	2740	2781	2726	910	650
	Six Pixels	957	679	2824	2771	2818	2762	910	650
	Whole Image	967	684	2861	2806	2853	2797	923	659

Table 126: Pixel shadowing for pixels that don't achieve texel coherence with four texels for the side viewpoint of the trees scene.

Shadow Map Resolution	Contour Thickness	Texel Coherence					
		Light			Shadow		
		Confirmed	Incorrectly Confirmed	Undecided	Confirmed	Incorrectly Confirmed	Undecided
1024x1024	Two Pixels	105 (0.77%)	0 (0.00%)	13540 (99.23%)	106 (0.77%)	0 (0.00%)	13663 (99.23%)
	Four Pixels	4552 (16.99%)	0 (0.00%)	22247 (83.01%)	4882 (17.83%)	0 (0.00%)	22501 (82.17%)
	Six Pixels	12547 (31.89%)	0 (0.00%)	26800 (68.11%)	13688 (33.45%)	0 (0.00%)	27231 (66.55%)
	Whole Image	643207 (95.26%)	0 (0.00%)	31998 (4.74%)	340528 (91.20%)	0 (0.00%)	32843 (8.80%)
2048x2048	Two Pixels	2340 (17.26%)	0 (0.00%)	11217 (82.74%)	2470 (18.02%)	0 (0.00%)	11240 (81.98%)
	Four Pixels	11886 (44.95%)	0 (0.00%)	14554 (55.05%)	12537 (46.15%)	0 (0.00%)	14626 (53.85%)
	Six Pixels	23125 (59.69%)	0 (0.00%)	15617 (40.31%)	24737 (61.13%)	0 (0.00%)	15727 (38.87%)
	Whole Image	659349 (97.59%)	0 (0.00%)	16282 (2.41%)	356521 (95.60%)	0 (0.00%)	16424 (4.40%)

Table 127: Pixel confirmation when using texel coherence with nine texels for the side viewpoint of the trees scene.

Shadow Map Lighting	Texel Shadowing	Shadow Map							
		1024x1024				2048x2048			
		Two Pixels	Four Pixels	Six Pixels	Whole Image	Two Pixels	Four Pixels	Six Pixels	Whole Image
Light	8 S-1 L	0	0	0	0	0	0	0	0
	8 S-1 L in RT Shadow	0	0	0	0	0	0	0	0
	7 S-2 L	6	6	6	6	6	6	6	6
	7 S-2 L in RT Shadow	2	2	2	2	1	1	1	1
	6 S-3 L	60	73	73	73	25	25	25	25
	6 S-3 L in RT Shadow	12	12	12	12	8	8	8	8
	5 S-4 L	118	165	182	182	28	32	32	32
	5 S-4 L in RT Shadow	27	28	28	28	6	6	6	6
	4 S-5 L	3102	4391	4942	5088	2210	2555	2556	2589
	4 S-5 L in RT Light	1549	2679	3219	4942	1295	1637	1638	1664
	3 S-6 L	7169	10923	12971	14459	5632	6941	7169	7439
	3 S-6 L in RT Light	6188	9870	11897	13363	5039	6327	6555	6820
	2 S-7 L	2404	3716	4307	5004	1873	2272	2409	2511
	2 S-7 L in RT Light	2400	3712	4303	5000	1868	2267	2404	2506
	1 S-8 L	681	2973	4319	7186	1443	2723	3420	3680
1 S-8 L in RT Light	681	2973	4319	7186	1443	2723	3420	3680	
Shadow	8 S-1 L	725	3144	4618	7814	1552	2903	3629	3903
	8 S-1 L in RT Shadow	719	3134	4603	7791	1552	2902	3627	3901
	7 S-2 L	2620	4024	4665	5427	1984	2412	2553	2665
	7 S-2 L in RT Shadow	2573	3972	4613	5372	1975	2403	2544	2656
	6 S-3 L	7282	11030	13096	14615	5613	6891	7123	7407
	6 S-3 L in RT Shadow	5897	9509	11528	113020	4850	6104	6336	6613
	5 S-4 L	3036	4303	4852	4987	2091	2420	2422	2449
	5 S-4 L in RT Shadow	1451	2536	3076	3195	1193	1513	1515	1535
	4 S-5 L	0	0	0	0	0	0	0	0
	4 S-5 L in RT Light	0	0	0	0	0	0	0	0
	3 S-6 L	0	0	0	0	0	0	0	0
	3 S-6 L in RT Light	0	0	0	0	0	0	0	0
	2 S-7 L	0	0	0	0	0	0	0	0
	2 S-7 L in RT Light	0	0	0	0	0	0	0	0
	1 S-8 L	0	0	0	0	0	0	0	0
1 S-8 L in RT Light	0	0	0	0	0	0	0	0	

Table 128: Pixel shadowing for pixels that don't achieve texel coherence with nine texels for the side viewpoint of the trees scene.

Shadow Map Resolution	Contour Thickness	Corrected		Turned Bad		Maintained Correct		Maintained Incorrect	
		L→S	S→L	L→S	S→L	L→L	S→S	L→L	S→S
1024x1024	Two Pixels	0	3023	0	442	11066	10304	2579	0
	Four Pixels	0	3350	0	1020	23988	23013	2811	0
	Six Pixels	0	3411	0	1751	36504	35757	2843	0
	Whole Image	0	3465	0	17120	672321	352786	2884	0
2048x2048	Two Pixels	1	1670	0	261	12029	11779	1527	0
	Four Pixels	1	1704	0	584	24888	24875	1551	0
	Six Pixels	1	1705	0	909	37190	37850	1551	0
	Whole Image	1	1719	0	8775	674067	362451	1563	0

Table 129: Pixel correction between the single texel approach and the shadow mapping approach for the side viewpoint of the trees scene.

Shadow Map Resolution	Contour Thickness	Corrected		Turned Bad		Maintained Correct		Maintained Incorrect	
		L→S	S→L	L→S	S→L	L→L	S→S	L→L	S→S
1024x1024	Two Pixels	2463	3023	0	99	11066	10647	116	0
	Four Pixels	2690	3350	0	136	23988	23897	121	0
	Six Pixels	2722	3411	0	185	36504	37323	121	0
	Whole Image	2763	3465	0	863	672321	369043	121	0
2048x2048	Two Pixels	1496	1670	0	28	12029	12012	32	0
	Four Pixels	1520	1704	0	38	24888	25421	32	0
	Six Pixels	1520	1705	0	55	37190	38704	32	0
	Whole Image	1532	1719	0	232	674067	370994	32	0

Table 130: Pixel correction between the neighbour texels approach using four neighbours and the shadow mapping approach for the side viewpoint of the trees scene.

Shadow Map Resolution	Contour Thickness	Corrected		Turned Bad		Maintained Correct		Maintained Incorrect	
		L→S	S→L	L→S	S→L	L→L	S→S	L→L	S→S
1024x1024	Two Pixels	2523	3023	0	34	11066	10712	56	0
	Four Pixels	2753	3350	0	43	23988	23990	58	0
	Six Pixels	2785	3411	0	63	36504	37445	58	0
	Whole Image	2826	3465	0	445	672321	369461	58	0
2048x2048	Two Pixels	1512	1670	0	9	12029	12031	16	0
	Four Pixels	1536	1704	0	10	24888	25449	16	0
	Six Pixels	1536	1705	0	20	37190	38739	16	0
	Whole Image	1548	1719	0	137	674067	371089	16	0

Table 131: Pixel correction between the neighbour texels approach using nine neighbours and the shadow mapping approach for the side viewpoint of the trees scene.

Shadow Map Resolution	Number of Neighbours	Triangle Average	Two Pixels	Four Pixels	Six Pixels	Whole Image
1024x1024	3	Used	0.9881	0.8686	0.8053	0.4583
		Available	1.0970	1.1280	1.1490	1.2337
	8	Used	1.2386	1.1561	1.0835	0.5663
		Available	1.2434	1.2621	1.2843	1.4649
2048x2048	3	Used	0.8207	0.7143	0.6731	0.4080
		Available	1.0665	1.0862	1.0968	1.1225
	8	Used	1.0383	0.9033	0.8327	0.4619
		Available	1.1358	1.1606	1.1760	1.2442

Table 132: Average of triangle intersections when using the neighbour texels approach for the side viewpoint of the trees scene.

Shadow Map Resolution	Contour Thickness	Corrected		Turned Bad		Maintained Correct		Maintained Incorrect	
		L→S	S→L	L→S	S→L	L→L	S→S	L→L	S→S
1024x1024	Two Pixels	0	3023	0	61	11066	10685	2579	0
	Four Pixels	0	3350	0	117	23988	23916	2811	0
	Six Pixels	0	3411	0	184	36504	37324	2843	0
	Whole Image	0	3465	0	1751	672321	368155	2884	0
2048x2048	Two Pixels	1	1670	0	26	12029	12014	1527	0
	Four Pixels	1	1704	0	50	24888	25409	1551	0
	Six Pixels	1	1705	0	77	37190	38682	1551	0
	Whole Image	1	1719	0	729	674067	370497	1563	0

Table 133: Pixel correction between the adjacent geometry approach with one level of adjacency and the shadow mapping approach for the side viewpoint of the trees scene.

Shadow Map Resolution	Contour Thickness	Corrected		Turned Bad		Maintained Correct		Maintained Incorrect	
		L→S	S→L	L→S	S→L	L→L	S→S	L→L	S→S
1024x1024	Two Pixels	0	3023	0	22	11066	10724	2579	0
	Four Pixels	0	3350	0	41	23988	23992	2811	0
	Six Pixels	0	3411	0	63	36504	37445	2843	0
	Whole Image	0	3465	0	1243	672321	368663	2884	0
2048x2048	Two Pixels	1	1670	0	18	12029	12022	1527	0
	Four Pixels	1	1704	0	30	24888	25429	1551	0
	Six Pixels	1	1705	0	38	37190	38721	1551	0
	Whole Image	1	1719	0	551	674067	370675	1563	0

Table 134: Pixel correction between the adjacent geometry approach with two level of adjacency and the shadow mapping approach for the side viewpoint of the trees scene.

Shadow Map Resolution	Adjacency Level	Triangle Average	Two Pixels	Four Pixels	Six Pixels	Whole Image
1024x1024	One Level	Used	2.0090	2.0216	2.0392	1.4243
		Available	4.0000	4.0000	4.0000	4.0000
	Two Levels	Used	7.2426	7.2979	7.3708	5.1081
		Available	14.4201	14.4402	14.4584	14.3456
2048x2048	One Level	Used	2.0114	2.0271	2.0435	1.4227
		Available	4.0000	4.0000	4.0000	4.0000
	Two Levels	Used	7.2488	7.3201	7.3906	5.1023
		Available	14.4156	14.4447	14.4662	14.3456

Table 135: Average of triangle intersections when using the adjacent geometry approach for the side viewpoint of the trees scene.

Contour Thickness		Two Pixels		Four Pixels		Six Pixels		Whole Image		
Lighting		L→S	S→L	L→S	S→L	L→S	S→L	L→S	S→L	
Shadow Map Resolution	1024x1024	Corrected by Both	0	3023	0	3350	0	3411	0	3465
		Turned Bad by Both	0	5	0	5	0	5	0	14
		Corrected by Neighbour Texels Only	2523	0	2753	0	2785	0	2826	0
		Corrected by Adjacent Geometry Only	0	0	0	0	0	0	0	0
		Turned Bad by Neighbour Texels Only	0	29	0	38	0	58	0	431
		Turned Bad by Adjacent Geometry Only	0	17	0	36	0	58	0	1229
	2048x2048	Corrected by Both	1	1670	1	1704	1	1705	1	1719
		Turned Bad by Both	0	1	0	1	0	1	0	9
		Corrected by Neighbour Texels Only	1511	0	1535	0	1535	0	1547	0
		Corrected by Adjacent Geometry Only	0	0	0	0	0	0	0	0
		Turned Bad by Neighbour Texels Only	0	8	0	9	0	19	0	128
		Turned Bad by Adjacent Geometry Only	0	17	0	29	0	37	0	542

Table 136: Pixel correction by the neighbour texels (9 texels) and the adjacent geometry (2 levels) approaches separated by lighting change for the side viewpoint of the trees scene.

Algorithm Step	Confirmations and Errors	1024x1024			2048x2048		
		Two Pixels	Four Pixels	Six Pixel	Two Pixels	Four Pixels	Six Pixel
Shadow Map	Total Contour Pixels	27414	54182	80266	27267	53603	79206
	Correct Light Pixels	11066 (81.10%)	23988 (89.51%)	36504 (92.77%)	12029 (88.73%)	24888 (94.13%)	37190 (95.99%)
	Correct Shadow Pixels	10746 (78.04%)	24033 (87.77%)	37508 (91.66%)	12040 (87.82%)	25459 (93.73%)	38759 (95.79%)
	Incorrect Light Pixels	2579 (18.90%)	2811 (10.49%)	2843 (7.23%)	1528 (11.27%)	1552 (5.87%)	1552 (4.01%)
	Incorrect Shadow Pixels	3023 (21.96%)	3350 (12.23%)	3411 (8.34%)	1670 (12.18%)	1704 (6.27%)	1705 (4.21%)
Texel Coherence	Confirmations in Light	2722 (19.95%)	12457 (46.48%)	24007 (61.01%)	6288 (46.38%)	18358 (69.43%)	30604 (78.99%)
	Confirmations in Shadow	2813 (20.43%)	12960 (47.33%)	25434 (62.16%)	6514 (47.51%)	19155 (70.52%)	32399 (80.07%)
	Wrong Confirmations in Light	0 (0.00%)	0 (0.00%)	0 (0.00%)	0 (0.00%)	0 (0.00%)	0 (0.00%)
	Wrong Confirmations in Shadow	0 (0.00%)	0 (0.00%)	1 (0.00%)	0 (0.00%)	0 (0.00%)	0 (0.00%)
Neighbouring Texels	Corrections in Light	2523 (18.49%)	2753 (10.27%)	2785 (7.08%)	1512 (11.15%)	1536 (5.81%)	1536 (3.96%)
	Confirmations in Shadow	10714 (77.81%)	23994 (87.62%)	37468 (91.57%)	12032 (87.76%)	25450 (93.69%)	38750 (95.76%)
Adjacent Geometry	Confirmations in Shadow	10741 (78.01%)	24028 (87.75%)	37504 (91.65%)	12039 (87.81%)	25458 (93.72%)	38758 (95.78%)
Final Lighting	Wrong Confirmations in Light	56 (0.41%)	58 (0.22%)	58 (0.15%)	16 (0.12%)	16 (0.06%)	16 (0.04%)
	Wrong Confirmations in Shadow	5 (0.04%)	5 (0.02%)	6 (0.01%)	1 (0.01%)	1 (0.00%)	1 (0.00%)

Table 137: Algorithm results of the side viewpoint of the trees scene.

Following below are the results for the “against” viewpoint of the “trees” scene.

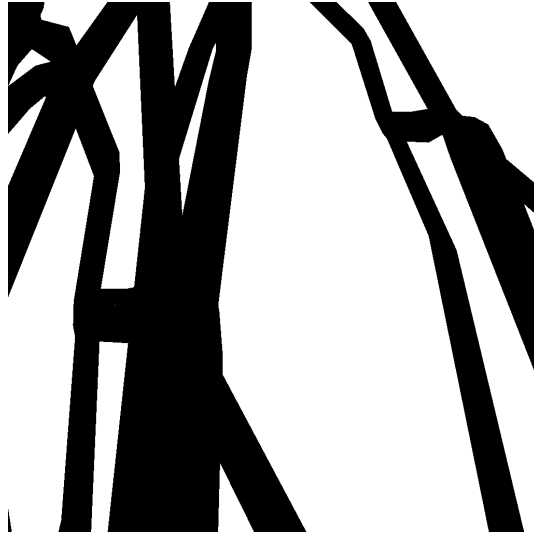


Figure 185: Result of the ray-tracing approach for the against viewpoint of the trees scene.



Figure 186: Result of the shadow mapping approach for the against viewpoint of the trees scene.



Figure 187: Result of texel coherence with four texels for the against viewpoint of the trees scene.



Figure 188: Result of texel coherence with nine texels for the against viewpoint of the trees scene.



Figure 189: Result of the single texel approach for the against viewpoint of the trees scene.



Figure 190: Result of the neighbour texels approach using four neighbours for the against viewpoint of the trees scene.



Figure 191: Result of the neighbour texels approach using nine neighbours for the against viewpoint of the trees scene.



Figure 192: Result of the adjacent geometry approach with one level of adjacency for the against viewpoint of the trees scene.



Figure 193: Result of the adjacent geometry approach with two level of adjacency for the against viewpoint of the trees scene.



Figure 194: Result of the algorithm with a six pixel thick contour and a 2048x2048 resolution shadow map for the against viewpoint of the trees scene.

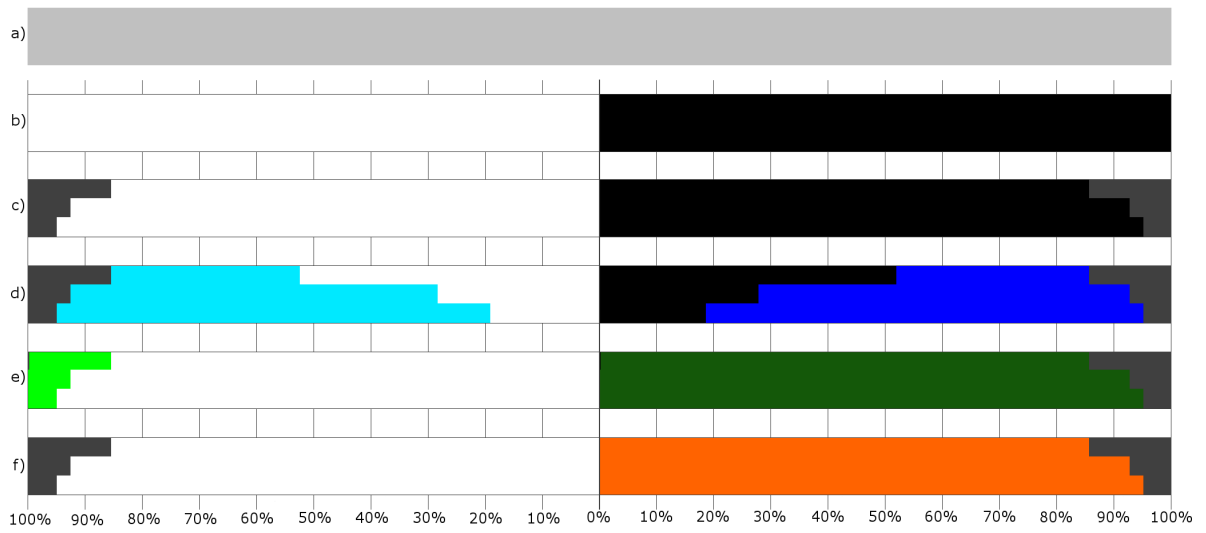
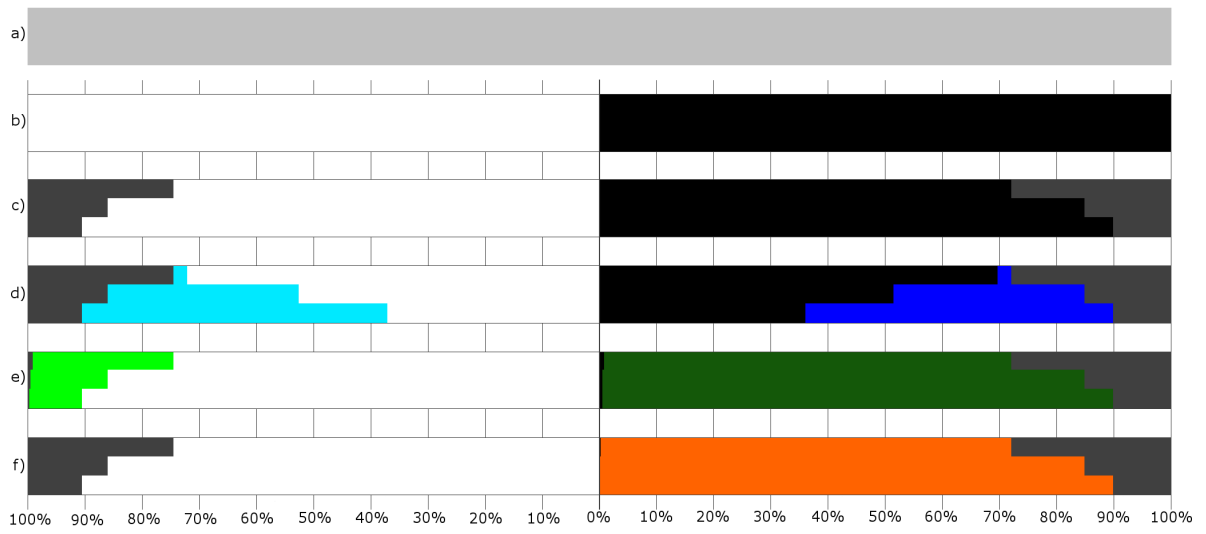


Figure 195: Corrected/confirmed/hinted contour pixels by each method for the against viewpoint of the trees scene using a 1024x1024 (top) and a 2048x2048 (bottom) resolution shadow map.

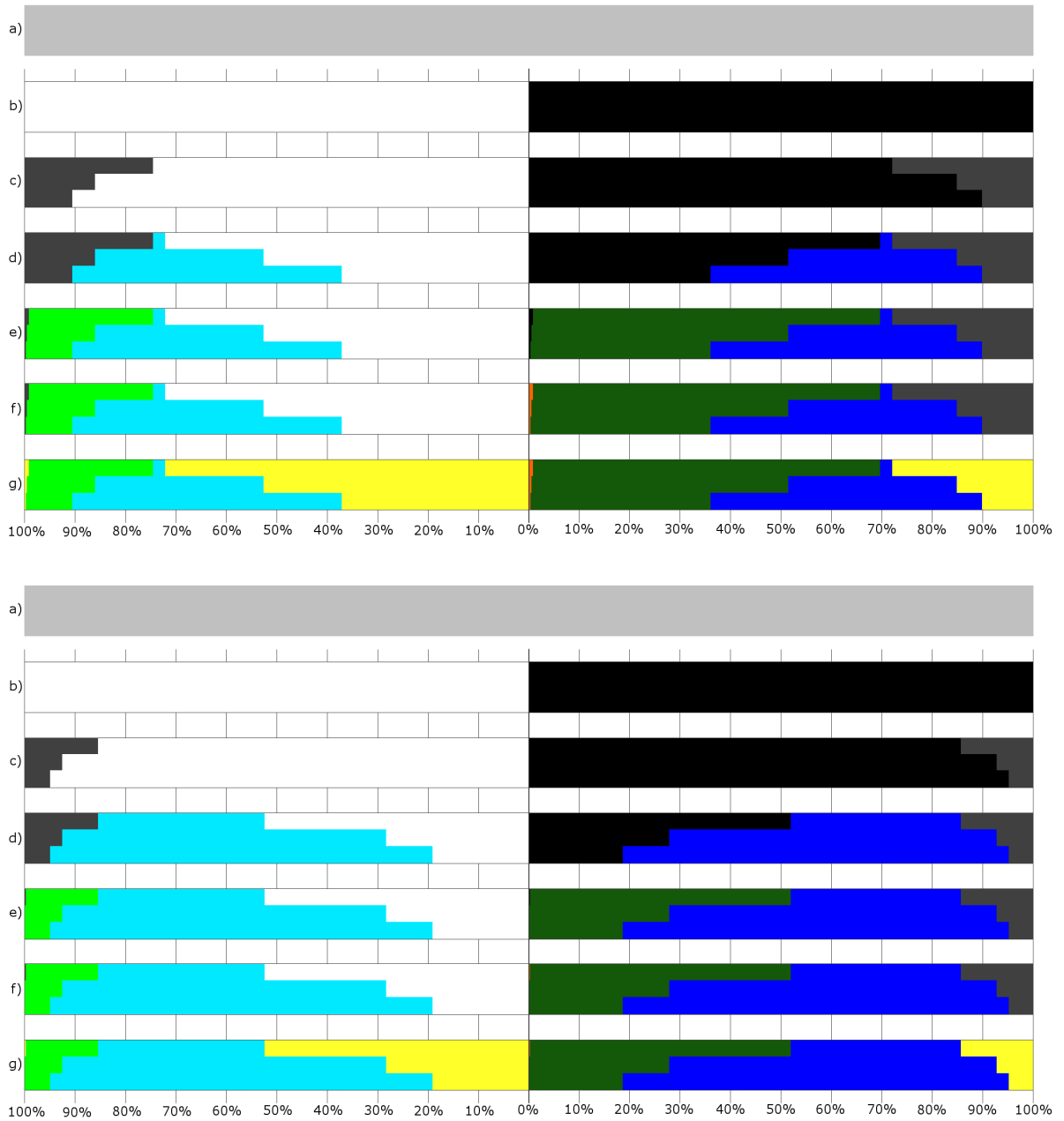


Figure 196: Corrected/confirmed/hinted contour pixels by the chaining of methods for the against viewpoint of the trees scene using a 1024x1024 (top) and a 2048x2048 (bottom) resolution shadow map.

Shadow Map Resolution	Approach	Contour Thickness			
		Two Pixels	Four Pixels	Six Pixels	Whole Image
1024x1024	Pixels in Contour	24929	49398	73522	1048576
	Shadow Map	6650 (26.68%)	7170 (14.51%)	7187 (9.78%)	7303 (0.70%)
	Single Texel	3592 (14.41%)	4261 (8.63%)	4867 (6.62%)	21192 (2.02%)
	Neighbour Texels (4 Neighbours)	387 (1.55%)	465 (0.94%)	543 (0.74%)	1215 (0.12%)
	Neighbour Texels (9 Neighbours)	269 (1.08%)	313 (0.63%)	313 (0.43%)	773 (0.07%)
	Adjacent Geometry (One Level)	3235 (12.98%)	3539 (7.16%)	3608 (4.91%)	4979 (0.47%)
	Adjacent Geometry (Two Level)	3193 (12.81%)	3469 (7.02%)	3498 (4.76%)	4583 (0.44%)
2048x2048	Pixels in Contour	24684	48825	72550	1048576
	Shadow Map	3551 (14.39%)	3556 (7.28%)	3557 (4.90%)	3605 (0.34%)
	Single Texel	1999 (8.10%)	2312 (4.74%)	2663 (3.67%)	10819 (1.03%)
	Neighbour Texels (4 Neighbours)	119 (0.48%)	132 (0.27%)	152 (0.21%)	289 (0.03%)
	Neighbour Texels (9 Neighbours)	69 (0.28%)	74 (0.15%)	84 (0.12%)	178 (0.02%)
	Adjacent Geometry (One Level)	1816 (7.36%)	1840 (3.77%)	1870 (2.58%)	2508 (0.24%)
	Adjacent Geometry (Two Level)	1806 (7.32%)	1814 (3.72%)	1822 (2.51%)	2378 (0.23%)

Table 138: Difference between the approaches that use ray-tracing and the actual ray-tracer for the against viewpoint of the trees scene.

Shadow Map Resolution	Contour Thickness		
	Two Pixels	Four Pixels	Six Pixels
1024x1024	6650 of 7303 (91.06%)	7170 of 7303 (98.18%)	7187 of 7303 (98.41%)
2048x2048	3551 of 3605 (98.50%)	3556 of 3605 (98.64%)	3557 of 3605 (98.67%)

Table 139: Wrongly defined pixels in the shadow mapping result which are inside the contour in the against viewpoint of the trees scene.

Shadow Map Resolution	Contour Thickness	Pixel Shading	
		Light	Shadow
1024x1024	Two Pixels	3162 of 12442	3488 of 12487
	Four Pixels	3423 of 24570	3747 of 24828
	Six Pixels	3430 of 36416	3757 of 37106
	Whole Image	3491 of 626198	3812 of 422378
2048x2048	Two Pixels	1784 of 12316	1767 of 12368
	Four Pixels	1787 of 24259	1769 of 24566
	Six Pixels	1787 of 35907	1770 of 36643
	Whole Image	1806 of 626526	1799 of 422050

Table 140: Pixels that the shadow map defines wrongly in the against viewpoint of the trees scene, separated in pixels defined in light and in shadow, compared to the total amount of pixels lighted in the same way.

Shadow Map Resolution	Contour Thickness	Texel Coherence					
		Light			Shadow		
		Confirmed	Incorrectly Confirmed	Undecided	Confirmed	Incorrectly Confirmed	Undecided
1024x1024	Two Pixels	301 (2.42%)	0 (0.00%)	12141 (97.58%)	296 (2.37%)	0 (0.00%)	12191 (97.63%)
	Four Pixels	8210 (33.41%)	0 (0.00%)	16360 (66.59%)	8302 (33.44%)	2 (0.01%)	16526 (66.56%)
	Six Pixels	19449 (53.41%)	0 (0.00%)	16967 (46.59%)	19976 (53.83%)	3 (0.01%)	17130 (46.17%)
	Whole Image	608706 (97.21%)	0 (0.00%)	17492 (2.79%)	404722 (95.82%)	4 (0.00%)	17656 (4.18%)
2048x2048	Two Pixels	4070 (33.05%)	0 (0.00%)	8246 (66.95%)	4175 (33.76%)	0 (0.00%)	8193 (66.24%)
	Four Pixels	15594 (64.28%)	0 (0.00%)	8665 (35.72%)	15955 (64.95%)	0 (0.00%)	8611 (35.05%)
	Six Pixels	27225 (75.82%)	0 (0.00%)	8682 (24.18%)	28018 (76.46%)	1 (0.00%)	8625 (23.54%)
	Whole Image	617708 (98.59%)	0 (0.00%)	8818 (1.41%)	413284 (97.92%)	3 (0.00%)	8766 (2.08%)

Table 141: Pixel confirmation when using texel coherence with four texels for the against viewpoint of the trees scene.

Shadow Map Resolution	Contour Thickness	Texel Shadowing							
		Light				Shadow			
		3 shadow/1 light	3 shadow/1 light in ray-tracer shadow	1 shadow/3 light	1 shadow/3 light in ray-tracer light	3 shadow/1 light	3 shadow/1 light in ray-tracer shadow	1 shadow/3 light	1 shadow/3 light in ray-tracer light
1024x1024	Two Pixels	1437	1086	2688	2627	2755	2640	1417	1131
	Four Pixels	1713	1187	4268	4199	4454	4316	1687	1248
	Six Pixels	1713	1187	4784	4713	4976	4832	1689	1248
	Whole Image	1771	1217	5141	5069	5335	5184	1725	1270
2048x2048	Two Pixels	861	610	2135	2088	2131	2082	818	595
	Four Pixels	864	610	2502	2452	2506	2457	819	595
	Six Pixels	864	610	2519	2469	2520	2471	819	595
	Whole Image	885	619	2584	2533	2589	2538	841	613

Table 142: Pixel shadowing for pixels that don't achieve texel coherence with four texels for the against viewpoint of the trees scene.

Shadow Map Resolution	Contour Thickness	Texel Coherence					
		Light			Shadow		
		Confirmed	Incorrectly Confirmed	Undecided	Confirmed	Incorrectly Confirmed	Undecided
1024x1024	Two Pixels	0 (0.00%)	0 (0.00%)	12442 (100.00%)	0 (0.00%)	0 (0.00%)	12487 (100.00%)
	Four Pixels	547 (2.23%)	0 (0.00%)	24023 (97.77%)	561 (2.26%)	0 (0.00%)	24267 (97.74%)
	Six Pixels	6035 (16.57%)	0 (0.00%)	30381(83.43%)	6318 (17.03%)	0 (0.00%)	30788(82.97%)
	Whole Image	591357 (94.44%)	0 (0.00%)	34841 (5.56%)	387142 (91.66%)	1 (0.00%)	35236 (8.34%)
2048x2048	Two Pixels	282 (2.29%)	0 (0.00%)	12034 (97.71%)	287 (2.32%)	0 (0.00%)	12081 (97.68%)
	Four Pixels	7891 (32.53%)	0 (0.00%)	16368 (67.47%)	7991 (32.53%)	0 (0.00%)	16575 (67.47%)
	Six Pixels	18870 (52.55%)	0 (0.00%)	17037 (47.45%)	19397 (52.94%)	0 (0.00%)	17246 (47.06%)
	Whole Image	609082 (97.22%)	0 (0.00%)	17444 (2.78%)	404380 (95.81%)	1 (0.00%)	17670 (4.19%)

Table 143: Pixel confirmation when using texel coherence with nine texels for the against viewpoint of the trees scene.

Shadow Map Lighting	Texel Shadowing	Shadow Map							
		1024x1024				2048x2048			
		Two Pixels	Four Pixels	Six Pixels	Whole Image	Two Pixels	Four Pixels	Six Pixels	Whole Image
Light	8 S-1 L	0	0	0	0	0	0	0	0
	8 S-1 L in RT Shadow	0	0	0	0	0	0	0	0
	7 S-2 L	22	25	25	25	4	4	4	4
	7 S-2 L in RT Shadow	9	9	9	9	0	0	0	0
	6 S-3 L	65	86	86	90	15	15	15	16
	6 S-3 L in RT Shadow	31	31	31	31	3	3	3	3
	5 S-4 L	105	146	159	160	49	55	55	55
	5 S-4 L in RT Shadow	29	30	30	30	17	17	17	17
	4 S-5 L	2381	3709	4132	4256	1806	2055	2055	2081
	4 S-5 L in RT Light	941	2120	2538	2631	1019	1267	1267	1282
	3 S-6 L	7567	14418	18048	19453	7371	9666	9758	9878
	3 S-6 L in RT Light	5917	12657	16285	17660	6395	8688	8780	8892
	2 S-7 L	1687	3223	3878	4056	1593	2031	2040	2073
	2 S-7 L in RT Light	1684	3220	3875	4053	1592	2030	2039	2072
	1 S-8 L	615	2416	4053	6801	1196	2542	3110	3337
1 S-8 L in RT Light	615	2416	4053	6801	1196	2542	3110	3337	
Shadow	8 S-1 L	686	2619	4382	7099	1217	2640	3215	3446
	8 S-1 L in RT Shadow	680	2608	4368	7083	1217	2640	3215	3446
	7 S-2 L	1795	3445	4191	4482	1660	2145	2160	2187
	7 S-2 L in RT Shadow	1772	3410	4152	4443	1650	2133	2147	2173
	6 S-3 L	7652	14585	18215	19549	7393	9724	9805	9935
	6 S-3 L in RT Shadow	5651	12475	16104	17407	6449	8780	8861	8979
	5 S-4 L	2338	3593	3975	4081	1811	2066	2066	2102
	5 S-4 L in RT Shadow	890	2013	2393	2478	998	1253	1253	1274
	4 S-5 L	16	25	25	25	0	0	0	0
	4 S-5 L in RT Light	10	11	11	11	0	0	0	0
	3 S-6 L	0	0	0	0	0	0	0	0
	3 S-6 L in RT Light	0	0	0	0	0	0	0	0
	2 S-7 L	0	0	0	0	0	0	0	0
	2 S-7 L in RT Light	0	0	0	0	0	0	0	0
	1 S-8 L	0	0	0	0	0	0	0	0
1 S-8 L in RT Light	0	0	0	0	0	0	0	0	

Table 144: Pixel shadowing for pixels that don't achieve texel coherence with nine texels for the against viewpoint of the trees scene.

Shadow Map Resolution	Contour Thickness	Corrected		Turned Bad		Maintained Correct		Maintained Incorrect	
		L→S	S→L	L→S	S→L	L→L	S→S	L→L	S→S
1024x1024	Two Pixels	0	3488	0	430	9280	8569	3162	0
	Four Pixels	0	3747	0	838	21147	20243	3423	0
	Six Pixels	0	3757	0	1437	32986	31912	3430	0
	Whole Image	0	3812	0	17701	622707	400865	3491	0
2048x2048	Two Pixels	1	1767	0	216	10532	10385	1783	0
	Four Pixels	1	1769	0	526	22472	22271	1786	0
	Six Pixels	1	1770	0	877	34120	33996	1786	0
	Whole Image	1	1799	0	9014	624720	411237	1805	0

Table 145: Pixel correction between the single texel approach and the shadow mapping approach for the against viewpoint of the trees scene.

Shadow Map Resolution	Contour Thickness	Corrected		Turned Bad		Maintained Correct		Maintained Incorrect	
		L→S	S→L	L→S	S→L	L→L	S→S	L→L	S→S
1024x1024	Two Pixels	2973	3488	0	198	9280	8801	189	0
	Four Pixels	3212	3747	0	254	21147	20827	211	0
	Six Pixels	3219	3757	0	332	32986	33017	211	0
	Whole Image	3280	3812	0	1004	622707	417562	211	0
2048x2048	Two Pixels	1729	1767	0	64	10532	10537	55	0
	Four Pixels	1732	1769	0	77	22472	22720	55	0
	Six Pixels	1732	1770	0	97	34120	34776	55	0
	Whole Image	1751	1799	0	234	624720	420017	55	0

Table 146: Pixel correction between the neighbour texels approach using four neighbours and the shadow mapping approach for the against viewpoint of the trees scene.

Shadow Map Resolution	Contour Thickness	Corrected		Turned Bad		Maintained Correct		Maintained Incorrect	
		L→S	S→L	L→S	S→L	L→L	S→S	L→L	S→S
1024x1024	Two Pixels	3055	3488	0	117	9280	8882	107	0
	Four Pixels	3306	3747	0	152	21147	20929	117	0
	Six Pixels	3313	3757	0	196	32986	33153	117	0
	Whole Image	3374	3812	0	656	622707	417910	117	0
2048x2048	Two Pixels	1752	1767	0	37	10532	10564	32	0
	Four Pixels	1755	1769	0	42	22472	22755	32	0
	Six Pixels	1755	1770	0	52	34120	34821	32	0
	Whole Image	1774	1799	0	146	624720	420105	32	0

Table 147: Pixel correction between the neighbour texels approach using nine neighbours and the shadow mapping approach for the against viewpoint of the trees scene.

Shadow Map Resolution	Number of Neighbours	Triangle Average	Two Pixels	Four Pixels	Six Pixels	Whole Image
1024x1024	3	Used	1.0563	0.9171	0.8294	0.5056
		Available	1.0692	1.1000	1.1277	1.2053
	8	Used	1.2201	1.2047	1.1357	0.6128
		Available	1.2201	1.2182	1.2372	1.4055
2048x2048	3	Used	0.8771	0.7322	0.6813	0.4552
		Available	1.0503	1.0759	1.0906	1.1078
	8	Used	1.0996	0.9549	0.8598	0.5088
		Available	1.1124	1.1390	1.1620	1.1240

Table 148: Average of triangle intersections when using the neighbour texels approach for the against viewpoint of the trees scene.

Shadow Map Resolution	Contour Thickness	Corrected		Turned Bad		Maintained Correct		Maintained Incorrect	
		L→S	S→L	L→S	S→L	L→L	S→S	L→L	S→S
1024x1024	Two Pixels	0	3488	0	73	9280	8926	3162	0
	Four Pixels	0	3747	0	116	21147	20965	3423	0
	Six Pixels	0	3757	0	178	32986	33171	3430	0
	Whole Image	0	3812	0	1488	622707	417078	3491	0
2048x2048	Two Pixels	1	1767	0	33	10532	10568	1783	0
	Four Pixels	1	1769	0	54	22472	22743	1786	0
	Six Pixels	1	1770	0	84	34120	34789	1786	0
	Whole Image	1	1799	0	703	624720	419548	1805	0

Table 149: Pixel correction between the adjacent geometry approach with one level of adjacency and the shadow mapping approach for the against viewpoint of the trees scene.

Shadow Map Resolution	Contour Thickness	Corrected		Turned Bad		Maintained Correct		Maintained Incorrect	
		L→S	S→L	L→S	S→L	L→L	S→S	L→L	S→S
1024x1024	Two Pixels	0	3488	0	31	9280	8968	3162	0
	Four Pixels	0	3747	0	46	21147	21035	3423	0
	Six Pixels	0	3757	0	68	32986	33281	3430	0
	Whole Image	0	3812	0	1092	622707	417474	3491	0
2048x2048	Two Pixels	1	1767	0	23	10532	10578	1783	0
	Four Pixels	1	1769	0	28	22472	22769	1786	0
	Six Pixels	1	1770	0	36	34120	34837	1786	0
	Whole Image	1	1799	0	573	624720	419678	1805	0

Table 150: Pixel correction between the adjacent geometry approach with two level of adjacency and the shadow mapping approach for the against viewpoint of the trees scene.

Shadow Map Resolution	Adjacency Level	Triangle Average	Two Pixels	Four Pixels	Six Pixels	Whole Image
1024x1024	One Level	Used	2.0036	2.0104	2.0188	1.6112
		Available	4.0000	4.0000	4.0000	4.0000
	Two Levels	Used	7.2241	7.2513	7.2870	5.8435
		Available	14.4222	14.4273	14.4386	14.5067
2048x2048	One Level	Used	2.0042	2.0126	2.0203	1.6100
		Available	4.0000	4.0000	4.0000	4.0000
	Two Levels	Used	7.2170	7.2547	7.2928	5.8400
		Available	14.4036	14.4187	14.4392	14.5093

Table 151: Average of triangle intersections when using the adjacent geometry approach for the against viewpoint of the trees scene.

Contour Thickness		Two Pixels		Four Pixels		Six Pixels		Whole Image		
Lighting		L→S	S→L	L→S	S→L	L→S	S→L	L→S	S→L	
Shadow Map Resolution	1024x1024	Corrected by Both	0	3488	0	3747	0	3757	0	3812
		Turned Bad by Both	0	11	0	12	0	13	0	16
		Corrected by Neighbour Texels Only	3055	0	3306	0	3313	0	3374	0
		Corrected by Adjacent Geometry Only	0	0	0	0	0	0	0	0
		Turned Bad by Neighbour Texels Only	0	106	0	140	0	183	0	640
		Turned Bad by Adjacent Geometry Only	0	20	0	34	0	55	0	1076
	2048x2048	Corrected by Both	1	1767	1	1769	1	1770	1	1799
		Turned Bad by Both	0	10	0	10	0	10	0	11
		Corrected by Neighbour Texels Only	1751	0	1754	0	1754	0	1773	0
		Corrected by Adjacent Geometry Only	0	0	0	0	0	0	0	0
		Turned Bad by Neighbour Texels Only	0	27	0	32	0	42	0	135
		Turned Bad by Adjacent Geometry Only	0	13	0	18	0	26	0	562

Table 152: Pixel correction by the neighbour texels (9 texels) and the adjacent geometry (2 levels) approaches separated by lighting change for the against viewpoint of the trees scene.

Algorithm Step	Confirmations and Errors	1024x1024			2048x2048		
		Two Pixels	Four Pixels	Six Pixel	Two Pixels	Four Pixels	Six Pixel
Shadow Map	Total Contour Pixels	24929	49398	73522	24684	48825	72550
	Correct Light Pixels	9280 (74.59%)	21147 (86.07%)	32986 (90.58%)	10532 (85.51%)	22472 (92.63%)	34120 (95.02%)
	Correct Shadow Pixels	8999 (72.07%)	21081 (84.91%)	33349 (89.87%)	10601 (85.71%)	22797 (92.80%)	34873 (95.17%)
	Incorrect Light Pixels	3162 (25.41%)	3423 (13.93%)	3430 (9.42%)	1784 (14.49%)	1787 (7.37%)	1787 (4.98%)
	Incorrect Shadow Pixels	3488 (27.93%)	3747 (15.09%)	3757 (10.13%)	1767 (14.29%)	1769 (7.20%)	1770 (4.83%)
Texel Coherence	Confirmations in Light	301 (2.42%)	8210 (33.41%)	19449 (53.41%)	4070 (33.05%)	15594 (64.28%)	27225 (75.82%)
	Confirmations in Shadow	296 (2.37%)	8302 (33.44%)	19976 (53.83%)	4175 (33.76%)	15955 (64.95%)	28018 (76.46%)
	Wrong Confirmations in Light	0 (0.00%)	0 (0.00%)	0 (0.00%)	0 (0.00%)	0 (0.00%)	0 (0.00%)
	Wrong Confirmations in Shadow	0 (0.00%)	2 (0.01%)	3 (0.01%)	0 (0.00%)	0 (0.00%)	1 (0.00%)
Neighbouring Texels	Corrections in Light	3055 (24.55%)	3306 (13.46%)	3313 (9.10%)	1752 (14.23%)	1755 (7.23%)	1755 (4.89%)
	Confirmations in Shadow	8882 (71.13%)	20945 (84.36%)	33210 (89.50%)	10564 (85.41%)	22760 (92.65%)	34837 (95.07%)
Adjacent Geometry	Confirmations in Shadow	8988 (71.98%)	21072 (84.87%)	33341 (89.85%)	10591 (85.63%)	22787 (92.76%)	24864 (95.15%)
Final Lighting	Wrong Confirmations in Light	107 (0.86%)	117 (0.48%)	117 (0.32%)	32 (0.26%)	32 (0.13%)	32 (0.09%)
	Wrong Confirmations in Shadow	11 (0.09%)	13 (0.05%)	14 (0.04%)	10 (0.08%)	10 (0.04%)	11 (0.03%)

Table 153: Algorithm results of the against viewpoint of the trees scene.

And following below are the results of the “side” viewpoint of the “flowers” scene.

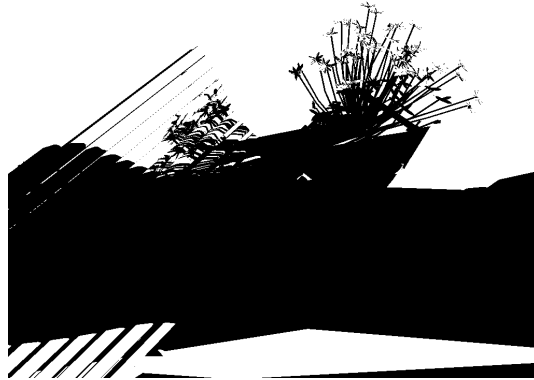


Figure 197: Result of the ray-tracing approach for the side viewpoint of the flowers scene.

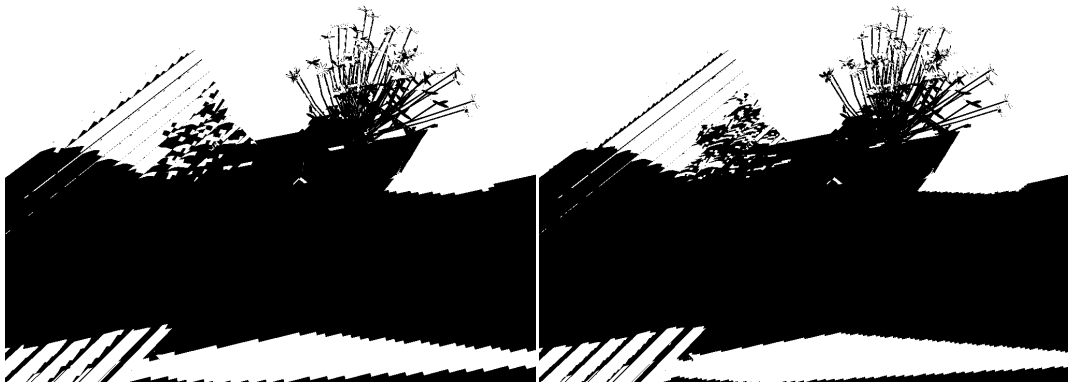


Figure 198: Result of the shadow mapping approach for the side viewpoint of the flowers scene.

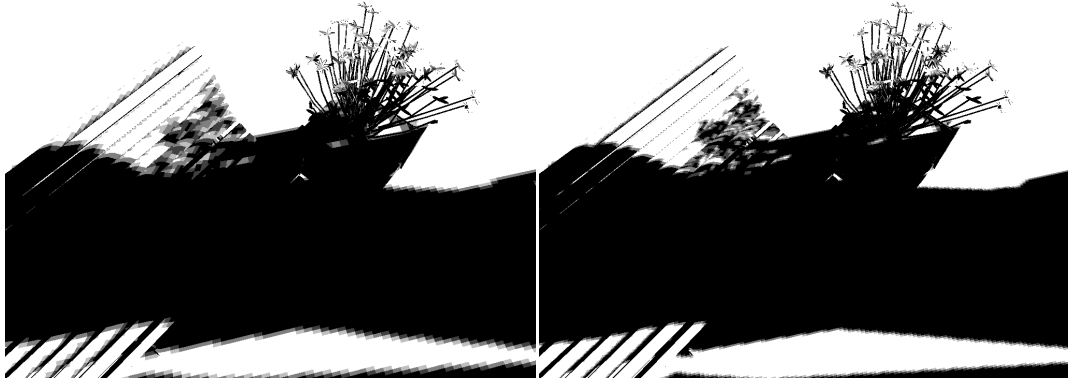


Figure 199: Result of texel coherence with four texels for the side viewpoint of the flowers scene.

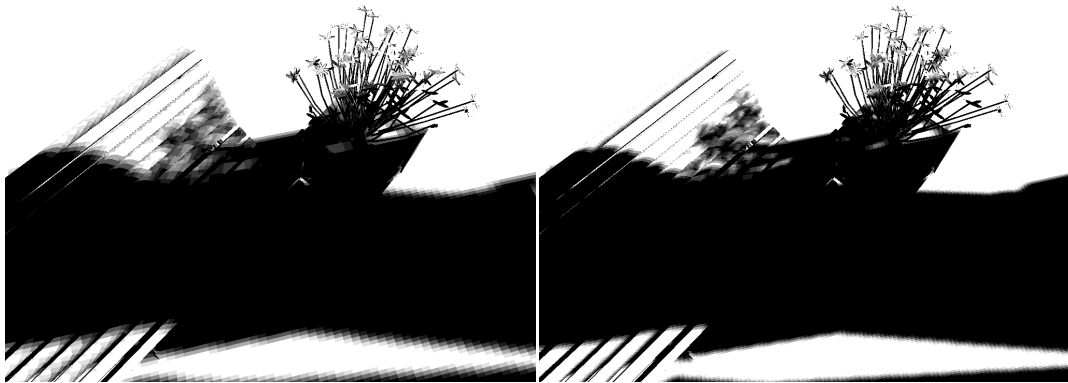


Figure 200: Result of texel coherence with nine texels for the side viewpoint of the flowers scene.

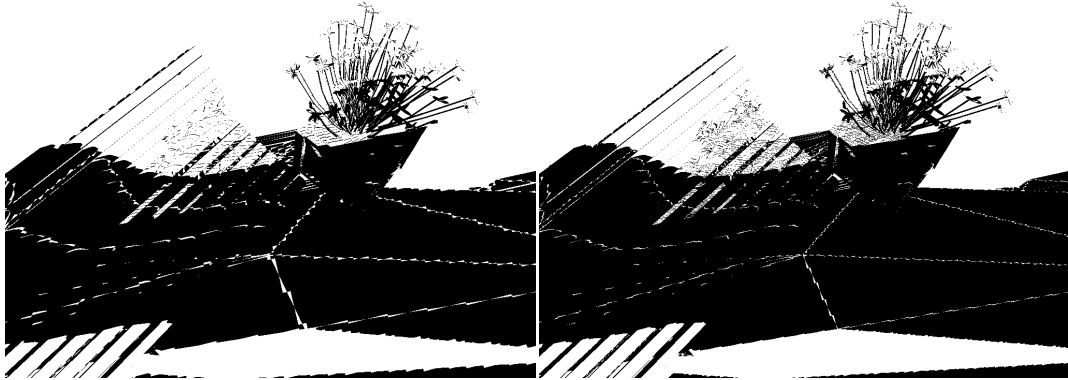


Figure 201: Result of the single texel approach for the side viewpoint of the flowers scene.

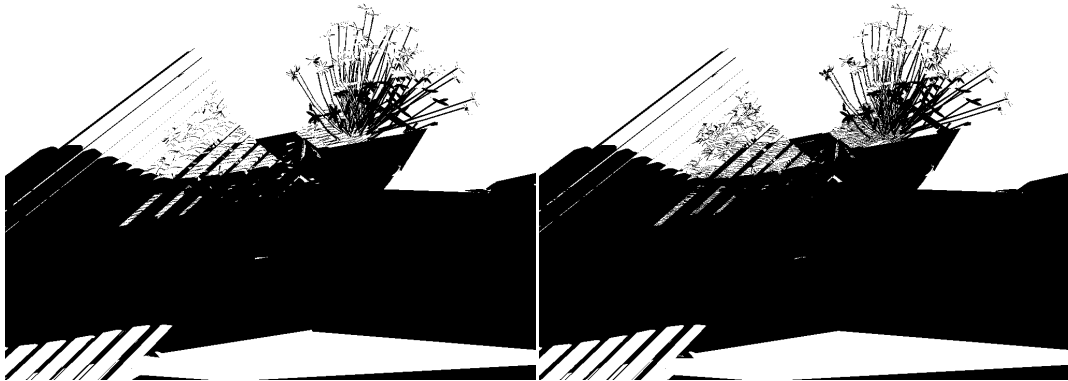


Figure 202: Result of the neighbour texels approach using four neighbours for the side viewpoint of the flowers scene.

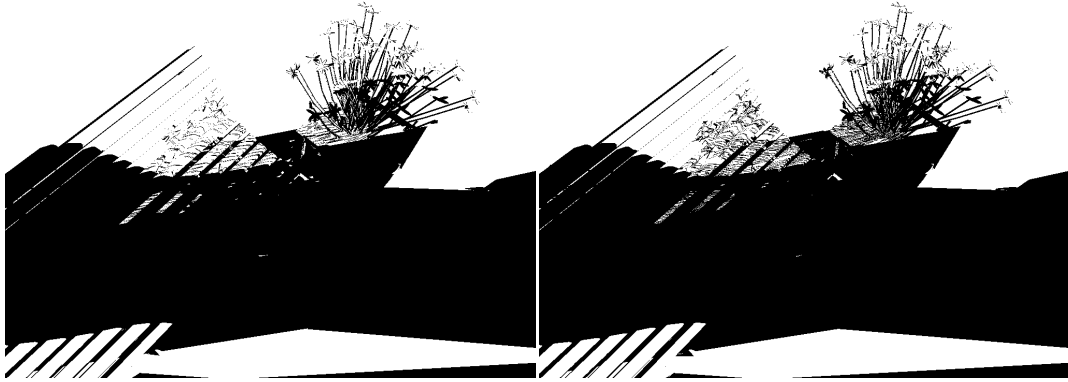


Figure 203: Result of the neighbour texels approach using nine neighbours for the side viewpoint of the flowers scene.

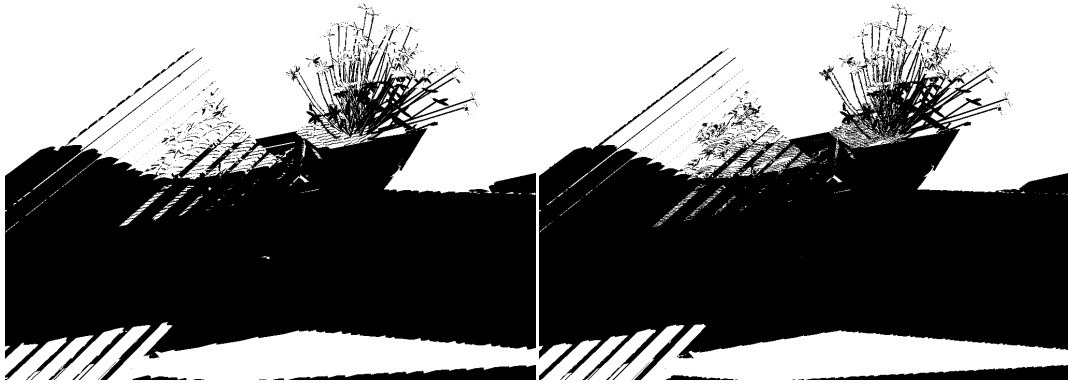


Figure 204: Result of the adjacent geometry approach with one level of adjacency for the side viewpoint of the flowers scene.

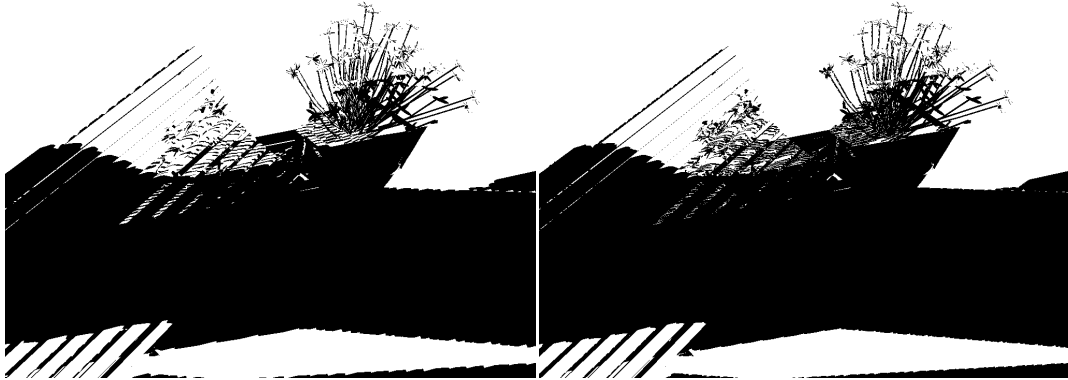


Figure 205: Result of the adjacent geometry approach with two levels of adjacency for the side viewpoint of the flowers scene.

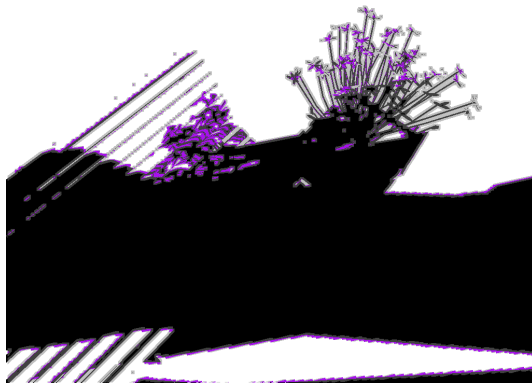


Figure 206: Result of the algorithm with a six pixel thick contour and a 2048x2048 resolution shadow map for the side viewpoint of the flowers scene.

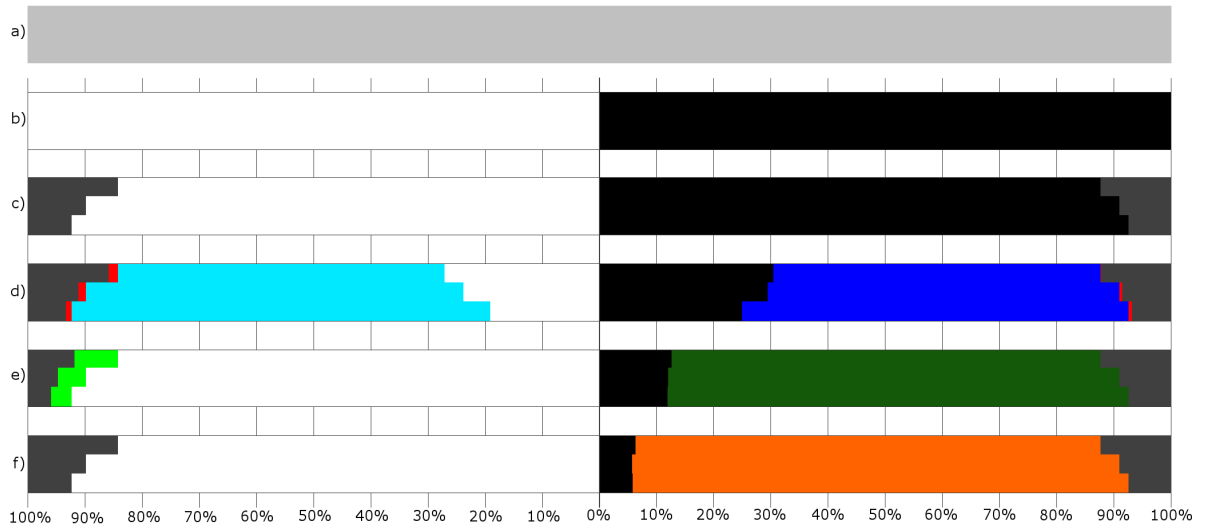
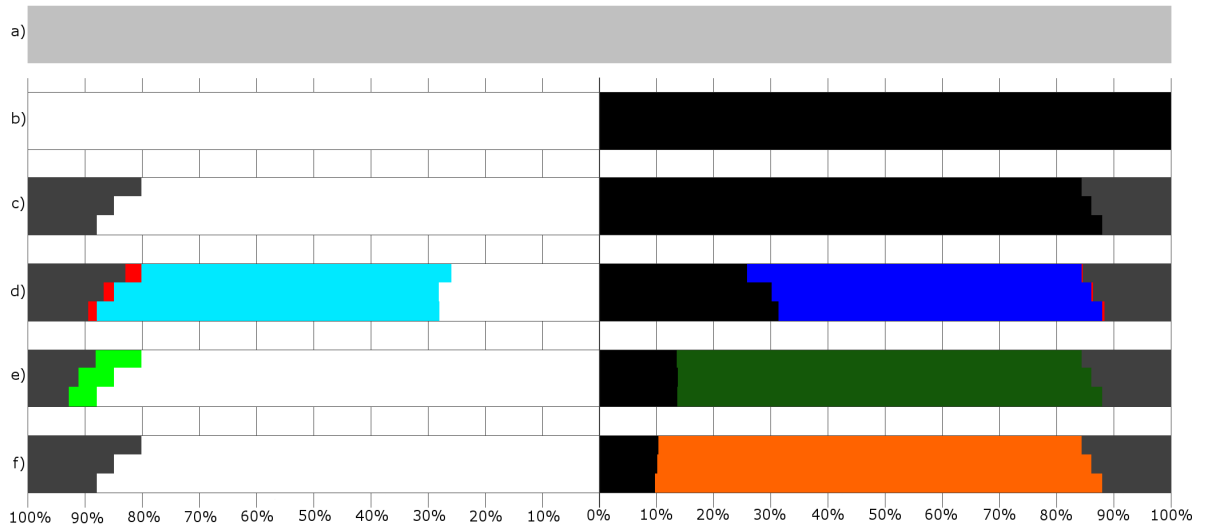


Figure 207: Corrected/confirmed/hinted contour pixels by each method for the side viewpoint of the flowers scene using a 1024x1024 (top) and a 2048x2048 (bottom) resolution shadow map.

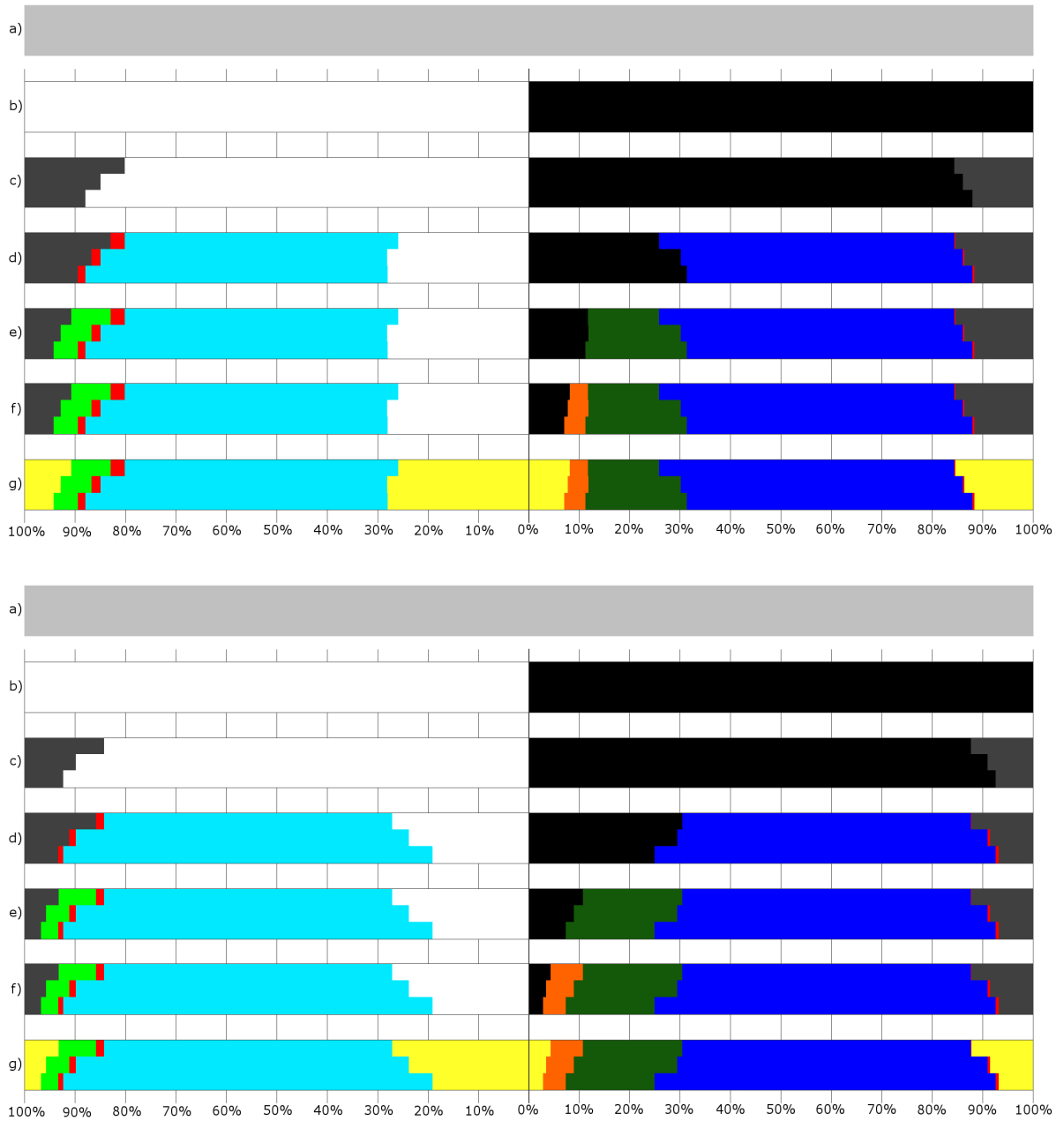


Figure 208: Corrected/confirmed/hinted contour pixels by the chaining of methods for the side viewpoint of the flowers scene using a 1024x1024 (top) and a 2048x2048 (bottom) resolution shadow map.

Shadow Map Resolution	Approach	Contour Thickness			
		Two Pixels	Four Pixels	Six Pixels	Whole Image
1024x1024	Pixels in Contour	47368	80814	106784	1048576
	Shadow Map	8434 (17.81%)	11724 (14.51%)	12834 (12.02%)	14226 (1.36%)
	Single Texel	8486 (17.92%)	12690 (15.70%)	15046 (14.09%)	35332 (3.37%)
	Neighbour Texels (4 Neighbours)	6287 (13.27%)	9444 (11.69%)	11295 (10.58%)	21596 (2.06%)
	Neighbour Texels (9 Neighbours)	6015 (12.70%)	8994 (11.13%)	10793 (10.11%)	19922 (1.90%)
	Adjacent Geometry (One Level)	7785 (16.44%)	11410 (14.12%)	13259 (12.42%)	23940 (2.28%)
	Adjacent Geometry (Two Level)	7067 (14.92%)	10156 (12.57%)	11546 (10.81%)	19721 (1.88%)
2048x2048	Pixels in Contour	49049	81863	106977	1048576
	Shadow Map	6923 (14.11%)	7825 (9.56%)	8049 (7.52%)	8547 (0.82%)
	Single Texel	8079 (16.47%)	10915 (13.33%)	12794 (11.96%)	26177 (2.50%)
	Neighbour Texels (4 Neighbours)	5775 (11.77%)	7881 (9.63%)	9325 (8.72%)	16347 (1.56%)
	Neighbour Texels (9 Neighbours)	5091 (10.38%)	6926 (8.46%)	8180 (7.65%)	13796 (1.32%)
	Adjacent Geometry (One Level)	6745 (13.75%)	8570 (10.47%)	9834 (9.19%)	16461 (1.57%)
	Adjacent Geometry (Two Level)	5259 (10.72%)	6345 (7.75%)	7041 (6.58%)	10510 (1.00%)

Table 154: Difference between the approaches that use ray-tracing and the actual ray-tracer for the side viewpoint of the flowers scene.

Shadow Map Resolution	Contour Thickness		
	Two Pixels	Four Pixels	Six Pixels
1024x1024	8434 of 14226 (59.29%)	11724 of 14226 (82.41%)	12834 of 14226 (90.22%)
2048x2048	6923 of 8547 (81.00%)	7825 of 8547 (91.55%)	8049 of 8547 (94.17%)

Table 155: Wrongly defined pixels in the shadow mapping result which are inside the contour in the side viewpoint of the flowers scene.

Shadow Map Resolution	Contour Thickness	Pixel Shading	
		Light	Shadow
1024x1024	Two Pixels	4866 of 24534	3568 of 22834
	Four Pixels	6604 of 43942	5120 of 36872
	Six Pixels	7144 of 59487	5690 of 47297
	Whole Image	7550 of 639660	6676 of 408916
2048x2048	Two Pixels	3967 of 25180	2956 of 23869
	Four Pixels	4422 of 43927	3403 of 37936
	Six Pixels	4485 of 58619	3564 of 48358
	Whole Image	4634 of 639507	3913 of 409069

Table 156: Pixels that the shadow map defines wrongly in the side viewpoint of the flowers scene, separated in pixels defined in light and in shadow, compared to the total amount of pixels lighted in the same way.

Shadow Map Resolution	Contour Thickness	Texel Coherence					
		Light			Shadow		
		Confirmed	Incorrectly Confirmed	Undecided	Confirmed	Incorrectly Confirmed	Undecided
1024x1024	Two Pixels	13931 (56.78%)	642 (2.62%)	10603 (43.22%)	13402 (58.69%)	39 (0.17%)	9432 (41.31%)
	Four Pixels	25723 (58.54%)	773 (1.76%)	18219 (41.46%)	20682 (56.09%)	81 (0.22%)	16190 (43.91%)
	Six Pixels	36427 (61.24%)	825 (1.39%)	23060 (38.76%)	26880 (56.83%)	144 (0.30%)	20417 (43.17%)
	Whole Image	612550 (95.76%)	956 (0.15%)	27110 (4.24%)	384379 (94.00%)	787 (0.19%)	24537 (6.00%)
2048x2048	Two Pixels	14763 (58.63%)	389 (1.54%)	10417 (41.37%)	13648 (57.18%)	17 (0.07%)	10221 (42.82%)
	Four Pixels	29524 (67.21%)	500 (1.14%)	14403 (32.79%)	23479 (61.89%)	125 (0.33%)	14457 (38.11%)
	Six Pixels	43425 (74.08%)	543 (0.93%)	15194 (25.92%)	32922 (68.08%)	234 (0.48%)	15436 (31.92%)
	Whole Image	623784 (97.54%)	633 (0.10%)	15723 (2.46%)	392923 (96.05%)	498 (0.12%)	16146 (3.95%)

Table 157: Pixel confirmation when using texel coherence with four texels for the side viewpoint of the flowers scene.

Shadow Map Resolution	Contour Thickness	Texel Shadowing							
		Light				Shadow			
		3 shadow/1 light	3 shadow/1 light in ray-tracer shadow	1 shadow/3 light	1 shadow/3 light in ray-tracer light	3 shadow/1 light	3 shadow/1 light in ray-tracer shadow	1 shadow/3 light	1 shadow/3 light in ray-tracer light
1024x1024	Two Pixels	2268	1623	3973	3053	3015	2524	2431	1582
	Four Pixels	3389	2247	7374	6060	5728	4896	3660	2225
	Six Pixels	3760	2360	10018	8527	7833	6791	4093	2400
	Whole Image	3898	2446	13286	11714	10890	9680	4286	2503
2048x2048	Two Pixels	2163	1345	3558	3011	3674	3232	1945	1277
	Four Pixels	2410	1423	5837	5156	6102	5522	2208	1365
	Six Pixels	2410	1423	6585	5887	6949	6332	2212	1367
	Whole Image	2462	1457	6932	6227	7421	6785	2275	1408

Table 158: Pixel shadowing for pixels that don't achieve texel coherence with four texels for the side viewpoint of the flowers scene.

Shadow Map Resolution	Contour Thickness	Texel Coherence					
		Light			Shadow		
		Confirmed	Incorrectly Confirmed	Undecided	Confirmed	Incorrectly Confirmed	Undecided
1024x1024	Two Pixels	11732 (47.82%)	323 (1.32%)	12802 (52.18%)	12701 (55.62%)	11 (0.05%)	10133 (44.38%)
	Four Pixels	21763 (49.53%)	403 (0.92%)	22179 (50.47%)	19290 (52.32%)	22 (0.06%)	17582 (47.68%)
	Six Pixels	30119 (50.63%)	420(0.71%)	29368(49.37%)	24059 (50.87%)	29 (0.06%)	23238(49.13%)
	Whole Image	589825 (92.21%)	449 (0.07%)	49835 (7.79%)	367989 (89.99%)	205 (0.05%)	40927 (10.01%)
2048x2048	Two Pixels	13147 (52.21%)	250 (0.99%)	12033 (47.79%)	12809 (53.66%)	4 (0.02%)	11060 (46.34%)
	Four Pixels	24443 (55.64%)	309 (0.70%)	19484 (44.36%)	19830 (52.27%)	19 (0.05%)	18106 (47.73%)
	Six Pixels	24856 (59.46%)	324 (0.55%)	23763 (40.54%)	25923 (53.61%)	47 (0.10%)	22435 (46.39%)
	Whole Image	611579 (95.63%)	402 (0.06%)	27928 (4.37%)	381863 (93.35%)	206 (0.05%)	27206 (6.65%)

Table 159: Pixel confirmation when using texel coherence with nine texels for the side viewpoint of the flowers scene.

Shadow Map Lighting	Texel Shadowing	Shadow Map							
		1024x1024				2048x2048			
		Two Pixels	Four Pixels	Six Pixels	Whole Image	Two Pixels	Four Pixels	Six Pixels	Whole Image
Light	8 S-1 L	176	213	214	214	135	144	144	144
	8 S-1 L in RT Shadow	113	134	134	134	79	80	80	80
	7 S-2 L	580	874	970	976	551	634	634	634
	7 S-2 L in RT Shadow	399	565	604	610	305	326	326	326
	6 S-3 L	802	1234	1407	1458	833	1005	1009	1010
	6 S-3 L in RT Shadow	477	659	734	752	383	419	423	424
	5 S-4 L	1088	1783	2178	2324	966	1254	1278	1280
	5 S-4 L in RT Shadow	562	817	907	920	375	417	422	422
	4 S-5 L	2489	4302	5578	7847	2527	3960	4541	4752
	4 S-5 L in RT Light	1142	2353	3434	5558	1311	2604	3183	3349
	3 S-6 L	3020	5293	7075	10355	3089	5087	6032	6351
	3 S-6 L in RT Light	2180	4231	5947	9130	2320	4254	5193	5503
	2 S-7 L	2402	4450	6224	10314	2365	4023	5047	5482
	2 S-7 L in RT Light	1956	3890	5631	9673	2001	3625	4637	5068
1 S-8 L	2245	4030	5722	16347	1567	3377	5078	8275	
1 S-8 L in RT Light	1886	3575	5242	15817	1341	3093	4775	7960	
Shadow	8 S-1 L	696	1443	2328	9873	895	2075	3487	6594
	8 S-1 L in RT Shadow	617	1295	2127	9438	807	1943	3315	6339
	7 S-2 L	1749	3301	4665	8372	2272	4014	5238	6023
	7 S-2 L in RT Shadow	1517	2961	4248	7746	2092	3765	4944	5698
	6 S-3 L	2752	4942	6786	10926	2904	5050	6192	6773
	6 S-3 L in RT Shadow	1945	3844	5591	9592	2267	4330	5449	6012
	5 S-4 L	2266	3924	5055	7111	2634	4096	4588	4866
	5 S-4 L in RT Shadow	1022	2003	2873	4726	1409	2700	3180	3401
	4 S-5 L	1151	1872	2172	2386	1125	1437	1468	1476
	4 S-5 L in RT Light	495	656	691	712	384	413	419	420
	3 S-6 L	756	1049	1127	1143	747	896	922	934
	3 S-6 L in RT Light	342	429	447	447	257	279	286	286
	2 S-7 L	623	890	942	953	392	440	442	442
	2 S-7 L in RT Light	313	457	479	483	137	147	147	147
1 S-8 L	140	161	163	163	91	98	98	98	
1 S-8 L in RT Light	45	49	49	49	44	48	48	48	

Table 160: Pixel shadowing for pixels that don't achieve texel coherence with nine texels for the side viewpoint of the flowers scene.

Shadow Map Resolution	Contour Thickness	Corrected		Turned Bad		Maintained Correct		Maintained Incorrect	
		L→S	S→L	L→S	S→L	L→L	S→S	L→L	S→S
1024x1024	Two Pixels	61	3568	0	3681	19668	15585	4805	0
	Four Pixels	66	5120	0	6152	37338	25600	6538	0
	Six Pixels	69	5690	0	7971	52343	33636	7075	0
	Whole Image	71	6676	0	27853	632110	374387	7479	0
2048x2048	Two Pixels	95	2956	0	4207	21213	16706	3872	0
	Four Pixels	105	3403	0	6598	39505	27935	4317	0
	Six Pixels	108	3564	0	8417	54134	36377	4377	0
	Whole Image	108	3913	0	21651	634873	383505	4526	0

Table 161: Pixel correction between the single texel approach and the shadow mapping approach for the side viewpoint of the flowers scene.

Shadow Map Resolution	Number of Neighbours	Contour Thickness	Corrected		Turned Bad		Maintained Correct		Maintained Incorrect	
			L→S	S→L	L→S	S→L	L→L	S→S	L→L	S→S
1024x1024	3	Two Pixels	1850	3568	0	3271	19668	15995	3016	0
		Four Pixels	2557	5120	0	5397	37338	26355	4047	0
		Six Pixels	2724	5690	0	6875	52343	34732	4420	0
		Whole Image	2889	6676	0	16935	632110	385305	4661	0
	8	Two Pixels	1957	3568	0	3106	19668	16160	2909	0
		Four Pixels	2700	5120	0	5090	37338	26662	3904	0
		Six Pixels	2877	5690	0	6472	52343	35135	4267	0
		Whole Image	3048	6676	0	15420	632110	386820	4502	0
2048x2048	3	Two Pixels	1675	2956	0	3483	21213	17430	2292	0
		Four Pixels	1824	3403	0	5283	39505	29250	2598	0
		Six Pixels	1829	3564	0	6669	54134	38125	2656	0
		Whole Image	1881	3913	0	13594	634873	391562	2753	0
	8	Two Pixels	1897	2956	0	3021	21213	17892	2070	0
		Four Pixels	2083	3403	0	4587	39505	29946	2339	0
		Six Pixels	2093	3564	0	5788	54134	39006	2392	0
		Whole Image	2148	3913	0	11310	634873	393846	2486	0

Table 162: Pixel correction between the neighbour texels approach and the shadow mapping approach for the side viewpoint of the flowers scene.

Shadow Map Resolution	Number of Neighbours	Triangle Average	Two Pixels	Four Pixels	Six Pixels	Whole Image
1024x1024	3	Used	2.1668	2.0608	1.9861	0.7183
		Available	2.6905	2.5855	2.5031	1.5644
	8	Used	4.0729	3.8122	3.6333	1.8020
		Available	5.0200	4.7517	4.5350	2.3070
2048x2048	3	Used	2.0622	1.9137	1.8058	0.6521
		Available	2.5513	2.4328	2.3459	1.4350
	8	Used	3.7121	3.4157	3.2112	0.9178
		Available	4.5758	4.2683	4.0352	1.9982

Table 163: Average of triangle intersections when using the neighbour texels approach for the side viewpoint of the flowers scene.

Shadow Map Resolution	Adjacency Level	Contour Thickness	Corrected		Turned Bad		Maintained Correct		Maintained Incorrect	
			L→S	S→L	L→S	S→L	L→L	S→S	L→L	S→S
1024x1024	One Level	Two Pixels	100	3568	0	3019	19668	16247	4766	0
		Four Pixels	124	5120	0	4930	37338	26822	6480	0
		Six Pixels	129	5690	0	6244	52343	35363	7015	0
		Whole Image	131	6676	0	16521	632110	385719	7419	0
	Two Levels	Two Pixels	170	3568	0	2371	19668	16895	4696	0
		Four Pixels	209	5120	0	3761	37338	27991	6395	0
		Six Pixels	215	5690	0	4617	52343	36990	6929	0
		Whole Image	222	6676	0	12393	632110	389847	7328	0
2048x2048	One Level	Two Pixels	155	2956	0	2933	21213	17980	3812	0
		Four Pixels	184	3403	0	4332	39505	30201	4238	0
		Six Pixels	187	3564	0	5536	54134	39258	4298	0
		Whole Image	187	3913	0	12014	634873	393142	4447	0
	Two Levels	Two Pixels	238	2956	0	1530	21213	19383	3729	0
		Four Pixels	290	3403	0	2213	39505	32320	4132	0
		Six Pixels	296	3564	0	2852	54134	41942	4189	0
		Whole Image	296	3913	0	6172	634873	398984	4338	0

Table 164: Pixel correction between the adjacent geometry approach and the shadow mapping approach for the side viewpoint of the flowers scene.

Shadow Map Resolution	Adjacency Level	Triangle Average	Two Pixels	Four Pixels	Six Pixels	Whole Image
1024x1024	One Level	Used	2.7295	2.6990	2.6858	1.7635
		Available	3.8489	3.8588	3.8681	3.9550
	Two Levels	Used	8.5830	8.4226	8.3134	5.7143
		Available	12.1029	12.0421	11.9728	12.8153
2048x2048	One Level	Used	2.8069	2.7537	2.7375	1.7690
		Available	3.8693	3.8748	3.8850	3.9583
	Two Levels	Used	9.0359	8.7366	8.6129	5.7363
		Available	12.4558	12.2932	12.2235	12.8352

Table 165: Average of triangle intersections when using the adjacent geometry approach for the side viewpoint of the flowers scene.

Contour Thickness		Two Pixels		Four Pixels		Six Pixels		Whole Image		
Lighting		L→S	S→L	L→S	S→L	L→S	S→L	L→S	S→L	
Shadow Map Resolution	1024x1024	Corrected by Both	76	3568	82	5120	85	5690	87	6676
		Turned Bad by Both	0	2148	0	3355	0	4072	0	10147
		Corrected by Neighbour Texels Only	1881	0	2618	0	2792	0	2961	0
		Corrected by Adjacent Geometry Only	94	0	127	0	130	0	135	0
		Turned Bad by Neighbour Texels Only	0	958	0	1735	0	2400	0	5273
		Turned Bad by Adjacent Geometry Only	0	223	0	406	0	545	0	2246
	2048x2048	Corrected by Both	128	2956	146	3403	150	3564	150	3913
		Turned Bad by Both	0	1240	0	1753	0	2268	0	4596
		Corrected by Neighbour Texels Only	1769	0	1937	0	1943	0	1998	0
		Corrected by Adjacent Geometry Only	110	0	144	0	146	0	146	0
		Turned Bad by Neighbour Texels Only	0	1781	0	2834	0	3520	0	6714
		Turned Bad by Adjacent Geometry Only	0	290	0	460	0	584	0	1576

Table 166: Pixel correction by the neighbour texels (9 texels) and the adjacent geometry (2 levels) approaches separated by lighting change for the side viewpoint of the flowers scene.

Algorithm Step	Confirmations and Errors	1024x1024			2048x2048		
		Two Pixels	Four Pixels	Six Pixel	Two Pixels	Four Pixels	Six Pixel
Shadow Map	Total Contour Pixels	47368	80814	106784	49049	81863	106977
	Correct Light Pixels	19668 (80.17%)	37338 (84.97%)	52343 (87.99%)	21213 (84.25%)	39505 (89.93%)	54134 (92.35%)
	Correct Shadow Pixels	19266 (84.37%)	31752 (86.11%)	41607 (87.97%)	20913 (87.62%)	34533 (91.03%)	44794 (92.63%)
	Incorrect Light Pixels	4866 (19.83%)	6604 (15.03%)	7144 (12.01%)	3967 (15.75%)	4422 (10.07%)	4485 (7.65%)
	Incorrect Shadow Pixels	3568 (15.63%)	5120 (13.89%)	5690 (12.03%)	2956 (12.38%)	3403 (8.97%)	3564 (7.37%)
Texel Coherence	Confirmations in Light	13931 (56.78%)	25723 (58.54%)	36427 (61.24%)	14763 (58.63%)	29524 (67.21%)	43425 (74.08%)
	Confirmations in Shadow	13402 (58.69%)	20682 (56.09%)	26880 (56.83%)	13648 (57.18%)	23479 (61.89%)	32922 (68.08%)
	Wrong Confirmations in Light	642 (2.62%)	773 (1.76%)	825 (1.39%)	389 (1.54%)	500 (1.14%)	543 (0.93%)
	Wrong Confirmations in Shadow	39 (0.17%)	81 (0.22%)	144 (0.30%)	17 (0.07%)	125 (0.33%)	234 (0.48%)
Neighbouring Texels	Corrections in Light	1936 (7.89%)	2677 (6.09%)	2853 (4.80%)	1852 (7.36%)	2020 (4.60%)	2027 (3.46%)
	Confirmations in Shadow	16610 (72.74%)	27430 (74.39%)	36408 (76.98%)	18349 (76.87%)	31241 (82.35%)	41442 (85.70%)
Adjacent Geometry	Confirmations in Shadow	17445 (76.40%)	28958 (78.54%)	38406 (81.20%)	19888 (83.32%)	33348 (87.91%)	43646 (90.26%)
Final Lighting	Wrong Confirmations in Light	2959 (12.06%)	3959 (9.01%)	4325 (7.27%)	2163 (8.59%)	2457 (5.59%)	2515 (4.29%)
	Wrong Confirmations in Shadow	1899 (8.32%)	2956 (8.02%)	3489 (7.38%)	1059 (4.44%)	1435 (3.78%)	1616 (3.34%)

Table 167: Algorithm results of the side viewpoint of the flowers scene.

Below are the results of the “against” viewpoint of the “flowers” scene.



Figure 209: Result of the ray-tracing approach for the against viewpoint of the flowers scene.

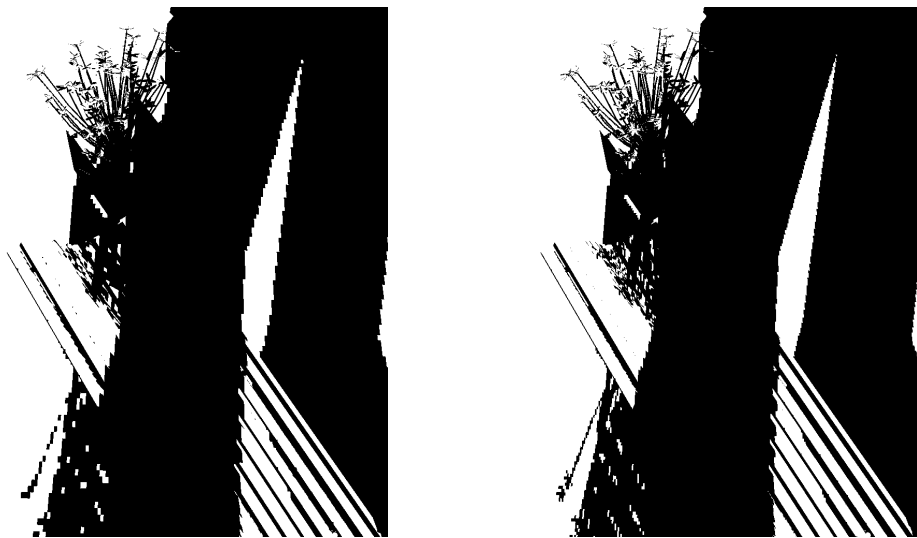


Figure 210: Result of the shadow mapping approach for the against viewpoint of the flowers scene.

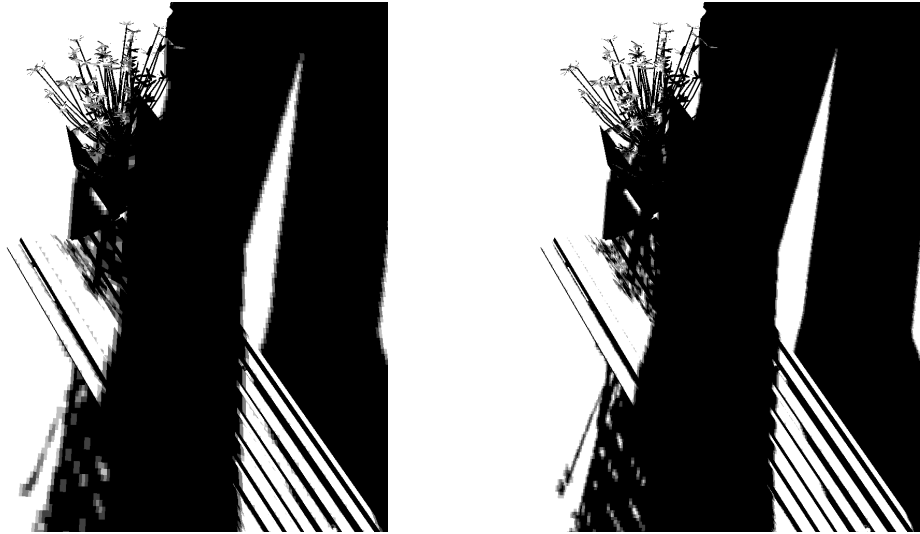


Figure 211: Result of texel coherence with four texels for the against viewpoint of the flowers scene.

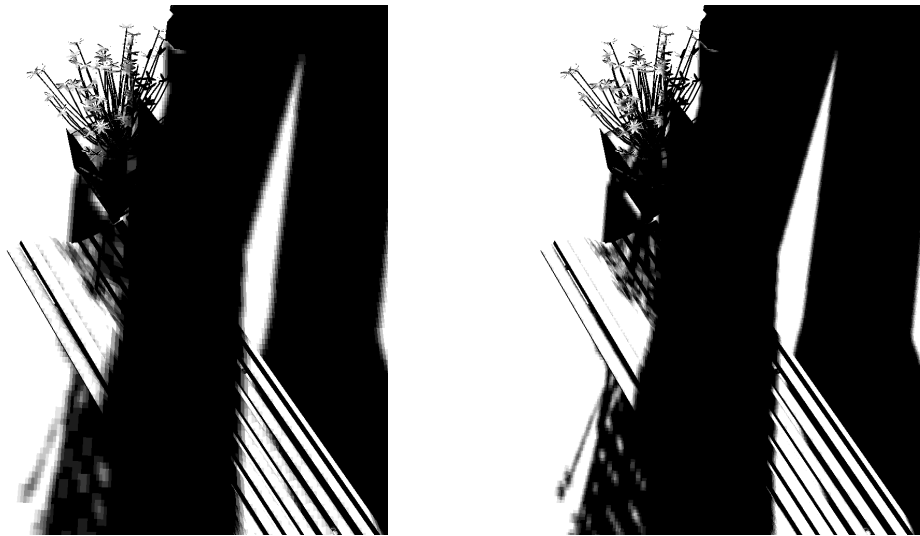


Figure 212: Result of texel coherence with nine texels for the against viewpoint of the flowers scene.

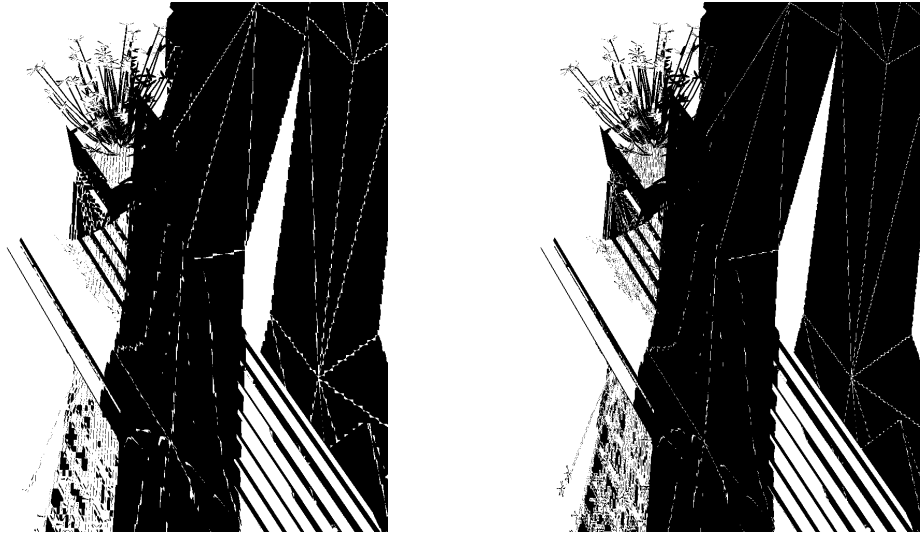


Figure 213: Result of the single texel approach for the against viewpoint of the flowers scene.



Figure 214: Result of the neighbour texels approach using four neighbours for the against viewpoint of the flowers scene.

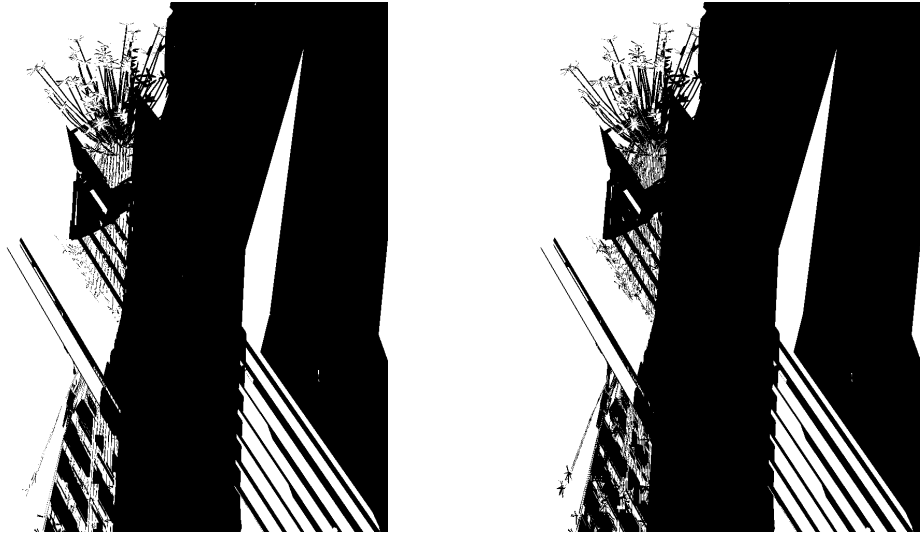


Figure 215: Result of the neighbour texels approach using nine neighbours for the against viewpoint of the flowers scene.

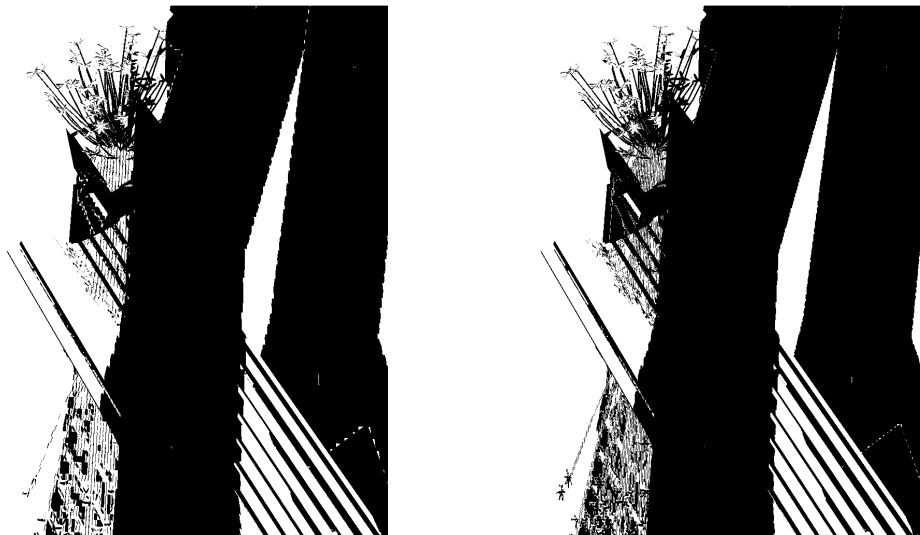


Figure 216: Result of the adjacent geometry approach with one level of adjacency for the against viewpoint of the flowers scene.

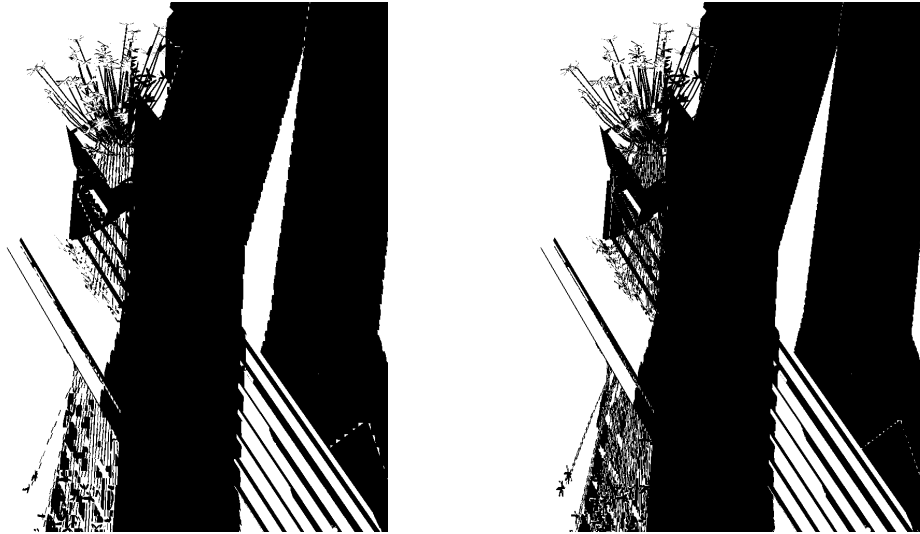


Figure 217: Result of the adjacent geometry approach with two levels of adjacency for the against viewpoint of the flowers scene.



Figure 218: Result of the algorithm with a six pixel thick contour and a 2048x2048 resolution shadow map for the against viewpoint of the flowers scene.

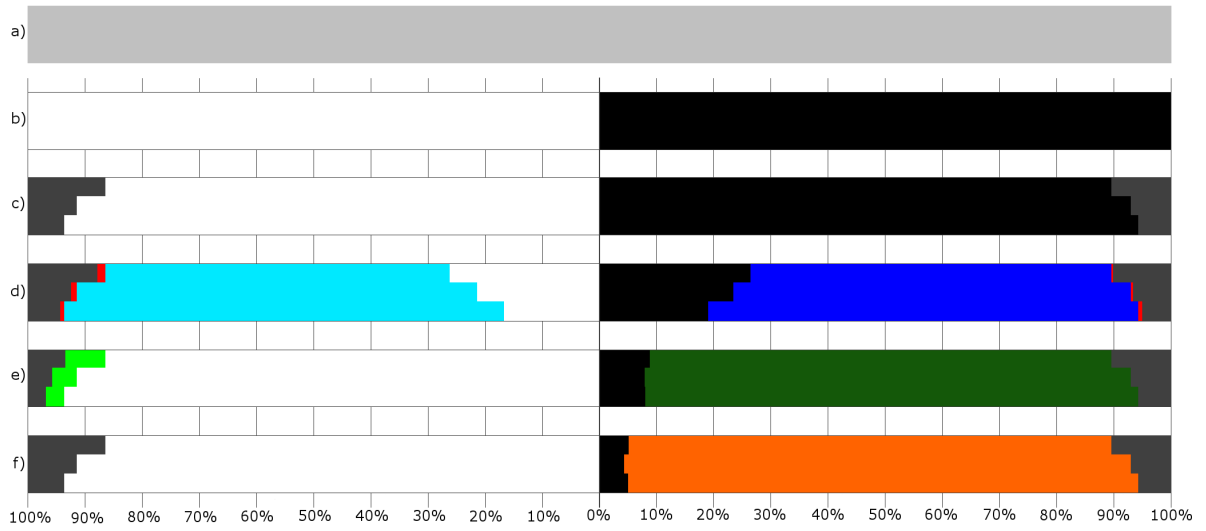
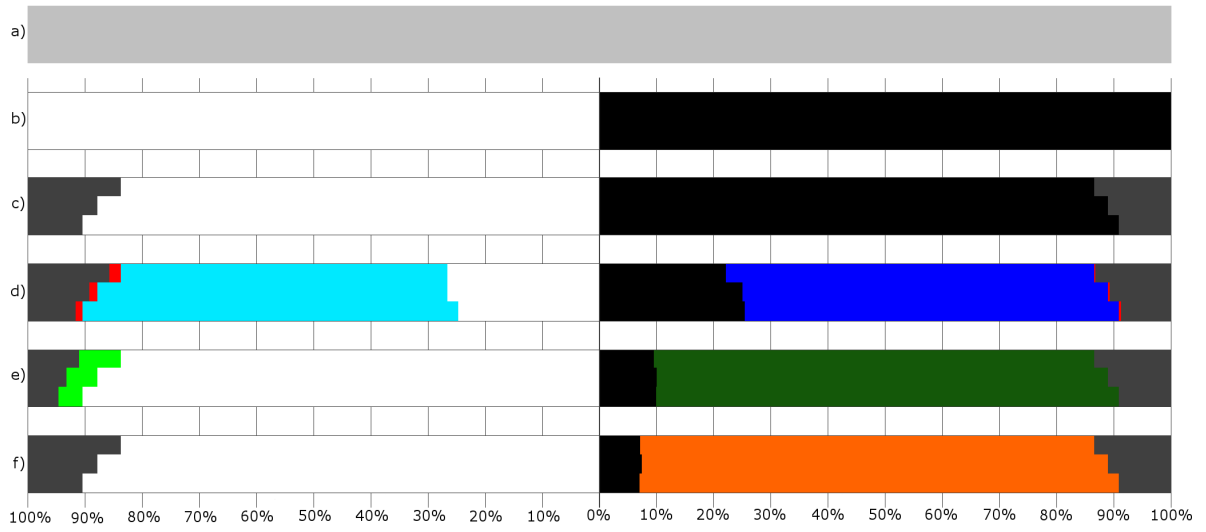


Figure 219: Corrected/confirmed/hinted contour pixels by each method for the against viewpoint of the flowers scene using a 1024x1024 (top) and a 2048x2048 (bottom) resolution shadow map.

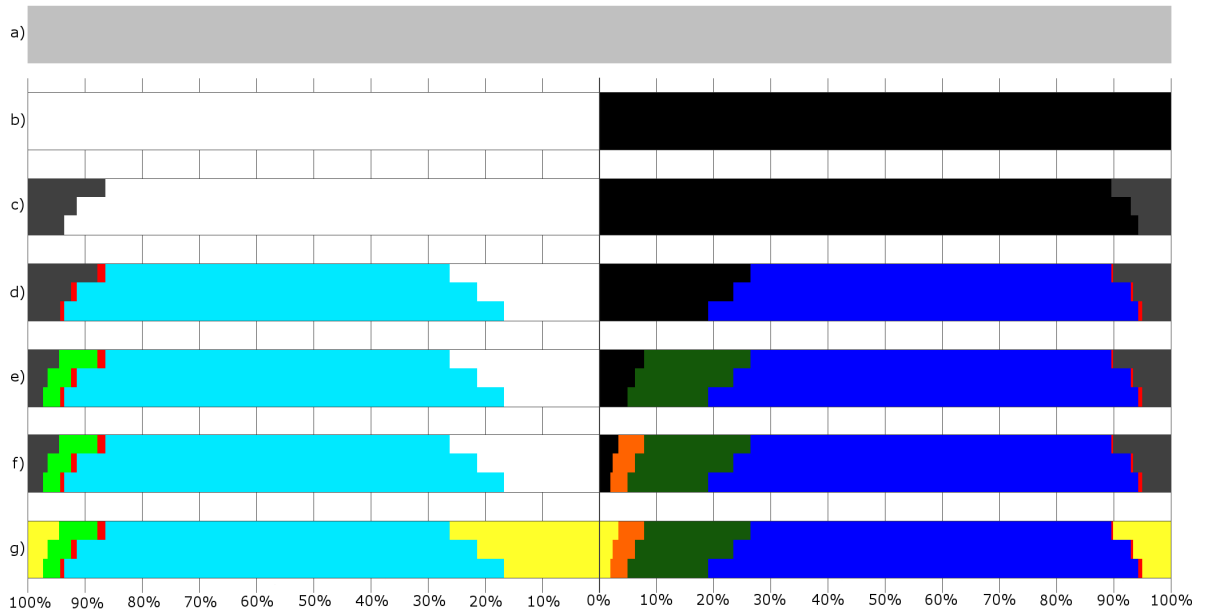
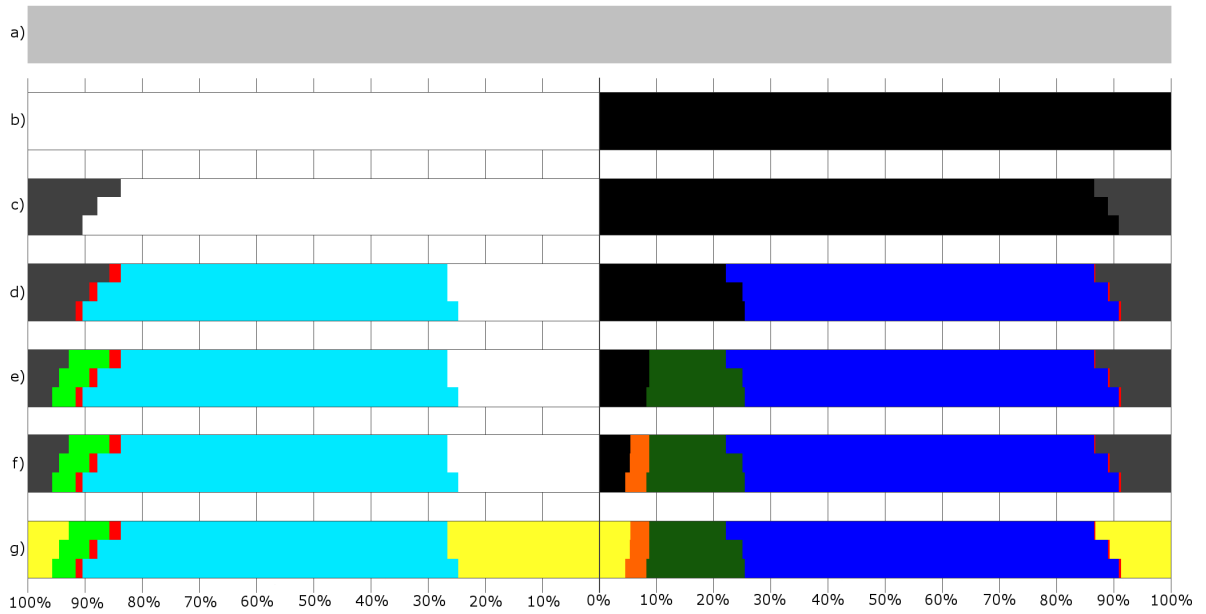


Figure 220: Corrected/confirmed/hinted contour pixels by the chaining of methods for the against viewpoint of the flowers scene using a 1024x1024 (top) and a 2048x2048 (bottom) resolution shadow map.

Shadow Map Resolution	Approach	Contour Thickness			
		Two Pixels	Four Pixels	Six Pixels	Whole Image
1024x1024	Pixels in Contour	48869	85292	114428	1048576
	Shadow Map	7239 (14.81%)	9885 (11.59%)	10649 (9.31%)	12037 (1.15%)
	Single Texel	6915 (14.15%)	10756 (12.61%)	13139 (11.48%)	48387 (4.61%)
	Neighbour Texels (4 Neighbours)	4905 (10.04%)	7778 (9.12%)	9575 (8.37%)	26983 (2.57%)
	Neighbour Texels (9 Neighbours)	4545 (9.30%)	7165 (8.40%)	8755 (7.65%)	22720 (2.17%)
	Adjacent Geometry (One Level)	6153 (12.59%)	9384 (11.00%)	11095 (9.70%)	32269 (3.08%)
	Adjacent Geometry (Two Level)	5514 (11.28%)	8143 (9.55%)	9315 (8.14%)	25575 (2.44%)
2048x2048	Pixels in Contour	51578	88386	117375	1048576
	Shadow Map	6154 (11.93%)	6869 (7.77%)	7091 (6.04%)	7398 (0.71%)
	Single Texel	7006 (13.58%)	9685 (10.96%)	12180 (10.38%)	35979 (3.43%)
	Neighbour Texels (4 Neighbours)	4727 (9.16%)	6511 (7.37%)	8109 (6.91%)	19187 (1.83%)
	Neighbour Texels (9 Neighbours)	3996 (7.75%)	5419 (6.13%)	6602 (5.62%)	14209 (1.36%)
	Adjacent Geometry (One Level)	5776 (11.20%)	7335 (8.30%)	9128 (7.78%)	22385 (2.13%)
	Adjacent Geometry(Two Level)	4581 (8.88%)	5461 (6.18%)	6502 (5.54%)	14343 (1.37%)

Table 168: Difference between the approaches that use ray-tracing and the actual ray-tracer for the against viewpoint of the flowers scene.

Shadow Map Resolution	Contour Thickness		
	Two Pixels	Four Pixels	Six Pixels
1024x1024	7239 of 12037 (60.14%)	9885 of 12037 (82.12%)	10649 of 12037 (88.47%)
2048x2048	6154 of 7398 (83.18%)	6869 of 7398 (92.85%)	7091 of 7398 (95.85%)

Table 169: Wrongly defined pixels in the shadow mapping result which are inside the contour in the against viewpoint of the flowers scene.

Shadow Map Resolution	Contour Thickness	Pixel Shading	
		Light	Shadow
1024x1024	Two Pixels	3951 of 24424	3288 of 24445
	Four Pixels	5267 of 43488	4618 of 41804
	Six Pixels	5617 of 59048	5032 of 55380
	Whole Image	5995 of 520136	6042 of 528440
2048x2048	Two Pixels	3469 of 25696	2685 of 25882
	Four Pixels	3785 of 44613	3084 of 43773
	Six Pixels	3826 of 59717	3265 of 57658
	Whole Image	3880 of 520545	3518 of 528031

Table 170: Pixels that the shadow map defines wrongly in the against viewpoint of the flowers scene, separated in pixels defined in light and in shadow, compared to the total amount of pixels lighted in the same way.

Shadow Map Resolution	Contour Thickness	Texel Coherence					
		Light			Shadow		
		Confirmed	Incorrectly Confirmed	Undecided	Confirmed	Incorrectly Confirmed	Undecided
1024x1024	Two Pixels	14408 (58.99%)	463 (1.90%)	10016 (41.01%)	15777 (64.54%)	47 (0.19%)	8668 (35.46%)
	Four Pixels	27199 (62.54%)	581 (1.34%)	16289 (37.46%)	26788 (64.08%)	106 (0.25%)	15016 (35.92%)
	Six Pixels	39441 (66.79%)	652 (1.10%)	19607 (33.21%)	36411 (65.75%)	163 (0.29%)	18969 (34.25%)
	Whole Image	498299 (95.80%)	759 (0.15%)	21837 (4.20%)	506648 (95.88%)	898 (0.17%)	21792 (4.12%)
2048x2048	Two Pixels	15783 (61.42%)	322 (1.25%)	9913 (38.58%)	16397 (63.35%)	53 (0.20%)	9485 (36.65%)
	Four Pixels	31631 (70.90%)	397 (0.89%)	12982 (29.10%)	30556 (69.81%)	156 (0.36%)	13217 (30.19%)
	Six Pixels	46289 (77.51%)	412 (0.69%)	13428 (22.49%)	43684 (75.76%)	294 (0.51%)	13974 (24.24%)
	Whole Image	506838 (97.37%)	426 (0.08%)	13707 (2.63%)	513766 (97.30%)	505 (0.10%)	14265 (2.70%)

Table 171: Pixel confirmation when using texel coherence with four texels for the against viewpoint of the flowers scene.

Shadow Map Resolution	Contour Thickness	Texel Shadowing							
		Light				Shadow			
		3 shadow/1 light	3 shadow/1 light in ray-tracer shadow	1 shadow/3 light	1 shadow/3 light in ray-tracer light	3 shadow/1 light	3 shadow/1 light in ray-tracer shadow	1 shadow/3 light	1 shadow/3 light in ray-tracer light
1024x1024	Two Pixels	2107	1387	3901	3243	2962	2401	2011	1347
	Four Pixels	3105	1894	6592	5655	5820	4944	2790	1763
	Six Pixels	3450	1975	8407	7352	8078	7055	3028	1845
	Whole Image	3503	2015	10191	8990	10330	9141	3056	1871
2048x2048	Two Pixels	1929	1255	3493	2991	3448	3062	1720	1111
	Four Pixels	2169	1334	5152	4562	5692	5200	1931	1195
	Six Pixels	2170	1334	5517	4914	6355	5832	1933	1196
	Whole Image	2210	1361	5702	5094	6526	5988	1964	1216

Table 172: Pixel shadowing for pixels that don't achieve texel coherence with four texels for the against viewpoint of the flowers scene.

Shadow Map Resolution	Contour Thickness	Texel Coherence					
		Light			Shadow		
		Confirmed	Incorrectly Confirmed	Undecided	Confirmed	Incorrectly Confirmed	Undecided
1024x1024	Two Pixels	11566 (47.36%)	264 (1.08%)	12858 (52.64%)	15275 (62.49%)	5 (0.02%)	9170(37.51%)
	Four Pixels	21589 (49.64%)	307 (0.71%)	21899 (50.36%)	25650 (61.36%)	13 (0.02%)	16154 (38.64%)
	Six Pixels	30745 (52.07%)	313 (0.53%)	28303 (47.93%)	33314 (60.16%)	28 (0.05%)	22066 (39.84%)
	Whole Image	477354 (91.77%)	327 (0.06%)	42782(8.23%)	488483 (92.44%)	404 (0.08%)	39957(7.56%)
2048x2048	Two Pixels	13556 (52.76%)	174 (0.68%)	12140 (47.24%)	15632 (60.40%)	14 (0.05%)	10250 (39.60%)
	Four Pixels	25933 (58.13%)	198 (0.44%)	18680 (41.87%)	26378 (60.26%)	32 (0.07%)	17395 (39.74%)
	Six Pixels	37926 (63.51%)	200 (0.33%)	21791 (36.49%)	35633 (61.80%)	53 (0.09%)	22025 (38.20%)
	Whole Image	496717 (95.42%)	203 (0.04%)	23828 (4.58%)	502859 (95.23%)	201 (0.04%)	25172 (4.77%)

Table 173: Pixel confirmation when using texel coherence with nine texels for the against viewpoint of the flowers scene.

Shadow Map Lighting	Texel Shadowing	Shadow Map							
		1024x1024				2048x2048			
		Two Pixels	Four Pixels	Six Pixels	Whole Image	Two Pixels	Four Pixels	Six Pixels	Whole Image
Light	8 S-1 L	304	501	576	576	121	135	135	141
	8 S-1 L in RT Shadow	153	218	226	226	75	81	81	87
	7 S-2 L	530	803	942	975	654	800	802	820
	7 S-2 L in RT Shadow	327	459	495	512	312	332	332	344
	6 S-3 L	673	1046	1207	1271	825	1069	1093	1103
	6 S-3 L in RT Shadow	314	427	463	505	357	392	402	403
	5 S-4 L	643	1048	1305	1434	756	1003	1048	1057
	5 S-4 L in RT Shadow	360	520	575	627	338	382	386	389
	4 S-5 L	2253	3607	4453	5485	2307	3461	3793	3865
	4 S-5 L in RT Light	1107	2017	2796	3753	1258	2343	2670	2726
	3 S-6 L	2840	4819	6243	8588	3182	4881	5625	5795
	3 S-6 L in RT Light	2113	3905	5270	7592	2460	4102	4837	5003
	2 S-7 L	2276	3940	5104	7613	2065	3317	3927	4186
	2 S-7 L in RT Light	1898	3452	4565	6979	1795	3014	3620	3875
1 S-8 L	3339	6135	8473	16840	2230	4014	5368	6861	
1 S-8 L in RT Light	3057	5791	8097	16404	2058	3814	5161	6649	
Shadow	8 S-1 L	987	2387	4033	14179	1035	2705	4693	7111
	8 S-1 L in RT Shadow	778	2013	3575	13375	945	2552	4487	6847
	7 S-2 L	1565	3024	4385	7702	2089	3934	5048	5453
	7 S-2 L in RT Shadow	1398	2765	4067	7273	1875	3645	4710	5103
	6 S-3 L	2168	3915	5467	8499	2898	4922	6046	6251
	6 S-3 L in RT Shadow	1550	3096	4596	7589	2294	4259	5347	5544
	5 S-4 L	2170	3566	4509	5651	2261	3339	3673	3774
	5 S-4 L in RT Shadow	1058	1958	2799	3871	1282	2273	2596	2680
	4 S-5 L	826	1185	1360	1498	885	1190	1253	1267
	4 S-5 L in RT Light	398	517	551	573	312	353	363	370
	3 S-6 L	685	1024	1158	1206	621	725	726	727
	3 S-6 L in RT Light	321	430	464	476	242	261	261	261
	2 S-7 L	548	767	852	918	375	450	456	457
	2 S-7 L in RT Light	332	442	472	505	187	207	208	209
1 S-8 L	221	286	302	304	86	130	130	132	
1 S-8 L in RT Light	126	156	160	161	43	60	60	62	

Table 174: Pixel shadowing for pixels that don't achieve texel coherence with nine texels for the against viewpoint of the flowers scene.

Shadow Map Resolution	Contour Thickness	Corrected		Turned Bad		Maintained Correct		Maintained Incorrect	
		L→S	S→L	L→S	S→L	L→L	S→S	L→L	S→S
1024x1024	Two Pixels	53	3288	0	3017	20473	18140	3898	0
	Four Pixels	58	4618	0	5547	38221	31639	5209	0
	Six Pixels	59	5032	0	7581	53431	42767	5558	0
	Whole Image	59	6042	0	42451	514141	479947	5936	0
2048x2048	Two Pixels	84	2685	0	3621	22227	19576	3385	0
	Four Pixels	86	3084	0	5986	40828	34703	3699	0
	Six Pixels	86	3265	0	8440	55891	45953	3740	0
	Whole Image	86	3518	0	32185	516665	492328	3794	0

Table 175: Pixel correction between the single texel approach and the shadow mapping approach for the against viewpoint of the flowers scene.

Shadow Map Resolution	Contour Thickness	Corrected		Turned Bad		Maintained Correct		Maintained Incorrect	
		L→S	S→L	L→S	S→L	L→L	S→S	L→L	S→S
1024x1024	Two Pixels	1616	3288	0	2570	20473	18587	2335	0
	Four Pixels	2122	4618	0	4633	38221	32553	3145	0
	Six Pixels	2195	5032	0	6153	53431	44195	3422	0
	Whole Image	2278	6042	0	23266	514141	499132	3717	0
2048x2048	Two Pixels	1526	2685	0	2784	22227	20413	1943	0
	Four Pixels	1607	3084	0	4333	40828	36356	2178	0
	Six Pixels	1613	3265	0	5896	55891	48497	2213	0
	Whole Image	1634	3518	0	16941	516665	507572	2246	0

Table 176: Pixel correction between the neighbour texels approach using four neighbours and the shadow mapping approach for the against viewpoint of the flowers scene.

Shadow Map Resolution	Contour Thickness	Corrected		Turned Bad		Maintained Correct		Maintained Incorrect	
		L→S	S→L	L→S	S→L	L→L	S→S	L→L	S→S
1024x1024	Two Pixels	1757	3288	0	2351	20473	18806	2194	0
	Four Pixels	2328	4618	0	4226	38221	32960	2939	0
	Six Pixels	2421	5032	0	5559	53431	44789	3196	0
	Whole Image	2520	6042	0	19245	514141	503153	3475	0
2048x2048	Two Pixels	1769	2685	0	2296	22227	20901	1700	0
	Four Pixels	1883	3084	0	3517	40828	37172	1902	0
	Six Pixels	1894	3265	0	4670	55891	49723	1932	0
	Whole Image	1918	3518	0	12247	516665	512266	1962	0

Table 177: Pixel correction between the neighbour texels approach using nine neighbours and the shadow mapping approach for the against viewpoint of the flowers scene.

Shadow Map Resolution	Number of Neighbours	Triangle Average	Two Pixels	Four Pixels	Six Pixels	Whole Image
1024x1024	3	Used	2.1533	2.1021	2.0545	0.9310
		Available	2.5577	2.4988	2.4580	1.6046
	8	Used	3.9267	3.8082	3.7200	1.4111
		Available	4.6192	4.4847	4.3664	2.3970
2048x2048	3	Used	2.0065	1.9038	1.8255	0.8386
		Available	2.3639	2.3097	2.2575	1.4568
	8	Used	3.5757	3.3819	3.2368	1.1931
		Available	4.1947	3.9851	3.8410	2.0553

Table 178: Average of triangle intersections when using the neighbour texels approach for the against viewpoint of the flowers scene.

Shadow Map Resolution	Contour Thickness	Corrected		Turned Bad		Maintained Correct		Maintained Incorrect	
		L→S	S→L	L→S	S→L	L→L	S→S	L→L	S→S
1024x1024	Two Pixels	108	3288	0	2310	20473	18847	3843	0
	Four Pixels	130	4618	0	4247	38221	32939	5137	0
	Six Pixels	135	5032	0	5613	53431	44735	5482	0
	Whole Image	135	6042	0	26409	514141	495989	5860	0
2048x2048	Two Pixels	170	2685	0	2477	22227	20720	3299	0
	Four Pixels	181	3084	0	3731	40828	36958	3604	0
	Six Pixels	181	3265	0	5483	55891	48910	3645	0
	Whole Image	181	3518	0	18686	516665	505827	3699	0

Table 179: Pixel correction between the adjacent geometry approach with one level of adjacency and the shadow mapping approach for the against viewpoint of the flowers scene.

Shadow Map Resolution	Contour Thickness	Corrected		Turned Bad		Maintained Correct		Maintained Incorrect	
		L→S	S→L	L→S	S→L	L→L	S→S	L→L	S→S
1024x1024	Two Pixels	198	3288	0	1761	20473	19396	3753	0
	Four Pixels	247	4618	0	3123	38221	34063	5020	0
	Six Pixels	256	5032	0	3954	53431	46394	5361	0
	Whole Image	256	6042	0	19836	514141	502562	5739	0
2048x2048	Two Pixels	240	2685	0	1352	22227	21845	3229	0
	Four Pixels	266	3084	0	1942	40828	38747	3519	0
	Six Pixels	266	3265	0	2942	55891	51451	3560	0
	Whole Image	266	3518	0	10729	516665	513784	3614	0

Table 180: Pixel correction between the adjacent geometry approach with two level of adjacency and the shadow mapping approach for the against viewpoint of the flowers scene.

Shadow Map Resolution	Adjacency Level	Triangle Average	Two Pixels	Four Pixels	Six Pixels	Whole Image
1024x1024	One Level	Used	2.8186	2.8161	2.8204	2.2372
		Available	3.8822	3.8900	3.8944	3.9568
	Two Levels	Used	8.7063	8.5779	8.5006	7.5952
		Available	11.9917	11.8492	11.7373	13.4333
2048x2048	One Level	Used	2.8608	2.8438	2.8525	2.2440
		Available	3.9049	3.9011	3.9022	3.9619
	Two Levels	Used	9.0159	8.7586	8.6815	7.6312
		Available	12.3064	12.0149	11.8764	13.4734

Table 181: Average of triangle intersections when using the adjacent geometry approach for the against viewpoint of the flowers scene.

Contour Thickness		Two Pixels		Four Pixels		Six Pixels		Whole Image		
Lighting		L→S	S→L	L→S	S→L	L→S	S→L	L→S	S→L	
Shadow Map Resolution	1024x1024	Corrected by Both	69	3288	77	4618	78	5032	78	6042
		Turned Bad by Both	0	1468	0	2562	0	3146	0	12504
		Corrected by Neighbour Texels Only	1688	0	2251	0	2343	0	2442	0
		Corrected by Adjacent Geometry Only	129	0	170	0	178	0	178	0
		Turned Bad by Neighbour Texels Only	0	883	0	1664	0	2413	0	6471
		Turned Bad by Adjacent Geometry Only	0	293	0	561	0	808	0	7332
	2048x2048	Corrected by Both	140	2685	147	3084	147	3265	147	3518
		Turned Bad by Both	0	957	0	1318	0	1902	0	5435
		Corrected by Neighbour Texels Only	1629	0	1736	0	1747	0	1771	0
		Corrected by Adjacent Geometry Only	100	0	119	0	119	0	119	0
		Turned Bad by Neighbour Texels Only	0	1339	0	2199	0	2768	0	6812
		Turned Bad by Adjacent Geometry Only	0	395	0	624	0	1040	0	5294

Table 182: Pixel correction by the neighbour texels (9 texels) and the adjacent geometry (2 levels) approaches separated by lighting change for the against viewpoint of the flowers scene.

Algorithm Step	Confirmations and Errors	1024x1024			2048x2048		
		Two Pixels	Four Pixels	Six Pixel	Two Pixels	Four Pixels	Six Pixel
Shadow Map	Total Contour Pixels	48869	85292	114428	51578	88386	117375
	Correct Light Pixels	20473 (83.82%)	38221 (87.89%)	53431 (90.49%)	22227 (86.50%)	40828 (91.52%)	55891 (93.59%)
	Correct Shadow Pixels	21157 (86.55%)	37186 (88.95%)	50348 (90.91%)	23197 (89.63%)	40689 (92.95%)	54393 (94.34%)
	Incorrect Light Pixels	3951 (16.18%)	5267 (12.11%)	5617 (9.51%)	3469 (13.50%)	3785 (8.48%)	3826 (6.41%)
	Incorrect Shadow Pixels	3288 (13.45%)	4618 (11.05%)	5032 (9.09%)	2685 (10.37%)	3084 (7.05%)	3265 (5.66%)
Texel Coherence	Confirmations in Light	14408 (58.99%)	27199 (62.54%)	39441 (66.79%)	15783 (61.42%)	31631 (70.90%)	46289 (77.51%)
	Confirmations in Shadow	15777 (64.54%)	26788 (64.08%)	36411 (65.75%)	16397 (63.35%)	30556 (69.81%)	43684 (75.76%)
	Wrong Confirmations in Light	463 (1.90%)	581 (1.34%)	652 (1.10%)	322 (1.25%)	397 (0.89%)	412 (0.69%)
	Wrong Confirmations in Shadow	47 (0.19%)	106 (0.25%)	163 (0.29%)	53 (0.20%)	156 (0.36%)	294 (0.51%)
Neighbouring Texels	Corrections in Light	1740 (7.12%)	2310 (5.31%)	2399 (4.06%)	1721 (6.70%)	1820 (4.08%)	1828 (3.06%)
	Confirmations in Shadow	19055 (77.95%)	33596 (80.37%)	45916 (82.91%)	21200 (81.91%)	38101 (87.04%)	51791 (89.82%)
Adjacent Geometry	Confirmations in Shadow	19865 (81.26%)	35082 (83.92%)	47966 (86.61%)	22382 (86.48%)	39781 (90.88%)	53562 (92.90%)
Final Lighting	Wrong Confirmations in Light	2226 (9.11%)	2976 (6.84%)	3238 (5.48%)	1790 (6.97%)	2009 (4.50%)	2042 (3.42%)
	Wrong Confirmations in Shadow	1386 (5.67%)	2316 (5.54%)	2708 (4.89%)	921 (3.56%)	1220 (2.79%)	1419 (2.46%)

Table 183: Algorithm results of the against viewpoint of the flowers scene.

Finally, the results of the “with” viewpoint of the “flowers” scene are presented below.



Figure 221: Result of the ray-tracing approach for the with viewpoint of the flowers scene.

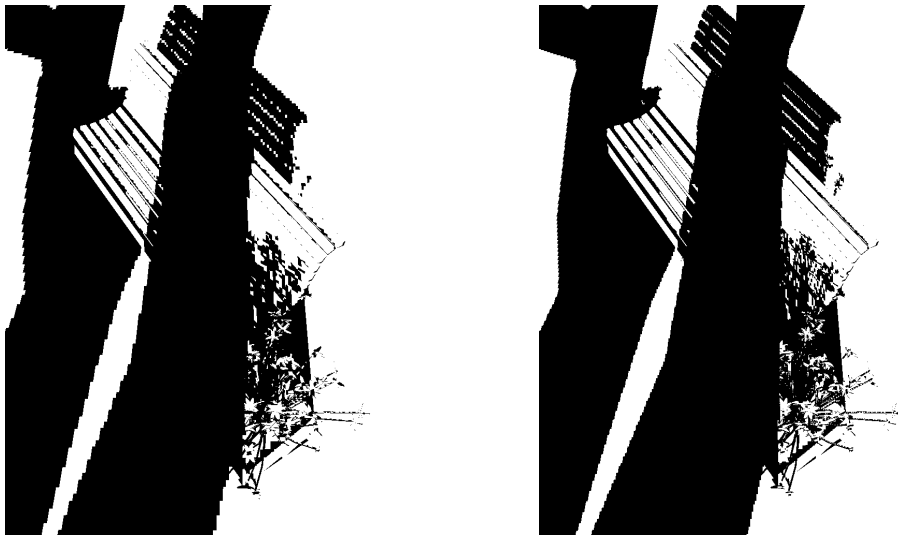


Figure 222: Result of the shadow mapping approach for the with viewpoint of the flowers scene.

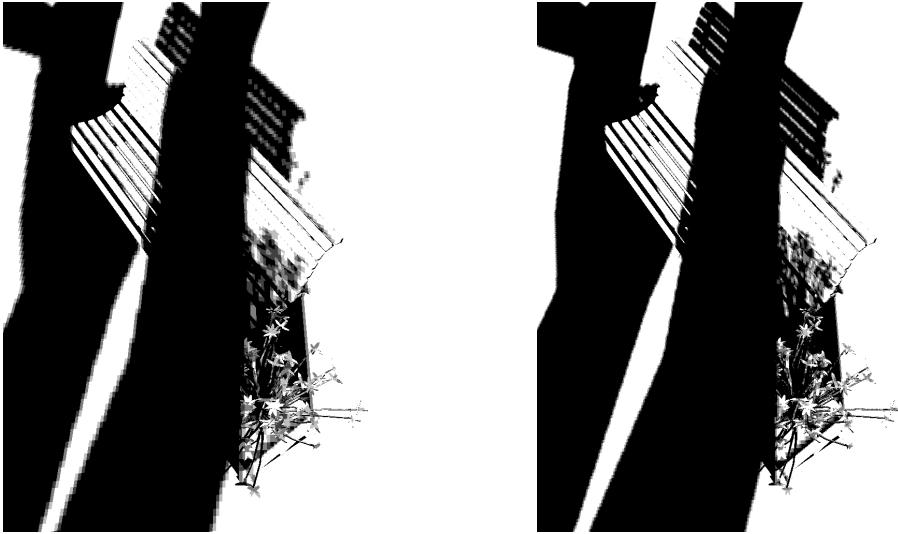


Figure 223: Result of texel coherence with four texels for the with viewpoint of the flowers scene.

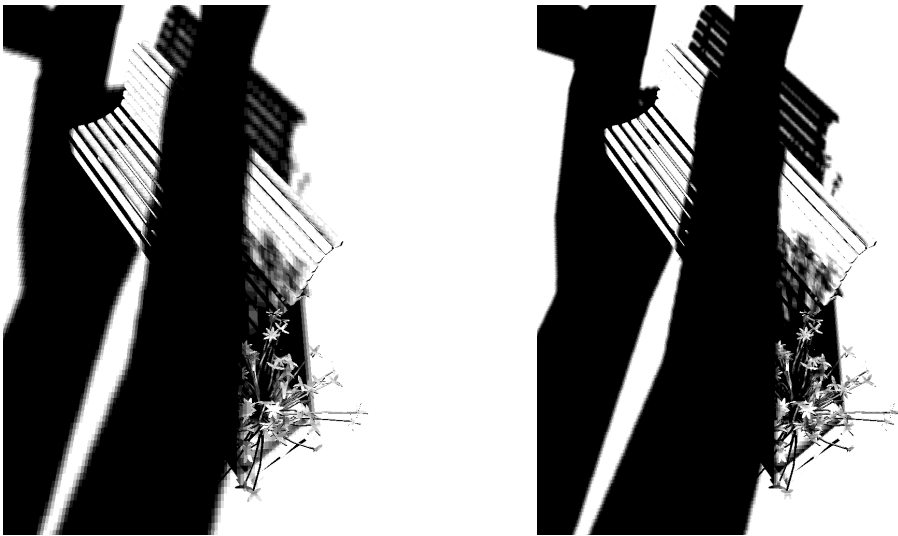


Figure 224: Result of texel coherence with nine texels for the with viewpoint of the flowers scene.

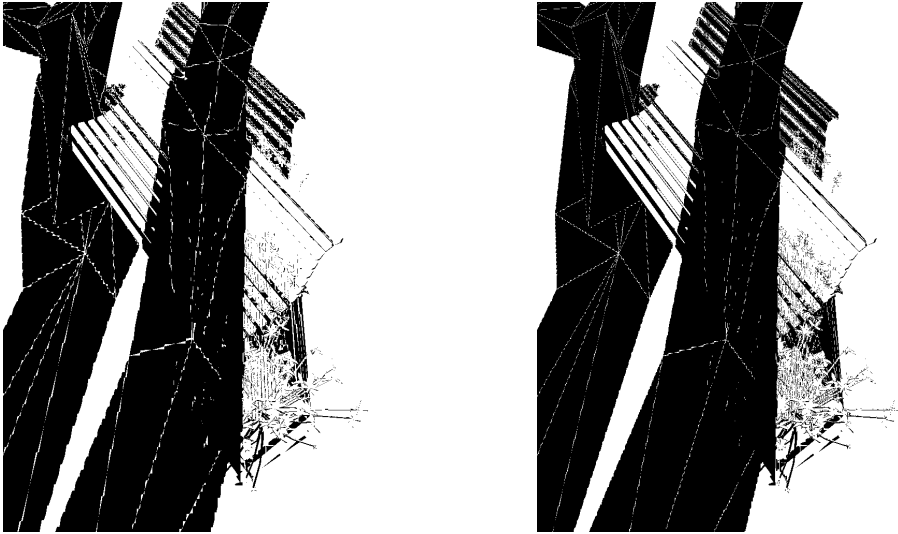


Figure 225: Result of the single texel approach for the with viewpoint of the flowers scene.

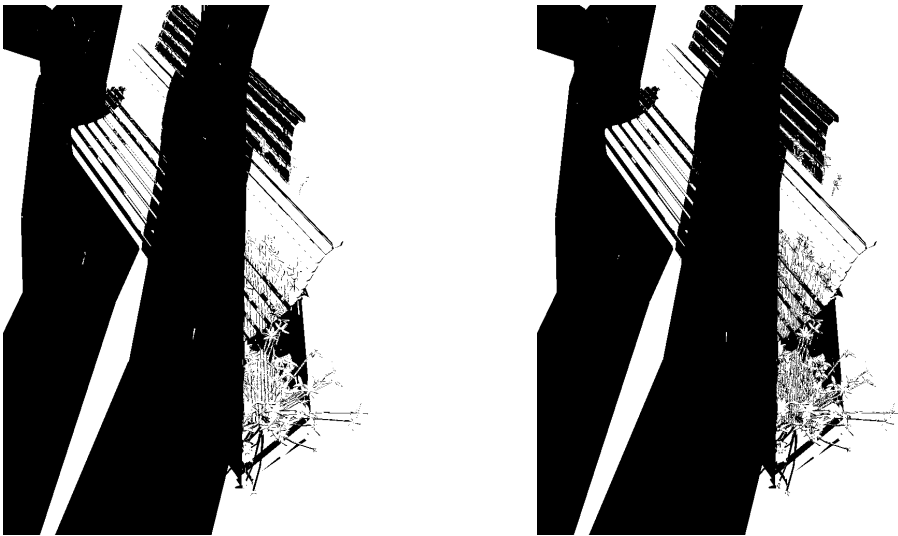


Figure 226: Result of the neighbour texels approach using four neighbours for the with viewpoint of the flowers scene.

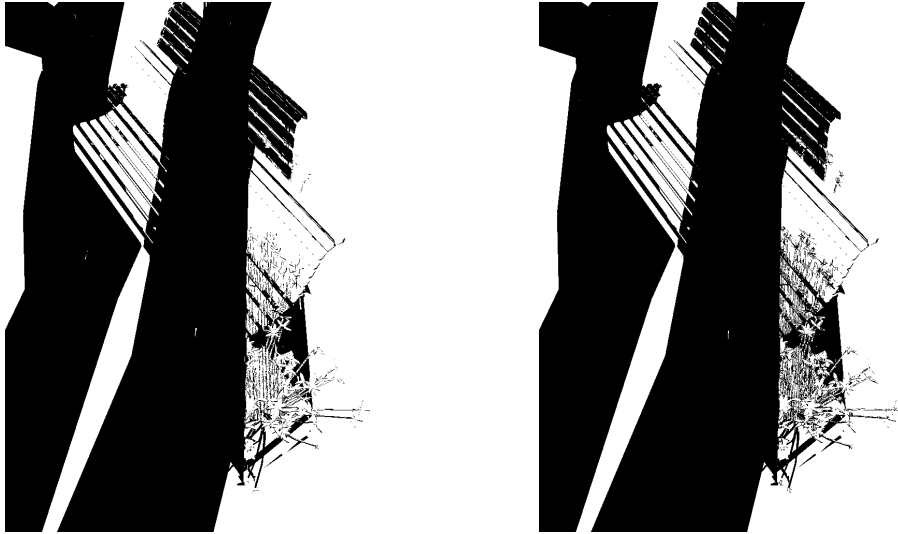


Figure 227: Result of the neighbour texels approach using nine neighbours for the with viewpoint of the flowers scene.



Figure 228: Result of the adjacent geometry approach with one level of adjacency for the with viewpoint of the flowers scene.

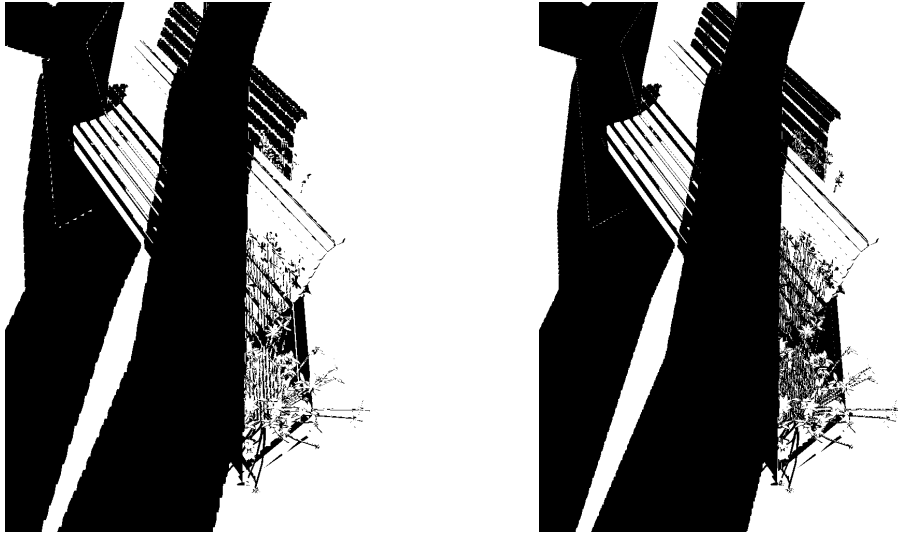


Figure 229: Result of the adjacent geometry approach with two levels of adjacency for the with viewpoint of the flowers scene.



Figure 230: Result of the algorithm with a six pixel thick contour and a 2048x2048 resolution shadow map for the with viewpoint of the flowers scene.

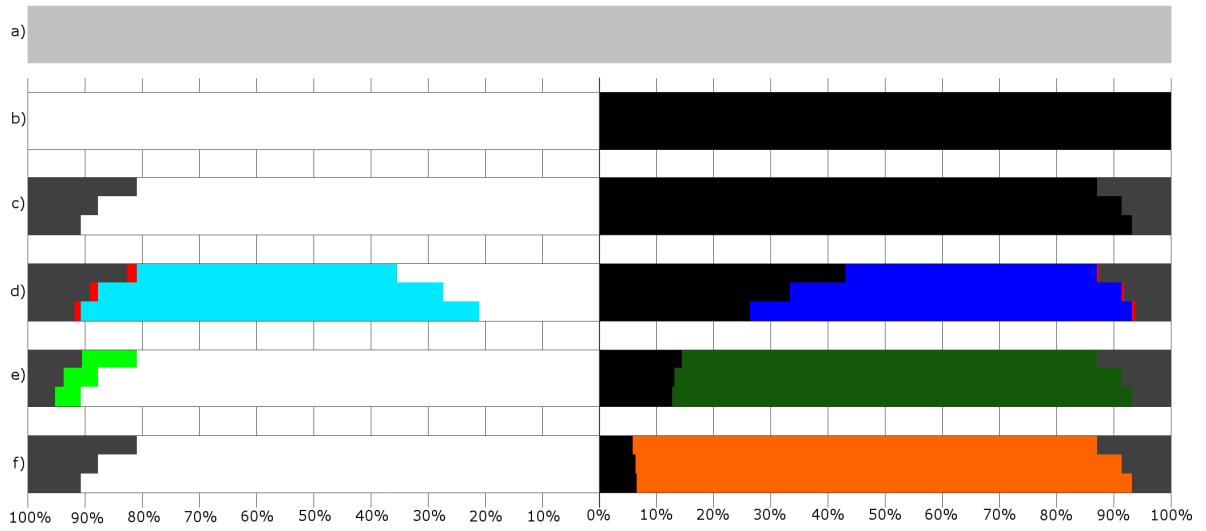
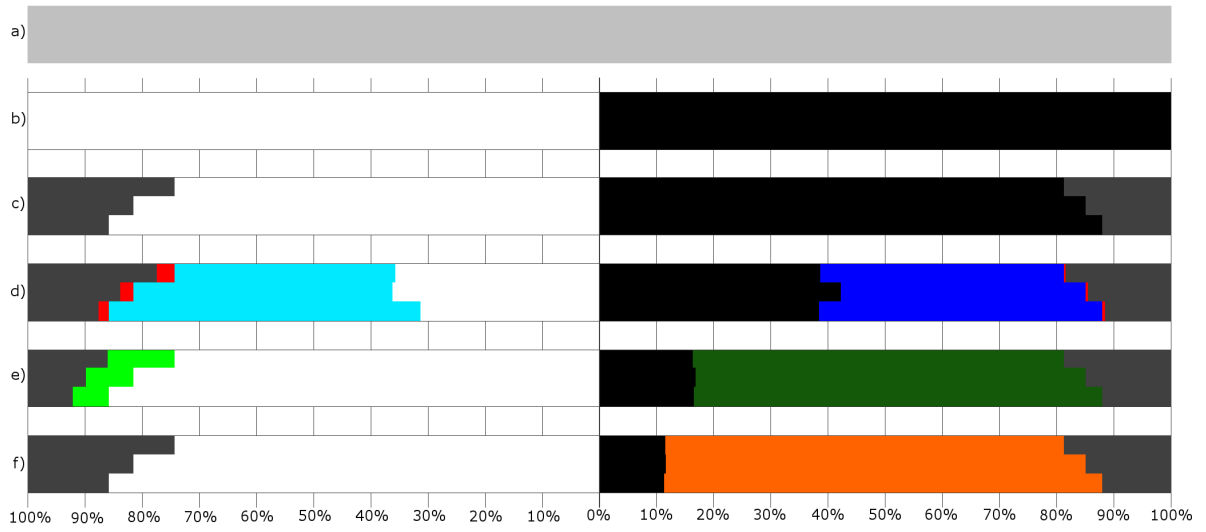


Figure 231: Corrected/confirmed/hinted contour pixels by each method for the with viewpoint of the flowers scene using a 1024x1024 (top) and a 2048x2048 (bottom) resolution shadow map.

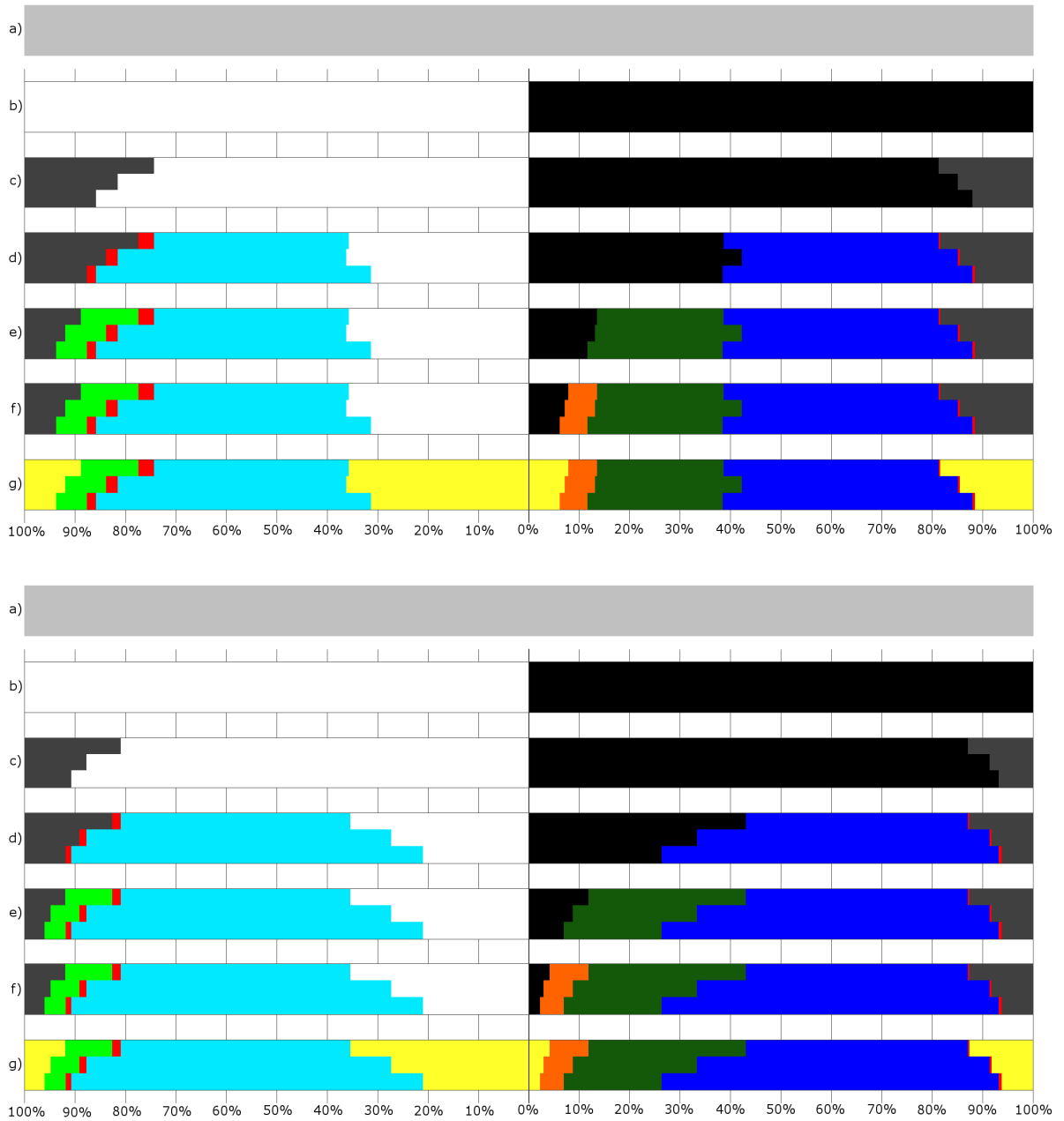


Figure 232: Corrected/confirmed/hinted contour pixels by the chaining of methods for the with viewpoint of the flowers scene using a 1024x1024 (top) and a 2048x2048 (bottom) resolution shadow map.

Shadow Map Resolution	Approach	Contour Thickness			
		Two Pixels	Four Pixels	Six Pixels	Whole Image
1024x1024	Pixels in Contour	47045	82557	111069	1048576
	Shadow Map	10457 (22.23%)	13806 (16.72%)	14567 (13.12%)	15230 (1.45%)
	Single Texel	11660 (24.78%)	18038 (21.85%)	21958 (19.77%)	43091 (4.11%)
	Neighbour Texels (4 Neighbours)	7994 (16.99%)	12578 (15.24%)	15247 (13.73%)	22742 (2.17%)
	Neighbour Texels (9 Neighbours)	7136 (15.17%)	11083 (13.42%)	13419 (12.08%)	19799 (1.89%)
	Adjacent Geometry (One Level)	9959 (21.17%)	14750 (17.87%)	17406 (15.67%)	26192 (2.50%)
	Adjacent Geometry (Two Level)	8585 (18.25%)	12121 (14.68%)	13820 (12.44%)	20171 (1.92%)
2048x2048	Pixels in Contour	50263	85450	113229	1048576
	Shadow Map	8050 (16.02%)	8919 (10.44%)	9099 (8.04%)	9245 (0.88%)
	Single Texel	10740 (21.37%)	15196 (17.78%)	18211 (16.08%)	30531 (2.91%)
	Neighbour Texels (4 Neighbours)	7054 (14.03%)	9821 (11.49%)	11739 (10.37%)	16311 (1.56%)
	Neighbour Texels (9 Neighbours)	6012 (11.96%)	8284 (9.69%)	9845 (8.69%)	13388 (1.28%)
	Adjacent Geometry (One Level)	8176 (16.27%)	10691 (12.51%)	12527 (11.06%)	17358 (1.66%)
	Adjacent Geometry(Two Level)	6169 (12.27%)	7498 (8.77%)	8501 (7.51%)	11249 (1.07%)

Table 184: Difference between the approaches that use ray-tracing and the actual ray-tracer for the with viewpoint of the flowers scene.

Shadow Map Resolution	Contour Thickness		
	Two Pixels	Four Pixels	Six Pixels
1024x1024	10457 of 15230 (68.66%)	13806 of 15230 (90.65%)	14567 of 15230 (95.65%)
2048x2048	8050 of 9245 (87.07%)	8919 of 9245 (96.47%)	9099 of 9245 (98.42%)

Table 185: Wrongly defined pixels in the shadow mapping result which are inside the contour in the with viewpoint of the flowers scene.

Shadow Map Resolution	Contour Thickness	Pixel Shading	
		Light	Shadow
1024x1024	Two Pixels	6196 of 24223	4261 of 22822
	Four Pixels	7878 of 42799	5928 of 39758
	Six Pixels	8205 of 57993	6362 of 53076
	Whole Image	8397 of 611823	6833 of 436753
2048x2048	Two Pixels	4860 of 25531	3190 of 24732
	Four Pixels	5328 of 43680	3591 of 41770
	Six Pixels	5379 of 58316	3720 of 54913
	Whole Image	5411 of 611836	3834 of 436740

Table 186: Pixels that the shadow map defines wrongly in the with viewpoint of the flowers scene, separated in pixels defined in light and in shadow, compared to the total amount of pixels lighted in the same way.

Shadow Map Resolution	Contour Thickness	Texel Coherence					
		Light			Shadow		
		Confirmed	Incorrectly Confirmed	Undecided	Confirmed	Incorrectly Confirmed	Undecided
1024x1024	Two Pixels	10080 (41.61%)	713 (2.94%)	14143 (58.39%)	9759 (42.76%)	34 (0.15%)	13063 (57.24%)
	Four Pixels	20347 (47.54%)	939 (2.19%)	22452 (52.46%)	17113 (43.04%)	105 (0.26%)	22645 (56.96%)
	Six Pixels	32596 (56.21%)	991 (1.71%)	25397 (43.79%)	26505 (49.94%)	199 (0.37%)	26571 (50.06%)
	Whole Image	584793 (95.58%)	1125 (0.18%)	27030 (4.42%)	408274 (93.48%)	568 (0.13%)	28479 (6.52%)
2048x2048	Two Pixels	12029 (47.12%)	426 (1.67%)	13502 (52.88%)	10932 (44.20%)	39 (0.16%)	13800 (55.80%)
	Four Pixels	26951 (61.70%)	562 (1.29%)	16729 (38.30%)	24353 (58.30%)	138 (0.33%)	17417 (41.70%)
	Six Pixels	41212 (70.67%)	591 (1.01%)	17104 (29.33%)	36967 (67.32%)	242 (0.44%)	17946 (32.68%)
	Whole Image	594584 (97.18%)	608 (0.10%)	17252 (2.82%)	418483 (95.82%)	340 (0.08%)	18257 (4.18%)

Table 187: Pixel confirmation when using texel coherence with four texels for the with viewpoint of the flowers scene.

Shadow Map Resolution	Contour Thickness	Texel Shadowing							
		Light				Shadow			
		3 shadow/1 light	3 shadow/1 light in ray-tracer shadow	1 shadow/3 light	1 shadow/3 light in ray-tracer light	3 shadow/1 light	3 shadow/1 light in ray-tracer shadow	1 shadow/3 light	1 shadow/3 light in ray-tracer light
1024x1024	Two Pixels	3149	2192	5563	4372	5024	4328	2853	1723
	Four Pixels	4242	2705	9334	7743	9917	8812	3916	2224
	Six Pixels	4408	2767	11154	9406	12362	11140	4180	2321
	Whole Image	4430	2778	12566	10785	13795	12546	4233	2357
2048x2048	Two Pixels	2475	1607	5362	4494	5545	5119	2458	1459
	Four Pixels	2627	1654	7306	6283	7607	7113	2690	1549
	Six Pixels	2627	1654	7579	6540	7987	7480	2695	1553
	Whole Image	2638	1662	7681	6640	8184	7672	2703	1559

Table 188: Pixel shadowing for pixels that don't achieve texel coherence with four texels for the with viewpoint of the flowers scene.

Shadow Map Resolution	Contour Thickness	Texel Coherence					
		Light			Shadow		
		Confirmed	Incorrectly Confirmed	Undecided	Confirmed	Incorrectly Confirmed	Undecided
1024x1024	Two Pixels	6946 (28.68%)	319 (1.32%)	17277 (71.32%)	8893 (38.97%)	5 (0.02%)	13929 (61.03%)
	Four Pixels	13915 (32.51%)	418 (0.98%)	28884 (67.49%)	14404 (36.23%)	23 (0.06%)	25354 (63.77%)
	Six Pixels	21354(36.8 2%)	426 (0.73%)	36639 (63.18%)	18524(34.9 0%)	27 (0.05%)	34552(65.1 0%)
	Whole Image	562833 (91.99%)	480 (0.08%)	48990 (8.01%)	387597 (88.75%)	187 (0.04%)	49156 (11.25%)
2048x2048	Two Pixels	9180 (35.96%)	222 (0.87%)	16351 (64.04%)	9315 (37.66%)	4 (0.02%)	15417 (62.34%)
	Four Pixels	18885 (43.23%)	293 (0.67%)	24795 (56.77%)	16234 (38.87%)	20 (0.05%)	25536 (61.13%)
	Six Pixels	30789 (52.80%)	302 (0.52%)	27527 (47.20%)	25273 (46.02%)	34 (0.06%)	29640 (53.98%)
	Whole Image	583005 (95.29%)	315 (0.05%)	28831 (4.71%)	405149 (92.77%)	101 (0.02%)	31591 (7.23%)

Table 189: Pixel confirmation when using texel coherence with nine texels for the with viewpoint of the flowers scene.

Shadow Map Lighting	Texel Shadowing	Shadow Map							
		1024x1024				2048x2048			
		Two Pixels	Four Pixels	Six Pixels	Whole Image	Two Pixels	Four Pixels	Six Pixels	Whole Image
Light	8 S-1 L	367	470	475	475	88	91	91	91
	8 S-1 L in RT Shadow	246	288	289	289	64	67	67	67
	7 S-2 L	861	1149	1179	1179	684	741	741	741
	7 S-2 L in RT Shadow	565	674	678	678	379	392	392	392
	6 S-3 L	1198	1730	1872	1881	924	1067	1070	1071
	6 S-3 L in RT Shadow	643	788	805	806	446	462	462	463
	5 S-4 L	1180	1736	1940	2001	1216	1524	1552	1558
	5 S-4 L in RT Shadow	570	709	736	738	541	584	585	585
	4 S-5 L	2695	4502	5601	6556	3310	4589	4813	4874
	4 S-5 L in RT Light	1109	2363	3363	4299	1924	3131	3355	3407
	3 S-6 L	3805	6505	8463	10362	4147	6449	7044	7151
	3 S-6 L in RT Light	2733	5219	7124	9001	3133	5338	5920	6022
	2 S-7 L	3285	5853	7757	10424	3018	4883	5397	5560
	2 S-7 L in RT Light	2691	5069	6913	9551	2535	4320	4822	4983
1 S-8 L	3886	6939	9352	16112	2964	5451	6819	7785	
1 S-8 L in RT Light	3285	6147	8502	15197	2639	5053	6405	7369	
Shadow	8 S-1 L	1625	4010	6919	14904	1986	5205	7222	8415
	8 S-1 L in RT Shadow	1464	3753	6602	14463	1900	5073	7058	8235
	7 S-2 L	2957	5622	7871	11072	3171	5510	6441	6779
	7 S-2 L in RT Shadow	2549	5026	7213	10347	2918	5227	6128	6451
	6 S-3 L	3300	6048	8241	10478	4000	6461	7243	7578
	6 S-3 L in RT Shadow	2281	4671	6807	8997	3343	5721	6474	6806
	5 S-4 L	3109	5291	6696	7775	3414	4855	5169	5229
	5 S-4 L in RT Shadow	1656	3319	4603	5639	2138	3496	3799	3846
	4 S-5 L	967	1510	1687	1730	1082	1366	1394	1409
	4 S-5 L in RT Light	382	518	555	562	276	322	327	327
	3 S-6 L	925	1423	1582	1621	938	1163	1192	1202
	3 S-6 L in RT Light	391	562	602	609	262	296	301	301
	2 S-7 L	695	960	1022	1026	673	779	782	782
	2 S-7 L in RT Light	321	435	459	462	304	349	352	352
1 S-8 L	351	490	534	550	153	197	197	197	
1 S-8 L in RT Light	121	188	217	230	72	90	90	90	

Table 190: Pixel shadowing for pixels that don't achieve texel coherence with nine texels for the with viewpoint of the flowers scene.

Shadow Map Resolution	Contour Thickness	Corrected		Turned Bad		Maintained Correct		Maintained Incorrect	
		L→S	S→L	L→S	S→L	L→L	S→S	L→L	S→S
1024x1024	Two Pixels	81	4261	0	5545	18027	13016	6115	0
	Four Pixels	104	5928	0	10264	34921	23566	7774	0
	Six Pixels	110	6362	0	13863	49788	32851	8095	0
	Whole Image	118	6833	0	34812	603426	395108	8279	0
2048x2048	Two Pixels	150	3190	0	6030	20671	15512	4710	0
	Four Pixels	167	3591	0	10035	38352	28144	5161	0
	Six Pixels	167	3720	0	12999	52937	38194	5212	0
	Whole Image	167	3834	0	25287	606425	407619	5244	0

Table 191: Pixel correction between the single texel approach and the shadow mapping approach for the with viewpoint of the flowers scene.

Shadow Map Resolution	Contour Thickness	Corrected		Turned Bad		Maintained Correct		Maintained Incorrect	
		L→S	S→L	L→S	S→L	L→L	S→S	L→L	S→S
1024x1024	Two Pixels	2467	4261	0	4265	18027	14296	3729	0
	Four Pixels	3080	5928	0	7780	34921	26050	4798	0
	Six Pixels	3166	6362	0	10208	49788	36506	5039	0
	Whole Image	3196	6833	0	17541	603426	412379	5201	0
2048x2048	Two Pixels	2113	3190	0	4307	20671	17235	2747	0
	Four Pixels	2213	3591	0	6706	38352	31473	3115	0
	Six Pixels	2216	3720	0	8576	52937	42617	3163	0
	Whole Image	2230	3834	0	13130	606425	419776	3181	0

Table 192: Pixel correction between the neighbour texels approach using four neighbours and the shadow mapping approach for the with viewpoint of the flowers scene.

Shadow Map Resolution	Contour Thickness	Corrected		Turned Bad		Maintained Correct		Maintained Incorrect	
		L→S	S→L	L→S	S→L	L→L	S→S	L→L	S→S
1024x1024	Two Pixels	2803	4261	0	3743	18027	14818	3393	0
	Four Pixels	3514	5928	0	6719	34921	27111	4364	0
	Six Pixels	3603	6362	0	8817	49788	37897	4602	0
	Whole Image	3635	6833	0	15037	603426	414883	4762	0
2048x2048	Two Pixels	2422	3190	0	3574	20671	17968	2438	0
	Four Pixels	2560	3591	0	5516	38352	32663	2768	0
	Six Pixels	2563	3720	0	7029	52937	44164	2816	0
	Whole Image	2577	3834	0	10554	606425	422352	2834	0

Table 193: Pixel correction between the neighbour texels approach using nine neighbours and the shadow mapping approach for the with viewpoint of the flowers scene.

Shadow Map Resolution	Number of Neighbours	Triangle Average	Two Pixels	Four Pixels	Six Pixels	Whole Image
1024x1024	3	Used	2.4112	2.3467	2.2626	0.7686
		Available	2.5506	2.4912	2.4558	1.5562
	8	Used	4.4772	4.3261	4.1689	1.1469
		Available	4.7030	4.5393	4.3816	2.2792
2048x2048	3	Used	2.2667	2.1329	2.0153	0.6925
		Available	2.4164	2.3558	2.2805	1.4165
	8	Used	4.0599	3.8321	3.6037	0.9629
		Available	4.2812	4.0566	3.8968	1.9494

Table 194: Average of triangle intersections when using the neighbour texels approach for the with viewpoint of the flowers scene.

Shadow Map Resolution	Contour Thickness	Corrected		Turned Bad		Maintained Correct		Maintained Incorrect	
		L→S	S→L	L→S	S→L	L→L	S→S	L→L	S→S
1024x1024	Two Pixels	165	4261	0	3928	18027	14633	6031	0
	Four Pixels	228	5928	0	7100	34921	26730	7650	0
	Six Pixels	244	6362	0	9445	49788	37269	7961	0
	Whole Image	257	6833	0	18052	603426	411868	8140	0
2048x2048	Two Pixels	287	3190	0	3603	20671	17939	4573	0
	Four Pixels	341	3591	0	5704	38352	32475	4987	0
	Six Pixels	346	3720	0	7494	52937	43699	5033	0
	Whole Image	346	3834	0	12293	606425	420613	5065	0

Table 195: Pixel correction between the adjacent geometry approach with one level of adjacency and the shadow mapping approach for the with viewpoint of the flowers scene.

Shadow Map Resolution	Contour Thickness	Corrected		Turned Bad		Maintained Correct		Maintained Incorrect	
		L→S	S→L	L→S	S→L	L→L	S→S	L→L	S→S
1024x1024	Two Pixels	268	4261	0	2657	18027	15904	5928	0
	Four Pixels	398	5928	0	4641	34921	29189	7480	0
	Six Pixels	429	6362	0	6044	49788	40670	7776	0
	Whole Image	452	6833	0	12226	603426	417694	7945	0
2048x2048	Two Pixels	395	3190	0	1704	20671	19838	4465	0
	Four Pixels	494	3591	0	2664	38352	35515	4834	0
	Six Pixels	504	3720	0	3626	52937	47567	4875	0
	Whole Image	507	3834	0	6345	606425	426561	4904	0

Table 196: Pixel correction between the adjacent geometry approach with two level of adjacency and the shadow mapping approach for the with viewpoint of the flowers scene.

Shadow Map Resolution	Adjacency Level	Triangle Average	Two Pixels	Four Pixels	Six Pixels	Whole Image
1024x1024	One Level	Used	3.0413	3.0660	3.0733	1.8966
		Available	3.8668	3.8695	3.8740	3.9621
	Two Levels	Used	9.6289	9.6693	9.6106	6.4508
		Available	12.2423	12.2033	12.1147	13.4759
2048x2048	One Level	Used	3.0904	3.1070	3.1055	1.9001
		Available	3.8679	3.8638	3.8649	3.9595
	Two Levels	Used	9.7832	9.6871	9.5584	6.4438
		Available	12.2443	12.0465	11.8957	13.4276

Table 197: Average of triangle intersections when using the adjacent geometry approach for the with viewpoint of the flowers scene.

Contour Thickness		Two Pixels		Four Pixels		Six Pixels		Whole Image		
Lighting		L→S	S→L	L→S	S→L	L→S	S→L	L→S	S→L	
Shadow Map Resolution	1024x1024	Corrected by Both	97	4261	128	5928	135	6362	143	6833
		Turned Bad by Both	0	2205	0	3825	0	4922	0	9037
		Corrected by Neighbour Texels Only	2706	0	3386	0	3468	0	3492	0
		Corrected by Adjacent Geometry Only	171	0	270	0	294	0	309	0
		Turned Bad by Neighbour Texels Only	0	1538	0	2894	0	3895	0	6000
		Turned Bad by Adjacent Geometry Only	0	452	0	816	0	1122	0	3189
	2048x2048	Corrected by Both	218	3190	250	3591	252	3720	252	3834
		Turned Bad by Both	0	1298	0	1923	0	2610	0	4227
		Corrected by Neighbour Texels Only	2204	0	2310	0	2311	0	2325	0
		Corrected by Adjacent Geometry Only	177	0	244	0	252	0	255	0
		Turned Bad by Neighbour Texels Only	0	2276	0	3593	0	4419	0	6327
		Turned Bad by Adjacent Geometry Only	0	406	0	741	0	1016	0	2118

Table 198: Pixel correction by the neighbour texels (9 texels) and the adjacent geometry (2 levels) approaches separated by lighting change for the with viewpoint of the flowers scene.

Algorithm Step	Confirmations and Errors	1024x1024			2048x2048		
		Two Pixels	Four Pixels	Six Pixel	Two Pixels	Four Pixels	Six Pixel
Shadow Map	Total Contour Pixels	47045	82557	111069	50263	85450	113229
	Correct Light Pixels	18027 (74.42%)	34921 (81.59%)	49788 (85.85%)	20671 (80.96%)	38352 (87.80%)	52937 (90.78%)
	Correct Shadow Pixels	18561 (81.33%)	33830 (85.09%)	46714 (88.01%)	21542 (87.10%)	38179 (91.40%)	51193 (93.23%)
	Incorrect Light Pixels	6196 (25.58%)	7878 (18.41%)	8205 (14.15%)	4860 (19.04%)	5328 (12.20%)	5379 (9.22%)
	Incorrect Shadow Pixels	4261 (18.67%)	5928 (14.91%)	6362 (11.99%)	3190 (12.90%)	3591 (8.60%)	3720 (6.77%)
Texel Coherence	Confirmations in Light	10080 (41.61%)	20347 (47.54%)	32596 (56.21%)	12029 (47.12%)	26951 (61.70%)	41212 (70.67%)
	Confirmations in Shadow	9759 (42.76%)	17113 (43.04%)	26505 (49.94%)	10932 (44.20%)	24353 (58.30%)	36967 (67.32%)
	Wrong Confirmations in Light	713 (2.94%)	939 (2.19%)	991 (1.71%)	426 (1.67%)	562 (1.29%)	591 (1.01%)
	Wrong Confirmations in Shadow	34 (0.15%)	105 (0.26%)	199 (0.37%)	39 (0.16%)	138 (0.33%)	242 (0.44%)
Neighbouring Texels	Corrections in Light	2767 (11.42%)	3468 (8.10%)	3556 (6.13%)	2355 (9.22%)	2472 (5.66%)	2475 (4.24%)
	Confirmations in Shadow	15496 (67.90%)	28704 (72.20%)	40702 (76.69%)	18630 (75.33%)	34623 (82.89%)	47617 (86.71%)
Adjacent Geometry	Confirmations in Shadow	16796 (73.60%)	31056 (78.11%)	43623 (82.19%)	20532 (83.02%)	37064 (88.73%)	50148 (91.32%)
Final Lighting	Wrong Confirmations in Light	3460 (14.28%)	4455 (10.41%)	4697 (8.10%)	2573 (10.08%)	2931 (6.71%)	2979 (5.11%)
	Wrong Confirmations in Shadow	1833 (8.03%)	2984 (7.51%)	3489 (6.57%)	1088 (4.40%)	1391 (3.33%)	1529 (2.78%)

Table 199: Algorithm results of the with viewpoint of the flowers scene.